Technical Report
TR-18-12
January 2019

Concrete caissons for 2BMA

Large scale test of design and material

Per Mårtensson
Carsten Vogt

SVENSK KÄRNBRÄNSLEHANTERING AB

SWEDISH NUCLEAR FUEL
AND WASTE MANAGEMENT CO

Box 3091, SE-169 03 Solna
Phone +46 8 459 84 00
skb.se

SVENSK KÄRNBRÄNSLEHANTERING

ISSN 1404-0344
SKB TR-18-12
ID 1605143
January 2019

Concrete caissons for 2BMA

Large scale test of design and material

Per Mårtensson, Svensk Kärnbränslehantering AB

Carsten Vogt, Betong- och Stålteknik

Keywords: Concrete, 2BMA, SFR, Repository.

Abstract

The repository for short-lived radioactive waste, SFR has been in operation since 1988 and hosts operational waste from the Swedish nuclear power plants and other nuclear facilities

At present, plans are made to increase the storage capacity of SFR through the construction of 6 new waste vaults which will be located at a depth of 120 metres. One of these vaults will be the rock vault for intermediate level waste (2BMA).

In 2BMA a number of caissons in which the waste will be disposed will be erected. According to the reference design valid when this work was conducted the caissons shall have the dimensions of $16.2 \times 16.2 \times 8.4$ meters and be made from unreinforced concrete with a thickness of the walls and base slab of 500 mm.

In order to demonstrate that SKB can construct the concrete caissons according to given specifications, a development program comprising the following activities has been carried out:

- Investigation of the suitability of the rock at the site of the SFR extension to be used as aggregates in the concrete.
- Identification of suitable quarries for aggregate production during development and large scale tests.
- Material development on a laboratory scale.
- Upscaling and mixing tests at concrete production scale plants.
- Casting of large concrete structures representative of the concrete caissons for 2BMA and long-term follow-up of material properties.

The first four activities have previously been reported in Lagerblad et al. (2016, 2017).

In this report, the observations and results from casting and long-term monitoring of 2 concrete structures representative of the concrete caissons aimed for the future 2BMA is presented, corresponding to the last bullet point in the list above.

The following conclusions can be drawn from the results presented in this report:

- Mixing of large amounts of concrete in a concrete production plant according to the mix design developed and tested in the preceding activities was successfully carried out and the properties of the fresh concrete immediately after mixing were according to the requirements.
- The control of the setting of concrete containing large amounts of fine-grained limestone filler, such as the concrete used in these experiments presents a challenging task. This is due to that the fine grained limestone acts as an accelerator; both shortening the time until hydration starts but also increasing the rate of hydration once hydration has been initiated. For that reason, a concrete production unit in close connection to the site of the casting need to be considered in future casting experiments and casting of the caissons in 2BMA.
- The difficulties to control the setting of the concrete also suggests that casting of base slab and walls in one uninterrupted sequence will be a very challenging task. The results presented in this study recommend that base slab and walls are cast on separate occasions. This is also supported by the fact that the hydraulic properties of the joint were similar to that of the bulk concrete.
- The foundation used in these experiments comprised a thick reinforced concrete slab with a smooth surface finish on which a reinforced plastic foil had been placed in order to promote unrestrained shrinkage of the concrete structures. From the results obtained up to 1 year after casting of section 1, this combination has fulfilled these requirements and no cracks have yet been identified. This in spite of that the concrete structures has deliberately been dried out in a relative humidity (RH) of 60 % and a temperature (T) of about 18 °C over a period of about 5 months.

- The properties of the hardened concrete were for both sections within the requirements, presenting a high strength and low hydraulic conductivity in combination with low shrinkage and low levels of strain.
- The hydraulic conductivity of joints and the interface between the joint seal and the concrete was found to be closely similar to that of the bulk concrete. This indicates that casting the base slab and the walls separately can be a suitable way forward in order to avoid a complicated casting process with a suspended formwork.

Altogether the results presented in this report indicate that the previously developed concrete can be used to cast the caissons for disposal of radioactive waste in 2BMA. However, further development of method for concrete mixing and method for casting needs to be considered. The updated reference design of the concrete caissons (with increased thickness of walls and base slab) needs also to be considered is the forthcoming method development.

Sammanfattning

I Slutförvaret för kortlivat radioaktivt avfall, SFR, vilket varit i drift sedan 1988 deponeras och slutförvaras driftsavfall från de svenska kärnkraftverken liksom kärntekniskt avfall från andra källor inom landet. I dagsläget planeras en utbyggnad av anläggningen för att ge plats till det avfall som förväntas uppkomma i samband med rivning av kärnkraftverken. Utbyggnaden omfattar totalt 6 stycken cirka 275 meter långa bergssalar på ett djup av cirka 120 meter varav en utgörs av Bergssalen för Medelaktivt Avfall, 2BMA.

I 2BMA kommer ett antal kassuner i vilka avfallet kommer att deponeras att uppföras. Enligt den referensdesign som var gällande när detta arbete genomfördes ska kassunerna ha måtten $16{,}2 \times 16{,}2 \times 8{,}4$ meter och vara gjorda av oarmerad betong. Väggar och bottenplatta ska vara 500 mm tjocka.

För att visa att SKB kan konstruera och uppföra kassunerna enligt givna specifikationer har ett utvecklingsprogram som omfattar följande aktiviteter genomförts:

- Undersökning av lämpligheten hos det entreprenadberg som kommer att uppkomma vid utsprängningen av SFR-utbyggnaden som ballast till betong.
- Identifiering av lämpliga täkter för tillverkning av ballast till utvecklingsarbetet och storskaliga tester.
- Materialutveckling i laboratorieskala.
- Uppskalning och blandningstester vid produktionsenheter.
- Gjutning av stora betongkonstruktioner som är representativa för betongkassunerna i 2BMA och långvarig uppföljning av materialegenskaper.

De första fyra aktiviteterna har tidigare rapporterats i Lagerblad et al. (2016, 2017).

I denna rapport presenteras observationer och resultat från gjutning och långsiktig övervakning av 2 betongkonstruktioner som är representativa för betongkassunerna i det framtida 2BMA, motsvarande den sista punkten i listan ovan.

Följande slutsatser kan dras ur de observationer och erfarenheter som presenteras i denna rapport.

- Blandning av stora mängder betong enligt det recept som utvecklats och testats i tidigare aktiviteter kunde framgångsrikt genomföras i en produktionsanläggning för betong och egenskaperna hos den färska betongen direkt efter blandning uppfyllde samtliga krav.
- Kontrollen av tillstyvnadsförloppet hos betong som innehåller stora mängder finkornig kalkstensfiller, såsom betongen som används i dessa experiment, utgör en stor utmaning. Detta beror på att mycket finmald kalksten fungerar som en accelerator och både förkortar tiden till dess att hydratationen påbörjar men ökar även hydratiseringshastigheten när hydratisering har initierats. Av denna anledning bör framtida storskaliga gjutningsexperiment och gjutning av kassuner i 2BMA utnyttja en anläggning för betongproduktion i nära anslutning till gjutplatsen.
- Svårigheten att styra betongens tillstyvnad innebär även att gjutning av bottenplatta och väggar i en oavbruten sekvens enligt den referensmetod som var gällande vid detta arbetes genomförande kommer att vara förenat med stora osäkerheter och risker. Resultaten som presenteras i denna studie rekommenderar i stället att bottenplatta och väggar gjuts vid separata tillfällen.
- Grundläggningen som användes i dessa experiment bestod av en tjock betongplatta med en slät yta på vilken en förstärkt plastfolie hade placerats för att främja fri krympning av betongkonstruktionerna. Från resultaten erhållna upp till 1 år efter gjutning av sektion 1 har denna kombination uppfyllt dessa krav och inga sprickor har ännu identifierats. Detta trots att betongkonstruktionerna avsiktligt har torkats ut i RF 60 % och T omkring 18 °C under en period av cirka 5 månader.
- Egenskaperna hos den härdade betongen var för båda sektionerna inom kraven och uppvisar en hög hållfasthet och låg hydraulisk konduktivitet i kombination med låg krympning och låga spänningsnivåer.

- Den hydrauliska konduktiviteten hos fogen mellan vägg och bottenplatta samt mellan betong och fogband var likvärdig betongens bulkegenskaper. Detta antyder att det kommer att vara möjligt att uppföra väggar och bottenplatta i två separata gjutningar och därmed undvika ett komplicerat och riskfyllt gjutningsförfarande.

Sammantaget visar resultaten som presenteras i denna rapport att den tidigare utvecklade betongen kan användas för att gjuta stora oarmerade betongkonstruktioner, såsom kassuner för slutförvaring av radioaktivt avfall. Ytterligare utveckling av metod för betongblandning och metod för gjutning måste emellertid övervägas och genomföras. Betydelsen av sådant arbete har nyligen ökat då ett beslut att ändra dimensionerna – huvudsakligen tjockleken på kassunernas väggar och bottenplatta – på betongkassunernas referensutformning tagits.

Contents

1 Background

1.1 The repository short-lived radioactive waste, SFR

The repository for short-lived radioactive waste, SFR has been in operation since 1988 and hosts operational waste from the Swedish nuclear power plants and from the other nuclear facilities. The repository includes underground waste vaults along with surface technical facilities. The waste vaults are located in granitic bedrock at a depth of about 60 meters below the Baltic Sea and are reached via two one-kilometre-long access tunnels from the ground surface.

The underground part of the existing facility, named SFR 1, consists of four 160-metre-long waste vaults and one 70-metre-high vault with a concrete silo with a total storage capacity of 63 000 m^3. The existing facility is shown in the top right part of Figure 1-1.

At present, plans are made to increase the storage capacity of SFR though the construction of 6 new waste vaults which will be located at a depth of 120 metres, i.e. at the same level as the bottom of the silo. These 6 waste vaults which are shown in the lower left part of Figure 1-1 will comprise 4 vaults for low-level waste (2–5BLA), one vault for intermediate level waste (2BMA) and one vault for reactor pressure vessels (BRT) each with a length of up to 275 meters. The work presented in this report relates primarily to 2BMA, see Section 1.2.

1.2 The rock vault for intermediate level waste, 2BMA

The rock vault for intermediate level waste, 2BMA will be in total about 275 meters long and contain a number of caissons in which the waste will be disposed, Figure 1-2. According to the reference design valid when the work presented in this report was conducted the caissons shall have the dimensions of 16.2 × 16.2 × 8.4 meters, Figure 1-3, and be made from unreinforced concrete with a thickness of the walls and base slab of 500 mm (SKB 2015).

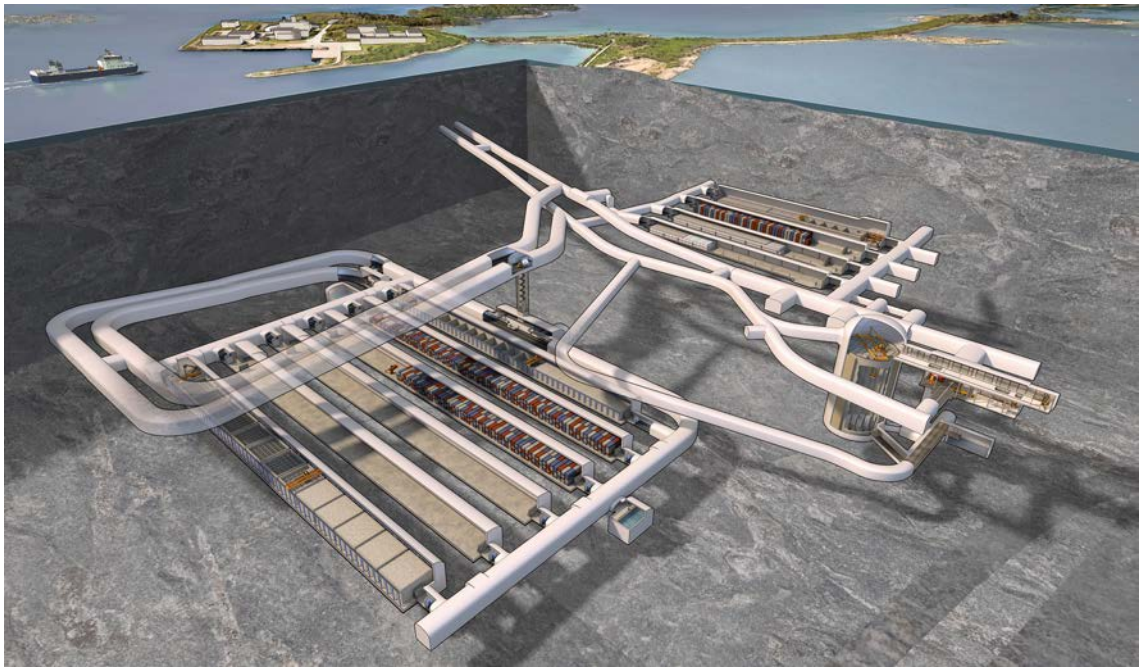

Figure 1-1. *An illustration of SFR. The existing facility is shown in the top right part and the planned extension in the lower left part of the illustration.*

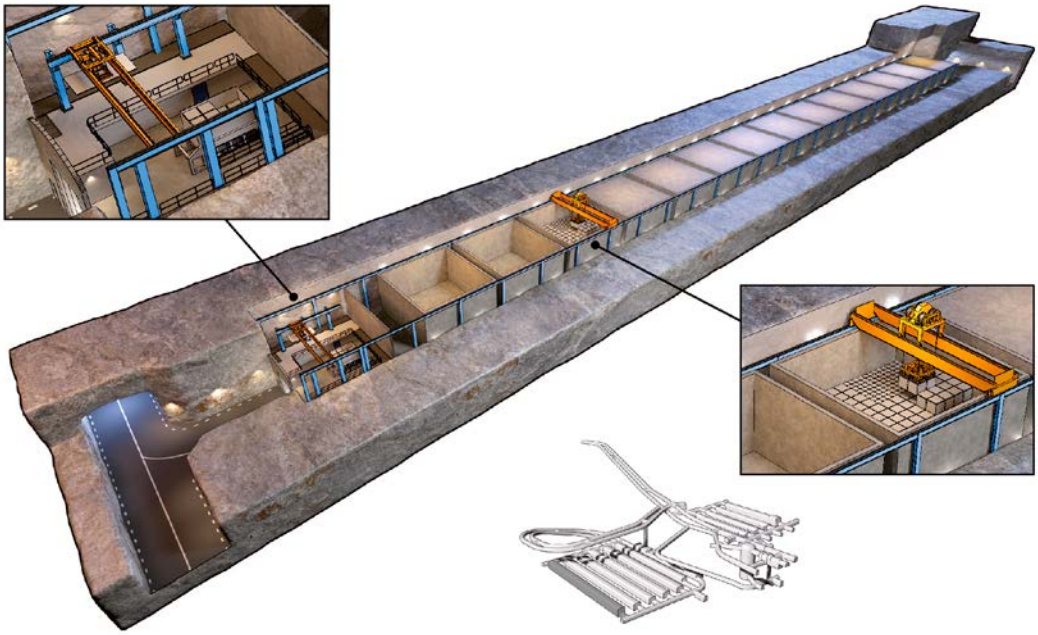

Figure 1-2. *The rock vault for intermediate level waste, 2BMA (SKB 2015).*

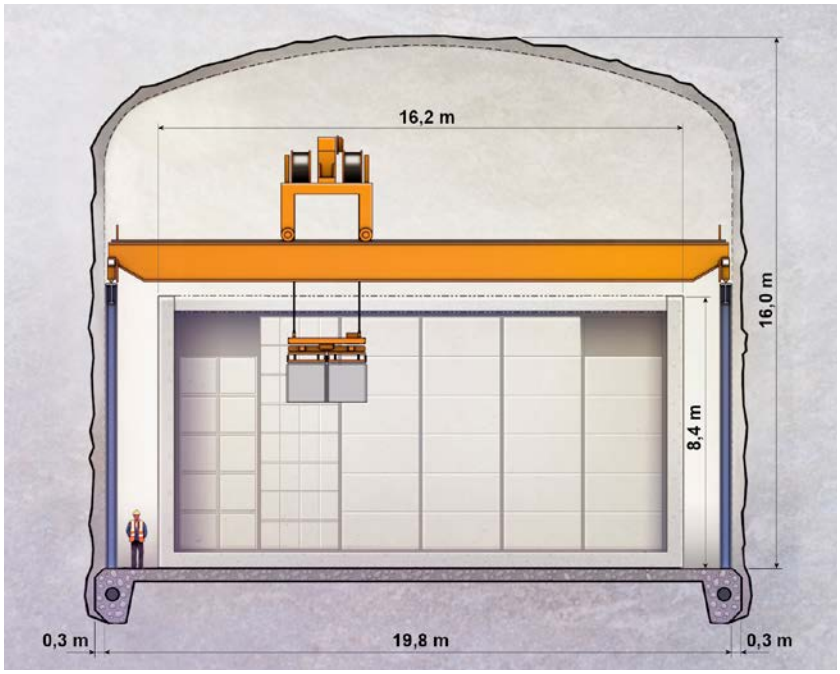

Figure 1-3. *Cross section of a caisson also showing the deposition of waste containers using the overhead crane.*

In order to achieve the desired hydraulic properties of the caissons, casting of the base slab and walls should according to the reference method preferably be done in one uninterrupted sequence to avoid the formation of casting joints. Further, the formwork must not contain form rods to avoid the formation of hydraulically conducting channels in the walls due to corrosion of these. For these reasons, a formwork in which the inner part is suspended in the outer part must be used. The maximum permissible width of a crack or joint is according to the reference design 0.1 mm.

To limit the stress concentration in the transition between walls and base slab or between adjacent walls, sharp 90-degree corners should be avoided. This is further discussed in Chapter 2.

1.3 Material development programme

1.3.1 Background

In order to demonstrate that SKB can construct the concrete caissons according to given specifications, a development program comprising the following activities has been undertaken:

- Investigation of the suitability of the rock at the site of the SFR extension to be used as aggregates in the concrete.
- Identification of suitable quarries for aggregate production for development and large scale tests.
- Material development on a laboratory scale.
- Upscaling and mixing tests at concrete production plants.
- Casting of large concrete structures representative of the concrete caissons for 2BMA and long-term follow-up of material properties.

Parts of this development programme have been reported previously in Lagerblad et al. (2016, 2017).

1.3.2 Prerequisites and requirements for concrete development

General prerequisites and requirements

When developing a concrete for 2BMA, the following conditions have been taken into account:

- **Dimensions**: The dimensions of the concrete caissons are $16.2 \times 16.2 \times 8.4$ m. ($l \times w \times h$) with a thickness of the walls and base slab of 500 mm.
- **Formwork**: Casting of the concrete caissons should be done using a formwork designed without the use of form rods to avoid the risk for future formation of hydraulically conducting channels through the walls.
- **Casting**: Casting should be done in one uninterrupted sequence to avoid the formation of casting joints.
- **Shrinkage**: The concrete should be designed in a way that minimizes shrinkage to avoid cracking during construction and operation.
- **Foundation**: The foundation of the caissons must permit unrestricted movements of the caissons caused by e.g. shrinkage and expansion due to the annual variations of temperature and relative humidity in the repository.
- **Load cases**: The following dimensioning loads have been taken into account in the design and construction of caissons:
  - Internal gas pressure due to gas formation from decomposition of waste.
  - Load from backfill material.
  - Pressure from backfilling the caisson with cement grout.
  - Load of waste.
  - Load of dropped waste container.
  - Accidental shock from overhead crane.
  - Load from falling block.
  - One-sided external water pressure during resaturation of the repository after closure.
- **Gas permeability**: No explicit requirements for the gas permeability of the concrete have been formulated. Instead, gas arising from corrosion of the waste, for example, will be expelled from the concrete structure through a dedicated gas-relief system.
- **Repository environment**: The concrete should be formulated with regard to the exposure class in the repository. Expected environment corresponds to marine environment.
- **Workability**: The concrete should be pumpable for at least three hours after mixing.
- **Setting**: The setting time of the concrete must be properly adjusted to avoid a very high form work pressure during casting of the walls but still long enough to facilitate proper homogenisation of the different casting layers, thus avoiding unintended joints.
- **Reinforcement**: No steel reinforcement can be used in the caissons.

Required properties of the fresh concrete

The following properties are required for the fresh concrete:

- **Setting time**: The concrete will be transported and wait at the site of casting for a total of up to three hours from mixing until the concrete truck has been emptied. This should not adversely affect the workability of the concrete. In addition, the concrete must not set in such a way that the successive casting layers cannot be vibrated together.
- **Workability**: The concrete must fill the mould completely and no cavities may be formed after vibration.
- **Stability**: Stone separation must not occur. Water separation may occur only to a very limited extent.
- **Pump ability**: The concrete should be pump able and not separate during pumping.

Required properties of the hardened concrete

The following properties are set on the hardened concrete:

- **Compressive strength:** The compressive strength at 90 days must exceed 50 MPa.
- **Tensile strength:** The tensile strength at 28 days must exceed 2.5 MPa.
- **Shrinkage:** Shrinkage should be minimized.
- **Internal strain:** Internal strain must be minimized in the finished structure to limit the risk of cracking.
- **Porosity:** Low porosity increases the chemical resistance of the concrete against leaching during the post closure period and thus improves the long term stability of the concrete.

Prerequisites for choice of concrete components

The following conditions for selecting the concrete components must be considered:

- **Cement type**: The cement should be sulphate resistant, low alkali and have a low heat development.
- **Cement content**: Low cement content is preferred. However, the amount of cement paste in the concrete must not be reduced to the extent that the workability of the concrete is adversely affected.
- **Aggregates**: Aggregates produced from material that has emerged from the excavation of the repository should preferably be used. Natural sand and gravel should not be used.
- **W/C-ratio**: The water/cement ratio should preferably not exceed 0.50.
- **Admixtures (Liquid)**: Modern admixtures can be used but the amounts should be limited as far as possible.
- **Additives (Solid)**: Solid additives, such as different types of commercially available filler materials, can be used.

1.3.3 Previous work within the material development programme

Suitability of the bedrock in SFR as aggregates in concrete

Lagerblad et al. (2016) investigated samples from the bedrock of the present and the future repositories in the Forsmark area with focus on its suitability as aggregates in concrete. The investigation showed that the excavated rock was acceptable, though not ideal for aggregate production and that suitable rock material would have to be selected for aggregate production during the excavation work whereas the less suitable material must be discarded. Lagerblad et al. (2016) also showed that there were quarries in the near region where rock material with similar properties as those of the material from the Forsmark area could be obtained for production of aggregates to be used in the material development programme.

Concrete development

Based on the prerequisites and requirement presented in Section 1.3.2 a concrete was developed and tested (Lagerblad et al. 2017). The concrete was based on the use of Degerhamn Anläggnings-cement from Cementa AB and aggregates obtained from crushing rock with similar properties as that expected to be obtained from the excavation of the repository. Further, also limestone filler was added to improve the workability of the concrete. Finally, superplasticiser was used to improve the workability while still keeping a W/C ratio of about 0.5.

1.4 Technology development programme

According to the reference design, the concrete caissons should be erected using certain principles in order to avoid the formation of hydraulically conducting zones in the walls and base slab or in joints between these parts. In combination with a carefully selected concrete developed within the material development programme, this would ensure the post-closure safety of the repository.

Within the requirements concerning the construction method for the concrete caissons the following main important features can be identified:

- The foundation of the concrete caissons should be made of crushed rock or macadam.
- Casting joints must be avoided and for that reason each caisson must be cast in one single uninterrupted sequence.
- Form rods must not be used to hold the formwork together.
- The inner part of the formwork must be suspended in the outer part and supports placed on the foundation cannot be used.
- Unrestrained shrinkage should be facilitated in order to reduce any strain in the concrete structure and thus reduce the risk of cracking.

With the dimensions of the concrete caissons in mind it is evident that the casting of the caissons according to these requirements will be a challenging task. For that reason, a technology development programme involving the focus areas described in Sections 1.4.1 to 1.4.3 was formulated with the aim of investigating alternative production methods.

1.4.1 Foundation

In order to promote unrestrained shrinkage of the concrete caisson and provide a very stiff foundation that helps distribute the loads from the concrete caisson it is suggested that the foundation should comprise a thick reinforced concrete slab which is erected on a draining layer of e.g. macadam.

In order to further reduce the bond between the foundation and the base slab of the concrete caisson it is suggested that a plastic foil is placed on the foundation prior to casting of the concrete caisson.

1.4.2 Casting base slab and walls separately

The main reason for casting the base slab and walls of the caissons in an uninterrupted sequence is that the formation of a joint with (possibly) poor hydraulic properties between these parts is avoided.

However, in the case that the walls and base slab are cast at separate occasions, the hydraulic properties of the joint could be improved by careful preparation of the joint surface prior to casting of the walls.

In order to investigate the possibility to cast the base slab and walls separately, the work presented in this report comprise two sections. Section 1 comprises the base slab and one L-shaped wall which are cast in one uninterrupted sequence according to the reference design. Section 2 comprises a second L-shaped wall which is cast against the base slab of section 1 in a position prepared for this purpose. In order to improve the hydraulic properties of the joint, a joint seal made of 300 mm wide and 1.5 mm thick copper sheet is placed in the centre of the joint during casting of the base slab.

1.4.3 Formwork design

According to the reference design the formwork comprises an outer wall which is supported against adjacent bedrock, caisson or supporting construction frames. Further, the formwork also comprises an inner part which is suspended in the outer part. Finally, also supporting bars between the pairs of opposite inner walls can be used to further enhance the stability of the formwork. Altogether, this results in a very complex formwork system.

Due to the high complexity of the reference formwork design, efforts to evaluate other construction methods involving alternative formwork designs can be motivated. Here, a less complex formwork design could be anticipated to reduce the risks connected with both the working environment and the casting process itself.

As an alternative to casting each caisson in one uninterrupted sequence casting of base slab and walls separately can be done instead. In doing so, the caissons can be erected using conventional methods for formwork construction.

First, casting of the base slab is done according to standard methods for base slabs. This is followed by casting of the walls which is done a couple of weeks later when the base slab has reached sufficient strength and the hydration process ceased. The wall formwork is erected on the base slab. Here, as previously mentioned, formwork tie rods cannot be used. Instead the inner and outer walls are supported by supporting construction frames or supporting rods between the formwork and adjacent rock walls or a previously cast caisson.

In the casting presented in this report, the formwork will be supported against adjacent rock wall and held together by the use of form rods. The use of form rods is here motivated by that it will not influence the properties of the concrete nor the monitoring programme.

It must though be recognized that form rods cannot be used in the formwork when casting the caissons in the future 2BMA. For that reason, other solutions such as e.g. supporting beams between the base slab and the caisson walls must be used instead. However, the value of using supporting beams in the current project is low. This is motivated by the fact that the dimensions of these components are much smaller than for the full scale caissons and very little information on the suitability of using supporting beams would be obtained from these small structures.

1.5 Purpose and goal of the work presented in this report

The main purposes of the work presented in this report are the following:

- To conduct a large scale production test of the concrete developed previously in order to verify that the concrete can be produced in a standard production unit with consistent quality.
- To perform a first large scale test of a concrete structure representative of the concrete caissons for 2BMA which will form the basis for future tests prior to casting of the caissons in 2BMA.
- To perform long term follow-up of the properties of the concrete and the effect of the climate in the repository on these properties.
- To investigate the possibility of reducing the degree of restraint between the foundation and the concrete structure by founding the concrete structure on a smooth concrete base slab covered with plastic foil to reduce the adhesion between these parts.
- To investigate the properties of a joint sealed with a joint seal made of a copper sheet between walls and base slab cast at two separate occasions.

1.6 Purpose and scope of this report

The purpose of this report is to present the results from the work covered by the bullet points presented in Section 1.5. It is further the purpose of this report to present well based conclusions from the results of the performed studies and to formulate a programme for future studies in order to improve the understanding of the requirements for casting of full-scale concrete caissons in 2BMA.

1.7 Structure of this report

The report is divided into 12 chapters and 3 appendices with the following content:

Chapter 1: Chapter 1 presents a background to the work presented in this report. Here concrete prerequisites and requirements as well as short descriptions of the material and technology development programmes are found.

Chapter 2: Chapter 2 presents the work leading to the suggested design of the representative sections of the concrete caissons to be cast in the tunnel section TAS05. The work takes off in an analysis of the available space in TAS05 as well as of the restraint situation in a full scale caisson.

Chapter 3: Chapter 3 presents the instrumentation programme. Here the different sensors and their position in the concrete structure are presented.

Chapter 4: Chapter 4 presents the preparations in TAS05 prior to casting.

Chapter 5: Chapter 5 presents the casting of section 1 including all steps from formwork design through casting but also including post casting inspection and material investigations.

Chapter 6: Chapter 6 presents the casting of section 2 including all steps from formwork design through casting but also including post casting inspection and material investigations.

Chapter 7: Chapter 7 presents the results from the extended material investigation programme. This mainly comprises investigations of cores extracted from the concrete structure about 1 year after casting.

Chapter 8: Chapter 8 presents the results from the long-term monitoring programme of section 1.

Chapter 9: Chapter 9 presents the results from the long-term monitoring programme of section 2.

Chapter 10: Chapter 10 presents the results from the stress test in which the concrete structure was covered by a tarpaulin and exposed to an atmosphere with a low relative humidity.

Chapter 11: Chapter 11 presents a summary of the work presented in this report and the results are briefly discussed.

Chapter 12: Chapter 12 finally presents the conclusions from this work.

Appendix A: Appendix A presents an analysis of material parameters for the concrete, to be used in calculations of the risk for thermal cracks in future constructions.

Appendix B: Appendix B presents computation details for section 1.

Appendix C: Appendix C presents computation details for section 2.

2 Design of a representative section of a concrete caisson for test casting

In this chapter the design of the representative section of a concrete caisson to be cast in a side tunnel (TAS05) at Äspö Hard Rock Laboratory is described.

2.1 Background and aim

The 2BMA barriers should limit the hydraulic flow through the waste. The proposed design prescribes the use of unreinforced concrete and minimized amounts of cast-in steel components. Therefore, tie rods through the barrier are not permitted, regardless of their material composition and a suspended formwork system will instead be required. In order to minimize the risk of cracking, the base slab and walls shall be cast in one uninterrupted sequence. The design shall be able to withstand different types of loading during (i) the construction phase, (ii) the operating phase and finally (iii) after the sealing of the SFR, Section 1.3.2.

A limited test casting shall be performed underground using the proposed concrete mix design. Within the test a representative section incorporating critical design elements, e.g. walls, edges and rounded fillets, shall be cast. The study shall include parameters such as the properties of the concrete mix design as well as temperature development, deformations (short and long-term) and, if possible, stresses within the structure. The study of the long-term shrinkage of the structure is of special interest. Therefore, the test casting shall have a foundation similar to the full scale caisson.

2.2 Prerequisites

2.2.1 Location and dimensions of TAS05

TAS05 is situated in the TASP section of the tunnels at Äspö HRL, approximately 3 100 m from the entrance at a depth of about 420 m. The dimensions of TAS05 are approximately 16 m in length, 6 m in height and 4.5 m in width. When the work was initiated, TAS05 had been cleaned from all rock debris from the excavation work and solid rock was exposed on all sides. An overview of the area around TAS05 is shown in Figure 2-1.

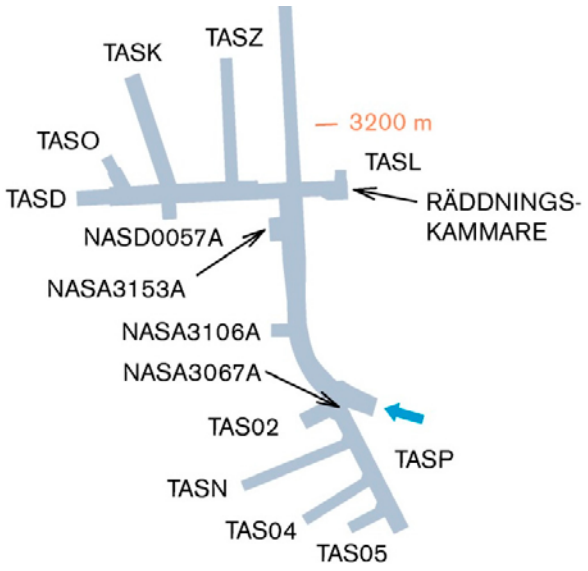

Figure 2-1. *The location of TAS05.*

2.2.2 Foundation

The reference design of the caisson structures in 2BMA states that the caisson shall be placed on a foundation of crushed rock levelled with gravel (SKB 2015). However, as stated in Section 1.4.1 one of the goals within this work is to investigate the possibility of reducing the degree of restraint between the caissons and the foundation by erecting the concrete structure on a smooth base slab provided with an adhesion reducing layer e.g. a plastic foil. For that reason a concrete base slab was cast in TAS05 as shown in Figure 2-2. Prior to casting, the slab was covered with a foil in order to reduce the degree of restraint between the base slab of the caisson and the foundation. For more details, see Chapter 4.

2.2.3 Available space after levelling and casting of foundation base slab

The reinforced concrete slab which is part of the foundation has the dimensions 15 x 4.05 x 0.5 m. The total height of the foundation was approximately 0.8 m. Therefore, the available height in TAS05 was about 5.2 m.

Further, when casting the concrete structures, allowance for formwork and required working space have to be considered. At least 1 m of free space has to be reserved in order to provide enough space for both the formwork and as an area in which to work. With regard to the actual cross section, this leaves, at best, an area of 2.5 x 3.5 m (w × h) as displayed in Figure 2-3 for the components. At the end of TAS05, 1.5 m of free space should be reserved, which gives a maximum available length of 13.5 m, see Figure 2-4.

Figure 2-2. *Levelling of TAS05 with a reinforced slab on the crushed rock.*

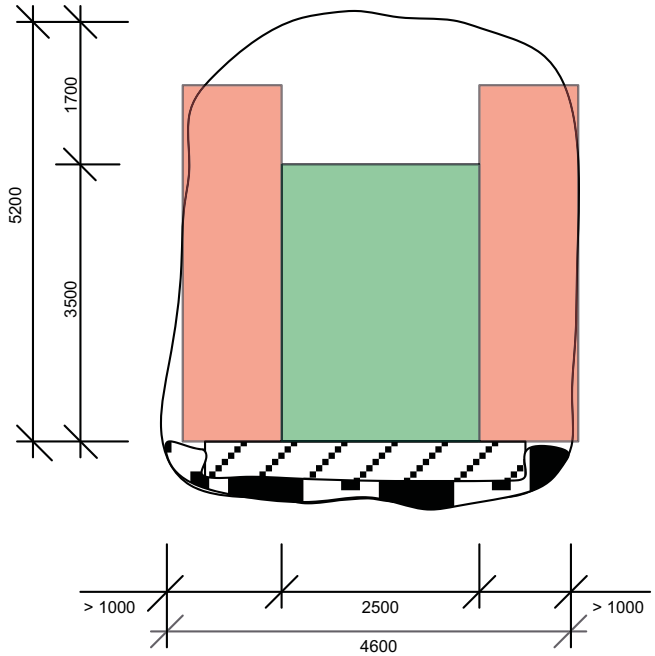

Figure 2-3. *Available space for casting of components (green) and required working space (red), cross section. All dimensions in mm.*

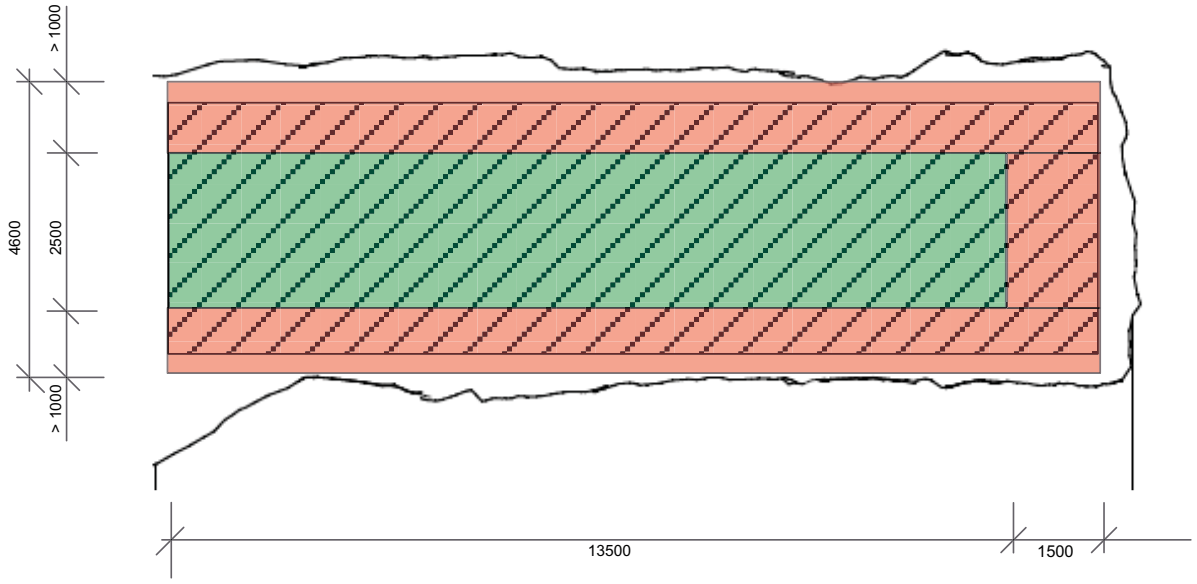

Figure 2-4. *Available space for casting of components (green) and required working space (red), section. All dimensions in mm.*

2.3 Formwork

As mentioned in the previous section only limited space is available in TAS05 which makes the use of lifting devices very difficult. The estimation of available space is therefore based on the assumption that the formwork will only occupy limited space. However, a suspended formwork, as required for the full scale casting according to the reference method occupies a considerable space and is difficult to install without proper lifting devices. Therefore, the use of a more traditional formwork system with tie rods made from composite material through the formwork was recommended here. Composite rods are preferred over steel rods since composite material has a heat transfer coefficient similar to concrete.

This is a deviation from the reference design but the advantages clearly outweigh the disadvantages. The use of tie rods will allow for larger components to be cast which will increase the similarity to the full scale caisson. The installation of the required sensors will be simplified when tie rods are available. Most importantly, the tie rods will not influence the behaviour of the components in any way with respect to temperature development, change of dimensions or change of humidity.

The major disadvantage is that a suspended formwork will not be tested in practice. However, since the dimensions of the components differ from the full scale caisson the representativeness from a technology point of view will be limited and the test of this type of suspended formwork therefore of less value.

In this work, the use of a lightweight framed formwork (manoeuvrable by hand) is recommended. Tie rods should consist of composite material (glass fibre or carbon fibre composite). The formwork should be designed for a formwork pressure of at least 40 kN/m^2. The design pressure is based on the assumption of a concrete with plastic consistency (not liquid) and that casting of the walls proceeds with about 0.5 m/h in height. Exact calculations need to be performed prior to formwork construction once the detailed properties of the concrete are known. Alternatively, the formwork could be designed to withstand the full hydrostatic pressure of the fresh concrete (72 kN/m^2).

2.4 Shape and dimensions of the test components

In order to compare the properties of a concrete structure erected according to the reference method (Section 1.2) and according to more conventional methods (Section 1.4.2) 2 different components are required. A corner section with one prolonged wall is considered as a desirable component for test casting, see Figure 2-5.

The use of unreinforced concrete stipulates the need to reduce stress peaks, likely to occur at e.g. corners. Therefore, the inner corner between walls shall be executed with a radius of at least 500 mm. The corner between wall and slab shall have a radius of at least 300 mm, see Figure 2-6. For further details, see Section 2.5.

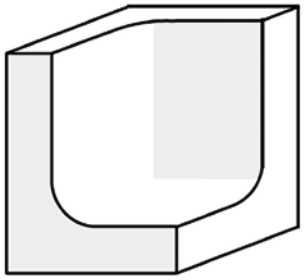

Figure 2-5. *Schematic design of a component for the test casting.*

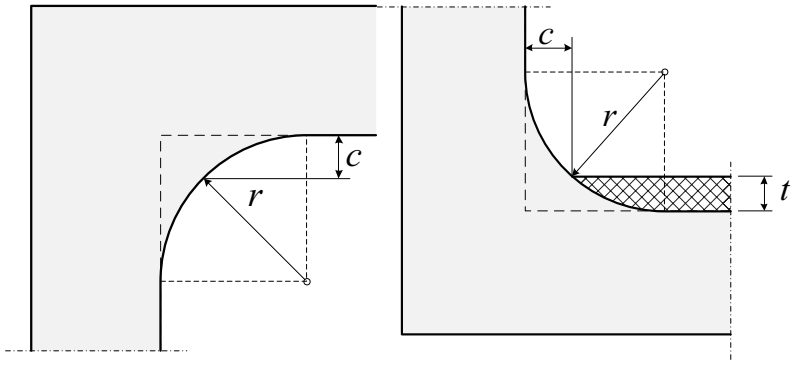

Figure 2-6. *Execution of fillets between walls with a radius of 500 mm (left) and between wall and base slab (radius 300 mm) (right). "t" is the thickness of a possible levelling casting to be cast in 2BMA.*

2.5 Design of a representative section of a concrete caisson

2.5.1 Dimensions and shape of components

The available space for the casting of the representative section of a concrete caisson was analysed in the previous section. There it was concluded that the maximum width available with regard to the construction phase is 2.5 m. However, the base slab of the components may be up to 0.5 m wider, Figure 2-7 and 2-8.

2.5.2 Joint seals

When casting section 2, joint seals shall be placed in the casting joint to the base slab. The joint seals shall be made of copper alloy and formed from long strips of copper sheets. In the wall, additional vertical "dummy" joint seals shall be placed vertically at both ends. The purpose of these is to test the installation process and the structural integrity of joint seals and concrete in such vertical joints. One part of the joint shall be equipped with a single joint seal and the other part with double as shown in Figure 2-9.

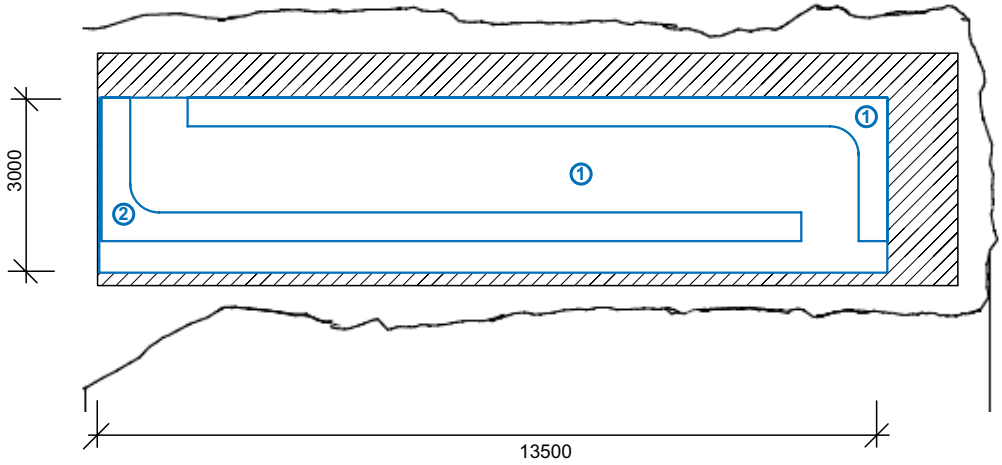

Figure 2-7. *Section of components 1 and 2 with a 3 m wide base slab. All dimensions in mm.*

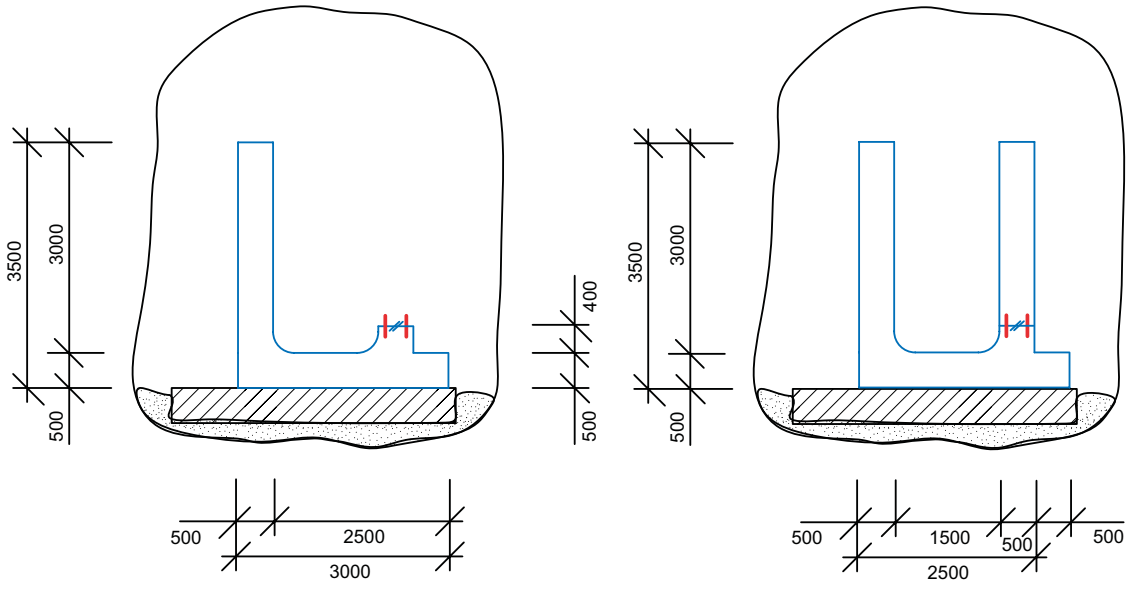

Figure 2-8. *Dimensions of components 1 and 2. The width of the base slab is 3 m. The red lines indicate the joint seals. All dimensions in mm.*

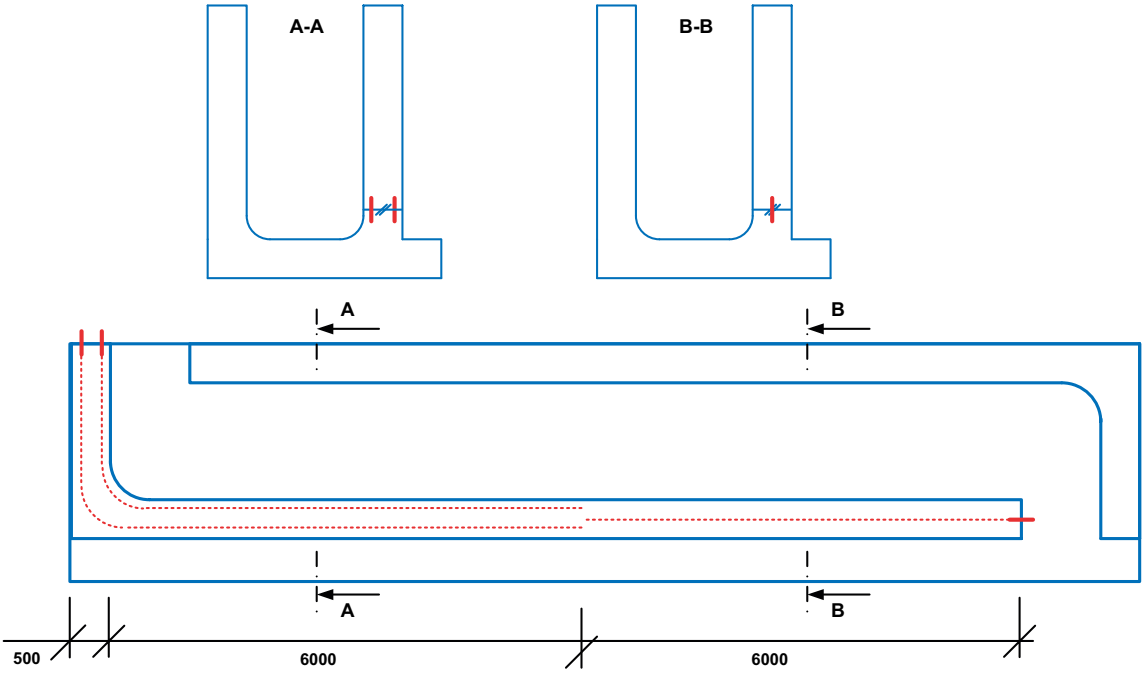

Figure 2-9. *Placement of joint seals in component no. 2. All dimensions in mm.*

2.5.3 Shape and position of casting joint and joint seals

After discussions it was late in the project decided to change the design of the joint between the base slab of section 1 and the wall of section 2. The new design is shown in the right hand illustration in Figure 2-10 and the original in the left. The main reason for this was to facilitate formwork construction and positioning of the joint seals.

As a consequence of this change, the position (height) of certain sensors in section 2 had to be adjusted and the new positions determined.

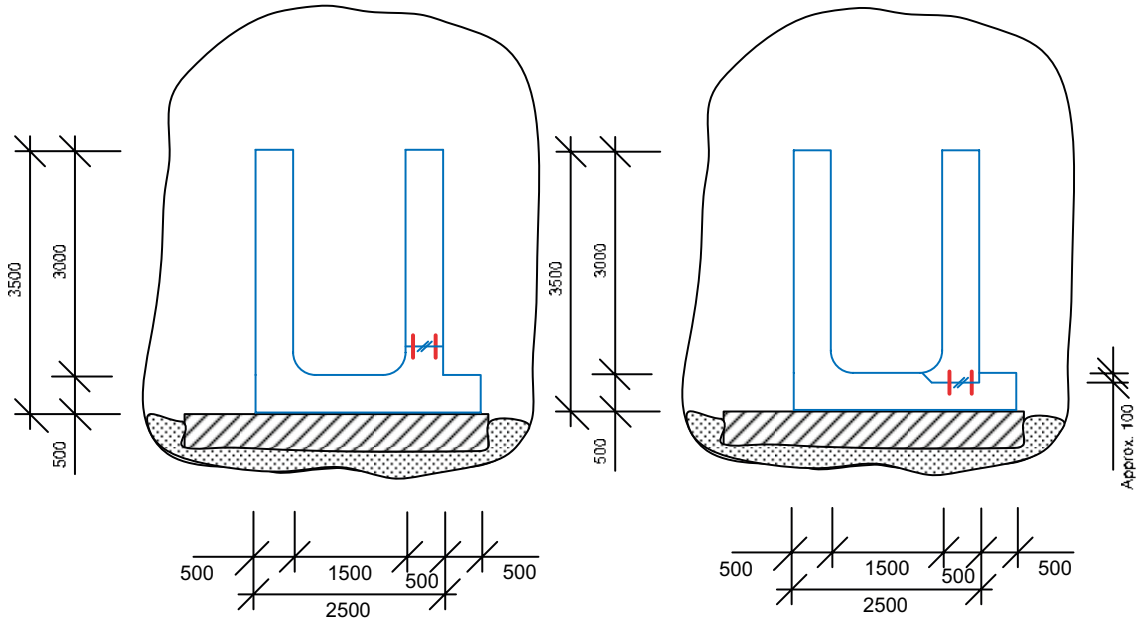

Figure 2-10. *Cross section of components 1 and 2 with a base slab (part of component 1) with a width of 3 m. The red lines indicate the joint seals. The left image illustrates the original design of the component whereas the right image shows the final design which was used for casting. All dimensions in mm.*

2.5.4 Restraint situation of the selected component

In this section calculations of the restraint situation for a number of components with different dimensions are presented and compared with the restraint situation for the full scale caisson.

In Figure 2-11 the calculated degree of restraint for the middle of a wall for different scale models of caissons are shown. The calculations show that the degree of restraint (for the scale models) increases with increasing length-height ratio. Figure 2-12 shows that the degree of restraint has its highest value close to the joint between the base slab and the wall and also that it is lower close to the ends of the component than closer to its central part.

The calculations behind the results presented in Figure 2-11 were based on geometries with a wider base slab (5 m) and a shorter wall segment on both ends. Therefore, the component suggested in Section 2.5.1 with a length of 12 m and a height of 3 m can be expected to experience a somewhat lower degree of restraint. This is due to the reduced base slab and only one "end wall". The difference will most likely be limited. In the analysis of the results from the test casting of the components, the actual degree of restraint for the components needs to be calculated.

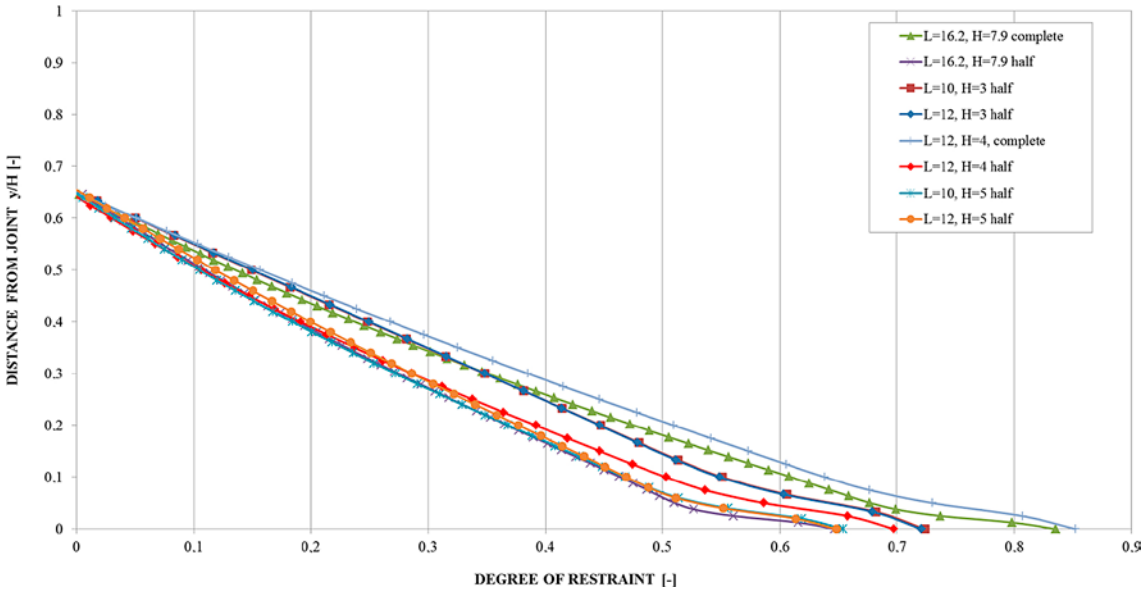

Figure 2-11. *Degree of restraint in the centre of the wall.*

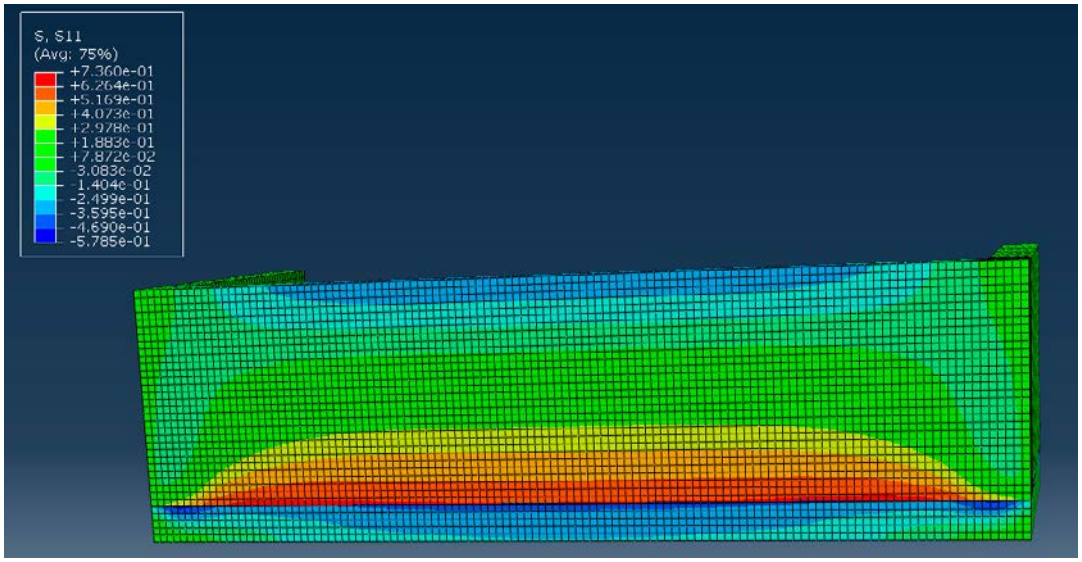

Figure 2-12. *Degree of restraint for a scale model, L = 12 m, H = 3 m and B = 5 m.*

3 Instrumentation

In this section the instrumentation programme is presented. The programme includes sensors for measuring internal strain, temperature, relative humidity and external dimensions. As a basis for the set-up, the analysis of the restraint situation presented in Section 2.5.4 was used.

3.1 Temperature

Temperature registration is usually done with commercially available ready-to-use sensors or simple thermocouples. The ready-to-use sensors are usually more accurate and designed to function for a long period of time. However, they are more costly and require more advanced and costly data acquisition devices. For the relatively simple purpose of logging the heat development of hardening concrete for approximately 2–3 weeks, thermocouples of type T (Cu-CuNi) have proven to be sufficient.

A total of 20 thermocouples positioned according to Figure 3-1 and 3-2 were used for monitoring the heat of hydration and the subsequent cooling of the concrete structure. For this purpose Pentronic P-24 (type k) temperature sensors were used.

Additionally temperature was also measured at the site of the strain gauges using the built in temperature sensors in these strain gauges; see Section 3.2.

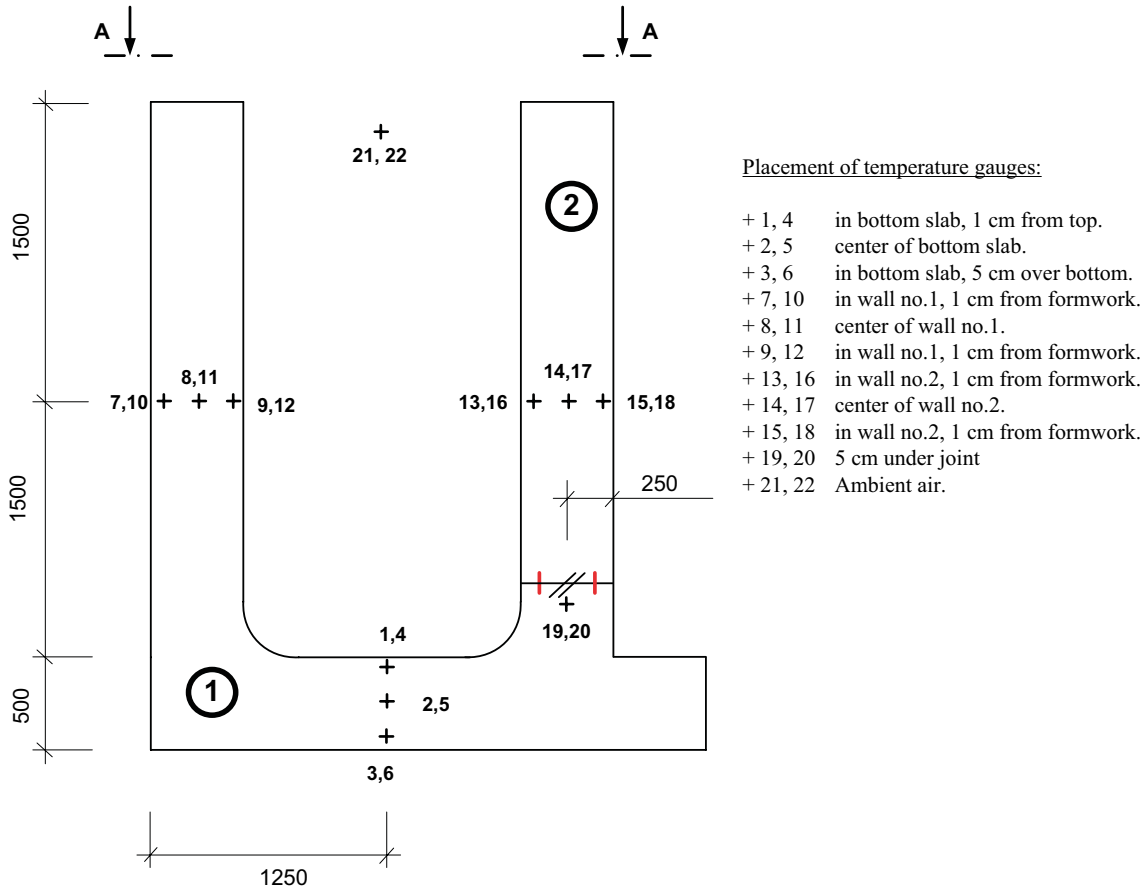

Figure 3-1. *Vertical placement of the temperature sensors.*

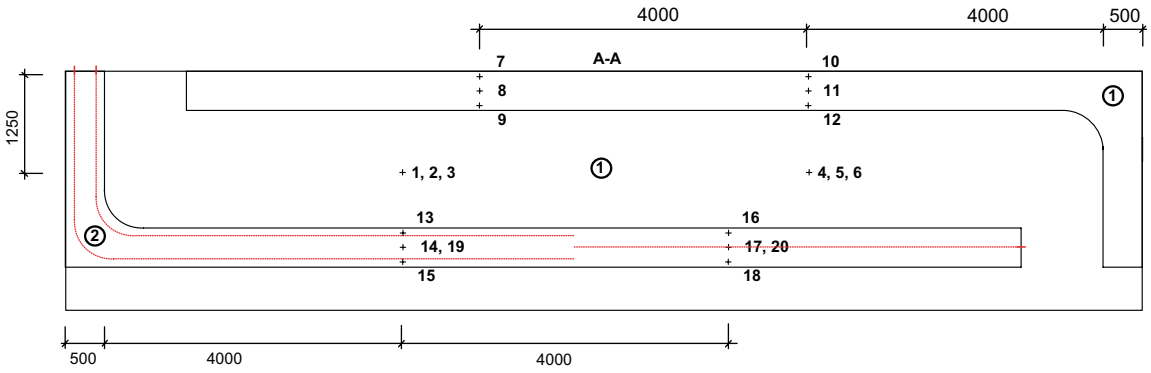

Figure 3-2. *Horizontal placement of the temperature sensors.*

3.2 Strain

In this work a combination of commercial (Section 3.2.1) and manufactured (Section 3.2.2) transducers was used in order to ensure redundancy. The commercial transducers were based on strain gauges which have proven to be reliable and provide results that are easy to analyse and correlate well with theoretical values.

3.2.1 Strain gauge transducer

This type of transducer works with strain gauges attached to a medium (usually some type of metal rod with attached end caps) and an outer sealing, see Figure 3-3. When the metal rod is subjected to forces, the strain gauge inside the transducer will deform and the resulting change in voltage can be related to the strain. The commonly used transducers typically have measuring lengths from 30 mm to 200 mm.

This type of sensor with a measuring length of 100 mm was used for the basic instrumentation of the dome plug in the domeplu experiments at Äspö in 2013, see Malm (2014).

In this work TML KM-100A and TML KM 200A commercial strain gauge transducers were used.

3.2.2 Manufactured strain transducers

Manufactured strain transducers are basically up-scaled commercial strain gauge transducers and have been successfully manufactured and installed in previous projects. These transducers have typical measuring lengths of 2 m. The longer measuring distance reduces the number of required channels for data recording and increases the probability of directly measuring "over" an eventual crack.

The basic setup of the transducer is simple. A strain gauge is attached to a metal bar with end caps. The metal bar is placed inside a tube (metal or plastic) for sealing off the strain gauge from the surrounding concrete and thus achieving a free strain length between the end caps. Manufactured strain transducers with a length of 2 m have been successfully used in projects with field measurements (Vogt et al. 2010). Figure 3-4 shows a manufactured strain transducer.

In this work TML (XY71-1.5/350) manufactured strain transducers were used.

Figure 3-3. *Strain gauge transducer.*

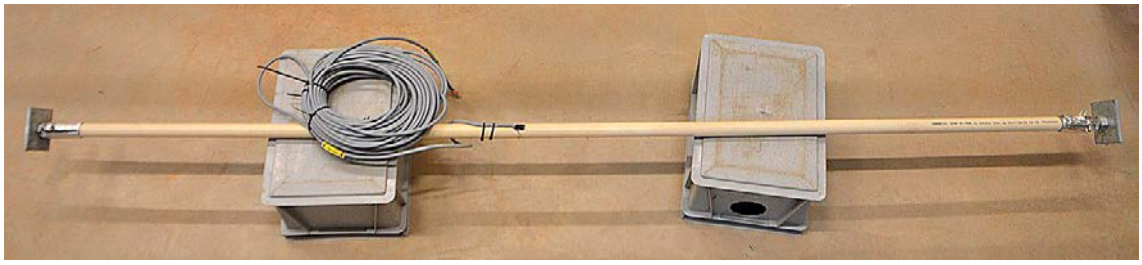

Figure 3-4. *Manufactured strain transducer with a length of 2.5 meters.*

3.2.3 Set-up

A total of 12 manufactured strain transducers, each with a length of 2 500 mm and 12 commercial strain gauges, each with a length of 100–200 mm, were used to monitor the internal strains in the components. The commercial strain transducers also included temperature registration. Figure 3-5 and 3-6 show the placement of the strain transducers.

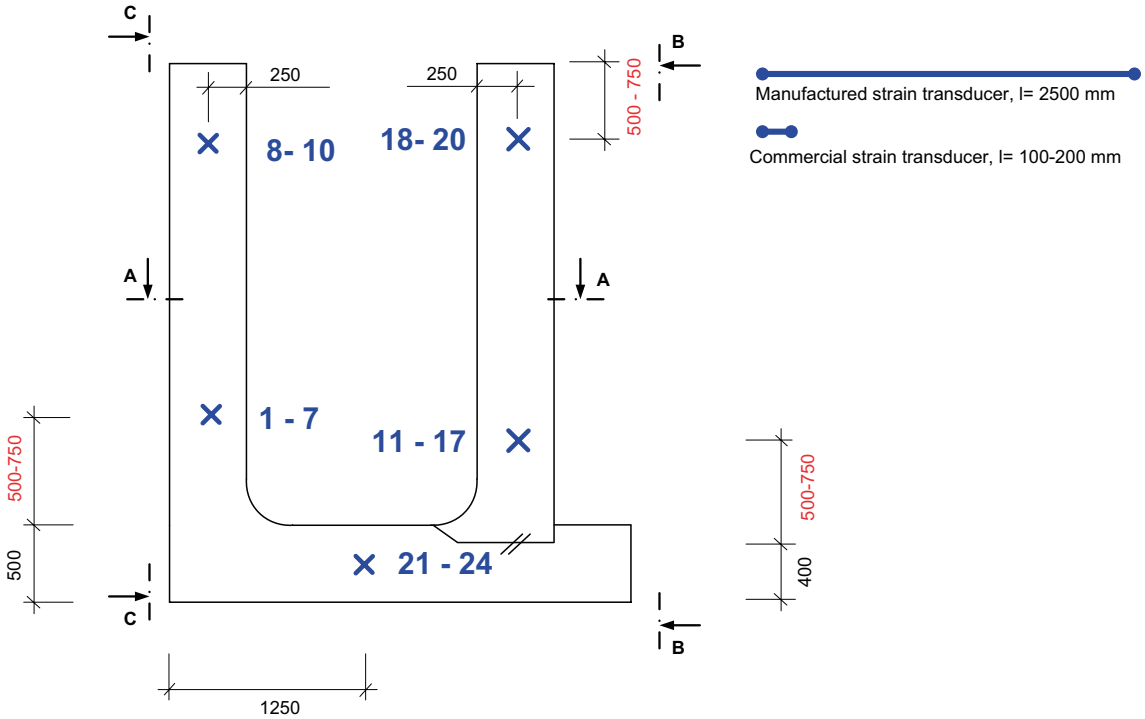

Figure 3-5. *Vertical placement of strain transducers.*

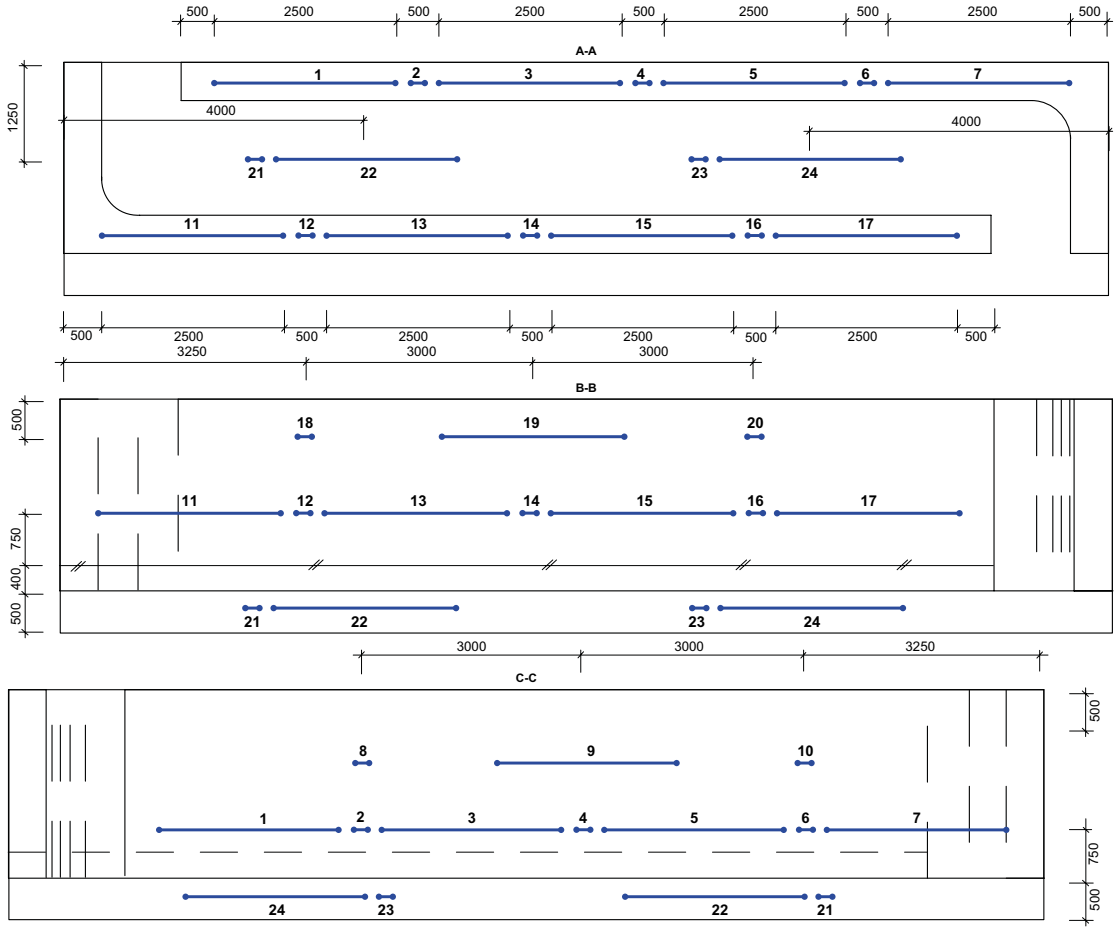

Figure 3-6. *Horizontal placement of strain transducers.*

3.3 External dimensions

The measurement of internal strains in the components was combined with external measurements of the dimensions of the components using external LVDT sensors (Linear Variable Differential Transformer). In TAS05, the LVDT sensors were attached directly to the adjacent rock. This was because it was judged unsuitable to attach the sensors to the foundation as it was rather recently cast and could shrink with time. A total of 8 LVDT sensors (HBM 1-WA/10MM-T), arranged as displayed in Figure 3-7 were used to monitor the external dimensions of the components. The sensors were installed after that the formwork had been removed.

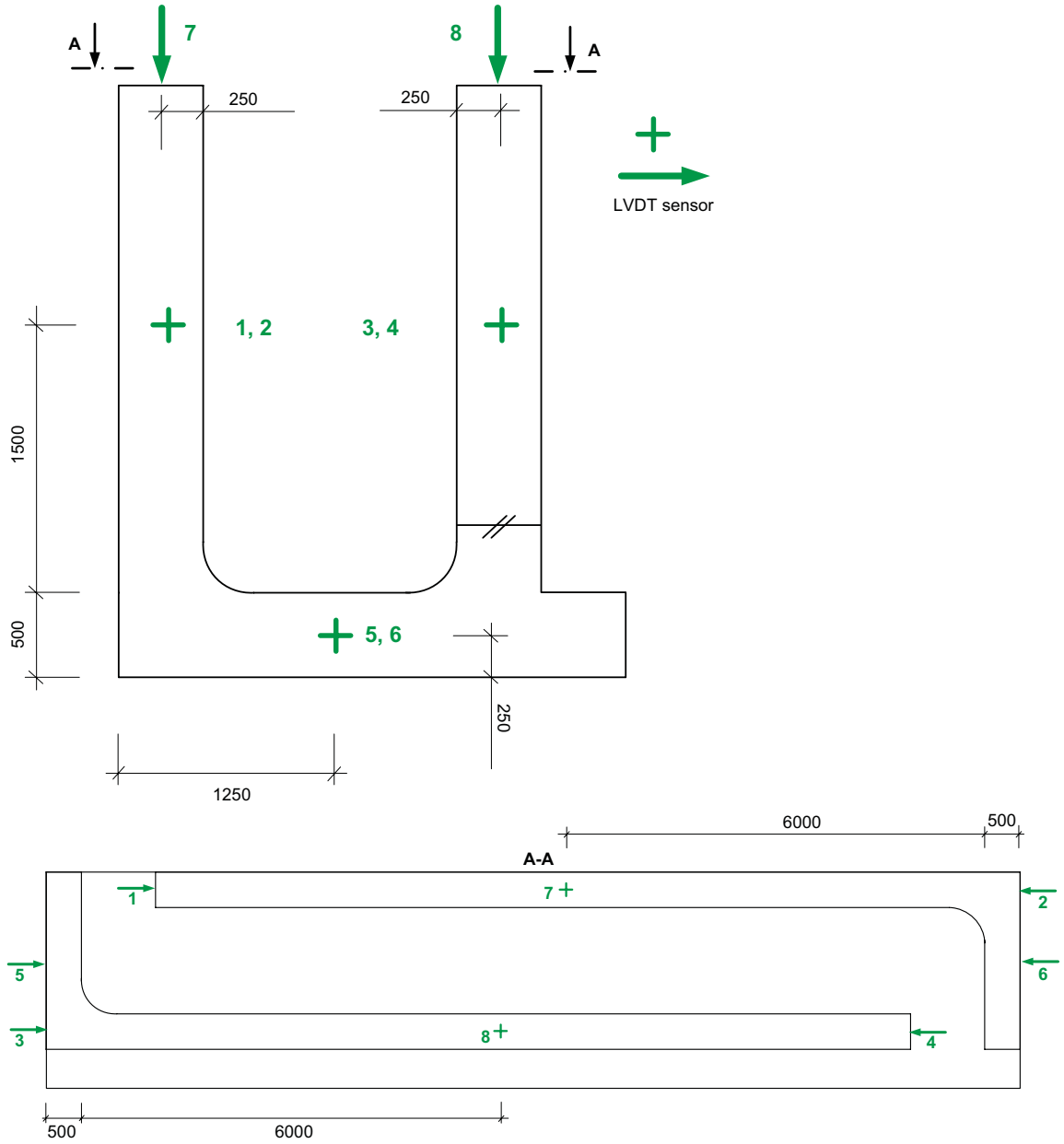

Figure 3-7. *Placement of LVDT sensors.*

3.4 RH sensors

Of special interest is the development of the relative humidity (RH) in the concrete and the environment. The shrinkage of the concrete can be related to the relative humidity inside the concrete and is one of the most important load independent deformation mechanisms which may lead to undesirable cracks.

Humidity sensors were installed in the walls and base slab of the components once curing of the concrete was finished. Additionally, the relative humidity of the ambient air was also monitored. A total of 5 humidity sensors (Vaisala HMP1109) positioned according to Figure 3-8 were installed after casting of section 1.

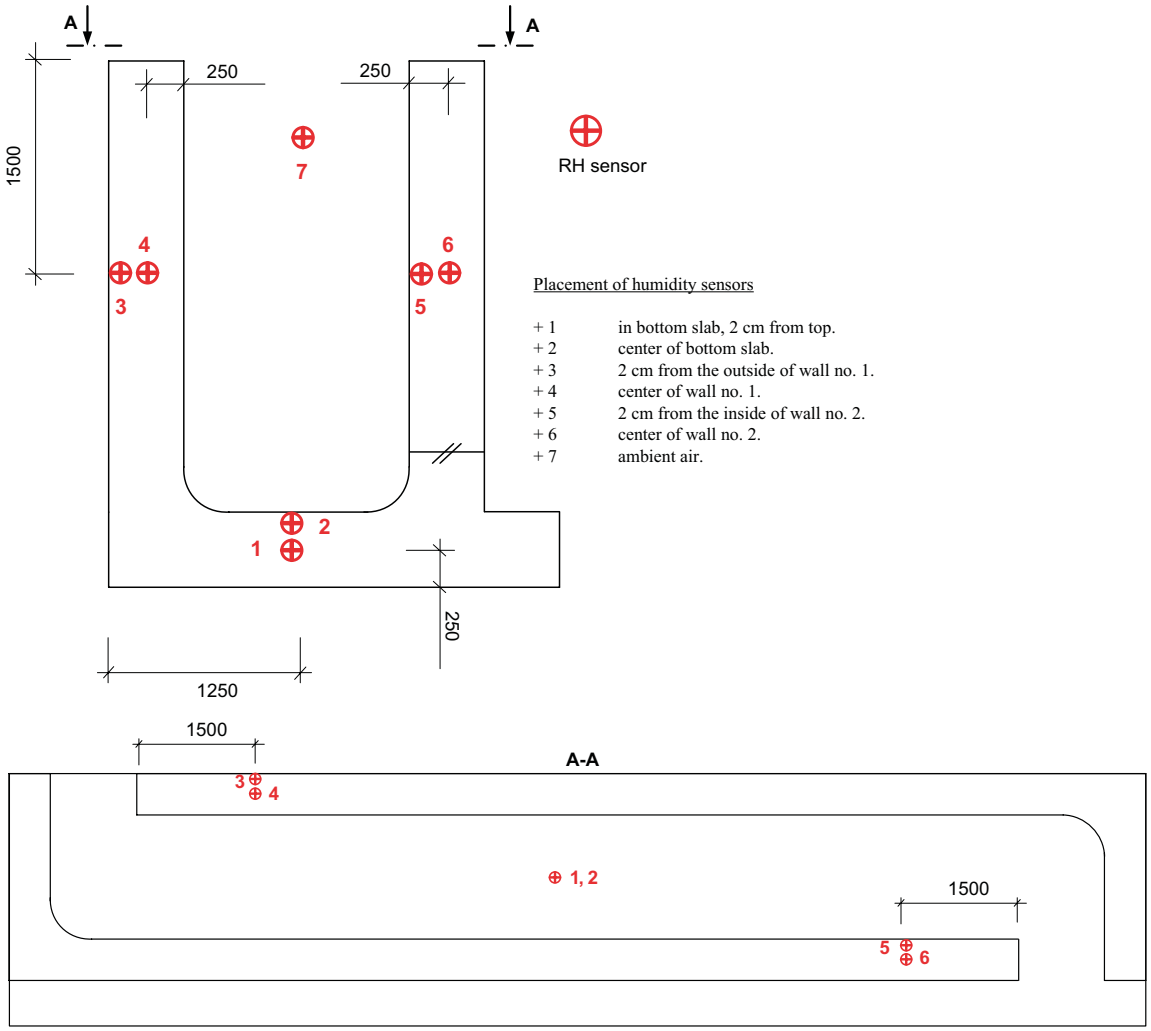

Figure 3-8. *Placement of humidity sensors according to the original plan.*

After casting of section 2 the following additional RH sensors were installed in both section 1 and section 2:

- Centre wall section 1
- Centre wall section 2
- Close to surface inside section 2
- Close to surface outside section 2
- Atmosphere between section 1 and 2
- Atmosphere in slit outside section 2

3.5 Formwork pressure

Formwork pressure was monitored using mechanical analogue load cells mounted on the tie rods of the form work, Figure 3-9. This was used only to follow the form work pressure during casting to ensure that form work pressure did not exceed the dimensioning loads.

Figure 3-9. *Load cell for control of formwork pressure during casting.*

3.6 Data acquisition and storage

A system for data acquisition and storage was installed, Figure 3-10. The installation was constructed to withstand the high humidity in the tunnel. Data could be remotely downloaded.

Figure 3-10. *All cables from the different sensors were collected into one bundle (left image) and signals were collected in the control cabinet (right image).*

3.7 Summary

In this chapter instrumentation programme for the test casting in TAS05 was outlined.

Temperatures, internal strains, external deformations, formwork pressure and humidity are of interest will be monitored. The type and number of sensors are summarized in Table 3-1.

The presented instrumentation is based on full redundancy (with exception of formwork pressure which is monitored while casting) and therefore quite comprehensive.

Table 3-1. Summary of sensors used in this work.

To be recorded	Number	Duration	Sensor type (example)
Temperature	20	Short term	Pentronic P-24 (type k)
Temperature at strain transducers	12	Long term	Included in the strain transducer
Internal strain	12	Long term	Manufactured strain gauge transducers
Internal strain	12	Long term	TML KM 100 with temperature registration
External deformation	8	Long term	HBM 1-WA/10MM T
Relative humidity	7	Long term	Vaisala HMP110 and Kimo

4 Preparations in TAS05

Prior to casting of the concrete structures, preparations were made in TAS05. These preparations comprised both means to ensure a healthy and safe working environment as well as preparation of the foundation on which the concrete structure should be erected.

4.1 Rock reinforcement and levelling of tunnel floor

The roof and walls of the tunnel had previously been reinforced by means of rock bolts. As an additional means to ensure a safe working environment the entire tunnel was covered with a net, Figure 4-1.

After excavation, TAS05 was cleaned from the debris caused by blasting leaving a bare but rather uneven rock floor. After the largest level differences in the tunnel floor were remedied, the floor was covered with a draining bed of macadam with a minimum thickness of about 100 mm. The bed was levelled and packed according to industry standard, Figure 4-1.

Figure 4-1. *TAS05 after rock reinforcement and levelling of the tunnel floor.*

4.2 Concrete slab

The concrete slab forms the foundation of the structures to be cast and its dimensions and amount of reinforcement was carefully determined.

4.2.1 Formwork construction and reinforcement

The formwork was made from simple wooden board kept in place by wooden studs fixed to the rock wall. A geo textile was placed on the drainage layer on which then the reinforcement was mounted. In Figure 4-2 all preparations for casting of the concrete slab have been made and the concrete hose laid out on the reinforcement bars.

4.2.2 Casting

The concrete slab (dimensions $15 \times 4 \times 0.5$ m) was cast from ordinary concrete class C45/55 according to the mix design presented in Table 4-1. In total about 30 m^3 of concrete was used.

Table 4-1. Nominal composition of the concrete used for casting the concrete slab.

Component	Amount (kg/m^3 concrete)
Gravel 0–8 mm	950
Stone 8–16 mm	800
Cement (Anläggningscement)	440
Water	180
Plasticiser Sika 26/50	2

4.2.3 Finishing

As a final step in the casting, the surface of the concrete slab was trowelled and then covered with a plastic foil to prevent evaporation and dehydration of the surface, Figure 4-4. The process began approximately 4 hours after the casting ended and lasted for a total of just over 4 hours. An extra tarpaulin was also set up to protect against water dripping from the tunnel roof, Figure 4-4.

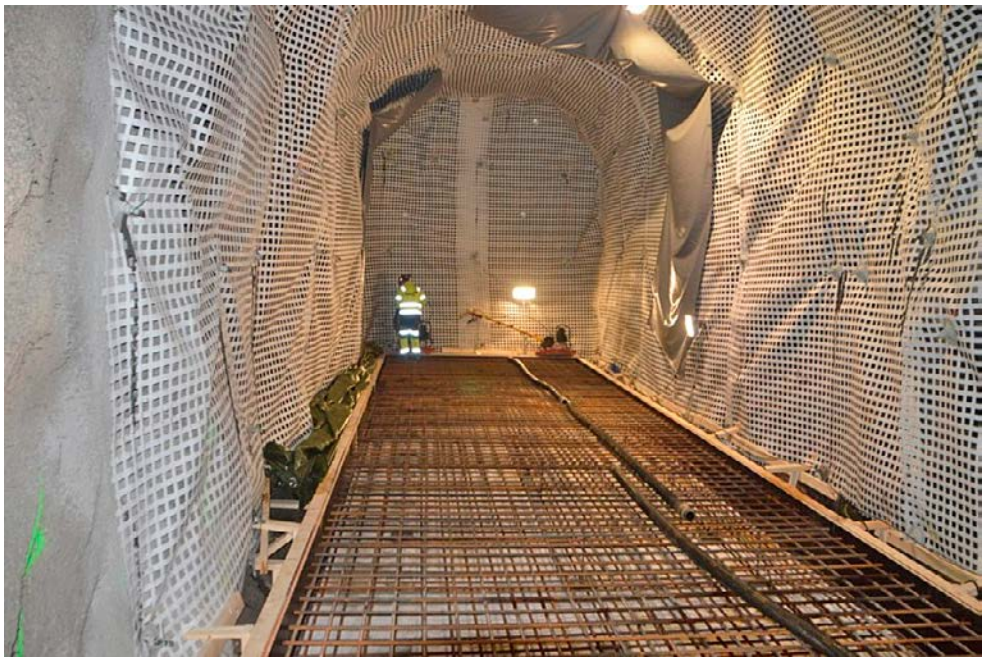

Figure 4-2. *All preparations have been made for casting of the concrete slab.*

Figure 4-3. *Casting of the concrete slab has started (left image) and casting and trowelling of the topmost layer (right image).*

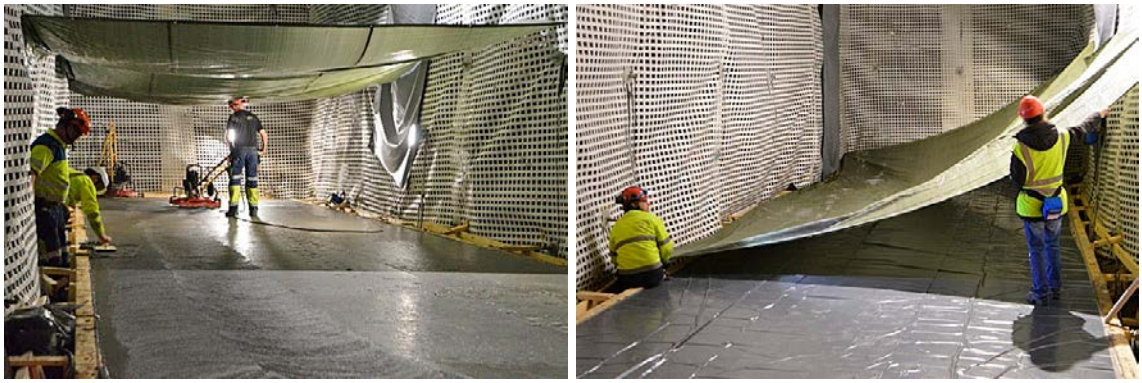

Figure 4-4. *Finishing of the concrete surface including surface trowelling and covering.*

4.3 Construction of a ramp

Finally, in order to facilitate easy access to the concrete slab during the following work, a ramp was constructed, Figure 4-5.

Figure 4-5. *All is ready for erecting the formwork for section 1.*

5 Preparations and casting of section 1

In this chapter the preparations made in TAS05 prior to casting as well as the casting and material analyses of the fresh and the hardened concrete are described. The base slab and walls of section 1 were cast in one continuous operation according to the reference design and method and no reinforcement was used. However, in order to facilitate the casting, the formwork was erected using traditional techniques rather than the suspended system required in the reference design as discussed in Section 1.4.3.

5.1 Formwork construction

The formwork (Doka system formwork) was erected on top of the foundation and fixed against the adjacent rock walls, Figure 5-1. In Figure 5-2 an example of the wooden structure made to shape the fillets is shown.

Figure 5-1. *The formwork under construction (left image) and ready just prior to casting (right image).*

Figure 5-2. *The part of the formwork used to shape the radius between the base slab and the wall of section 1.*

5.2 Installation of the sensors and signal control system

The sensors were mounted in the mould and fastened on the tie rods or other rods mounted in the mould for that sole purpose after the mould had been erected, Figure 5-3. From the sensors in the base slab, all cables were loosely laid on the adhesion reducing layer on top of the foundation and then pulled out through the formwork in a single bundle, Figure 5-4.

5.3 Adhesion reducing layer

In order to reduce the adhesion between the base slab of section 1 and the foundation, the concrete slab was covered with a reinforced plastic foil, Figure 5-4. This foil was put in place when the base slab was covered so that it would not be damaged during formwork construction.

Figure 5-3. *Sensors suspended on the system of rods inside the form work of the wall of section 1.*

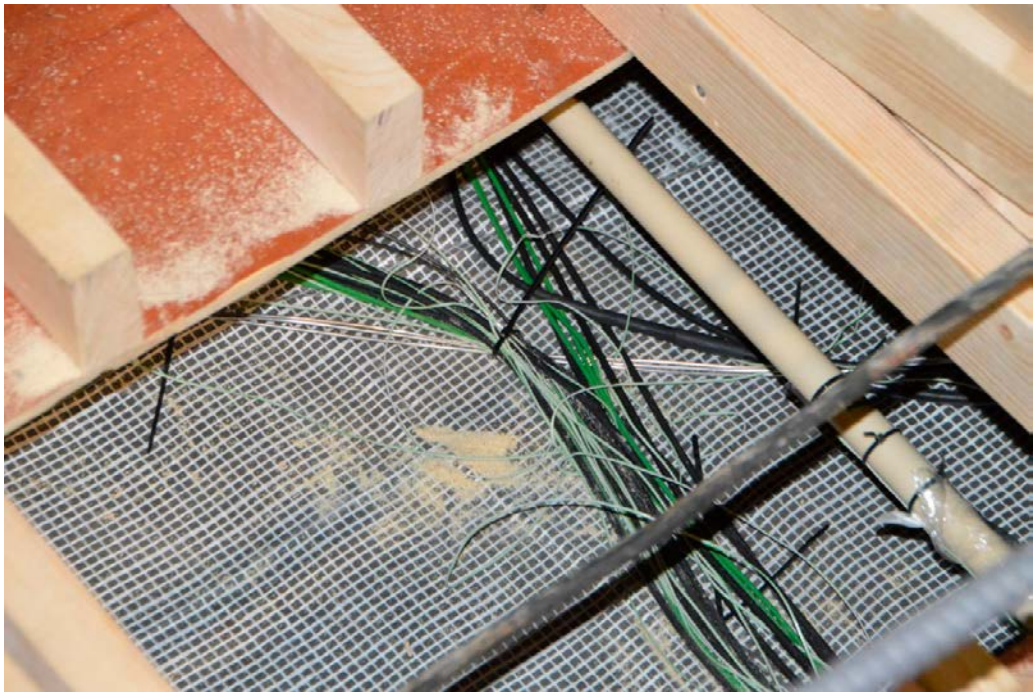

Figure 5-4. *Cables from the sensors placed on the plastic foil on top of the concrete slab. Note that the cables are loose and unprotected.*

5.4 Joint seals: manufacturing and mounting

The joint seals were manufactured from 1.5 mm thick and 300 mm wide copper sheets on site. The copper sheets were then welded together to the required length, Figure 5-5, and mounted in the formwork of section 1, Figure 5-6, according to the outline in Section 2.5.2.

Figure 5-5. *Welded copper sheets.*

Figure 5-6. *A copper joint seal is mounted in the radius between the two walls of section 1.*

5.5 Manufacturing and transport of the concrete

The concrete was manufactured at Swerock concrete production unit in Kalmar, Figure 5-7. In total, about 50 m^3 of concrete was mixed and transported to TAS05 in 7 concrete trucks.

5.5.1 Concrete components

The following components were used:

Cement

Degerhamn Anläggningscement, a CEM I product from Cementa was used.

Aggregates

4 different aggregate fractions were used, 0–4 mm, 4–8 mm, 8–16 mm and 16–22 mm. All fractions consisted of crushed granitic rock produced at a quarry near the concrete plant.

Filler materials

2 types of fillers were used to improve the workability of the concrete, OMYACARB 2GU and Myanit 10. OMYACARB 2GU is a pure limestone filler with an average grain size of 2 µm and Myanit 10 is a Dolomite product with an average grain size of about 10 µm.

Admixtures

3 different additives were used: Master Glenium Sky 558 (Superplasticiser), Master Sure 910 (Superplasticiser which also improves pump ability) and Master Set RT 401 (Retarder).

Figure 5-7. *Swerock concrete production plant in Kalmar which was used for mixing of the concrete.*

5.5.2 Concrete mix design, mixing and production quality control

The concrete was mixed in a standard production mixer with a capacity of 6 m^3. The concrete was mixed in batches of 2.33 or 2.67 m^3 depending on whether the total amount in the concrete truck was 7 or 8 m^3. The production was carried out according to standard routines and with the mix design according to Table 5-1. All materials except for Myanit 10 were added with the factory's dosing and weighing equipment. Myanite 10 was added manually from 20 kg sacks. Concrete properties from plant production control are shown in Table 5-2.

Table 5-1. Concrete mix design for section 1.

Component	Product/Supplier	Amount (kg/m^3)
Cement	Degerhamn Anläggningscement/Cementa AB	320
Filler (2 µm)	OMYACARB 2GU /OMYA	130
Filler (10 µm)	Myanit 10 /OMYA	33.3
Water*		156.8
Aggregates 16–22 mm	Crushed rock	393.3
Aggregates 8–16 mm	Crushed rock	425.7
Aggregates 4–8 mm	Crushed rock	92.0
Aggregates 0–4 mm	Crushed rock	840.9
Superplasticiser	Master Glenium Sky 558 / BASF	1.30
Superplasticiser	Master Sure 910 / BASF	1.70
Retarder	Master Set RT 401 / BASF	0.96

* A mixture of warm and cold water was used.

Table 5-2. Concrete properties from plant production control.

Truck #	Time	Temperature (°C)	Slump (mm)	Air content (%)
1	17:00	–	210	2.4
2	17:30	14.5	220	2.5
3	18:05	14.8	240	2.4
4	18:30	19.1	230	3.0
5	19:20	17.0	240	2.5
6	20:50	15.9	230	2.6
7	22:10	14.6	240	2.4

5.6 Quality control on site prior to casting and adjustments of concrete composition

The concrete slump was measured on arrival at the main tunnel TASP, Table 5-3. In cases where the concrete did not meet the requirements and the slump was too low, adjustments were made by adding water, superplasticiser or air entraining agent according to Table 5-4. In several cases water was added immediately upon arrival without any prior measurement of the slump. This was motivated by the fact that when the truck arrived, a rattling sound from the mixer indicated that the concrete was already very stiff and that setting had already started.

It should be noted that adding water is an emergency solution chosen here to be able to complete the casting. Water addition causes the concrete properties to change but when the option was to terminate the casting, this was considered the best option.

When the concrete was ready for pumping, small cubes were cast for later testing of compressive strength. Also, a larger cube from which drill cores were extracted for measurement of 6 months tensile and compressive strength was cast. This cube had the approximate dimensions $500 \times 500 \times 300$ mm (l × w × h).

Table 5-3. Concrete properties on arrival at TAS05.

Truck #	Time	Temperature (°C)	Slump (mm)	Air (%)	Comment
1	18:40	12	210	1,8	At 19:00, slump 210 with about 2 m^3 used.
2	19:30	16	100	Not measured	Pump stop. Adjustments according to Table 5-4. Rejected with about 2 m^3 left in the truck.
3	20:15	16	90	Not measured	Concrete too stiff. Rejected upon arrival. Cube K1 + K2.
4	21:00	Not measured	120	Not measured	Concrete very stiff upon arrival. Slump value after adjustments according to Table 5-4. Cube K3 + K4.
5	22:30	Not measured	70	Not measured	Adjustments according to Table 5-4. Cube K5+K6.
6	23:30	17	170	2,7	Adjustments according to Table 5-4. Cube K7+K8.
7	00:45	Not measured	150	Not measured	Casting of large cube and specimens for shrinkage measurements Cube K9–K12.

Table 5-4. Adjustments made to improve concrete workability.

Truck #	Water (amount added)	Additive (l/m^3 concrete)	Comment
1			No adjustments were made
2	50 litres added: slump 90 mm 20 litres added with 4m^3 left in truck	2 litres Master Glenium SKY558 0.5 litre Air entraining agent	Rejected with about 2 m^3 left in the truck.
3			Concrete too stiff. Rejected upon arrival.
4	A total of 160 litres added	2 litres Master Glenium SKY558.	Concrete very stiff upon arrival.
5	A total of 120 litres added upon arrival		
6	A total of 140 litres added upon arrival	2 litres Master Glenium SKY558	
7	A total of 120 litres added upon arrival. (slump:150 mm)		

Figure 5-8. *A typical example of a stiff concrete from one of the concrete trucks prior to adjustments.*

5.7 Casting

The casting process was severely influenced by that the concrete in all trucks was very stiff and that hydration already had started. Due to this, a lot of time was spent on initially trying to pump the concrete and later to make adjustments and improve workability.

The fact that the transport time from the concrete production plant was close to 90 minutes also meant that many trucks were already on their way once problems were encountered. For that reason the possibility to make adjustments of the concrete composition or changes in the schedule for delivery were not immediately possible

5.7.1 Base slab

Due to limited experience of large scale castings using the type of concrete used for casting of section 1 it was decided that the formwork of the base slab should be completely covered with a lid. The motivation for this was the identified risk that high pressures from the concrete in the wall could push the concrete out of the mould in the case the concrete in the base slab had not stiffened sufficiently to counteract this pressure. Covering the mould of the base slab with a securely fastened lid was considered the best option to ensure that the concrete would stay in the mould. Filling the base slab mould and vibrating the concrete was done through openings which could be closed and secured, Figure 5-9.

Immediately when casting commenced it was noted that the concrete did not flow in the mould as expected and large efforts had to be put on vibration already at this stage. It was also found that the stiff concrete moved around the cables from the sensor system; see Figure 5-4, which threatened the function of the sensor system.

For those reasons, the casting of the base slab was very time consuming. This caused further delays and concrete trucks had to wait for unacceptable long periods of time for delivery. As a consequence, the concrete started to set due to the delays which caused further needs for adjustments and slow delivery into the mould. For that reason it was finally decided to terminate the casting of the base slab just before the mould was completely filled in order not to compromise the entire casting and instead focus on casting the walls.

5.7.2 Walls

Casting of the walls of section 1 was by no means effortless but still less troublesome than casting of the base slab, Figure 5-10. The main difference was that the formwork of the walls was completely open and that gravity worked in the favour of the casting team. Still, the delays caused during the casting of the base slab resulted in that the concrete from the first few trucks delivered to the walls was very stiff. For that reason, large efforts had to be made by the casting team in order to ensure a dense and homogeneous concrete without the formation of unintended joints in the structure.

Figure 5-9. *Casting of the base slab.*

Figure 5-10. *Casting of the walls of section 1 and vibrating the concrete.*

5.8 Visual inspection immediately after demoulding

5.8.1 Overview

Immediately after demoulding, an inspection was carried out where the result of the casting was investigated. The focus was on surface smoothness, occurrence of air blisters or other surface imperfections, adhesion to joint seals and finally mould filling where the main focus was on mould filling in the base slab. An overview image is shown in Figure 5-11.

As shown in Figure 5-11, section 1 has the expected shape with joint seals at the location where the wall to section 2 is to be erected. At first glance the wall looks fine while the base slab is rough and very uneven.

Figure 5-11. *Section 1 just after disassembling of the formwork.*

5.8.2 Base slab

As shown in Figure 5-12, full form filling of the base slab has not been obtained. This is explained by the fast stiffening of the concrete during casting of the base slab. For a more detailed discussion of the problems encountered during this work, please refer to Section 5.7.1.

5.8.3 Walls and fillets

The mould filling in the walls and fillets was considerably better than the base slab and the surfaces were smooth with only a few very small imperfections, Figure 5-13.

Figure 5-12. *Images showing details of different types of imperfections in the base slab.*

Figure 5-13. *The surface of the walls were smooth and only a very few imperfections were detected. Also, the concrete was dense and homogeneous in spite of the encountered problems.*

Figure 5-14. *Image showing the complete filing of the fillet between the wall and the base slab of section 1. However, in this image it is also shown that the concrete has not entirely covered the surface of the base slab due to low mobility.*

5.8.4 Joint seals

Figure 5-15 right image shows that the filling between two parallel joint seals is good. Certainly, some imperfections are noted, but it could have been significantly worse considering the problems that occurred during casting. The holes and dikes seen in the left-hand image cannot be considered as an effect of the joint seals but are due to the abandonment of this part of the mould as the entire casting was compromised due to the concrete's fast stiffening.

As shown in the left image in Figure 5-16 the connection between joint seal and concrete was good and no gaps were noted. In addition, the right picture in Figure 5-16 shows that the adhesion was strong enough to withstand the forces occurring during demoulding.

Figure 5-15. *The joint seal mounted in the base slab at the position of the future section 2 of the concrete structure.*

Figure 5-16. Images showing the adhesion between the concrete and the joint seal.

5.9 Material properties

5.9.1 Compressive strength

28 days compressive strength

The 28 days compressive strength was measured on the cubes made from concrete from 5 of the concrete trucks, Table 5-5. The compressive strength varied between 45.0 and 54.5 MPa with an average of 49.0 MPa, i.e. just below the 90 days requirement of 50 MPa.

Table 5-5. 28 days compressive strength of concrete from trucks 3-7.

Specimen	Truck	Weight (g)	Weight (g)	Density (kg/m$^{3)}$	Density (kg/m$^{3)}$)	Force (kN)	Compressive strength (Mpa)
K1	3	8 102		2 401		1 226	54.5
K2	3	8 078		2 393		1 213	53.9
K3	4	8 044		2 383		1 010	44.9
K4	4	7 987		2 367		1 012	45.0
K5*	5	8 239	4 789	2 441	2 388	1 104	49.1
K6	5	8 227		2 438		1 114	49.5
K7	6	8 067		2 390		1 048	46.6
K8	6	8 166		2 420		1 069	47.5
K9	7	8 176		2 423		1 137	50.5
K10	7	8 168		2 420		1 093	48.6
K11*	7	8 009	4 655	2 373	2 388	1 082	48.1
K12	7	8 130		2 409		1 107	49.2

* The dimensions of cubes K5 and K11 were outside the requirements for this method. Instead the density calculations were based of the weight of the cube immersed in water.

6 months compressive strength

6 months compressive strength of the concrete was measured on ∅ 100 mm cores drilled from the small cube made from concrete from truck #7, Figure 5-17. The results are shown in Table 5-6.

From Table 5-6, the 6 months average compressive strength is 67.7 MPa. This exceeds by a large margin the requirement on a 90 days compressive strength of 50 MPa.

Table 5-6. 6 months compressive strength for cores from the small cube shown in Figure 5-17.

Core	Weight (g)	Density (kg/m^3)	Force (kN)	Compressive strength (Mpa)
1	1 833	2 360	527.2	67.0
2	1 852	2 360	527.6	67.2
5	1 821	2 360	539	68.4
8	1 822	2 340	529.9	67.3
9	1 820	2 360	540.6	68.6

Figure 5-17. *The small cube cast from concrete from truck #7 after drilling of cores for testing of compressive and tensile strength. Numbers refer to specimens numbers in Table 5-6 and 5-7.*

5.9.2 Tensile strength

6 months tensile strength of the concrete was measured using ∅ 100 mm cores drilled from the small cube made from concrete from truck #7, Figure 5-17. The results are shown in Table 5-7.

Table 5-7. 6 months tensile strength for cores from the small cube shown in Figure 5-17.

Core	∅ (mm)	L (mm)	Weight (g)	Force (kN)	Tensile strength (Mpa)
1	100	197.5	3684	13.58	1.73
2	100	200.5	3740	20.43	2.60
5	100	199.0	3716	19.26	2.45
8	100	200.1	3717	25.17	3.20
9	100	202.8	3773	25.11	3.20

As shown in Table 5-7, tensile strength varies around the average (2.64 MPa) with a standard deviation of 0.55 MPa. The values can be compared with the 2.5 MPa requirement, but testing of more samples would have been useful for obtaining a better statistics. Note that for tests 1, 5 and 9, fracturing has occurred partially very close to or in the glue between metal plate and concrete sample, Figure 5-18. For that reason the reliability of these measurements might be slightly lower than for samples 2 and 8 where fracturing occurred further into the specimen. Detailed enlargements of the fracture surfaces are shown in Figure 5-19.

Figure 5-18. *Cores used for measurements of tensile strength after testing.*

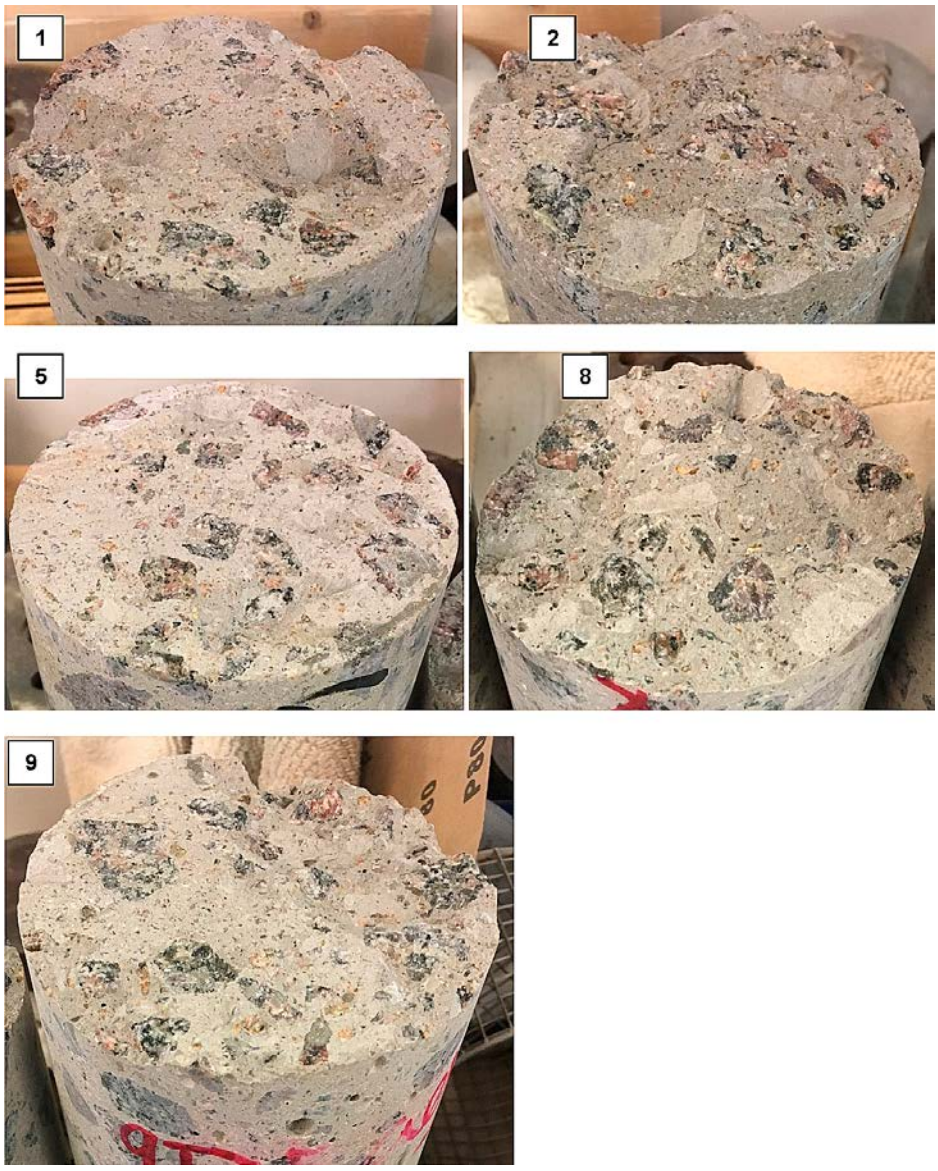

Figure 5-19. *Enlargments of fracture surfaces from the specimens used for measuring the tensile strength of the concrete.*

5.9.3 Shrinkage

The casting of the specimens for shrinkage measurements is shown in Figure 5-20. Results from shrinkage measurements according to SIS (2000) and for sealed samples where dehydration shrinkage was prevented are presented in Figure 5-21. Concrete from truck # 7 was used for casting of the specimens.

As shown in Figure 5-21, drying shrinkage represents the dominant part of the total shrinkage of the concrete. This would mean that the appearance of cracks in 2BMA can be significantly limited by choosing a concrete-favourable climate with a high humidity or protecting the concrete structure from drying-out during the operational period. This will, however, be countered by the fact that other installations can benefit from a dry climate.

Figure 5-20. *Casting of specimens for shrinkage measurements.*

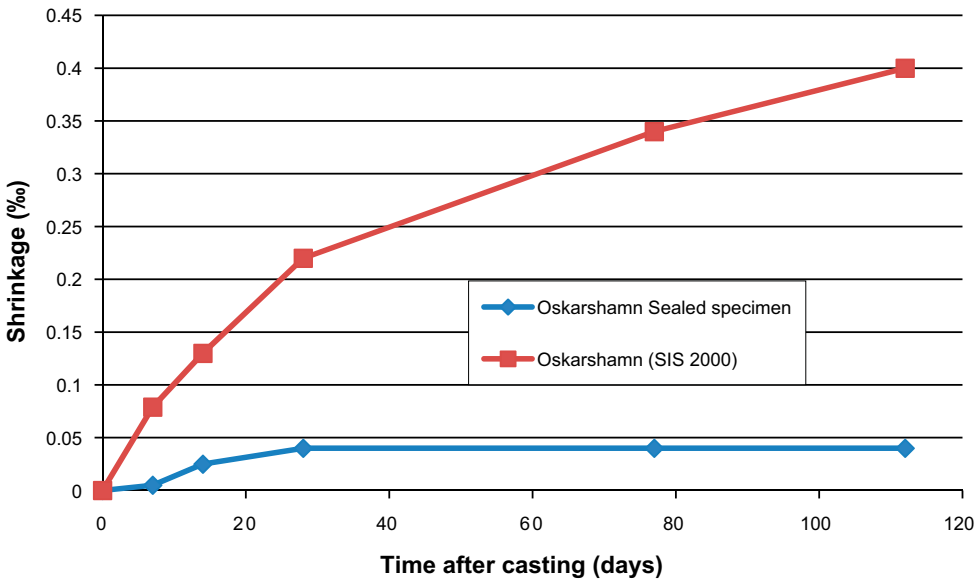

Figure 5-21. *Results from shrinkage measurements (SIS 2000) and sealed specimens.*

5.10 Casting of section 1: Summary

In this section the most important experiences from the casting of section 1 are presented (Section 5.10.1) as well as a summary of the material properties, Section 5.10.2.

5.10.1 Construction

Formwork

The formwork was designed for a high hydrostatic pressure from the fresh concrete due to that the understanding of the concrete hardening properties was not completely known. For that reason, also the formwork of the base slab was covered with a lid with closable hatches for filling of the mould with concrete and vibration.

The most important experience from this work was that the use of a lid with closable hatches for the base slab in combination with a very stiff concrete caused many problems and considerably delayed the casting process. For that reason an open formwork also for the base slab would have been beneficial for the casting process given the properties of the concrete used here. However, with the concrete used for casting of section 2 the lid would on the other hand have been crucial for a successful casting, see Section 6.6.

Monitoring system

Installation of the sensors was made after construction of the formwork and was successful. The main issue with the monitoring system was that the cables between the sensors and the control cabinet were not securely fastened. Due to that, the cables were moved around by the fresh concrete during casting and only thanks to skilful operation from the workers only one of the sensors was lost. To avoid this in future experiments, the cables must be securely fastened prior to casting.

Concrete production and transport

Concrete production did not face any major obstacles and even though some manual handling of one of the limestone fillers was required all other materials were handled through the plants standard production control system. Also concrete transport worked well.

However, due to the long transport times, production and transport could not respond fast enough to the required change of schedule caused by the delays during casting of the base slab.

With a mobile concrete production plant placed just at the entrance to the tunnel, response time would have been much shorter and the effect of the early delays significantly mitigated.

Composition and properties of the fresh concrete

The quality control at the concrete production plant showed that the properties of the fresh concrete were according to requirements and also according to previous experience from tests at a production plant (Lagerblad et al. 2017).

However, at production some warm water was added to the concrete mix. This was motivated by the low outside temperature and that the concrete was expected to cool during transport. As the chemical reactions in the concrete are temperature dependent a low temperature was expected to slow down the hydration and setting of the concrete. As a very slow setting of the concrete could give rise to very high formwork pressures, means to counteract this was decided to be taken, thus increasing the temperature of the mixing water in the concrete.

However, as was noticed here, the warm mixing water in combination with the use of the limestone filler and insufficient amounts of retarder caused the concrete to set unexpectedly early. Further, also the setting proceeded at a higher rate than previously experienced, causing the problems reported in Section 5.7.

With these experiences in mind the use of warm mixing water should be avoided in future production scale testing when this concrete is used. Also, to further reduce the rate of the hydration process a larger amount of retarder should be used during longer transports. For an investigation on the influence of temperature and lime-stone filler on concrete hydration, please refer to Lagerblad et al. (2017, Appendix A).

5.10.2 Properties of the hardened concrete

The properties of the hardened concrete were studied using several methods and the following results obtained:

- The compressive strength of the concrete was measured on cubes which were manufactured in connection with casting of section 1. The 28 day compressive strength varied between 45–55 MPa, which can be compared to the 90 day 50 MPa requirement. After six months the compressive strength had increased to almost 70 MPa with a very low spread.
- The tensile strength of the concrete was measured on cores drilled from a small cube which was made in connection with casting of section 1. The average tensile strength was 2.64 MPa, but the spread was quite large with a standard deviation of 0.55 MPa. These results, however, are associated with some uncertainties because fracturing has occurred partially in or very close to the glue between concrete samples and metal plate.
- Concrete shrinkage was measured according to SIS (2000) where samples were stored in a climate room with RH 50 % and on sealed samples where dehydration was prevented. After 112 days, shrinkage was 0.4 ‰ and 0.04 ‰ respectively for these methods. This indicates that drying shrinkage is the dominant shrinkage process.

6 Preparations and casting of section 2

In this chapter the preparations made in TAS05 prior to casting of section 2 as well as the casting and material analyses of the fresh and the hardened concrete are described.

6.1 Formwork construction

The formwork (Doka system formwork) was erected on top of the base slab of section 1 and fixed against the adjacent rock walls and floor, Figure 6-1. Also in section 2 tie rods were accepted, both to ensure the stability of the formwork but the tie rods were also used for suspension of the sensor system, including cables and sensors.

6.2 Installation of the sensors and signal control system

The sensors were mounted in the formwork according to principles used for section 1, Figure 6-2. See Chapter 3 for details on the sensors used and their respective positions.

Figure 6-1. *The formwork just before start of casting.*

Figure 6-2. *Sensor suspended on the system of rods inside the formwork of the wall of section 2.*

6.3 Joint seals

Single or double vertical joint seals were placed in both ends of section 2 as shown in Figure 2-9. For details on material and manufacturing, see Section 5.4.

The purpose of these vertical joint seals was to serve as input to a future decision on method for construction of the caissons and in particular whether it would be possible to erect the walls one by one with joint seals sealing the joints between the individual walls.

6.4 Manufacturing and transport of the concrete

6.4.1 Concrete components

The same concrete components were used as in section 1. See Section 5.5.1 for details.

6.4.2 Concrete mix design, mixing and production quality control

The concrete was produced in the same plant and according to the same procedures as for section 1. See Section 5.5.2 for details. Compared with the concrete used in section 1, the amount of retarder was increased from 0.96 to 4.16 kg/m^3 fresh concrete. No other adjustments were made. The mix design is shown in Table 6-1 and the properties prior to transport are shown in Table 6-2.

Table 6-1. Concrete mix design for section 2.

Component	Product /Supplier	Amount (kg/m^3)
Cement	Degerhamn Anläggningscement / Cementa AB	320
Filler 2 µm	OMYACARB 2GU / OMYA	130
Filler 10 µm	Myanit 10 / OMYA	33.3
Water		156.8
Aggregates 16–22 mm	Crushed rock	393.3
Aggregates 8–16 mm	Crushed rock	425.7
Aggregates 4–8 mm	Crushed rock	92.0
Aggregates 0–4 mm	Crushed rock	840.9
Superplasticiser	MasterGlenium Sky 558 /BASF	1.30
Superplasticiser	Master Sure 910 /BASF	1.70
Retarder	Master Set RT 401 /BASF	4.16*

* Note the large increase in the amount of retarder compared to section 1.

Table 6-2. Concrete properties from production plant control.

Truck #	Time	Temperature (°C)	Slump (mm)
1	16:20	15.9	180
2	17:15	15.6	200
3	18:05	15.4	190
4	19:00	15.3	180

6.5 Quality control on site prior to casting and adjustments of concrete composition

On arrival at the main tunnel, TASP, the concrete slump, temperature and air content were measured, Table 6-3. Also, small cubes were cast for later testing of compressive strength as well as a larger cube from which cores for later studies of 6 month tensile and compressive strength were drilled, Figure 6-9. This cube had the approximate dimensions 500 × 500 × 300 mm (l × w × h).

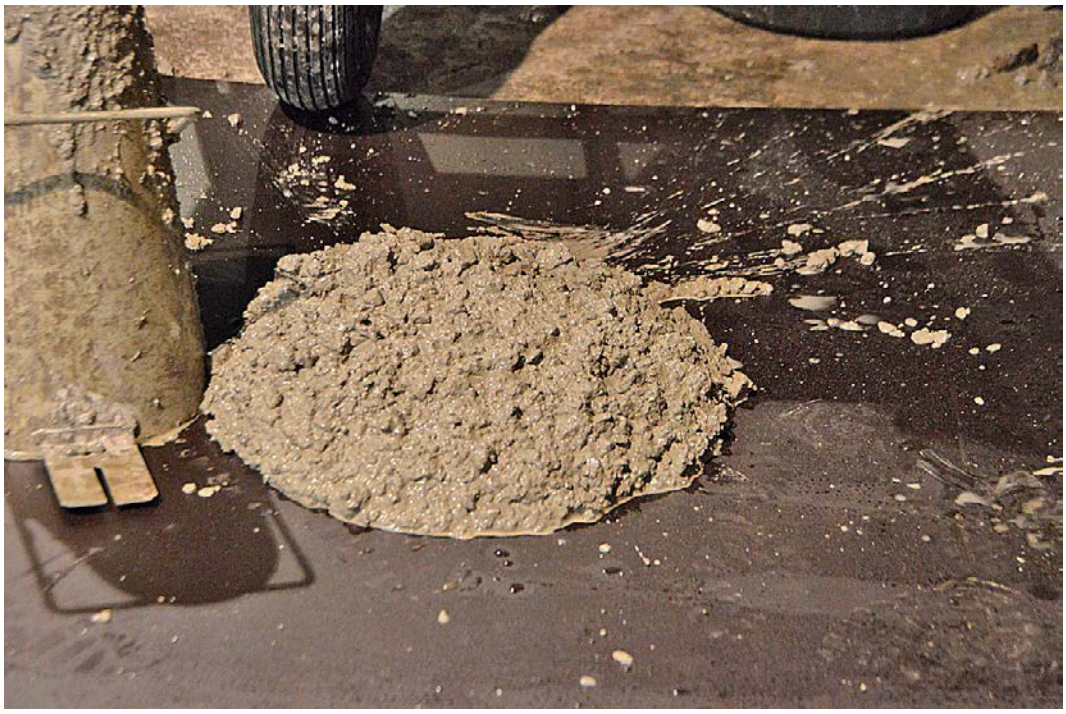

Figure 6-3. *A typical example the concrete used for casting of section 2.*

The properties of the fresh concrete were for all trucks according to requirements and no adjustments were made before casting was started.

Table 6-3. Concrete properties on arrival at TAS05.

Truck #	Time	Temperature (°C)	Slump (mm)	Air (%)	Comment
1	18:00	15.5	200	2.4	Cubes for compressive strength 1:1,1:2,1:3
2	19:05	15.5	200	2.2	Cubes for compressive strength 2:1,2:2,2:3
3	19:55	15.4	170	2.9	Cubes for compressive strength 3:1,3:2,3:3
4	20:55	14.9	140	2.9	Cubes for compressive strength 4:1,4:2,4:3

6.6 Casting

The casting of section 2 proceeded smoothly and without any delays or mishaps. This was of course partly due to that section 2 only comprised a wall section with a formwork whose top was completely open. However, the main reason for the rather effortless casting was the fact that the pump ability of the concrete was excellent during the entire casting process, Figure 6-4.

During casting it was also noticed that the addition of a larger amount of retarder than for section 1 delayed the setting and hydration of the concrete considerably. Indications from the temperature sensors during casting showed that hydration had not started at time the casting was completed; see also Section 9.1. This caused some concern as a very slow setting could cause an undesired high form work pressure. However, there was no real concern that the form work would collapse as it was designed for full hydrostatic pressure from the fresh concrete.

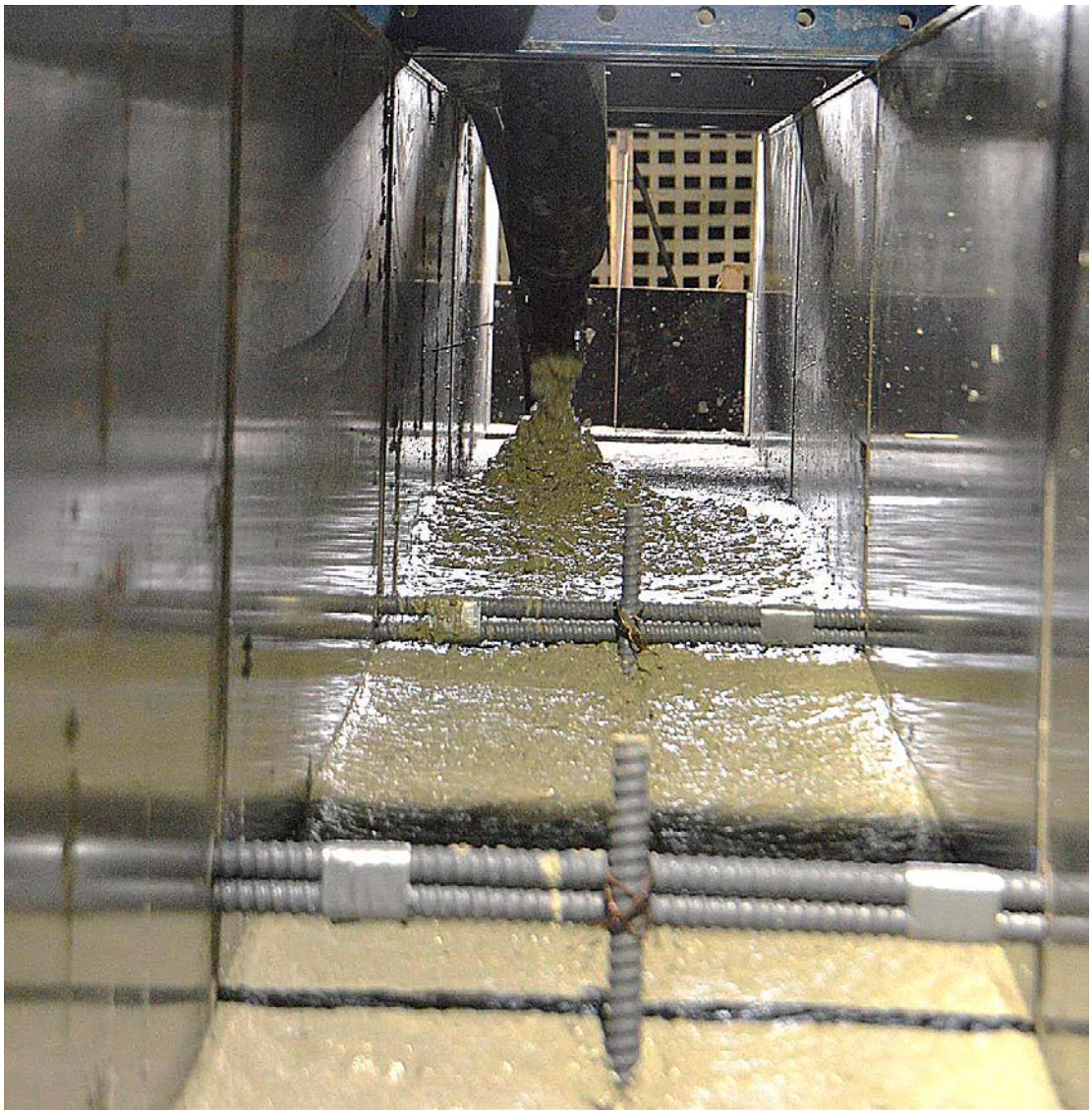

Figure 6-4. *Casting of the top-most section of section 2. Note how the concrete flows very well in the formwork. At this stage only little vibration were made due to concern of high form pressure.*

6.7 Visual inspection immediately after demoulding

Immediately after demoulding, an inspection was carried out where the result of the casting was investigated. The focus was on surface smoothness, occurrence of air blisters or other surface imperfections, adhesion to joint seals and finally mould filling. An overview image is shown in Figure 6-5.

6.7.1 Overview

As shown in Figure 6-5 and 6-6, section 2 has the expected shape and all surfaces looks fine. Vertical joint seals can be seen at the end of the short wall.

Figure 6-5. *An overview image of section 1 (left part) and section 2 (right part). The horizontal joint seal in the base slab and the vertical joint seal in the wall of section 2 are clearly visible.*

Figure 6-6. *The interior of the concrete structure with section 2 to the left and section 1 to the right. Note the rather large amount of water on the base slab caused by ground water dripping from tunnel roof.*

6.7.2 Form filling and surface quality

The form filling in the walls and in the fillet between walls and between walls and base slab was excellent, Figure 6-7, and only a very few air blisters were detected in the concrete surface.

6.7.3 Joint seals

As shown in Figure 6-7, filling between the double joint seals is complete. This was expected thanks to the excellent properties of the fresh concrete. An image of the interface between the joint seal and the concrete is shown in Figure 6-8. Here it is shown that the connection between the joint seal and the concrete is also of high quality and no gao has been formed. Attempts to measure the tensile strength of the bond between the concrete and the copper sheet were, however, not successful due to debonding during specimen preparation.

Figure 6-7. *Form filling in the fillet between section 2 and the base slab of section 1. This image also shows that the filling between the vertical joint seals in section 2 is complete.*

Figure 6-8. *Image showing the interface between the concrete and the joint seal.*

6.8 Material properties

6.8.1 Compressive strength

28 days compressive strength

The 28 days compressive strength was measured on the cubes made from concrete from all of the 4 concrete trucks, Table 6-4. The compressive strength varied between 46.3 and 53.1 MPa with an average of 49.6 MPa, i.e. just below the 90 day requirement of 50 MPa. The corresponding value for section 1 was 49.0 MPa.

Table 6-4. 28 days compressive strength of concrete from trucks 1-4.

Specimen	Truck	Weight (g)	Density (kg/m^3)	Force (kN)	Compressive strength (Mpa)
1:1	1	7997	2370	1117	49.7
1:2	1	7996	2370	1126	50.0
1:3	1	7986	2370	1137	50.5
2:1	2	8023	2380	1170	52.0
2:2	2	8183	2420	1195	53.1
2:3	2	8090	2400	1195	53.1
3:1	3	8072	2390	1086	48.3
3:2	3	7928	2350	1052	46.7
3:3	3	8061	2390	1043	46.3
4:1	4	8017	2380	1113	49.5
4:2	4	8003	2370	1078	47.9
4:3	4	7806	2310	1088	48.4

6 months compressive strength

6 months compressive strength of the concrete was measured on ∅ 100 mm cores drilled from the small cube made from concrete from truck #4, Figure 6-9. The results are shown in Table 6-5.

From Table 6-5, the 6 months average compressive strength is 67.8 MPa. The corresponding value for section 1 was 67.7 MPa.

Figure 6-9. *The small cube cast from concrete from truck #4 after drilling of cores for testing compressive and tensile strength. Numbers refer to specimens numbers in Table 6-5 and 6-6.*

Table 6-5. 6 months compressive strength for cores from the small cube shown in Figure 6-9.

Core	Weight (g)	Density (kg/m^3)	Force (kN)	Compressive strength (Mpa)
1	1830	2340	522.0	66.5
3	1815	2340	522.8	66.4
5	1830	2360	527.0	67.0
7	1822	2360	557.7	70.9
8	1816	2360	541.0	68.6
9	1853	2360	527.6	67.2

6.8.2 Tensile strength

6 months tensile strength of the concrete was measured using ∅ 100 mm cores extracted from the small cube made from concrete from truck #4, Figure 6-9. The results are shown in Table 6-6.

Table 6-6. 6 months tensile strength for cores from the small cube shown in Figure 6-9.

Core	∅ (mm)	L (mm)	Weight (g)	Force (kN)	Tensile strength (Mpa)
1	99.9	200.0	3812	25.2	3.21
3	100.0	200.0	3781	21.0	2.67
5	99.9	200.0	3793	11.1	1.41
7	100.0	200.0	3690	27.8	3.54
8	100.0	200.0	3711	10.6	1.35
9	99.9	200.0	3722	14.5	1.85

As shown in Table 6-6, 6 months tensile strength varies considerably with an average of 2.33 MPa. The values can be compared with the 2.5 MPa requirement. Note that for tests 5, 8 and 9, fracturing has occurred partially very close to or in the glue between metal plate and the concrete. This could possibly make the reliability of these measurements slightly lower than for samples 1, 3 and 7 where fracturing occurred further into the specimens.

6.8.3 Shrinkage

The casting of the specimens for shrinkage measurements was done according to the same method as used for the section 1 specimens, Figure 5-20. Concrete from truck # 4 was used here. The results from the measurements are shown in Figure 6-10 for two different methods (SIS 2000) and for sealed samples where dehydration was prevented.

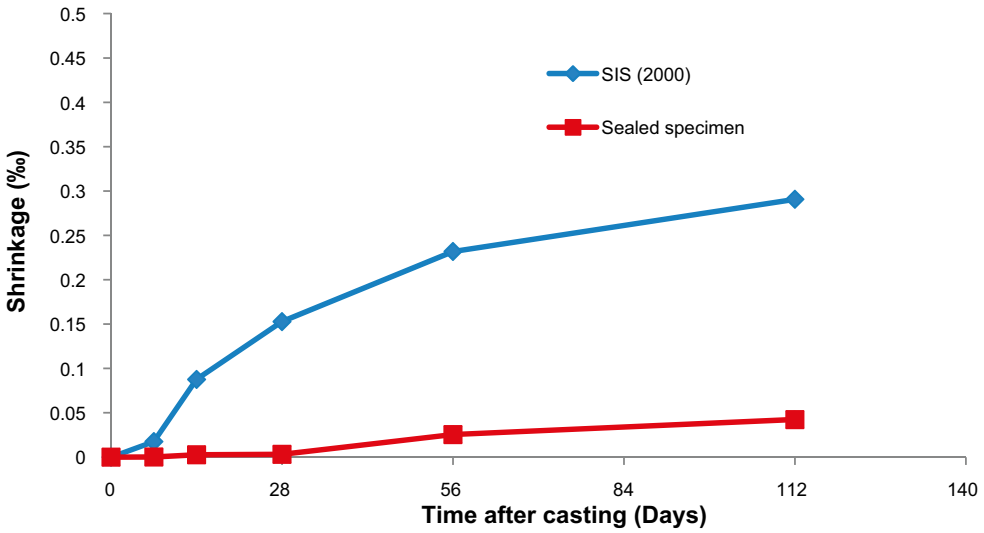

Figure 6-10. Results from shrinkage measurements using two methods: SIS (2000) and sealed specimens.

As shown in Figure 6-10, drying shrinkage represents the dominant part of the total shrinkage of this concrete used. This would mean that the appearance of cracks in the future caissons in 2BMA can be significantly limited by choosing a concrete-favourable climate with a high humidity or through protecting the concrete from drying-out.

6.9 Casting of section 2: Summary

In this section the most important experiences from the casting of section 2 are presented (Section 6.9.1) as well as a summary of the material properties, Section 6.9.2. Over all, all parts of the work were accomplished according to expectations and material properties were satisfactory.

6.9.1 Construction

Formwork

The formwork was designed for a full hydrostatic pressure from the fresh concrete. The formwork was very well built and the preparations for casting complete.

Monitoring system

Installation of the sensors was made after construction of the formwork and was successful. No sensors were lost during casting of section 2.

Concrete production and transport

Concrete production and transport worked well.

Composition and properties of the fresh concrete

Compared to the concrete in section 1 the amount of retarder was increased and the temperature of the mixing water decreased in the concrete for section 2. No other adjustments were made. The consequence of this was that the properties of the fresh concrete were basically the same when it arrived at TAS05 as right after production. No adjustments were thus required and casting could proceed immediately.

6.9.2 Material properties

The properties of the hardened concrete were studied using several methods with the following results:

- The compressive strength of the concrete was measured on cubes which were manufactured in connection with casting of section 2. The 28 day compressive strength varied between 46–53 MPa. After six months the compressive strength had increased to an average of 67.8 MPa with a very low spread.
- The tensile strength of the concrete was measured on cores drilled from a small cube which was made in connection with casting of section 2. The average tensile strength was 2.33 MPa, but the spread was large. These results, however, are associated with some uncertainties because fracturing occurred partially in or very close to the glue between concrete samples and metal plate in several of the measurements.
- Concrete shrinkage was measured according to SIS (2000) where samples were stored in a climate room with RH 50 % but also on sealed samples where dehydration was prevented. After 112 days, total shrinkage was 0.3 ‰ and 0.04 ‰, respectively for these methods. This indicates that drying shrinkage is the dominant shrinkage process.

7 Extraction of drill cores and extended characterization programme

7.1 Extraction of cores

A total of 10 cores (∅ 100 mm and length of about 500 mm) were extracted from the concrete structure according to the illustrations in Figure 7-1. After extraction, the cores were wrapped in plastic foil while waiting for further analyses.

7.2 Concrete homogeneity

A visual inspection of the cores showed that the concrete was homogeneous and only minor variations in the distribution of paste and aggregates were observed. An image of core TAS05_10 as a typical example is shown in Figure 7-2 and a close-up showing the distribution of smaller and larger particles is shown in Figure 7-3.

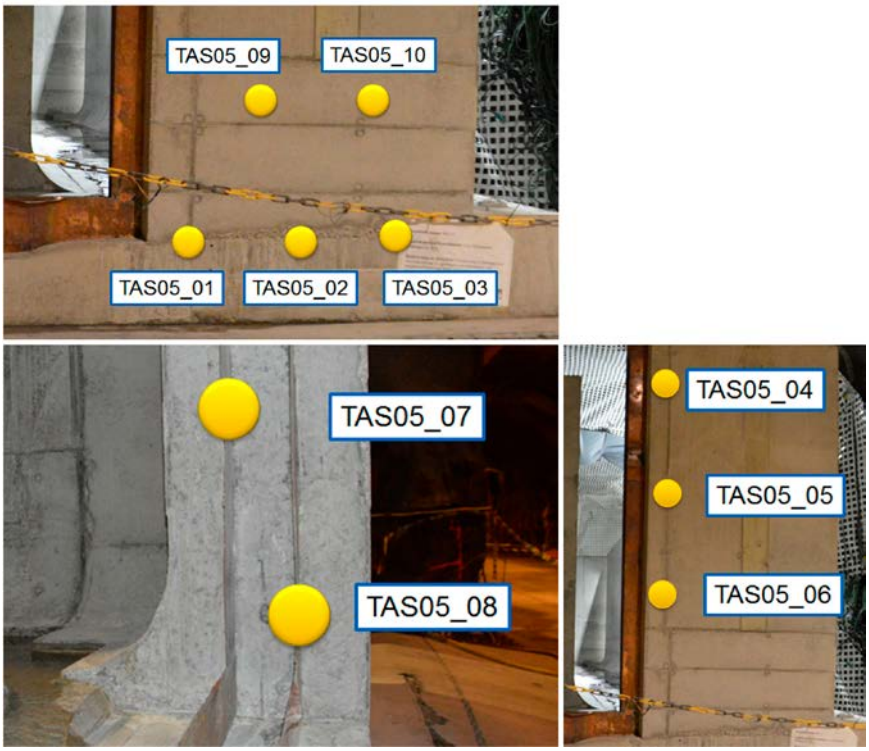

Figure 7-1. *Positions for core drilling.*

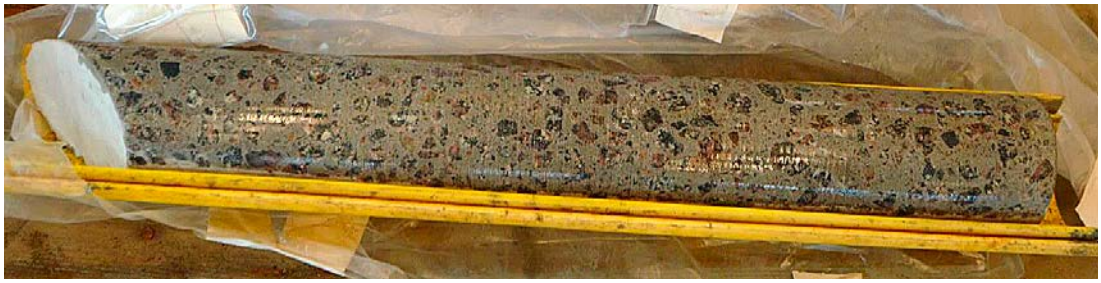

Figure 7-2. *An overview image showing the core TAS05_10 as an example of a typical core.*

Figure 7-3. *Particle distribution in the concrete from core TAS05_08. This image is from the inner part of the core, approximately 500 mm from the surface of the concrete structure.*

7.3 Joint and joint seal

7.3.1 Joint

The joint between the base slab of section 1 and the wall of section 2 was provided with joint seals made of copper sheets as shown in Sections 2.5.2 and 5.8.4. The reason for using these joint seals was to reduce the hydraulic conductivity of the joint in the case that the adhesion between the base slab and the wall was insufficient.

In Figure 7-4 images from core TAS05_01 showing the joint between the base slab and the inside of the wall (left image) and the centre of the wall (right image) are shown. From these images the joint looks perfectly tight with no obvious pores or voids. However, from these images it is also clear that the aggregate distribution is different in this part of the base slab and the wall with a much lower content of larger particles in the base slab than in the wall. The reason for this is not clear but as the same mix design was used for casting section 1and 2 this difference has probably been caused during the casting procedure by e.g. excessive vibration.

7.3.2 Joint seal

The properties of the interface between the concrete and the joint seals could only be studied on core TAS05_08. The reason for this is that the adhesion between the concrete and the copper sheets was too low and that intact interfaces could not be obtained in cores TAS05_01 and TAS05_03. In these cores the copper sheets separated from the concrete during drilling.

Figure 7-5 shows that the interface between the concrete and the copper sheet is free from pores and larger voids and that the concrete has a similar aggregate distribution close to the copper sheet and further away. The rough surface on the upper side of the copper sheet was most likely caused during drilling.

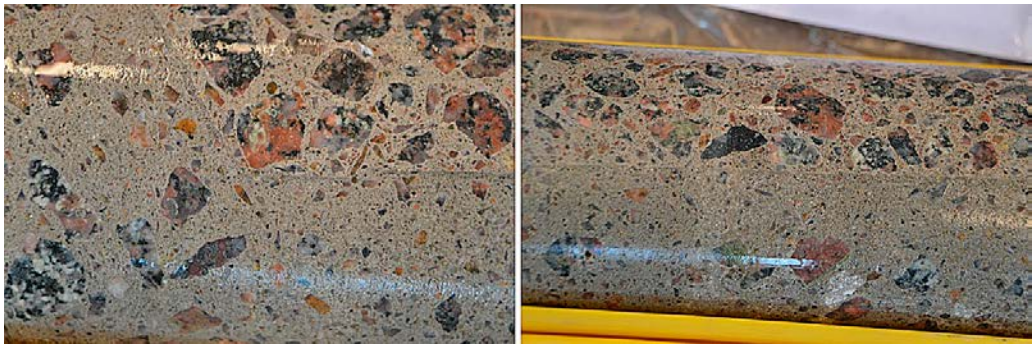

Figure 7-4. *The joint between the base slab and the wall of section 2. Images from core TAS05_01.*

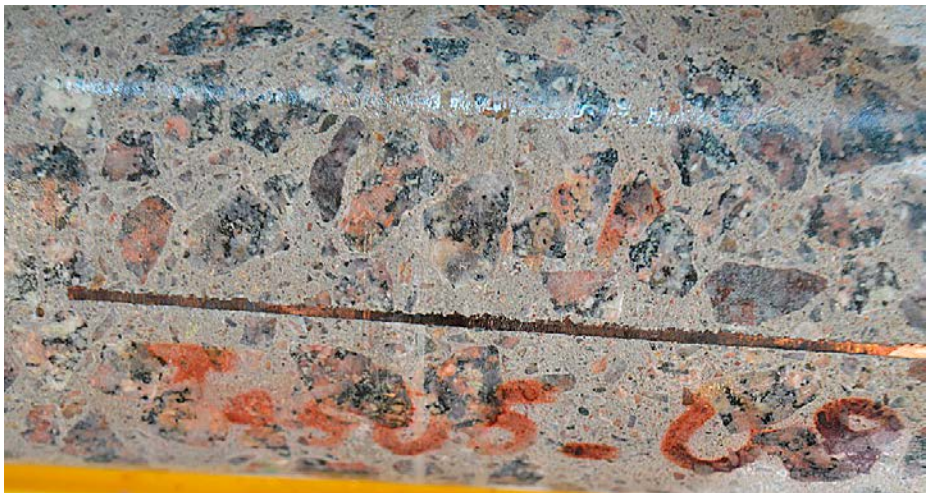

Figure 7-5. Image showing the contact zone between concrete and joint seal from core TAS05_08.

7.4 Material properties

7.4.1 Compressive strength

Compressive strength was measured according to SIS (2011) on specimens obtained from core TAS05_04. The average compressive strength from 2 specimens was 61.5 MPa. Surprisingly, this is a bit lower than the 6 months compressive strength, Table 6-5 which was on an average 67.8 MPa. A plausible explanation for this is that different batches of concrete were used in the measurements.

7.4.2 Hydraulic conductivity

The hydraulic conductivity of the concrete was measured using a standard permeameter on specimens obtained from cores TAS05_02, TAS05_4 and TAS05_7. The length and diameter of the specimens were both 50 mm. The method relies on the use of a water saturated specimen which is placed in a sealed pressurised cell. The specimen is connected to water inlet and outlet and a pressure gradient which forces water through the specimen is applied across the specimen. Typically the maximum cell pressure is 6 bars with a pressure gradient across the specimen of about 1 bar. On the outlet side of the specimen the cell is connected to a very thin hose and the amount of water that has passed through the specimen is measured as the distance travelled by the water meniscus.

Figure 7-6. Core containing a joint seal. Note that it was not possible to prepare specimens where the 2 halves of the specimen were completely separated by the joint seal as this caused the specimen to split.

Unfortunately, this method was found not suitable for materials with very low hydraulic conductivity and the measurements could only tell that the hydraulic conductivity was $<1 \times 10^{-11}$ m/s for all specimens. No measurable difference could be obtained between cores with and without a joint seal or a joint between the base slab and the wall.

It should though be mentioned that indications of a slightly higher hydraulic conductivity outside the measurable range of the method in specimens containing a joint seal was noticed during the measurements. This was indicated by that the meniscus had moved forward a hardly measurable distance further for samples containing the joint seal or a joint without a joint seal than for bulk concrete samples.

8 Section 1: Monitoring programme

In this chapter the results from the monitoring programme of section 1 is presented. The results are presented separately for different time periods after casting in order to be able to distinguish between variations caused by different events.

8.1 Section 1: The first 3 weeks after casting

8.1.1 Temperature

Base slab

As shown in Figure 8-1 a strong temperature increase is experienced in the base slab of section 1 immediately from the beginning of the casting indicating that hydration had started already when the concrete was pumped into the mould. About 24 hours after casting was started a maximum temperature of about 38 °C is reached in the centre of the base slab. The maximum temperature is lower on the underside of the base slab due to the cooling effect of the foundation. After this initial temperature rise, the concrete structure slowly cooled down and about 100 hours after casting the temperature was between 20–25 °C in the entire base slab.

Wall

As shown in Figure 8-2, after a delay of about 4 hours, corresponding to the time required to cast the base slab, a strong temperature increase is experienced in the wall of section 1 indicating that concrete have now reached the sensors and that hydration has started. About 24 hours after casting was started a maximum temperature of about 41 °C is reached. After this initial temperature rise, the concrete structure cooled down and about 100 hours after casting the temperature was between 20–25 °C in the entire wall.

Figure 8-2 also shows the effect of the depth of the temperature sensors. Here the two centrally located sensors exhibit a significantly higher maximum temperature than the temperature sensors closer to the surface of the wall.

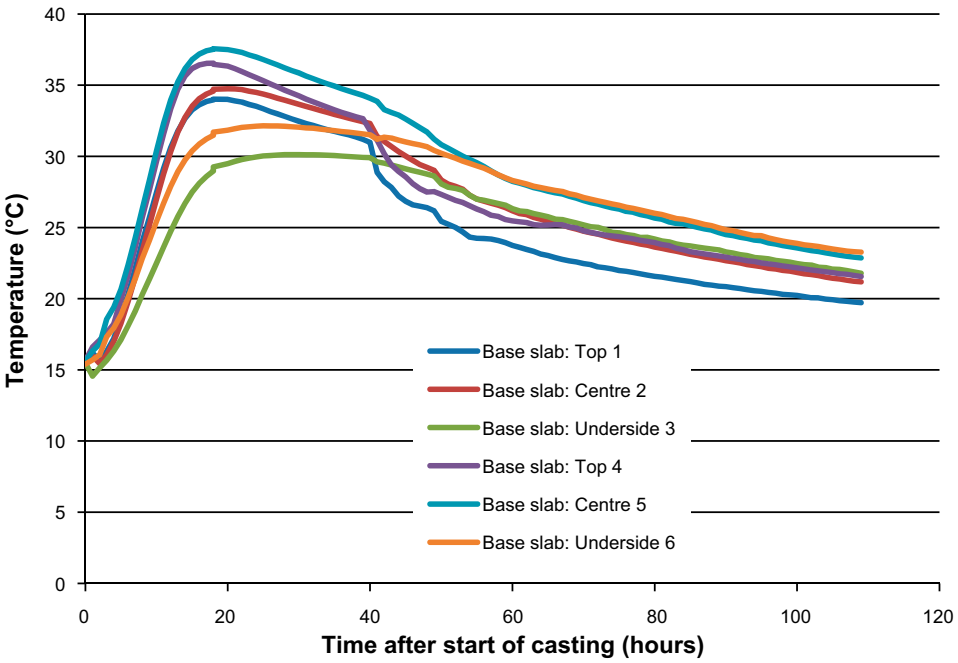

Figure 8-1. *Temperature development in the base slab of section 1 during the first 110 hours after that the casting was started.*

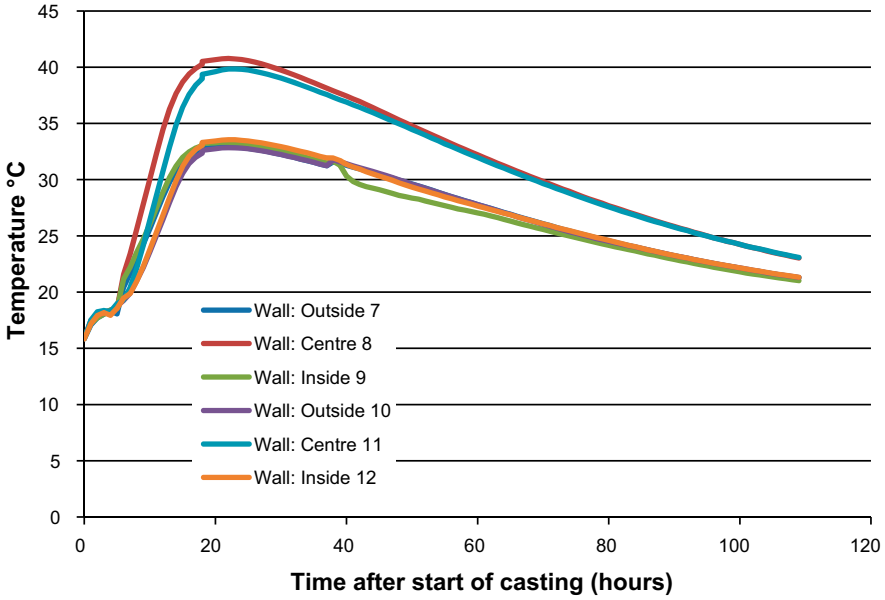

Figure 8-2. *Temperature development in the wall of section 1 the first 110 hours after that the casting was started.*

8.1.2 Internal strain

Temperature and level of strain were measured in the positions of the wall and the base slab of section 1 shown in Figure 3-5 and 3-6. Summaries of the strain in the wall and in the base slab during the first 25 days (600 hours) are shown in Figure 8-3 (base slab) and Figure 8-4 (wall).

The sharp temperature increase is accompanied by an increase in the compressive strain in the concrete as shown in Figure 8-5. This is explained by the expansion of the warm and stiffening concrete. Both the temperature and the compressive strain reach their maximum values at about 24 hours after casting was started. Once the exothermic chemical reactions in the concrete diminishes the concrete starts to cool down and contract. This contraction is expressed in a decrease in the compressive strain in the concrete as shown in Figure 8-5. However, still 3 weeks after casting and with the concrete having reached the ambient temperature, section 1 is in a state of compressive strain and there are no indications in the figures that tensile strain would prevail in the near future.

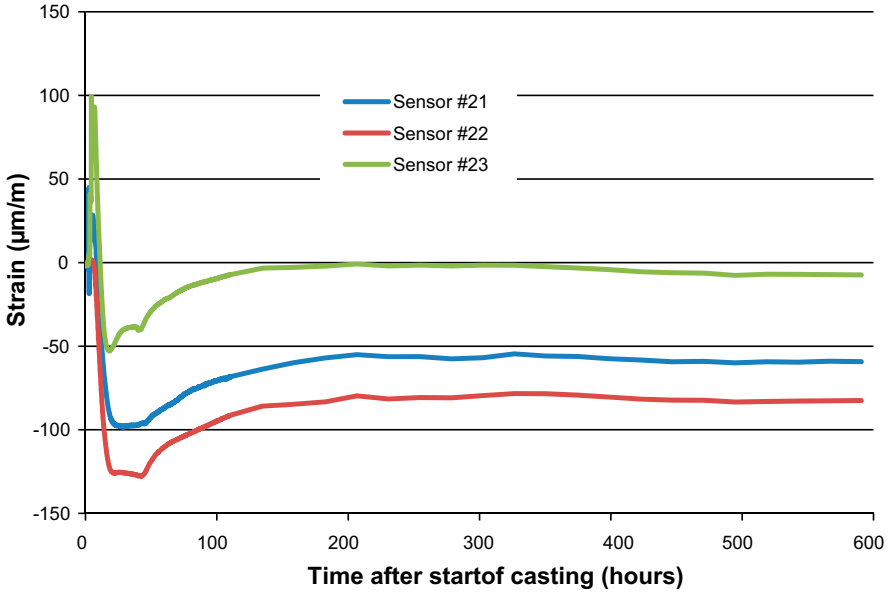

Figure 8-3. *Internal strain in the base slab after casting of section 1. Please refer to Figure 3-5 and 3-6 for details on position of the different sensors.*

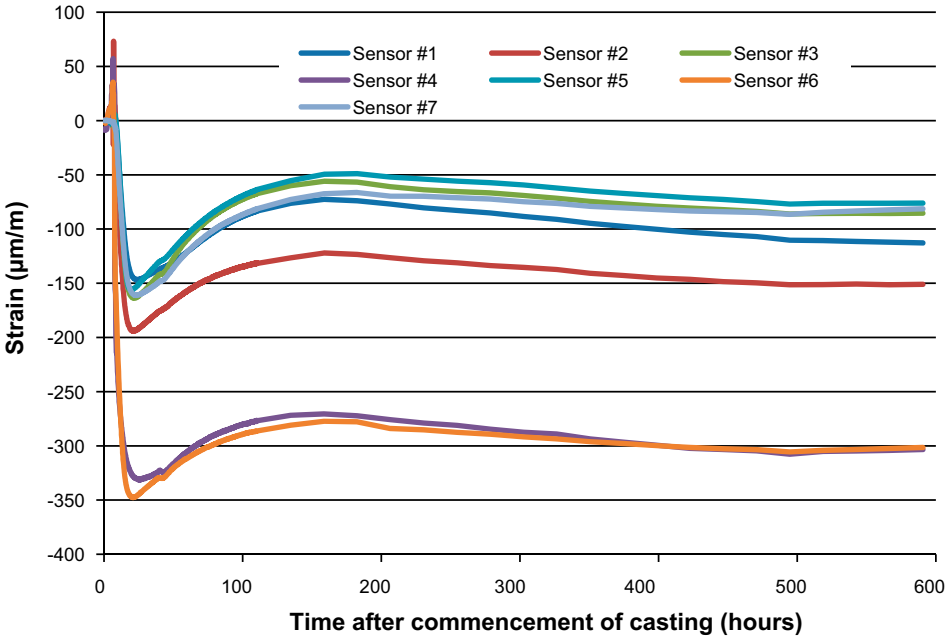

Figure 8-4. *Internal strain in the wall after casting of section 1. Please refer to Figure 3-5 and 3-6 for details on position of the different sensors.*

The response from strain transducers can in part be understood if the signals from the built-in temperature sensors in the strain sensors are considered. See Figure 8-5 for an example. However, it should be noted that the levels of strain are too large to be fully explained by the temperature increase. For that reason, at the time of writing investigations are still ongoing in order to find a plausible explanation for the very large early compressive strain in the concrete structure. For further discussions on the response from the strain transducers, please refer to Chapter 11 and Appendix A.

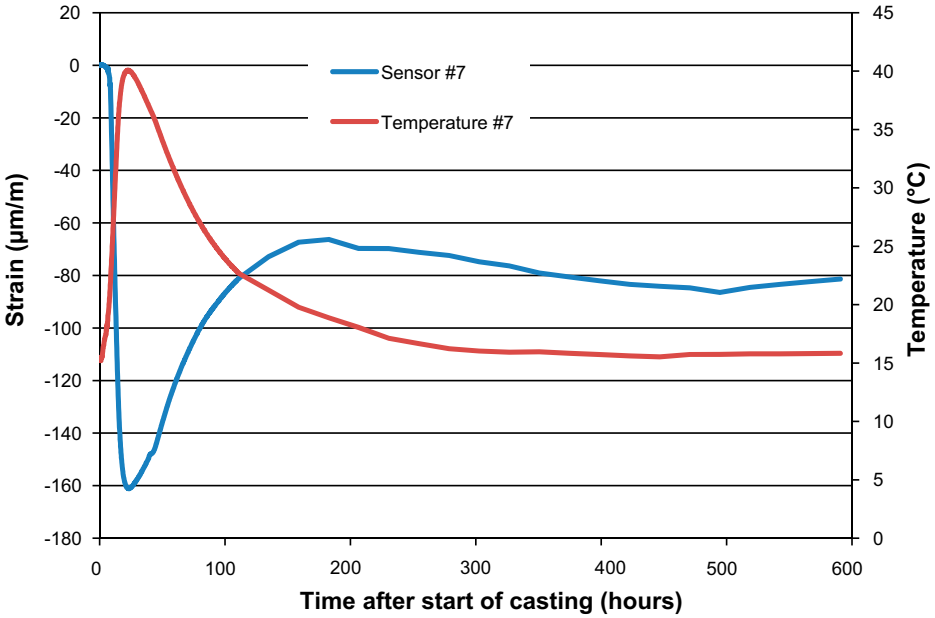

Figure 8-5. *Internal strain and temperature from sensor at position #7 in the wall of section 1. The signals from the sensors at the other positions in section 1 were in principle identical and are therefore not included in this report.*

8.1.3 Crack monitoring

During the first 3 weeks after casting no cracks were detected in any part of section 1. This confirms the findings in Section 8.1.2 that section 1 is subjected to strain well below the tensile strength of the concrete.

8.2 Section 1: The period until casting of section 2

In this section results from the long term monitoring programme during the period until casting of section 2 is presented. This period covers a total of four and a half months.

8.2.1 Temperature

As shown in Figure 8-6 only minor temperature changes were observed in section 1 after that the concrete had cooled down after the initial temperature increase discussed in Section 8.1.1. These small changes can all be explained by the temperature variations in TAS05.

8.2.2 Internal strain

As shown in Figure 8-7 the level of internal strain continues to change also after that the temperature in the concrete has reached the temperature in the tunnel. The overall tendency is that the initial increase in compressive strain caused by the increased temperature during early hydration is followed by a period of increased tensile strain during cooling of the concrete and then a long-term increase in compressive strain.

The reason for the long-term increase in compressive strain can only be speculated upon. However, a possible reason is that the slow drying of the concrete's surface causes a contraction in the surface and thus an increase in compressive strain in the centre where drying is slower and also where the sensors are positioned.

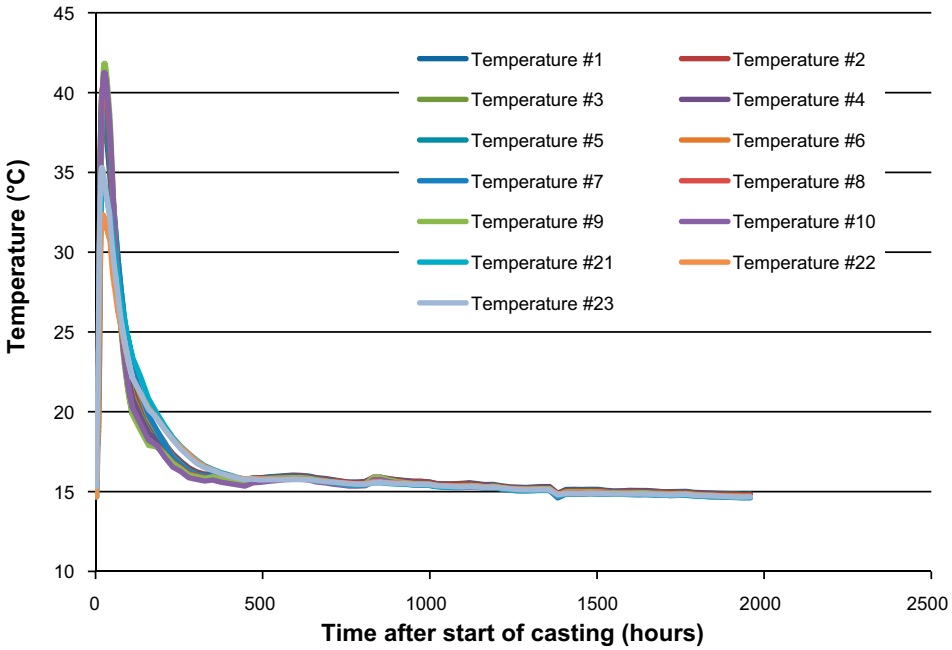

Figure 8-6. *Temperature development in the wall of section 1 during the period until casting of section 2. The diagram covers the period from November 16 2016 to February 5 2017.*

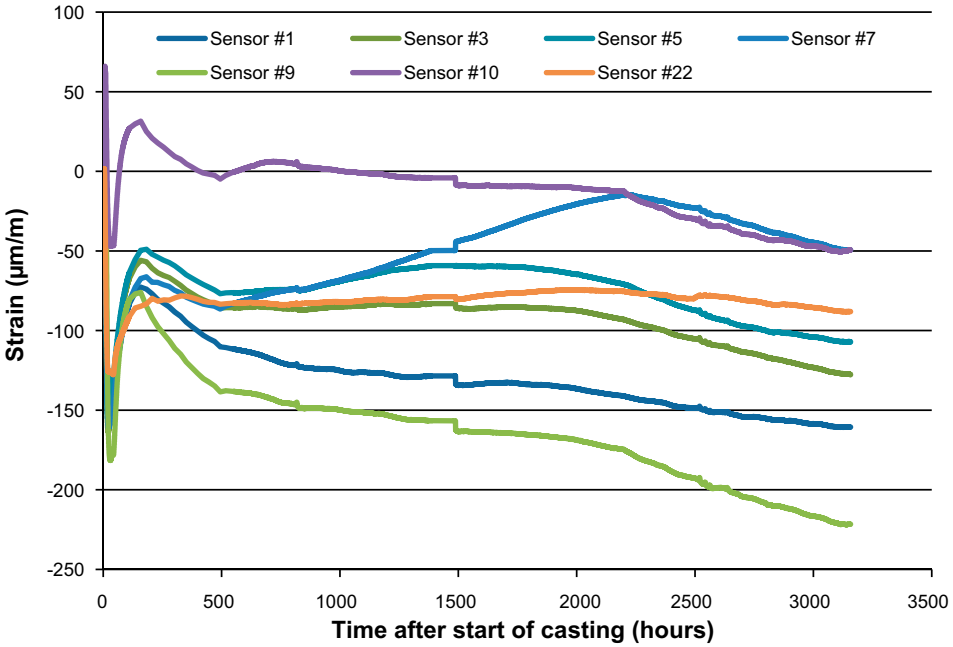

Figure 8-7. *Internal strain in section 1. The diagram covers the period from November 16 2016 to March 28 2017.*

8.2.3 Relative humidity

The RH sensors were not installed until about 1 month after casting of section 1 and data is therefore only available from about mid-December 2016. In Figure 8-8, the relative humidity in different parts of section 1 until the time of casting of section 2 is shown.

From Figure 8-8, the relative humidity in the centre of the base slab follows that of the ambient atmosphere. As such rapid changes are not possible in concrete, this is an indication of that this sensor is in fact in direct contact with the atmosphere and that the hole in which it is positioned is poorly sealed.

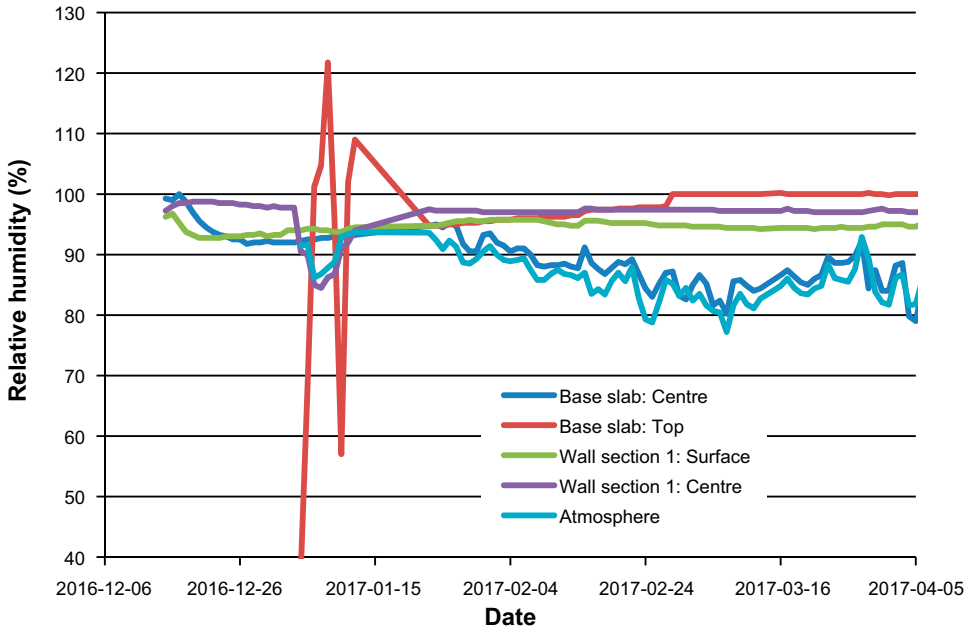

Figure 8-8. *Relative humidity in the concrete in different parts of section 1 as well in the ambient atmosphere in TAS05.*

The response from the sensor in the surface region of the base slab is a bit peculiar. The most likely reason for this behaviour is that the sensor is malfunctioning due to exposure of water. This is logical considering that water has been present on the surface during the major part of the time after casting, see Figure 6-6. See also Section 10.5.3 and Figure 10-9 where this sensor seems to have regained its function after a long period of drying-out of the concrete

For the remaining sensors, only minor variations of RH were noticed. Here, the response was slightly faster in the surface region of the wall than in its centre.

In conclusion, only minor changes of the relative humidity in the concrete was experienced during the first 4,5 months after casting and RH was above 95 % until the start of the stress test in mid-July 2017, Chapter 10.

8.2.4 External dimensions

Changes in the external dimensions of section 1 have been followed by means of LVDT-sensors since from about 1 month after casting of section 1. The results from the measurements are shown in Figure 8-9. The positions of the sensors are shown in Figure 3-7.

From Figure 8-9, the dimensional changes in the different parts of section 1 follows the trend of reduced dimensions during winter when the concrete dries out and a sudden increase in conjunction with casting of section 2. The total shrinkage of the wall is obtained from adding the values from sensor 1 and 2 and corresponds to about 0.55 mm. For an overview of the annual climatic variations in the tunnel, please refer to Figure 8-10.

8.2.5 Crack monitoring

No cracks were observed in section 1 during the period until casting of section 2 corresponding to a period of about 4 months.

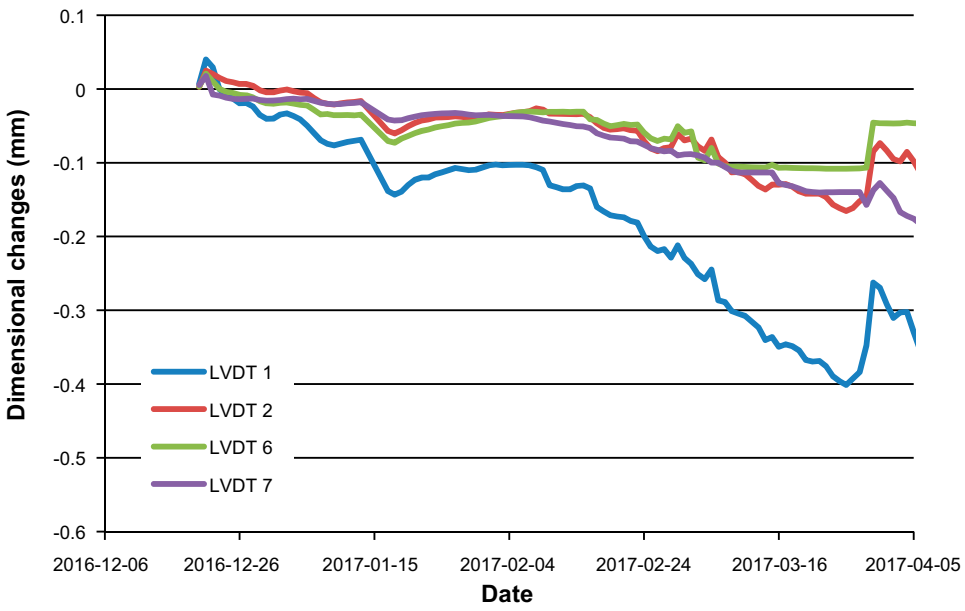

Figure 8-9. *Changes in external dimensions of section 1, from about one month after casting until immediately after casting of section 2.*

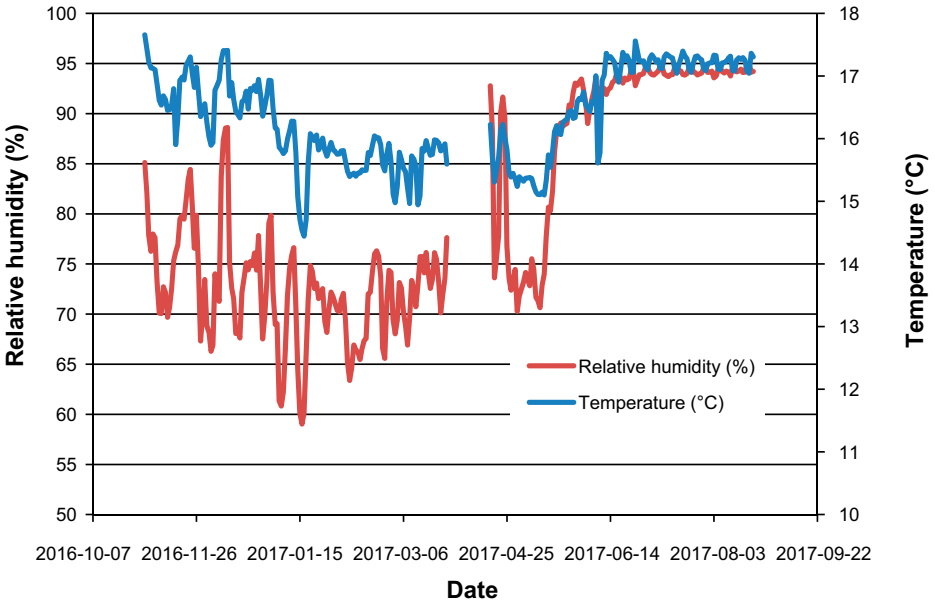

Figure 8-10. *Temperature and RH in the main tunnel just outside its connection with TASP.*

8.3 Section 1: The first 3 weeks post casting of section 2

8.3.1 Temperature

Base slab

As shown in Figure 8-11, only a very limited temperature increase was observed in the base slab of section 1 after casting of section 2. Figure 8-11 also shows that the temperature increase was faster close to the top surface of the base slab and the slowest and lowest close to the underside.

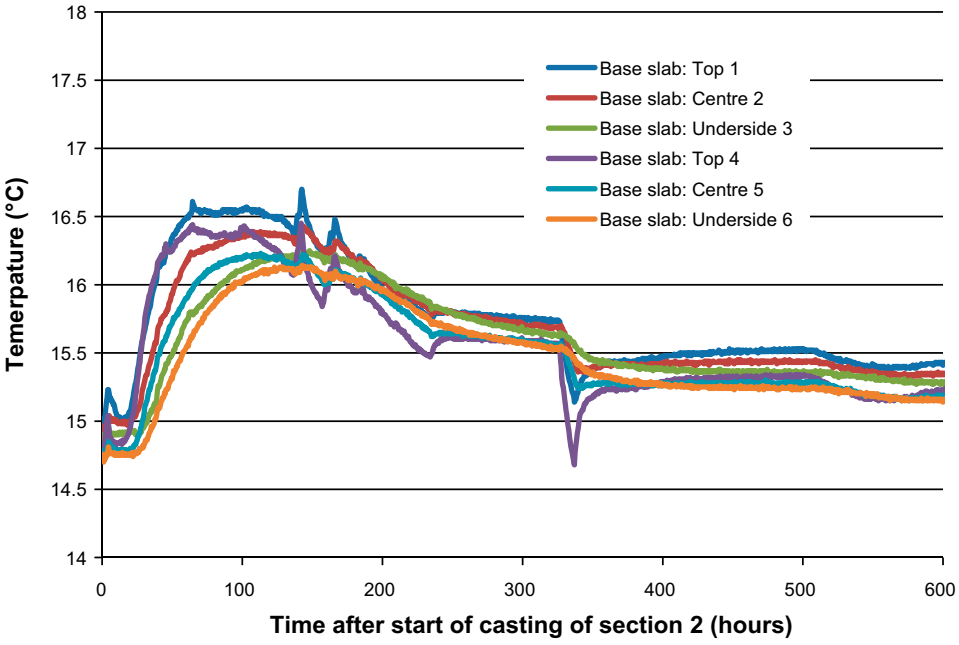

Figure 8-11. *Temperature development in the base slab of section 1 during the first 600 hours after that casting of section 2 was started.*

How much of the observed increase in temperature that can be attributed to the presence of personnel and vehicles in the tunnel during casting of section 2 and the concrete's heat of hydration, respectively, is difficult to determine here. However, Figure 8-11 shows a slight increase in temperature associated with the casting while the large increase is only after 24 hours. This would thus suggest that the main temperature increase can be derived from the hydration heat emitted from section 2 in connection with the concrete's hardening.

Finally, the temperature peaks noted 140 and 165 hours after casting section 2 can be explained by that during these days staff and heavier equipment were present in TAS05 for demoulding.

Wall of section 1

Analogously to the base slab, the temperature also rose in the wall in section 1 in conjunction with the casting of section 2, Figure 8-12. It is also noted that the temperature rise was considerably higher on the side facing section 2 while the lowest temperature increase was noted on the outside which faces the adjacent rock wall. Here too, a smaller temperature increase occurs in conjunction with the casting of section 2, while the large temperature increase occurs with about one day delay.

Temperature peaks noted 140 and 165 hours after casting of section 2 are again explained by that during these days, demoulding was carried out with the presence of personnel and heavier equipment in TAS05.

Together, these observations indicate that the main contribution to the temperature increase in section 1 associated with casting section 2 can be deduced to delivered hydration heat from section 2 and not from the presence of staff and heavier equipment in TAS05.

8.3.2 Internal strain

During casting of section 2 and the following period also the level of strain in all parts of section 1 was affected. These effects were similar in all parts of the section 1 and for that reason only the response from sensor # 23 in the base slab is shown here as a representative example, Figure 8-13. The following discussion can thus apply for all parts of section 1. For exact location of the sensors, refer to Figure 3-5 and 3-6.

In the very short perspective, all sensors exhibit an initial low peak where tensile strain increase somewhat, which occurs some hours after the lowest measured temperature. The time for maximum tensile strain corresponds to the time of the casting end.

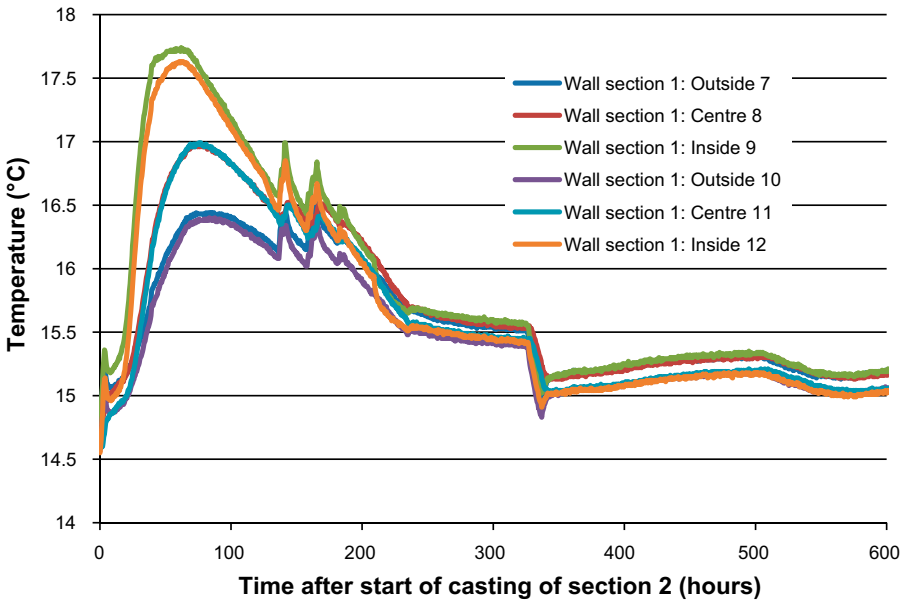

Figure 8-12. *Temperature development in the wall of section 1 during the first 600 hours after that casting of section 2 was started.*

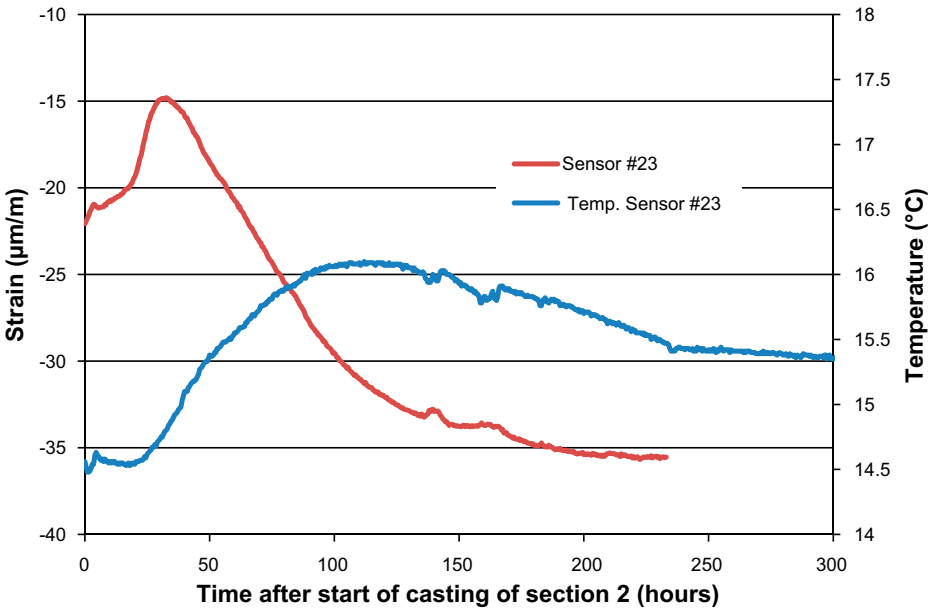

Figure 8-13. *Level of strain and temperature in the base slab of section 1 during the first 300 hours after casting of section 2.*

In the somewhat longer term, all sensors exhibit a slow and small increase in tensile strain until about 31–32 hours after casting of section 2. This is about 20 hours before the maximum temperature in section 1 but very close to the time of maximum temperature in section 2; see Section 9.1.1. After this period, the levels of tensile strain decrease again and apart from the familiar small peak at 140 and 165 hours after the casting of section 2 the strain levels are soon close to those just before casting of section 2 started.

8.3.3 Relative humidity

See Section 8.4.3.

8.3.4 External dimensions

See Section 8.4.4.

8.3.5 Crack monitoring

No cracks were detected in the wall of section 1 or in the base slab during the first 3 weeks after casting of section 2, corresponding to about 5 months after casting of section 1.

8.4 Section 1: The period until the start of the stress test

The results presented in this section covers the period from casting of section 2 in mid-March 2017 until start of the stress test in the end of July 2017.

8.4.1 Temperature

As shown in Figure 8-14 only minor temperature changes occurred in section 1 during the period from casting of section 2 until the start of the stress test, corresponding to a period from 4 to 8 months after casting of section 1. Besides the small variations during the first 300 hours after casting of section 2, these variations can be explained by climatic variations in the tunnel.

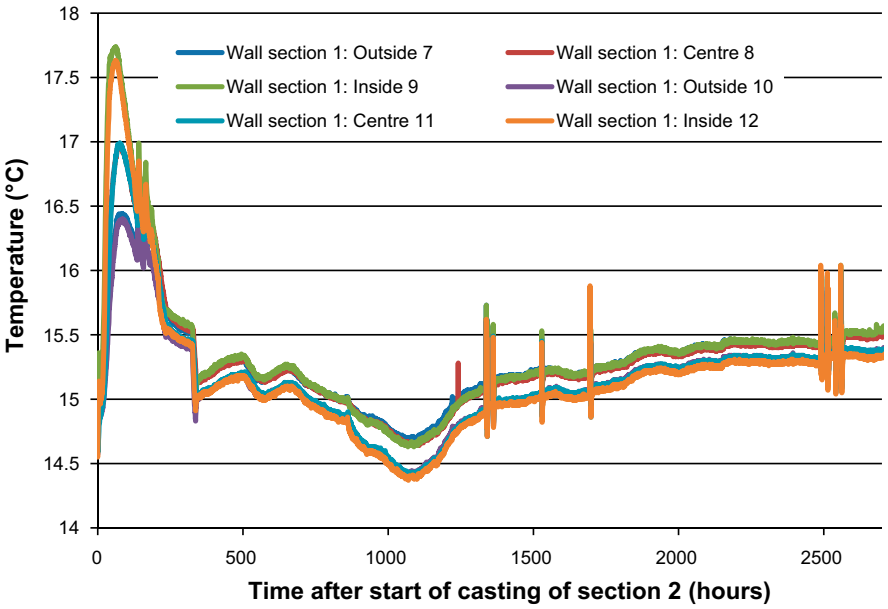

Figure 8-14. *Temperature development in section 1 from casting of section 2 until start of the stress test.*

8.4.2 Internal strain

As shown in Figure 8-15, only minor changes in the levels of internal strain was observed in section 1 from the time of casting of section 2 until the start of the stress test.

8.4.3 Relative humidity

The RH sensors were not installed until about 1 month after casting of section 1 and data is therefore only available from about mid-December 2016. In Figure 8-16, the relative humidity in different parts of section 1 from casting of section 2 until a few weeks into the stress test is shown. See also the discussion in Section 8.2.3 concerning suspected malfunction of some of the sensors. In Figure 8-16, also the sensor showing the RH in the atmosphere shows a strange behaviour from early July, i.e. a few weeks prior to the start of the stress test.

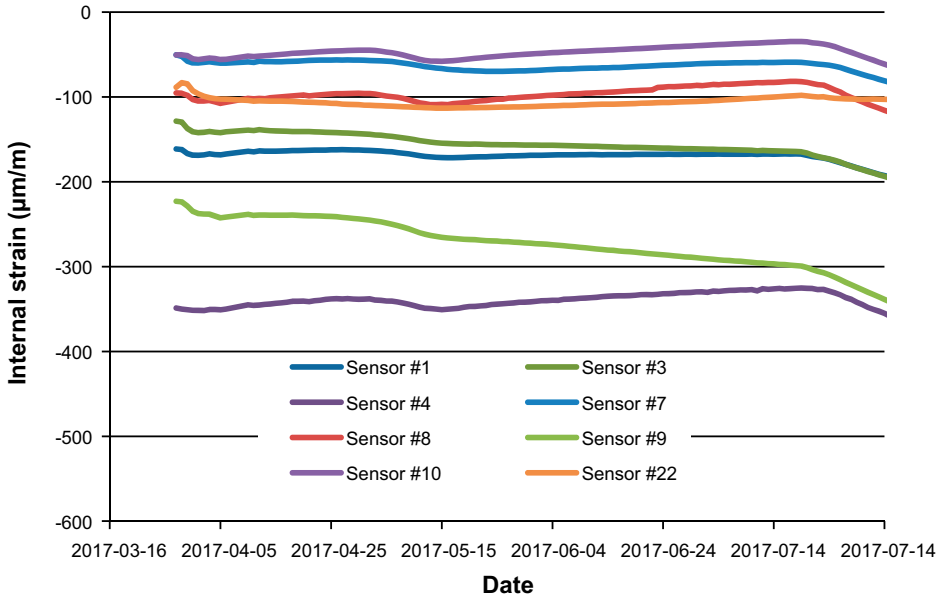

Figure 8-15. *The internal strain in section 1 during the period between casting of section 2 and start of the stress test. Some sensors have been excluded for readability.*

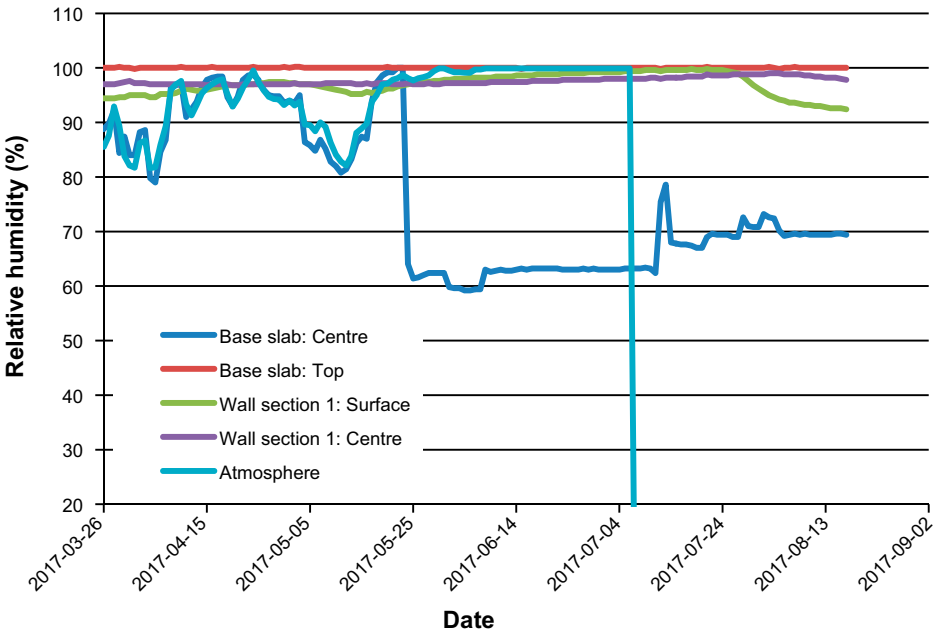

Figure 8-16. *Relative humidity in the concrete in different parts of section 1 as well in the ambient atmosphere in TAS05 from the time of casting of section 2 until a few weeks into the stress test.*

8.4.4 External dimensions

Variations in the external dimensions of section 1 during the period from casting of section 2 until the a few weeks into the stress test are shown in Figure 8-17. From this figure, a slight increase in the external dimensions – probably caused by increased RH and temperature during the summer – is observed. Once the stress test starts, shrinkage is experienced due to the drying of the concrete.

8.4.5 Crack monitoring

No cracks were detected during the first 8 months from casting of section 1 until July 20, 2017 when the stress test started.

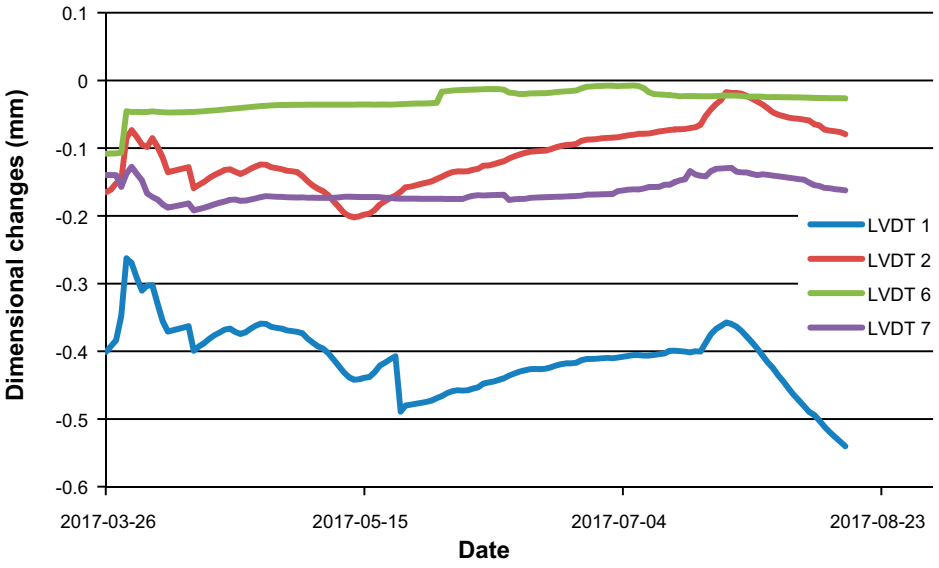

Figure 8-17. *Dimensional changes of the concrete structure during the period from casting of section 2 until a few weeks into the stress test.*

8.5 Monitoring of section 1: Summary

In this chapter the results from the long-term monitoring programme of section 1 covering the period from the day of casting in mid-November 2016 until the start of the stress test in the end of July 2017 has been presented. This period also covers the casting of section 2. The following observations have been made:

- Temperature: After an early and rather fast temperature increase during hydration with a maximum temperature in the centre of the structure of about 41 °C the temperature soon cooled down and after a few weeks the temperature of the concrete structure had returned to that prevailing in the tunnel. During casting of section 2, the temperature increased by about 2 °C but soon regained that of the tunnel. During the following period, the temperature in the concrete followed that of the tunnel.
- Internal strain: The internal strain in the concrete has been monitored by means of a large number of strain transducers. Typically all of these show a similar pattern with a sharp increase in compressive strain during the very early hydration period. This is followed by a period where the compressive strain is reduced but interestingly tensile strain is never reached. In the longer term compressive strain again increases in all parts of the structure. This is in agreement with the fact that no cracks have been observed up to 8 months post casting of section 1.

  The response from strain transducers can in part be understood if the signals from the built-in temperature sensors in the strain sensors are considered. However, it should be noted that the levels of strain are too large to be fully explained by the temperature increase. At the time of writing investigations are still ongoing in order to find a plausible explanation for the observations made.
- Relative humidity: The monitoring of the relative humidity has suffered from malfunctioning of several of the RH sensors. Those that have been functioning have shown that the relative humidity in all parts of the concrete structure is very high and close to 100 %.
- External dimensions: The external dimensions in section 1 were monitored from about 1 month after casting. The general observation is that the external dimensions have followed the relative humidity in the concrete and thus also in the tunnel. During the dry winter and early spring a slight contraction could be observed. This was followed by a small expansion, beginning in the end of May and continuing until the start of the stress test when the concrete was exposed to an in this context very dry environment. This is discussed further in Chapter 10.
- Crack formation: No cracks were observed in the concrete during the first 8 months post casting of section 1.

9 Section 2: Monitoring programme

9.1 The first 3 weeks post casting

9.1.1 Temperature

As shown in Figure 9-1, after a delay of about 15 hours, a strong temperature increase is experienced in the wall of section 2 indicating that hydration has started. About 35 hours after casting was started a maximum temperature of about 38 °C is reached in the centre of the wall. After this initial temperature increase, the concrete structure cooled slowly and about 2 weeks after completion of casting, the temperature had reached the ambient temperature.

Figure 9-1 also shows the cooling effect at the surface of the wall as the two centrally located sensors exhibit a significantly higher maximum temperature than those closer to the surface. A temperature increase of about 10 °C is also observed in the base slab close to the joint, sensors 19 and 20.

In Figure 9-2 the temperature development in section 2 is compared with that of section 1. Here the experiences from the casting of section 1 and section 2 respectively are confirmed. For section 1 the rapid hydration is shown as a very early and sharp temperature increase. This is in contrast to the long delay before temperature starts to increase in section 2 which reflects the much delayed hydration process and the effect of the increased amount of retarder.

9.1.2 Internal strain

Temperature and level of strain were measured in 7 different positions in the wall of section 2 shown in Figure 3-5 and 3-6. Internal strain during the first 10 days (250 hours) after casting is shown in Figure 9-3. Please note that sensor #14 is the only sensor which indicates tensile strain, whereas all others show compressive strain or basically zero strain.

The changes in internal strain in section 2 follows the same trend as in section 1 and are understood if the signals from the built-in temperature sensors in the strain transducers are considered, see Figure 9-4 for an example. Please see Section 8.1.2 for a discussion on this topic.

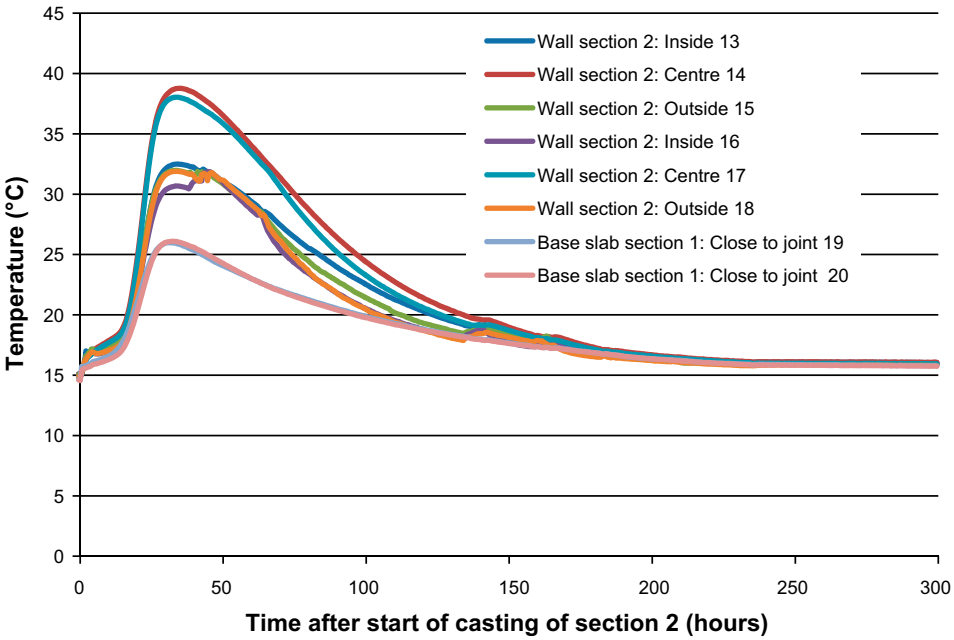

Figure 9-1. *Temperature development in the wall of section 2 during the first 300 hours after casting.*

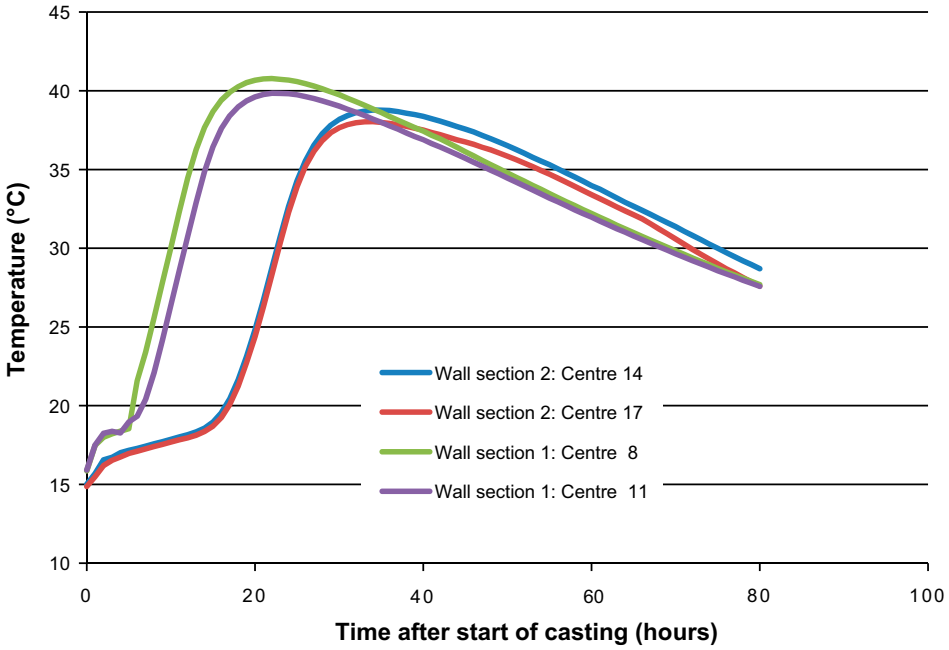

Figure 9-2. *Comparison of temperature development in section 1 and section 2. For section 1 a much more rapid hydration process is indicated by the very early temperature increase as compared to section 2 where hydration was considerably delayed by the addition of a larger amount of retarder.*

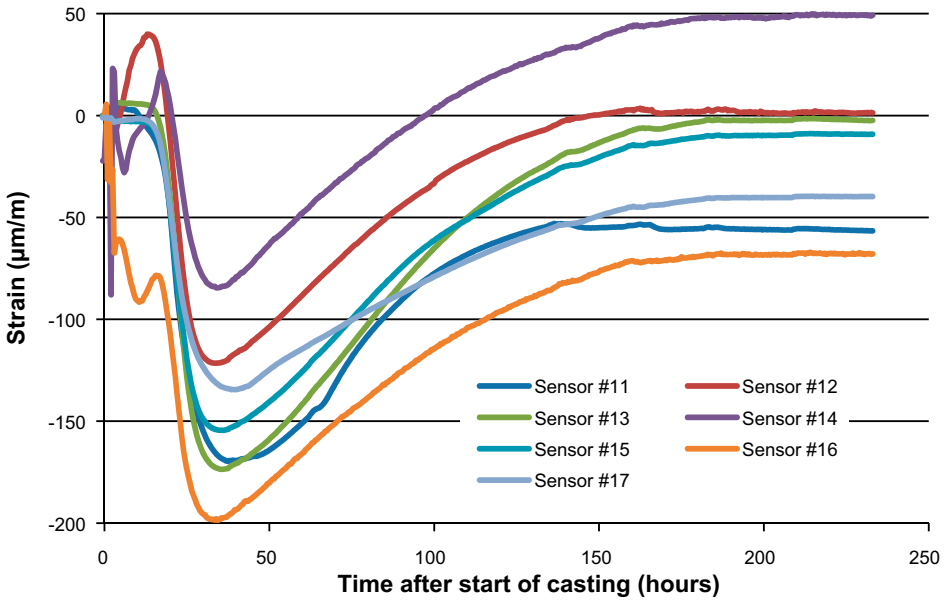

Figure 9-3. *Internal strain in the lower parts of the wall of section 2 during the first 250 hours after start of casting of section 2.*

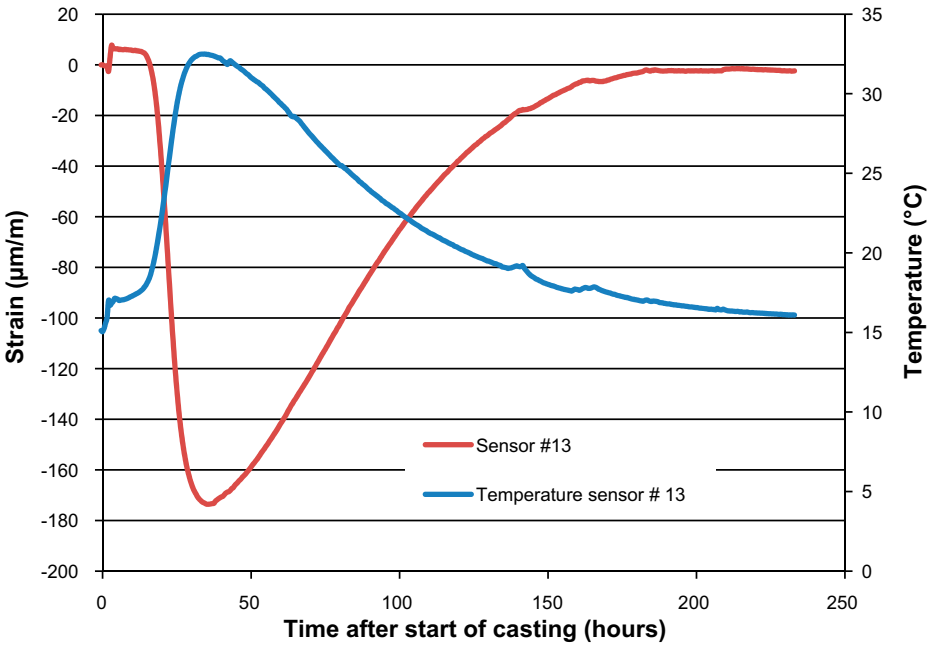

Figure 9-4. *Temperature and internal strain in in the wall of section 2 during the first 250 hours after start of casting of section 2.*

9.1.3 Relative humidity

Relative humidity in the concrete was not measured in section 2 during the first 3 weeks after casting.

9.1.4 External dimensions

Changes in the external dimensions were not measured in section 2 during the first 3 weeks after casting.

9.1.5 Crack monitoring

No cracks were detected either in the wall of section 2 or in the base slab of section 1 during the first 3 weeks after casting of section 2.

9.2 The first 4 months post casting of section 2

In this section the results from the long-term monitoring programme from the day of casting until the start of the stress test, Chapter 10, is presented.

9.2.1 Temperature

The long-term temperature development in section 2 during the first 3.5 months after casting of section 2 is shown in Figure 9-5.

Figure 9-5 shows that after the initial temperature increase during casting, the concrete cools down and within 2 weeks it has reached that of the ambient atmosphere in TAS05 characterised by a slow cooling during spring followed by a weak but steady increase during the warm summer. The distinct temperature increase at about 2 700 hours after casting corresponds to the start of the stress test in July 2017.

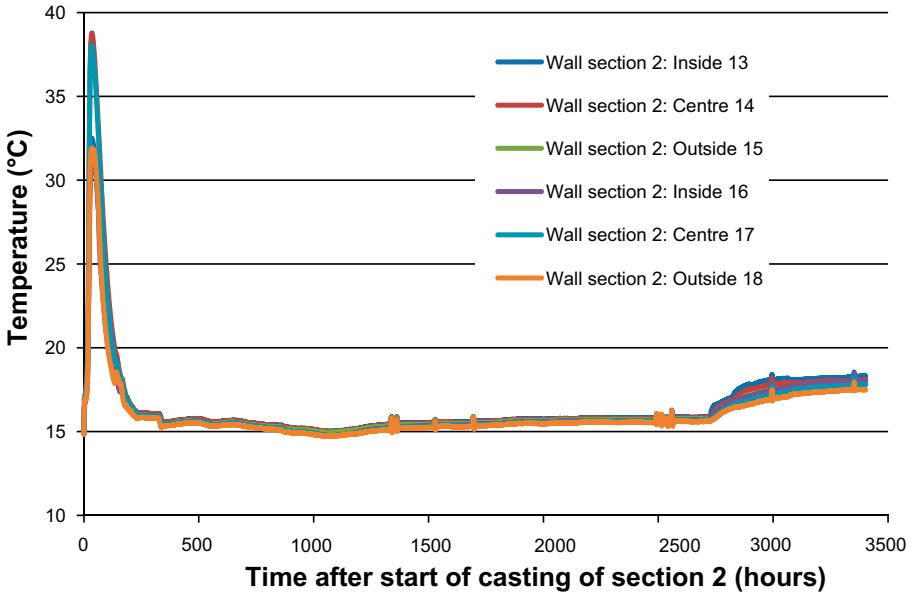

Figure 9-5. Temperature development in section 2 during the first 3 300 hours (3.5 months) after casting.

9.2.2 Internal strain

The strain in the wall of section 2 about 750 mm above the joint between the wall and the base slab and about 500 mm from the top of the wall of section 2 is shown in Figure 9-6 and 9-7 respectively.

The levels of strain in the two parts of the wall follow a similar pattern. After the initial 300 hours after casting previously discussed in Section 9.1.2 the levels of strain follow the evolution of the relative humidity in the concrete with increased compression during the drier periods and reduced compression during the more humid. The large increase in compressive strain experienced from July is explained by the start of the stress test.

The response from the strain transducers is discussed in Section 8.1.2 and 8.2.2 and is not repeated here.

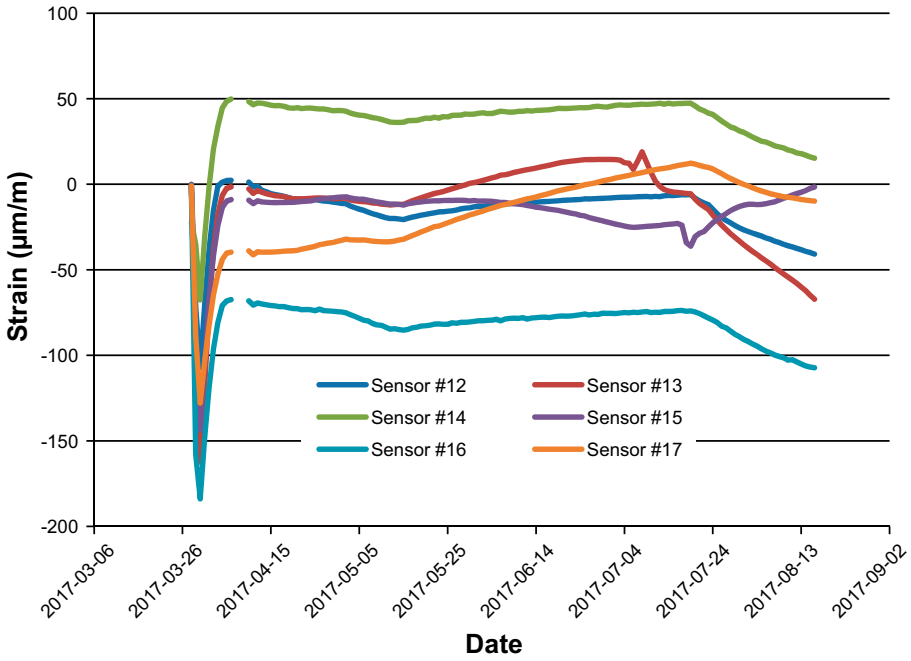

Figure 9-6. Long-term evolution of the levels of strain in the wall of section 2 about 750 mm above the joint between the base slab and the wall of section 2. The signal from sensor #11 indicated the sensor was malfunctioning and for that reason it has been excluded from this figure and the following discussion.

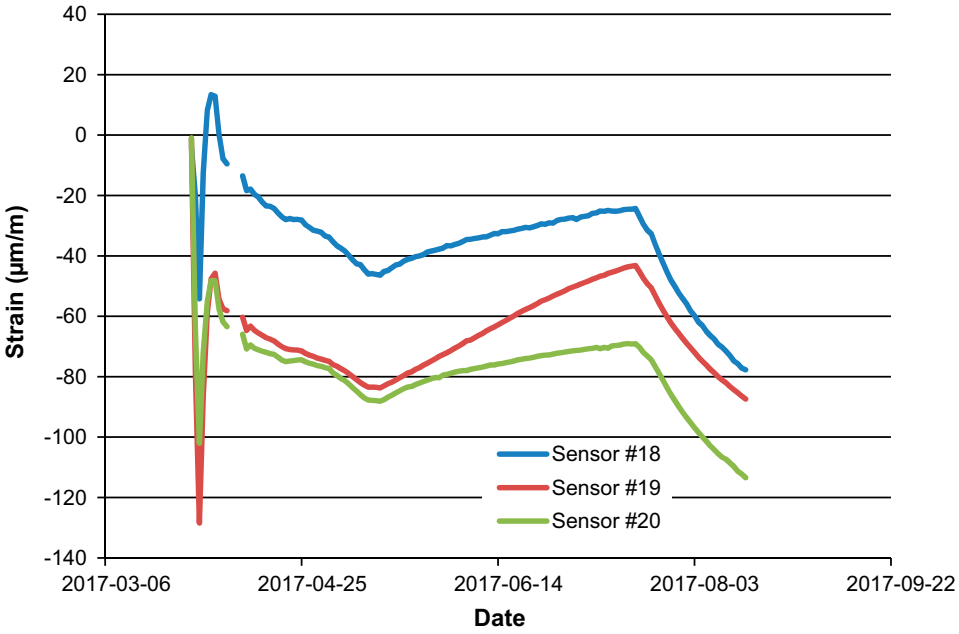

Figure 9-7. *Long-term evolution of the levels of strain in the wall of section 2 about 500 mm below the top of the wall of section 2.*

9.2.3 Relative humidity

Measurements of the relative humidity in section 2 were initiated mid-July 2017, i.e. just one week before the stress test was started. For that reason the period of undisturbed conditions is too short to provide sufficient data to be used in any kind of evaluation.

9.2.4 External dimensions

The changes in external dimensions of section 2 from about 2 months after casting and forward are shown in Figure 9-8. The figure shows that the concrete structure is constantly expanding from mid-May until the start of the stress test in the end of July, i.e. during the warm and humid summer months. Once drying starts, a sudden contraction is initiated.

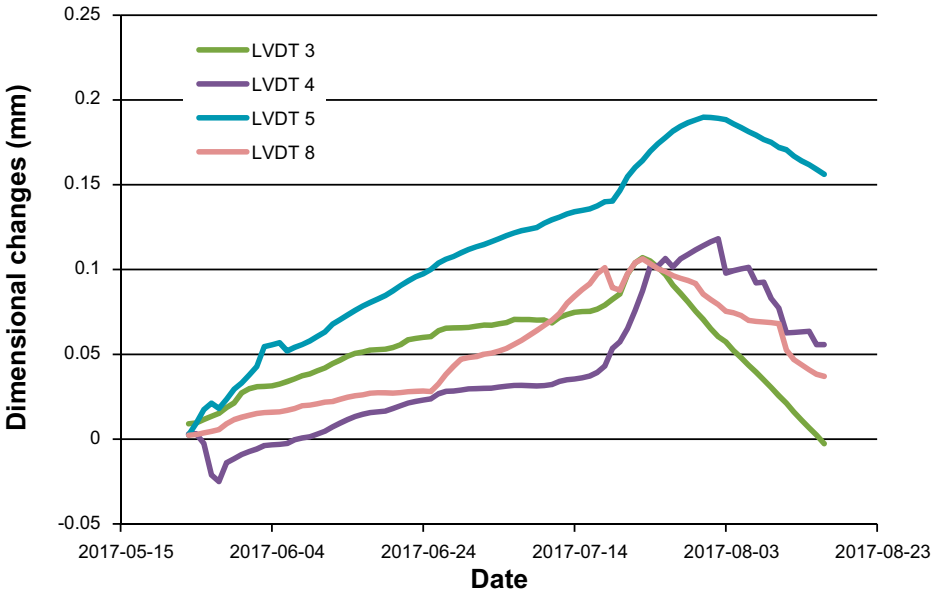

Figure 9-8. *The evolution of the external dimensions in the wall of section 2 for the period beginning mid-May until mid-August.*

9.2.5 Crack monitoring

No cracks had formed in section 2 until the start of the stress test, i.e. about 4 months after casting of section 2.

9.3 Monitoring of section 2: Summary

In this chapter the results from the long-term monitoring programme of section 2 covering the period from the day of casting in mid-March 2017 until the start of the stress test in the end of July 2017 has been presented. The following observations have been made:

- Temperature: After an early and rather fast temperature increase during hydration with a maximum temperature in the centre of the structure of about 38 °C the temperature soon cooled down and after a few weeks the temperature of the concrete structure had returned to that prevailing in the tunnel.
- Internal strain: The internal strain in the concrete has been monitored by means of a large number of strain transducers. Typically all of these show a similar pattern with a sharp increase in compressive strain during the very early hydration period. This is followed by a period where the compressive strain is reduced. In the longer term, compressive strain again increases in all parts of the structure.
- Relative humidity: RH sensors were not installed until just one week prior to the start of the stress test and no data were available here.
- External dimensions: The external dimensions in section 2 were monitored from about 2 months after casting. The general observation is that the external dimensions have followed the relative humidity in the concrete and thus also in the tunnel with a small expansion during the more humid period of the year. When the stress test started and the concrete was exposed to a dry environment contraction was instead observed. This is discussed further in Chapter 10.
- Crack monitoring: No cracks were observed in the concrete during the first 4 months post casting of section 2.

10 Stress test

10.1 General description and purpose

Four months post casting of section 2 the stress test was initiated. The main purpose of the stress test was thus to serve as a background to future decisions on climate control in 2BMA by providing information on the rate with which the concrete dries out in a very dry environment and the effect on concrete properties and crack formation.

10.2 Construction of tent and installation of dehumidifiers

Erection of the tent made from roof trusses and tarpaulin was commenced beginning mid July 2017, i.e. just below 4 months post casting of section 2 and about 8 months post casting of section 1, Figure 10-1 left image. The tent covered the entire concrete structure and the use of roof trusses allowed a spacing of about 0.5 meters on all sides of the concrete structure, Figure 10-1 right image. This permitted the air to flow freely and ensured homogeneous climate conditions around the concrete structure.

The dehumidifiers – essentially similar those used in private homes – were placed one on each side of the base slab between the walls; see Figure 10-2 right image. To each dehumidifier a ventilation pipe which ended outside the tent was connected, Figure 10-1 left image.

10.3 Installation of new RH sensors

As a complement to the RH sensors installed in section 1, the following additional sensors were also installed:

- Centre wall section 1
- Centre wall section 2
- Close to surface inside section 2
- Close to surface outside section 2
- Atmosphere between section 1 and 2
- Atmosphere in slit outside section 2

Figure 10-1. *The tent covering the concrete structure during the stress test.*

10.4 Visual inspection

10.4.1 Drying of the concrete surface

Figure 10-2 shows that the surface of the base slab of the concrete structure has completely dried out about 1 month into the stress test.

10.4.2 Crack monitoring

Still 5 months into the stress test, no cracks had been detected in any parts of the concrete structure.

10.5 Monitoring programme

10.5.1 Temperature

As shown in Figure 10-3 a temperature increase of about 2–3 degrees can be attributed to the heat released by the dehumidifiers. As also shown in this figure, temperature increase was lower underneath the base slab than closer to the surface. This can be attributed to the cooling effect of the foundation. The trend was identical for the walls and for that reason these data are not presented.

10.5.2 Internal strain

Level of strain was measured in the positions of the wall and the bottom slab of section 1 and section 2 shown in Figure 3-5 and 3-6.

Base slab

The levels of strain in the base slab of the concrete structure are shown in Figure 10-4.

The levels of strain are slightly different for the different sensors. The long sensor (# 22) shows increasing tensile strain from the start of drying period. This is opposed to the two shorter sensors placed on either side of the long one which exhibit increasing compressive strain with progression of the dehydration. No valid explanation for this behavior has yet been found.

Figure 10-2. *The space between section 1 and section 2 prior to start of stress test (Left image) and about 1 month after the start of the stress test (Right image).*

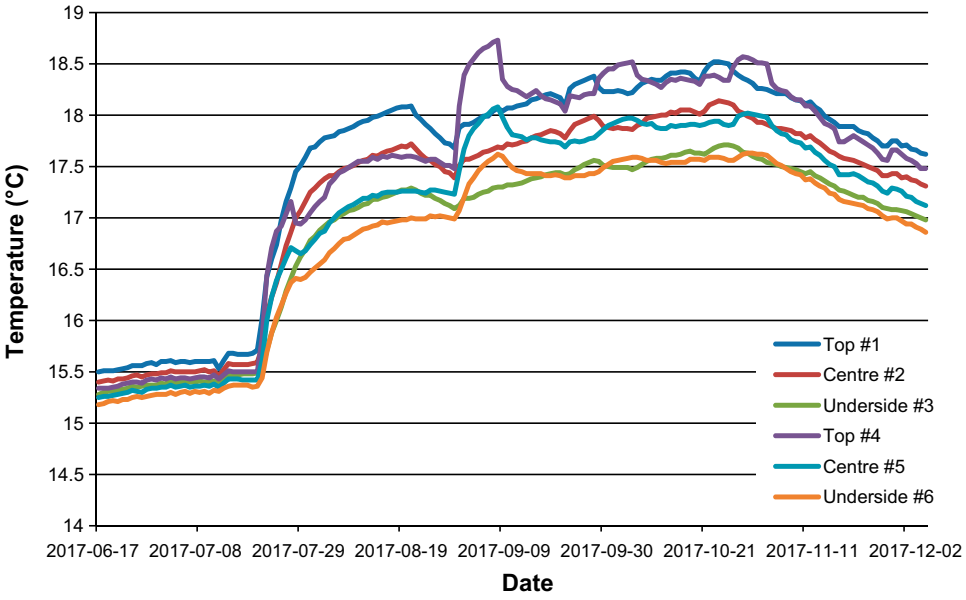

Figure 10-3. *Temperature development in the base slab during the period covering about one month prior to start of the stress test and the 4 first months of the stress test.*

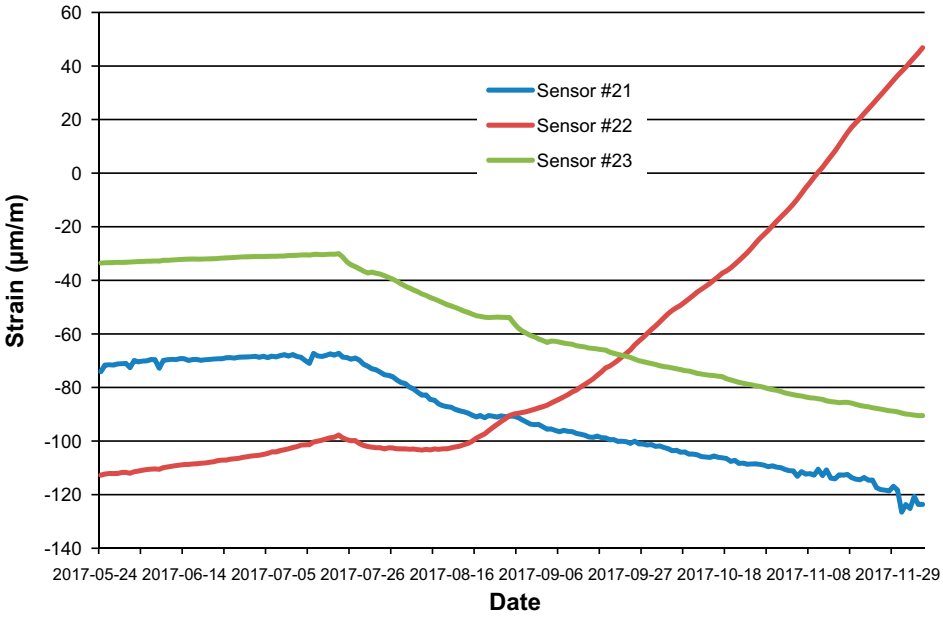

Figure 10-4. *Levels of strain in the base slab during the first 4 months of the stress test and the 2 months preceding this test.*

Section 1: Wall 750 mm above the top surface of the base slab

The levels of strain in the wall of section 1 750 mm above the top surface of the base slab are shown in Figure 10-5.

The concrete structure exhibits increasing compressive strain in all parts of the length of the wall at 750 mm above the top surface of the base slab, whereby the dehydration progresses. All sensors exhibit a small ”bump” in the curve just in early September. This can probably be derived from the sudden temperature changes that occurred during this time period, see Figure 10-3.

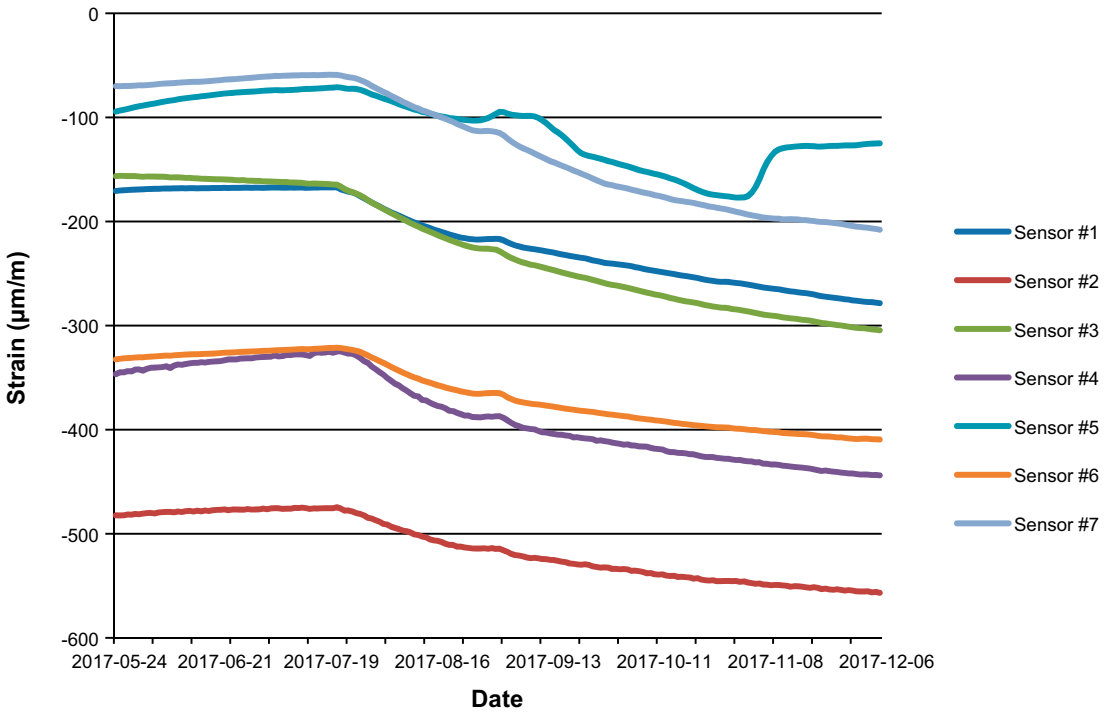

Figure 10-5. *Levels of strain in the wall of section 1 750 mm above the top surface of the base slab during the first 4 months of the stress test and the 2 months preceding this test.*

Section 1: Wall 500 mm below the top of the wall

The levels of strain in the wall of section 1 500 mm below the top of the wall are shown in Figure 10-6.

The levels of strain in the wall of section 1 500 mm below the top of the wall exhibits a similar pattern as in the wall 750 mm above the top surface of the base slab; see above.

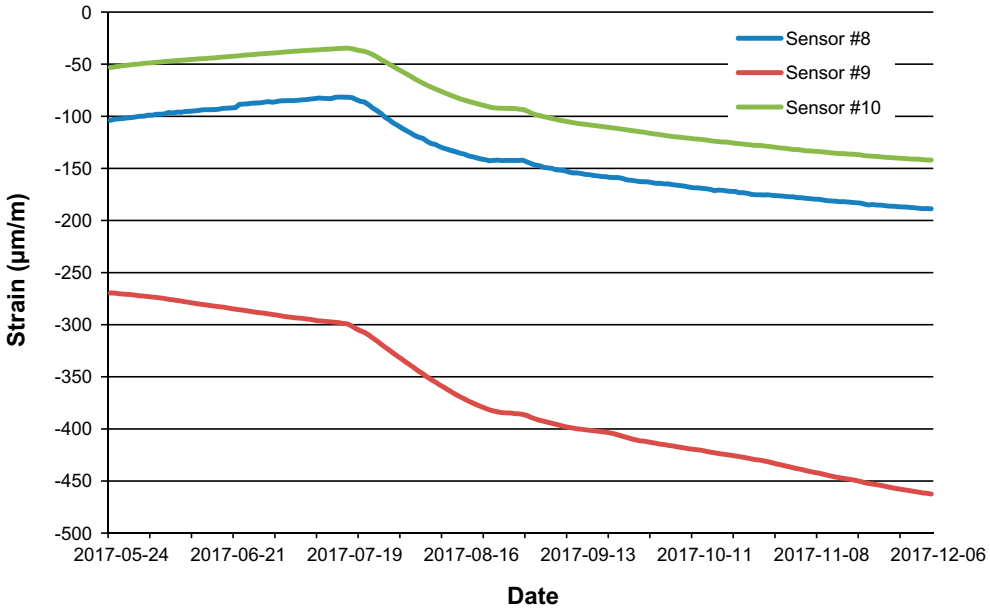

Figure 10-6. *Levels of strain in the wall of section 1 500 mm below the top of the wall during the first 4 months of the stress test and the 2 months preceding this test.*

Section 2: Wall 750 mm above the joint between the base slab and the wall of section 2

The levels of strain in the wall of section 2 750 mm above the joint between the base slab and the wall of section 2 are shown in Figure 10-7.

The concrete structure exhibits increasing compressive strain in all parts of the wall at 750 mm above the joint between the base slab and the wall. The exceptions are sensors # 15 and #17 which show a somewhat different behaviour.

Section 2: Wall about 500 mm below the top of the wall

The levels of strain in the wall of section 1 500 mm below the top of the wall are shown in Figure 10-8.

The concrete structure exhibits increasing compressive strain in all parts of the length of the wall at 500 mm below the top of the wall, whereby the dehydration progresses. The net change in the levels of strain in the wall 500 mm below its top is similar to those 750 mm above the joint between the wall of section 2 and the base slab; see above.

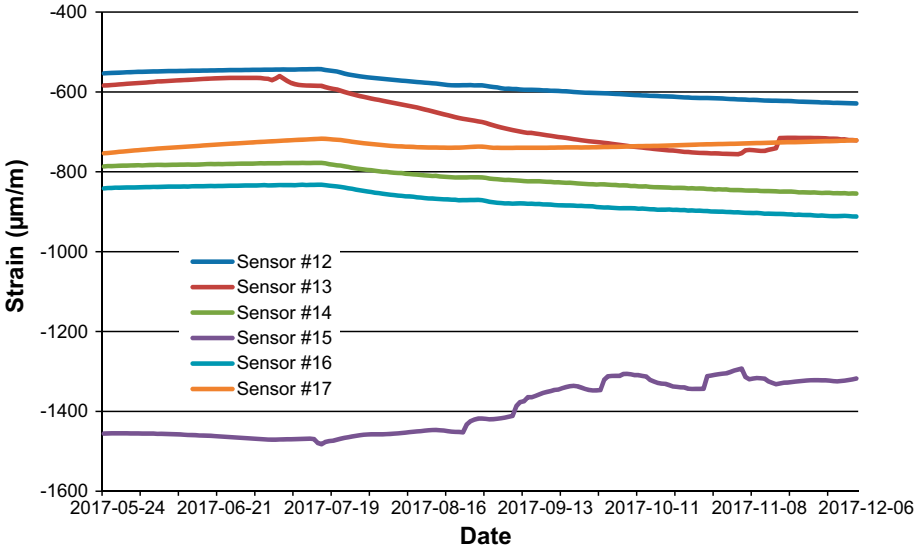

Figure 10-7. *Levels of strain in the wall of section 2 750 mm above the joint between the base slab and the wall.*

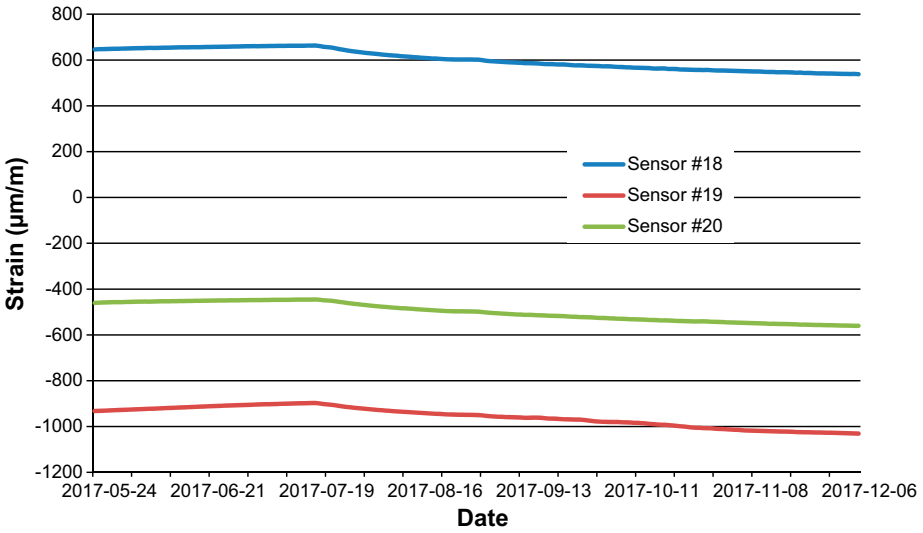

Figure 10-8. *Levels of strain in the wall of section 1 500 mm below the top of the wall during the first 4 months of the stress test and the 2 months preceding this test.*

Internal strain: Summary

The follow-up of the internal strain in the various parts of the concrete structure has shown that there have been mainly increasing compressive strain after the dehydration was started. Only a few sensors show increasing tensile strain but the reason for this is unclear. For a discussion on the influence of moisture gradients in the concrete on levels of strain, please see Section 8.2.2.

10.5.3 Relative humidity

The relative humidity of the concrete was measured with both the original system in section 1, as well as a new system installed prior to the start of the stress test, Section 3.4.

The original sensor system

The relative humidity in different parts of the concrete in section 1 is shown in Figure 10-9.

As shown in Figure 10-9, the relative humidity of the concrete's various parts is around 100 % when the dehydration begins in the end of July. It can also be noted that there is probably a malfunction of the sensor in the center of the base slab, as this exhibits a very strange behavior. This may be explained by that it has been destroyed by exposure to water in the hole where it was installed. The variations in the wall follow more the expected pattern with a faster dehydration in the outer parts than in the center of the wall where only a minor dehydration is observed only during this period.

The new sensor system

Just before the start of the stress test, a number of new RH sensors were installed in different parts of the concrete structure. These sensors are referred to in this report "The new sensor system".

As can be seen from Figure 10-10, the relative humidity in the space between the two walls ("inner atmosphere") has been below 60 %, basically throughout the period covered by this test.

During the dehydration period, the concrete has slowly dried out. This is most evident in the outer parts of the walls where RH has fallen to around 80 % both on the inside as well as on the outside. RH in the central parts of the walls, on the other hand is still after 4 months of dehydration close to 95 %, which means a decrease of about 1–3 % compared to the original value.

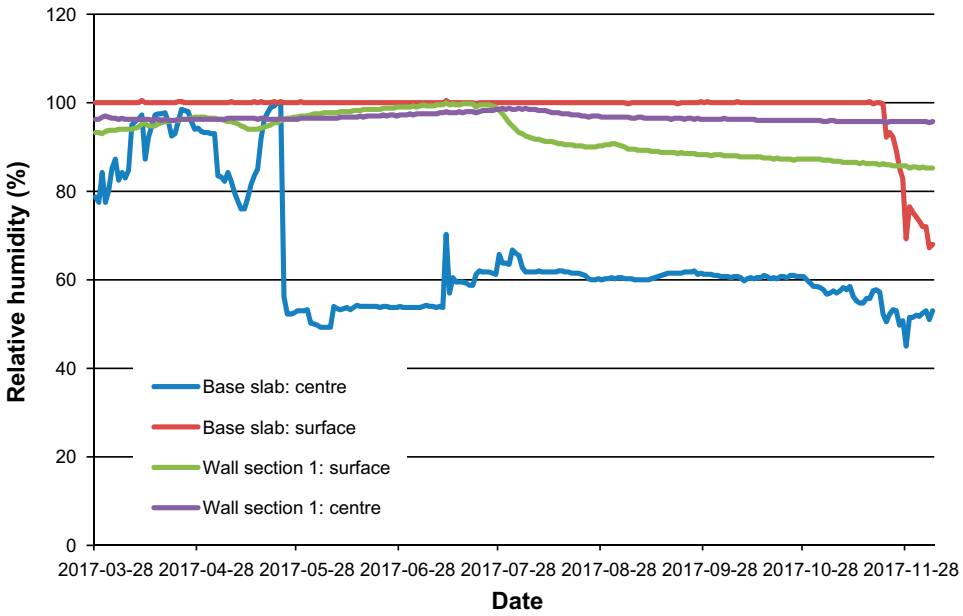

Figure 10-9. *Relative humidity in the concrete in different parts of section 1 during the first 4 months of the dehydration and the 2 months prior to this. Data from the original sensor system which was installed just after casting of section 1.*

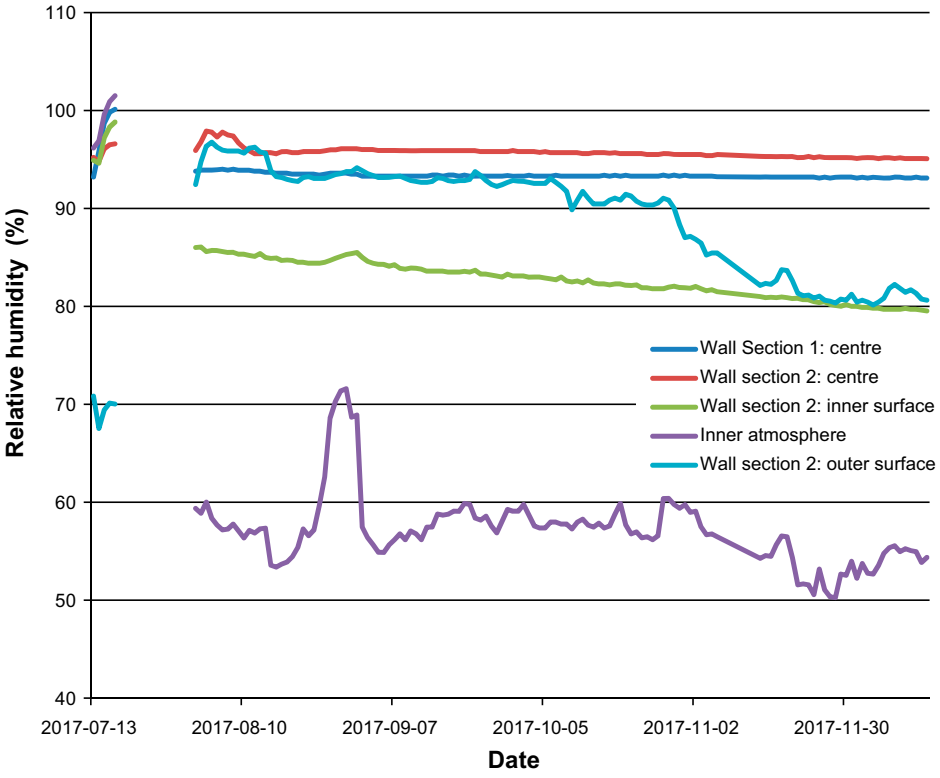

Figure 10-10. *Relative humidity of the concrete in different parts of section 2 and in the surrounding atmosphere during the first 4 months of the stress test.*

10.5.4 External dimensions

Measurements of the external dimensions were performed beginning 2016-12-20 for section 1 and beginning 2017-05-24 for section 2. The results from measurements from late May to December 2017 are shown in Figure 10-11 to 10-13 and the location of the sensors is shown in Figure 3-7.

Base slab

The changes in the external dimensions of the base slab are shown in Figure 10-11.

As can be seen from Figure 10-11, it is mainly LVDT 5 (Placed in the outer part of TAS05) which shows some changes both in terms of expansion in connection with the summer's entry but also in the form of contraction beginning with the dehydration. On the contrary, no shrinkage is observed in the part of the concrete structure located in the inner parts of TAS05 (i.e. LVDT 6). The reason for this discrepancy is not understood. The net shrinkage is estimated from Figure 10-11 to a total of 0.4 mm, which when distributed over a total length of 13 meters gives an average shrinkage of 0.03 ‰.

Wall section 1

The changes in external dimensions in the wall of section 1 are shown in Figure 10-12.

As shown in Figure 10-12, LVDT1 and LVDT 2 show a similar net shrinkage, corresponding to 0.42 mm for LVDT 2 and 0.57 mm for LVDT 1 from the start of the dehydration. This gives a total shrinkage of about 1 mm, corresponding to an average of 0.077 ‰. The vertical shrinkage (LVDT 7) is on the other hand negligible.

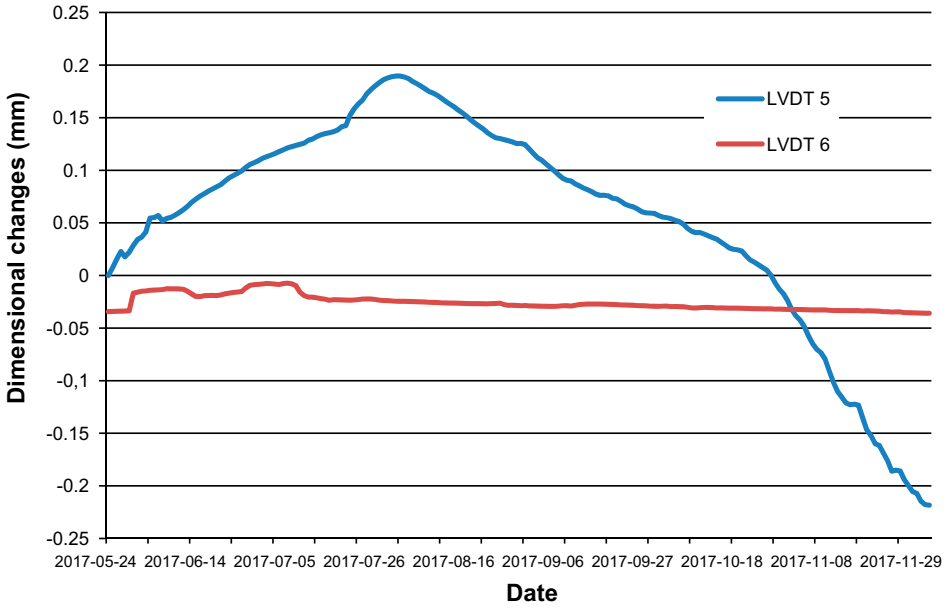

Figure 10-11. *Changes in the external dimensions of the base slab.*

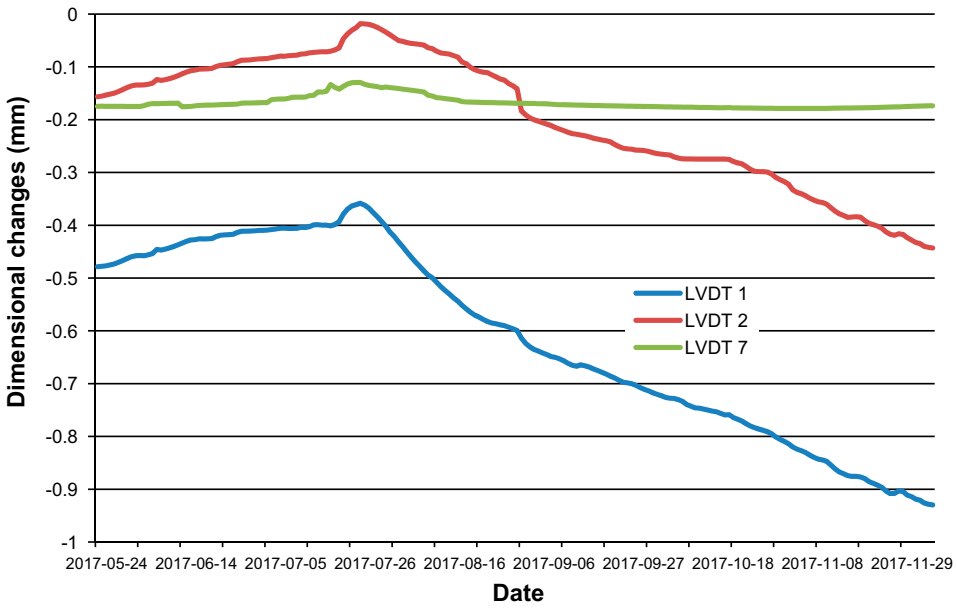

Figure 10-12. *Changes in external dimensions in the wall of section 1.*

Wall section 2

The changes in external dimensions in the wall of section 2 are shown in Figure 10-13.

As shown in Figure 10-13, the LVDT 3 and LVDT 4 show a similar net shrinkage, corresponding to 0.55 mm for LVDT 3 and 0.42 mm for LVDT 4 from the start of dehydration. This gives a total shrinkage of about 1 mm, corresponding to 0.077 ‰. The vertical shrinkage (LVDT 8) is slightly larger than for section 1 and corresponds to 0.13 mm or 0.04 ‰.

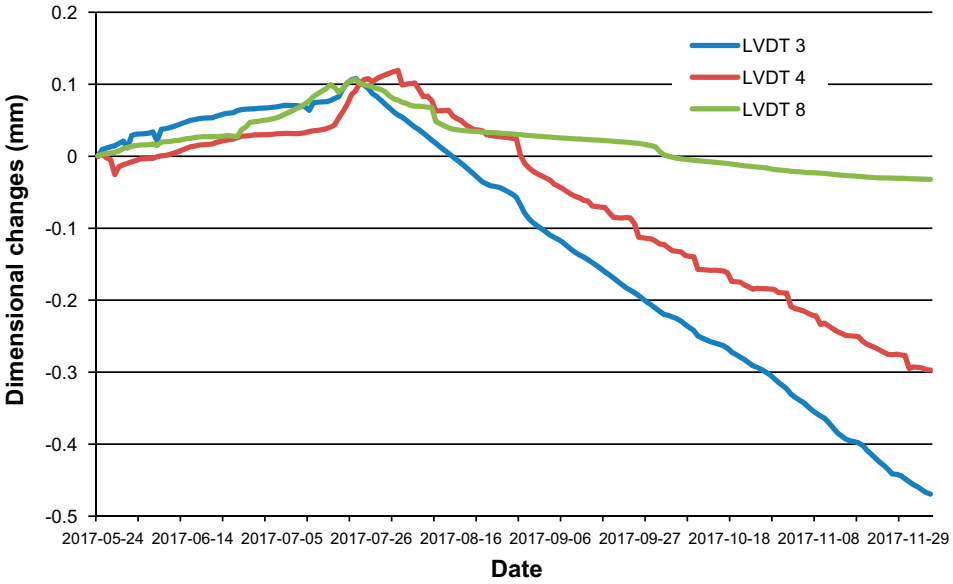

Figure 10-13. *Changes in external dimensions in the wall of section 2.*

10.6 Stress test: Summary

In this chapter the results from the monitoring programme of the stress test covering the period from the end of July 2017 until end of November 2017 has been presented. The following observations have been made:

- Temperature: The installation of 2 dehumidifiers caused the temperature in the concrete to increase by about 2 °C.
- Relative humidity: The relative humidity in the ambient atmosphere has been close to 60 % since the start of the stress test. After 4 months of dehydration RH in the surface region and in the centre of the concrete structure had fallen to about 80 % and about 95 % respectively. Drying-out is thus as expected much faster close to the surface than in the centre.
- External dimensions: Shrinkage has been somewhat larger in the horizontal plane than in the vertical. An average horizontal shrinkage of up to 0.08 ‰ has been identified while the vertical shrinkage has been about 0.04 ‰.
- Internal strain: Drying of the concrete´s surface parts has caused the compressive strain in the central parts of the (basically) entire concrete structure to increase. Only 2 out of close to 20 strain transducers show reducing compressive strain or tendencies of tensile strain.
- Crack monitoring: No cracks were observed in the concrete during the first 4 months of the stress test.

In summary, the stress test has shown that the concrete dries very slowly and that shrinkage is very low. Consequently, no cracks have yet been detected still 1 year after casting of section 1 and 8 months after casting of section 2.

11 Summary

11.1 Overview

The work presented in this report has comprised casting and long-term monitoring of the properties of 2 concrete structures representative of the concrete caissons planned to be erected in the future 2BMA in SFR. In total these two structures contain about 100 m^3 of concrete.

The first concrete structure – section 1 – comprised a based slab with the dimensions of 3×13.5 meters and an L-shaped wall with a total length of about 16 meters and a height of 3.5 meters which were cast in one uninterrupted sequence. As a foundation, a thick reinforced concrete slab covered with a reinforced plastic foil in order to reduce adhesion between these parts was used.

The second concrete structure – section 2 – comprised an L-shaped wall of the same dimensions as the wall in section 1. This wall was erected on the base slab of section 1 and the joint between these two parts were sealed with joint seals made of 1.5 mm thick and 300 mm wide copper sheets.

The concrete used in these experiments had previously been developed and tested by Lagerblad et al. (2017). The concrete was based on Degerhamn Anläggningscement from Cementa AB and the aggregates were obtained entirely from crushed rock. Additionally also rather large amounts of commercial lime stone filler was added in order to obtain the desired workability of the concrete.

For the experiments, the concrete was produced at Swerock concrete production plant in Kalmar situated close to 100 km from the Äspö laboratory where casting was performed. The concrete was transported to the site in standard concrete trucks.

11.2 Section 1

11.2.1 Casting and short-term

For section 1; the following observation were made:

Formwork

The formwork was designed for a high pressure from the fresh concrete due to that the understanding of the concrete hardening properties was not complete. For that reason, also the formwork of the base slab was covered with a lid with closable hatches for filling of the mould with concrete and vibration.

The most important experience from this work was that the use of a lid with closable hatches for the base slab in combination with a very stiff concrete caused many problems and considerably delayed the casting process. For that reason an open formwork also for the base slab would have been beneficial for the casting process given the properties of the concrete used here.

Monitoring system

Installation of the sensors was made after construction of the formwork and was successful. The main issue with the monitoring system was that the cables between the sensors and the control cabinet were not securely fastened. Due to that, the cables were moved around by the fresh concrete during casting and only thanks to skilful operation from the workers only one of the sensors was lost. To avoid this in future experiments, the cables must be securely fastened prior to casting.

Concrete production and transport

Concrete production did not face any major obstacles and even though some manual handling of one of the limestone fillers was required all other materials were handled through the plants standard production control system. Also concrete transport worked well.

However, due to the long transport times, production and transport could not respond fast enough to the required change of schedule caused by the delays during casting of the base slab.

With a mobile concrete factory placed just at the entrance to the tunnel, response time would have been much faster and the effect of the early delays significantly mitigated.

Composition and properties of the fresh concrete

The quality control at the concrete production plant showed that the properties of the fresh concrete were according to requirements and also according to previous experience from tests at a production plant (Lagerblad et al. 2017).

However, at production some warm water was added to the concrete mix. This was motivated by the low outside temperature and that the concrete was expected too cool during transport. As the chemical reactions in the concrete are temperature dependent a low temperature was expected to slow down the hydration and setting of the concrete. As a very slow setting of the concrete could give rise to very high formwork pressures means to counteract this was decided to be taken, thus increasing the temperature of the mixing water in the concrete.

However, as was noticed here, the warm mixing water in combination with the use of the limestone filler and insufficient amounts of retarder caused the concrete to set unexpectedly early. Further, also the setting proceeded at a higher rate than previously experienced.

With these experiences in mind the use of warm mixing water should be avoided in future production scale testing when this concrete is used. Also, to further reduce the rate of the hydration process a larger amount of retarder should be used during longer transports.

Material properties

The properties of the hardened concrete were studied using several methods and the following results obtained:

Compressive strength: The compressive strength of the concrete was measured on cubes which were manufactured in connection with casting of section 1. The 28 days compressive strength varied between 45–55 MPa with an average value of 48.9 MPa. After six months the compressive strength had increased to 67.7 MPa with a very low spread.

Tensile strength: The tensile strength of the concrete was measured on cores drilled from a small cube which was made in connection with casting of section 1. The average tensile strength was 2.64 MPa, but the spread was quite large with a standard deviation of 0.55 MPa. These results, however, are associated with some uncertainties because fracturing occurred partially in or very close to the glue between concrete samples and metal plate in several of the measurements.

Shrinkage: Concrete shrinkage was measured according to SIS (2000) where samples were stored in a climate room with RH 50 % but also on sealed samples where dehydration was prevented. After 112 days, total shrinkage was 0.4 ‰ and 0.04 ‰, respectively for these methods. This indicates that drying shrinkage is the dominant shrinkage process.

11.2.2 Monitoring and follow-up

The following observations were made during the long-term follow-up programme:

- Temperature: After an early and rather fast temperature increase during hydration with a maximum temperature in the centre of the structure of about 41 °C the concrete soon cooled down and after a few weeks the temperature of the concrete structure had returned to that prevailing in the tunnel. During casting of section 2, the temperature in section 1 increased by about 2 °C but soon regained that of the tunnel. During the following period, the temperature in the concrete followed that of the tunnel.
- Internal strain: The internal strains in the concrete were monitored by means of a large number of strain transducers. Typically all of these showed a similar pattern with a sharp increase in compressive strain during the very early hydration period. This was followed by a period where the compressive strain was reduced. Interestingly tensile strain was never observed. In the longer term compressive strain again increased in all parts of the structure.

Analyses of the data indicate that the levels of compressive strain during the early hydration of the concrete are too large to be fully explained by the temperature increase during this period. Typically, the levels of early compressive strain are much lower for standard concrete and consequently tensile strain is obtained some time after casting. Investigations carried out in order verify the function of the strain transducers have not been able to shed any light upon this issue. Instead of providing answers, these studies caused more questions to arise. Further studies are currently planned within a separate project.

- Relative humidity: The monitoring of the relative humidity has suffered from malfunctioning of several of the RH sensors. Those that have been functioning have shown that the relative humidity in all parts of the concrete structure is very high and close to 100 %.
- External dimensions: The external dimensions in section 1 were monitored from about 1 month after casting. The general observation is that the external dimensions have followed the relative humidity in the concrete and thus also in the tunnel. During the dry winter and early spring a slight contraction could be observed. This was followed by a small expansion, beginning in the end of May and continuing until the start of the stress test when the concrete was exposed to an in this context very dry environment.
- Crack monitoring: No cracks were observed in the concrete during the first 8 months post casting of section 1, i.e. until the start of the stress test.

11.3 Section 2

11.3.1 Casting and short term

For section 2; the following observations were made:

Formwork

The formwork (DOKA system) was designed for a full hydrostatic pressure from the fresh concrete and was assembled according to standard methods used for this type of formwork. During casting, it was noted that setting of the concrete was very slow with a (not measured) high formwork pressure as a consequence. This did not have any adverse effects on the formwork which thus proved to be very well assembled.

Monitoring system

Installation of the sensors was made after construction of the formwork and was successful.
No sensors were lost during casting of section 2.

Concrete production and transport

Concrete production and transport worked well.

Composition and properties of the fresh concrete

Compared to the concrete in section 1 the amount of retarder was increased and the temperature of the mixing water decreased in the concrete for section 2. No other adjustments were made. The consequence of this was that the properties of the fresh concrete were basically the same when it arrived at TAS05 as right after production and it could therefore be used without any adjustments.

Material properties

Compressive strength: The compressive strength of the concrete was measured on cubes which were manufactured in connection with casting of section 2. The 28 days compressive strength varied between 46–53 MPa. After six months the compressive strength had increased to an average value of 67.8 MPa with a very low spread.

Tensile strength. The tensile strength of the concrete was measured on cores drilled from a small cube which was made in connection with casting of section 2. The average tensile strength was 2.33 MPa, but the spread was large. These results, however, are associated with some uncertainties because fracturing occurred partially in or very close to the glue between concrete samples and metal plate in several of the measurements.

Shrinkage: Concrete shrinkage was measured according to SIS (2000) where samples were stored in a climate room with RH 50 % but also on sealed samples where dehydration was prevented. After 112 days, total shrinkage was 0.3 ‰ and 0.04 ‰, respectively for these methods. This indicates that drying shrinkage is the dominant shrinkage process.

11.3.2 Monitoring and follow-up

The following observations were made in the long-term monitoring program:

- Temperature: After an early temperature increase during hydration with a maximum temperature in the centre of the structure of about 38 °C the concrete soon cooled down. A few weeks after casting the temperature of the concrete structure had returned to that prevailing in the tunnel.
- Internal strain: Typically all sensors showed a similar pattern with a sharp increase in compressive strain during the very early hydration period. This was followed by a period where the compressive strain was reduced. In the longer term compressive strain again increased in all parts of the structure and tensile strain was not observed.
- Relative humidity: RH sensors were not installed until just one week prior to the start of the stress test and no data were available here.
- External dimensions: The external dimensions in section 2 were monitored from about 2 months after casting. The general observation is that the external dimensions have followed the relative humidity in the concrete and thus also in the tunnel with a small expansion beginning in the end of May and continuing until the start of the stress test when the concrete was exposed to an in this context very dry environment.
- Crack monitoring: No cracks were observed in the concrete during the first 4 months post casting of section 2, i.e. until the start of the stress test.

11.4 Section 1 and 2: Stress test

The following observations were made during the stress test:

- Temperature: The installation of 2 dehumidifiers caused the temperature in the concrete to increase by about 2 °C.
- Relative humidity: The relative humidity in the ambient atmosphere was close to 60 % from just after the start of the stress test. After 4 months of dehydration RH in the surface region and in the centre of the concrete structure had fallen to about 80 % and about 95 % respectively. Drying-out is thus as expected much faster close to the surface than in the centre.
- External dimensions: Shrinkage were more pronounced in the horizontal plane than in the vertical. The average horizontal shrinkage was 0.08 ‰ while the vertical shrinkage was up to 0.04 ‰.
- Internal strain: Drying of the concrete´s surface parts has caused the compressive strain in the central parts of the (basically) entire concrete structure to increase. Only 2 out of close to 20 strain transducers showed reducing compressive strain or tendencies of tensile strain.
- Crack monitoring: No cracks were observed in the concrete during the first 4 months of the stress test.

In summary, the stress test has so far shown that the concrete dries very slowly and that shrinkage is very low. This explains the absence of cracks still 1 year after casting of section 1 and 8 months after casting of section 2.

12 Conclusions

The results presented in this report in terms of observations during concrete production and transport, formwork construction, casting, material investigations and long-term monitoring of the properties of the concrete structure have provided vast amounts of data which will be of great value in the future development of material and method for casting the concrete caissons in 2BMA.

The following conclusions can be drawn from the results presented in this report:

- Mixing of large amounts of concrete in a concrete production plant according to the mix design developed and tested in the preceding activities was successfully carried out and the properties of the fresh concrete immediately after mixing were according to the requirements.
- The control of the setting of concrete containing large amounts of fine-grained limestone filler, such as the concrete used in these experiments, presents a challenging task. This is due to that the fine grained limestone acts as an accelerator; both shortening the time until hydration starts but also increasing the rate of hydration once hydration has been initiated. For that reason future casting experiments and casting of the caissons in 2BMA must utilise a concrete production unit in close connection to the site of the casting.
- The difficulties to control the setting of the concrete also suggests that casting of base slab and walls in one uninterrupted sequence will be a very challenging task. The results presented in this study recommend that base slab and walls are cast on separate occasions. This is also supported by the fact that the hydraulic properties of the joint were similar to that of the bulk concrete thanks to a careful preparation of the surface of the base slab prior to casting of the walls.
- The foundation used in these experiments comprised a thick reinforced concrete slab with a smooth surface finish on which a reinforced plastic foil had been placed in order to promote unrestrained shrinkage of the concrete structures. From the results obtained up to 1 year after casting of section 1, this combination has fulfilled these requirements and no cracks have yet been identified. This in spite of that the concrete structures has deliberately been dried out in RH 60 % and T about 18 °C over a period of about 5 months.
- The properties of the hardened concrete were for both sections within the requirements, presenting a high strength and low hydraulic conductivity in combination with low shrinkage and levels of strain below the tensile strength of the concrete.
- The hydraulic conductivity of joints and the interface between the joint seal and the concrete was found to be closely similar to that of the bulk concrete. This indicates that casting the base slab and the walls separately can be a suitable way forward in order to avoid a complicated casting process with a suspended formwork.

Altogether the conclusions from the work presented in this report indicate that the previously developed concrete can be used to cast the caissons for disposal of radioactive waste in 2BMA. However, further development of method for concrete production and method for casting need to be considered. This importance of such work has recently increased as a decision to alter the dimensions – mainly concrete thickness – of the reference design of the concrete caissons recently has been taken.

References

SKB's (Svensk Kärnbränslehantering AB) publications can be found at www.skb.com/publications.

Arizona Leisure, 2014. Construction history of Hoover Dam – A brief overview of Hoover Dam construction. Available at: http://www.arizona-leisure.com/hoover-dam-building.html

Bamforth P B, 2007. CIRIA C660, Early-age thermal crack control in concrete. London: CIRIA, Classic House.

Eckfeldt L, 2005. Möglichkeiten und Grenzen der Berechnung von Rissbreiten in veränderlichen Verbundsituationen. PhD thesis. Technische Universität Dresden, Germany. (In German.)

Hedlund H, 2000. Hardening concrete: measurements and evaluation of non-elastic deformation and associated restraint stresses. PhD thesis. Luleå University of Technology, Sweden.

Hösthagen A, 2017. Thermal crack risk estimation and material properties of young concrete. Lic thesis. Luleå University of Technology, Sweden.

Jonasson J-E, Wallin K, Emborg M, Gram A, Saleh I, Nilsson M, Larson M, Hedlund H, 2001. Temperatursprickor i betongkonstruktioner – Handbok med diagram för sprickriskbedömning inklusive åtgärder för några vanliga typfall. LTU rapport 2001:14, Luleå University of Technology, Sweden. (In Swedish.)

Lagerblad B, Golubeva M, Cirera Rui J, 2016. Lämplighet för krossberg från Forsmark och SFR att användas som betongballast. SKB P-16-13, Svensk Kärnbränslehantering AB. (In Swedish.)

Lagerblad, B, Rogers P, Vogt C, Mårtensson P, 2017. Utveckling av konstruktionsbetong till kassunerna i 2BMA. SKB R-17-21, Svensk Kärnbränslehantering AB.

Leonhardt F, 1988. Cracks and crack control in concrete structures. PCI Journal 33, 124–145.

Löfquist B, 1946. Temperatureffekter i hårdnande betong (Temperature effects in hardening concrete). PhD thesis. Chalmers University of Technology, Sweden. (In Swedish.)

Malm R, 2014. Instrumentation and evaluation of the concrete dome plug DOMPLU. TRITA-BKN Report 147, Royal Institute of Technology, Stockholm, Sweden.

RILEM, 1998. Prevention of thermal cracking in concrete at early ages: state-of-the-art report. RILEM, Technical Committee 119, Technical University of Munich, Germany.

SIS, 2000. SS 13 72 15: Betongprovning – hårdnad betong – krympning (Concrete testing – Hardened concrete – Shrinkage). Stockholm: Swedish Standards Institute. (In Swedish.)

SIS, 2011. SS-EN 12390-3:2009: Provning av hårdnad betong. Del 3: Tryckhållfasthet hos provkroppar (Testing hardened concrete – Part 3: Compressive strength of test specimens). Stockholm: Swedish Standards Institute. (In Swedish.)

SKB, 2015. Safety analysis for SFR, Long-term safety. Main report for the safety assessment SR-PSU. Revised edition. SKB TR-14-01, Svensk kärnbränslehantering AB.

Vogt C, Lagerblad B, Wallin K, Baldy F, Jonasson J-E, 2009. Low pH self-compacting concrete for deposition tunnel plugs. SKB R-09-07, Svensk Kärnbränslehantering AB.

Vogt C, Hedlund H, Wallin K, Baldy F, Pettersson D, 2010. Beständiga undervattensgjutna konstruktioner – SBUF projekt 11940 (Durable quay constructions cast under water – SBUF project 11940). Stockholm: Svenska Byggbranschens Utvecklingsfond. (In Swedish.)

Appendix A

Evaluation of material parameters for thermal crack risk calculations

The caissons in 2BMA shall be made of unreinforced concrete with the requirement of a maximum crack width or joint is 0.1 mm. In order to reduce the extent of thermal cracking in a structure where reinforcement cannot be used, two possibilities can be identified. The primary option is to cast the base slab and the walls in one uninterrupted sequence. This limits the risk for thermal cracks during hardening as there will be no joints in the structure, but imposes very strict requirements on the formwork.

The second option is to cast the base slab first and the walls later. This simplifies construction but increases the risk for crack formation caused by restraint between the different parts of the structure. The mature slab will prevent the movements of the walls during hardening of the concrete with an increased risk for crack formation as a consequence. In order to reduce the risk for crack formation, the base slab will need to be pre-heated prior to casting of the walls. Pre-heating causes the base slab to expand and through simultaneous cooling down of walls and base slab the risk for thermal cracks is reduced.

The required heating effect and heating time needs to be calculated prior to casting of the walls in order to meet the requirements on the risk of cracking. To be able to do that, material parameters for the hardening concrete have to be known. In this Appendix, existing material parameters are adjusted to the measured temperature development and strain measurements obtained from the sensor system installed in the concrete structures. Computation details are presented in Appendixes B and C.

Normally, measurements of temperature and strain for hardening concrete on real size structures are used to verify laboratory results and results from simulations. Here, the approach is vice-versa and thus, certain errors and problems have to be expected. Especially strain measurements on hardening concrete are prone to errors. It is for example very difficult to exactly define the starting point (when does strain actually develop in the structure) from the measurements. Another source of errors are measuring artifacts such as disturbance by casting and vibration of the fresh concrete.

The special composition of the actual concrete may have an influence on the strain measurements. The concrete incorporates rather large amounts of ultrafine limestone filler which may have an influence on early age deformations (shrinkage) and also speeds up the early hydration. These factors may result in early volume changes which can superpose the early thermal deformations in the strain measurements. Also, the thermal dilation coefficient of the concrete may be lower than the generally accepted value, resulting in additional strain induced in the strain gauges. These uncertainties could not be examined closer within the context of the present report but are focused on in the follow-up project.

A1 Thermal cracking: background

Tensile stresses and resulting cracks in a concrete structure may develop from loading or from restrained load-independent deformations such as those emanating from the heat of hydration of the concrete during hardening (see Figure A-1). The thermal shrinkage of the newly cast element may be restrained by inner restraint (risk of surface cracks) or adjacent structures (external restraint, risk of through-cracks). Autogenous deformations (self-desiccation and chemical shrinkage) of the hardening concrete add to the thermal shrinkage when cooling takes place after the hydration process.

The cracking which may result from this type of deformation is of special importance for massive structures (generally defined as a structure with a thickness of more than 800 mm). This is a result of the more pronounced temperature rise inside the structure during hardening and also the comparably lower amount of reinforcement in massive structures. Early age cracking due to heat of hydration and early autogenous deformations will be denoted temperature cracking in the following as a simplification. It is not to be confused with stresses and cracks resulting from external temperature loads such as seasonal temperature variations.

The basic mechanism of temperature cracking is explained in the section below (Hedlund 2000, Hösthagen 2017).

Figure A-1. *Early age cracks in retaining walls, left picture: Anders Hösthagen, BOSTEK, right picture: Jonatan Paulsson-Tralla, BOSTEK.*

During hardening (hydration) of concrete, heat is generated due to the exothermal cement hydration processes. Usually, the temperature varies within the cross section; it is lower in the surface layers than in the centre. This temperature difference leads to a differential movement, i.e. the inner parts expand more than the outer parts in the so-called expansion phase of the hydration. If the temperature difference between inner and outer parts is large, the developing stresses may exceed the tensile strength of the young concrete and surface cracks may form. This principle is illustrated in Figure A-2.

The tensile stresses in the surface of the cross section will later turn to compression, thus reducing the crack width. However, due to a certain interlocking effect of the cracked surfaces, a complete crack closure will not be achieved. Later developing through-cracks are related to the average volume decrease due to both temperature drop and the relatively homogenous basic shrinkage during the critical contraction phase, as illustrated in Figure A-2. Typically, through-cracks are generated over the entire cross section as a result of the restraint from the adjacent existing structural concrete or subgrade.

Depending on dimensions and other prevailing conditions, the cracks may appear weeks, months and in extreme cases even years after a section has been casted. The critical time period for later through cracks starts from the point of "zero stress" shortly after the temperature maximum (see Figure A-2) and continues until cracking occurs or until the ratio between the maximum tensile stresses to tensile strength has been reached. Cracks formed in the cooling phase tend to remain open permanently. Prevailing drying shrinkage will increase the crack width with time. Therefore, through-cracks are often considered as being more critical than surface cracks, concerning appearance and durability.

The consequences of these restrained early movements lead to cracks more often than expected. Even relatively thin cross sections generate enough heat to cause early age cracking, as stated in Bamforth (2007): "As a rule of thumb, any concrete element cast against an adjacent element of

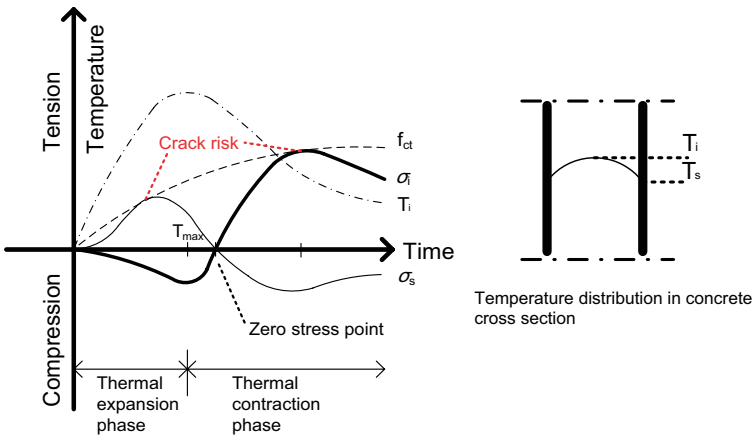

Figure A-2. *Schematic demonstration of the stress development at the surface and the interior of a concrete construction, and the development of surface tensile strength. Stress development showed is representative for a freely cast construction or an undisturbed (i.e. no cooling or heating) part of a construction. T_s and T_i is the surface and interior temperature, σ_s and σ_i is the surface and interior stress and f_{ct} is the surface tensile strength (Hösthagen 2017).*

the same thickness or greater, and which achieves a temperature rise in excess of about 20 °C, has a significant risk of early thermal cracking if the length of the joint exceeds about 5 m. A 20 °C rise would typically be achieved in a 300 mm thick wall cast in plywood formwork using C30/37 concrete with CEM I."

Common measures to control the heat development and thus temperature cracking are adjustment of the concrete mix design, use of special cements, replacement of cement or active measures such as cooling of newly cast structures with cast in cooling pipes. The margins of the stresses developing depend not only on the heat development but also on the degree of restraint. The dimensions, especially the length, of the newly cast structural member, but also the dimensions of the restraining structures are of importance.

Temperature cracks in concrete structures may also be limited by means of reinforcement. However, reinforcement may only help to control the crack width for the actual exposure acceptable crack widths, never avoid cracking in general. For massive structures, this results in technically and economically unrealistic amounts of reinforcement; especially for small crack widths (Leonhardt 1988, Eckfeldt 2005).

The topic of temperature cracks was first described in literature in the 1920s when the construction of several massive concrete dams was initiated in the USA. During the construction of the Hoover dam in the 1930s, the importance of the heat of hydration of young concrete was noted and the Hoover dam was constructed using cast-in cooling pipes (Arizona Leisure 2014).

Early calculations and design of measures to control the risk of temperature cracks were based on tabularized values of heat- and strength development or simple temperature restrictions. The first attempt to use the strain development in concrete to characterize the crack risk was done by Löfquist (1946). Later, the importance of the restraint was realized, and first attempts were made to calculate the stresses resulting from restrained thermal movements and to compare those with the developing tensile strength of the hardening concrete (RILEM 1998). In recent time, the use of 2D and 3D finite element analysis (FEA) has become increasingly common to evaluate the risk of early age cracking.

A2 Parametrization of test results

A2.1 Theoretical background and formulas

In order to be able to perform numerical calculations of early age cracking in FEA, the mechanical properties of the concrete material need to be transformed into material parameters as input. The parametrization required for software ConTest Pro is described in e.g. Jonasson et al. (2001). For a complete setup of material parameters, a number of tests have to be performed in order to determine material properties to be used in temperature and stress calculations. The following properties have to be evaluated based on tested data:

- Maturity functions.
- Heat of hydration.
- Strength growth at variable temperature.
- Young´s modulus and early age creep.
- Free deformation at variable temperature.
- Stress growth at totally restraint conditions.

The following section is extracted from Jonasson et al. (2001), Hösthagen (2017) and Vogt et al. (2009) and corresponding references therein. In this report only the most essential formulas are given.

Maturity function

$$t_e = \beta_\Delta \int_t \beta_T \cdot dt + t_{e,0} \qquad \text{(A-1)}$$

where $\beta\Delta$ = adjustment factor to be used for different admixtures [-], here = 1, β_T = temperature sensitivity factor [-], see further Equation (A-2), t = clock time [h], and $t_{e,0}$ = starting time of t_e (at $t = 0$) to be used for different admixtures [-], here = 0.

β_T is often called the maturity function, which can be expressed by:

$$\beta_T = \begin{cases} \exp\left[\theta \cdot \left(\frac{1}{293} - \frac{1}{T+273}\right)\right] & \text{for T} > -10\ ^\circ C \\ 0 & \text{for T} \leq -10\ ^\circ C \end{cases} \quad \text{(A-2)}$$

where θ = "activation temperature" [K] = (formally:) activation energy divided by general gas constant, which here is expressed by:

$$\theta = \theta_{ref} \cdot \left(\frac{30}{T+10}\right)^{\kappa_3} \quad \text{(A-3)}$$

where θ_{ref} [K] and κ_3 are fitting parameters according to best fit with test data.

Heat of hydration

$$W_B = \frac{W_{tot}}{B} = W_U \cdot \exp\left[-\lambda_1 \cdot \left(\ln(1+\frac{t_e}{t_1})\right)^{\kappa_1}\right] \quad \text{(A-4)}$$

where W_B = generated heat by weight of binder as a function of equivalent time [J/kg], B = binder content, here the sum of cement and fly ash content [kg/m^3], W_{tot} = generated heat at testing [J], W_U = ultimate generated heat by weight of binder [J/kg], and λ_1 [-], t_1 [h] and κ_1 [-] are fitting parameters.

Strength growth

The growth of the compressive strength for a series of equivalent points of time can be expressed by:

$$f_{cc}(t_e(i)) = \frac{\eta_i}{1000} \cdot f_{cc,28d} \quad \text{(A-5)}$$

The compressive strength is given for the following points of time:

$t_e\,(i)$ = [4, 6, 8, 12, 18, 24, 72, 168, 672 h]$^{-1}$

Thus, the strength development starts formally at $t_e = 4\ h$ and is always related to $t_e = 28\ d$, which results in

$\eta_1 = 0$

$\eta_9 = 1\,000$

Young's modulus and early age creep

The Young's modulus at loading age t_0, $E(t_0)$, can be expressed by:

$$E(t_0) = \frac{1}{J(\Delta t_0, t_0)} = \frac{1}{J(0.001, t_0)} \quad \text{(A-6)}$$

where $J(0.001,t_0)$ is the measured deformation 0.001d (≈ 1.5 minutes) after loading [1/Pa], and t_0 = equivalent age at loading [d].

The total deformation, $J\Delta_{load}$, t_0, can now be expressed by:

$$J(\Delta t_{load}, t_0) = \frac{1}{E_0(t_0)} + \Delta J(\Delta t_{load}, t_0) \quad \text{(A-7)}$$

where $\Delta l_{load} = t - t_0$ = load duration, [d], $\Delta J(\Delta t_{load},t_0)$ = "creep" part of the total deformation [1/Pa].

The Young's modulus is expressed by:

$$E_c(t_0) = \left[\exp\left\{ s_E \cdot \left(1 - \sqrt{\frac{28 - t_{SE}}{t_0 - t_{SE}}} \right) \right\} \right]^{0.5} \cdot E_{28d} \qquad \text{(A-8)}$$

where t_0 = equivalent age at loading [d], t_{SE} = equivalent time, where deformations start to create stresses [d], E_{28} = Young's modulus at equivalent time = 28d [GPa], and s_E = shape parameter for the growth of the Young's modulus [-].

With two straight lines in the logarithmic time scale the creep portion can be formulated as:

$$\Delta J(\Delta t_{load}, t_0) = \begin{cases} a_1 \cdot \log\left(\dfrac{\Delta t_{load}}{\Delta t_0} \right) & \text{for } \Delta t_0 \le \Delta t_{load} < \Delta t_1 \\ a_1 \cdot \log\left(\dfrac{\Delta t_1}{\Delta t_0} \right) + a_2 \cdot \log\left(\dfrac{\Delta t_{load}}{\Delta t_1} \right) & \text{for } \Delta t_{load} \ge \Delta t_1 \end{cases} \qquad \text{(A-9)}$$

where Δt_1 = time duration for the distinct break point in the creep behaviour [d], a_1 and a_2 are inclinations, dependent on the loading ages, in the linear-logarithmic plot of the creep behaviour [10^{-12}/(Pa log-unit)].

Free deformation at variable temperature

The model for free deformation at variable temperature is expressed by:

$$\varepsilon_{\text{tot}} = \varepsilon_T^o + \varepsilon_{SH}^o \qquad \text{(A-10)}$$

$$\varepsilon_T^o = \Delta T \cdot \alpha_{\text{T}} \qquad \text{(A-11)}$$

$$\varepsilon_{SH}^o = \begin{cases} 0 & \text{for } t_e \le t_{s1} \\ \dfrac{t_e - t_{s1}}{t_{s2} - t_{s1}} \cdot \varepsilon_{s1} & \text{for } t_{s1} < t_e \le t_{s2} \\ \varepsilon_{s1} + \exp\left[-\left(\dfrac{t_{SH}}{t_e - t_{s2}} \right)^{\eta_{SH}} \right] \cdot \varepsilon_{s2} & \text{for } t_e > t_{s2} \end{cases} \qquad \text{(A-12)}$$

where ε_{tot} = the measured strain [-], ε_T^o = the stress free strain related to changes in temperature [-], ε_{SH}^o = the stress free strain not related to changes in temperature [-], ΔT = change in temperature [°C], α_T = thermal dilation coefficient [1/°C], t_{s1} [h], t_{s2} [h], ε_{s1} [-] ε_{s2} [-], t_{SH} [h] and η_{SH} [-] are fitting parameters.

Stress growth at full restrained conditions

The tensile strength is related to the compressive strength according to:

$$f_{ct} = (f_{cc} / f_{cc}^{ref})^{\beta_1} \cdot f_{ct}^{ref} \qquad \text{(A-13)}$$

where f_{ct} = tensile strength [MPa], f_{cc}^{ref} = reference compressive strength [MPa], f_{ct}^{ref} = reference tensile strength [MPa}, and β_1 = exponent [-].

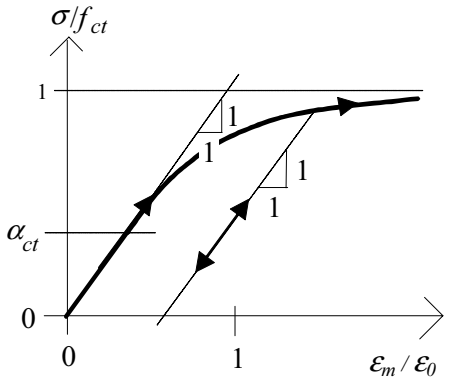

Figure A-3. *Non-linear stress-strain curve for the concrete in tension.*

The stress-strain curve used in the calculation is illustrated in Figure A-3, and α_{ct} denotes the upper limit of the linear stress-strain at 1st loading. Remaining denotations in Figure A-3 are: σ = (uniaxial) stress in the concrete [MPa], ε_m = strain related to stresses in concrete (= "material" strain) [-], ε_0 is the strain related to a linear behaviour all the way up to $\sigma = f_{ct}$.

A3 Basis for material parameters

For the present investigation, the material parameters of the actual concrete were not determined from laboratory investigations. This was due to logistical and economic reasons in the present step of the material development. Moreover, any required change in concrete composition due to observations from the test casting would result in time consuming and expensive re-testing. Instead, the material parameters of a comparable concrete were chosen as basis (self-compacting concrete with limestone filler, Anläggningscement Degerhamn and w/c = 0.47). These material parameters will be modified in order to fit the obtained data as good as possible.

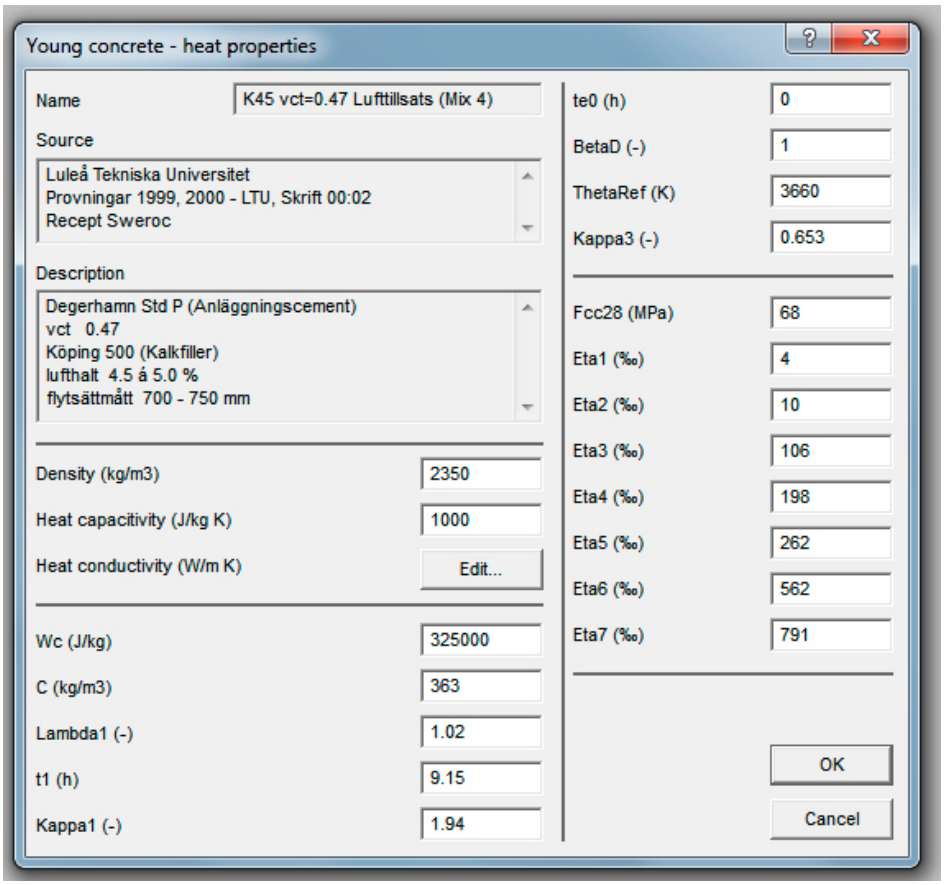

Figure A-4. *Original heat parameters for SCC with w/c of 0.47. For denotation, see previous section.*

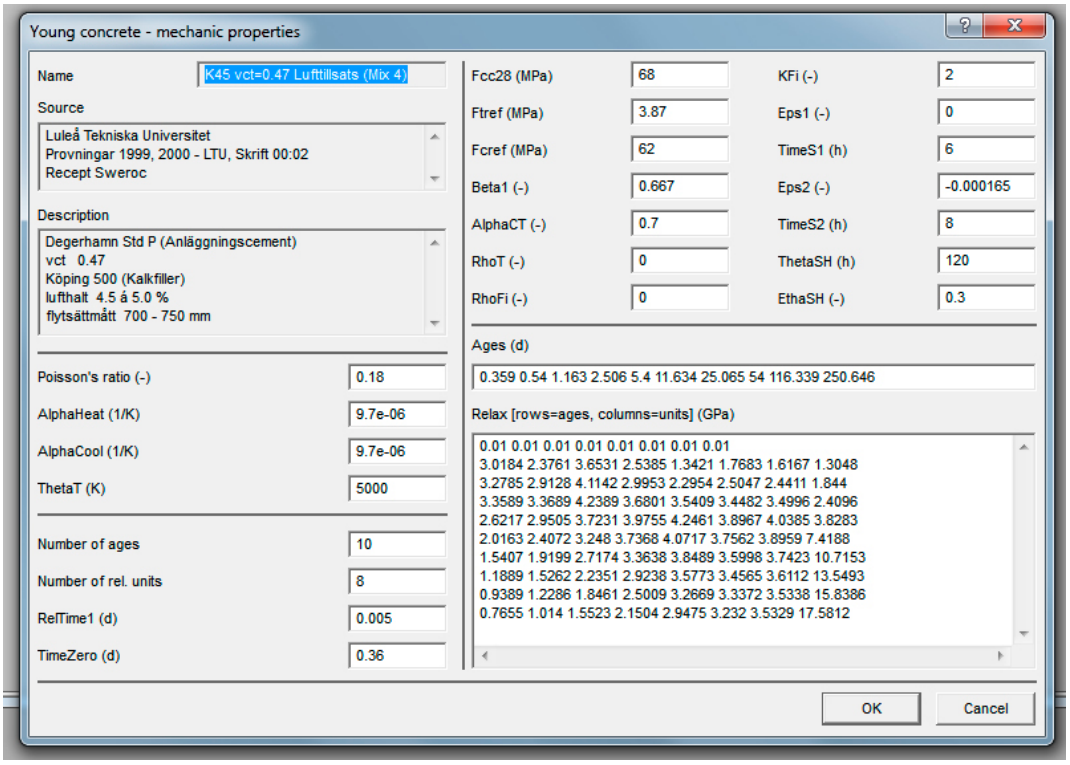

Figure A-5. *Original stress parameters for SCC with w/c of 0.47. For denotation, see previous section.*

A4 Adaption of basic material parameters

A4.1 Input data

Geometry and boundary conditions

The exact dimensions of the test casting were modelled and meshed in Software ConTest Pro. Figure A-6 displays the FE-mesh.

The boundary conditions in the simulation are summarized in Table A-1. The thermal properties of the fresh concrete are displayed in Figure A-4.

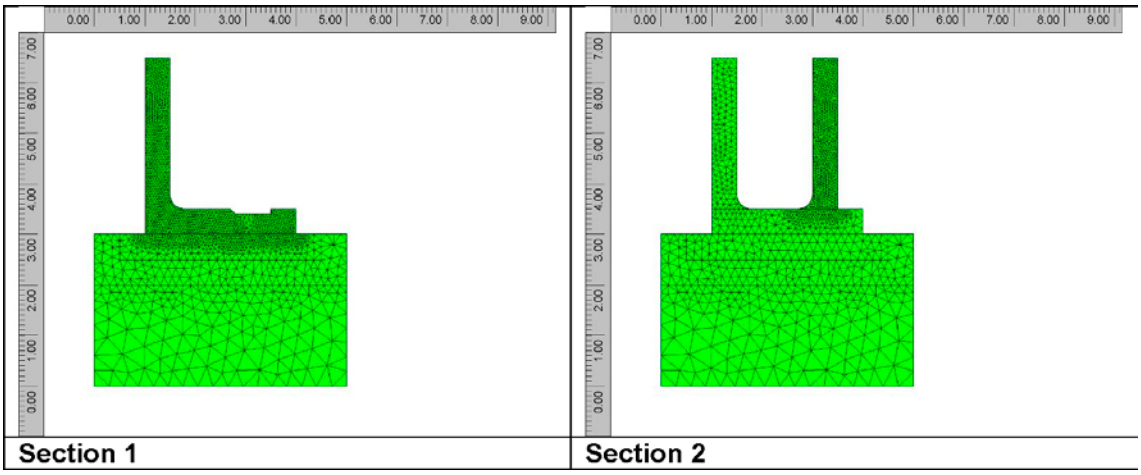

Figure A-6. *FE-mesh in the models for section 1 and section 2.*

Table A-1. Boundary conditions for the analysis.

Boundary/material	Thickness (mm)	Wind speed (m/s)	Conductivity/HTC (W/m K)/(W/m² K)	Density (kg/m³)	Heat capacitivity (J/kg K)
Free surface	–	2	13.0		
Plywood 21 mm (wall)	21	2	4.46		
Plywood 18 mm (on top of the slab)	18	2	4.93		
Plywood 40 mm (fillets and box-out for wall 2)	40	2	2.78		
Rock	–	–	3.7	2650	850
Gravel	–	–	2.1	2200	1400
Mature concrete	–	–	1.7	2350	1000

A4.2 Casting of section 1

Temperature

The temperature measurements from the thermocouple setup was used for evaluation, see Table A-2, Figure A-7 and Figure A-8. Sensors #4, #5 and #6 were chosen for the slab and sensors #10, #11 and #12 for the wall. This is due to the similar starting temperature (temperature of the fresh concrete) which simplifies the analysis. The temperature increase for the boundaries after casting until 72 hours after casting fits temperature readings from castings section 2. A slight increase in the temperature of the mature concrete in wall 1 was noticed after casting section 2. This can only result from an increase in the air temperature in TAS05 due to heat of hydration and machinery.

Table A-2. Temperatures used in the analysis. Linear interpolation is done automatically in the used software. Calculation time 1 000 h.

Boundary	Time (h)	Temperature (°C)
Air, formwork	0	18
	24	20
	48	20
	72–1 000	17
Rock, gravel, mature slab	0–1 000	17
Fresh concrete	0	18

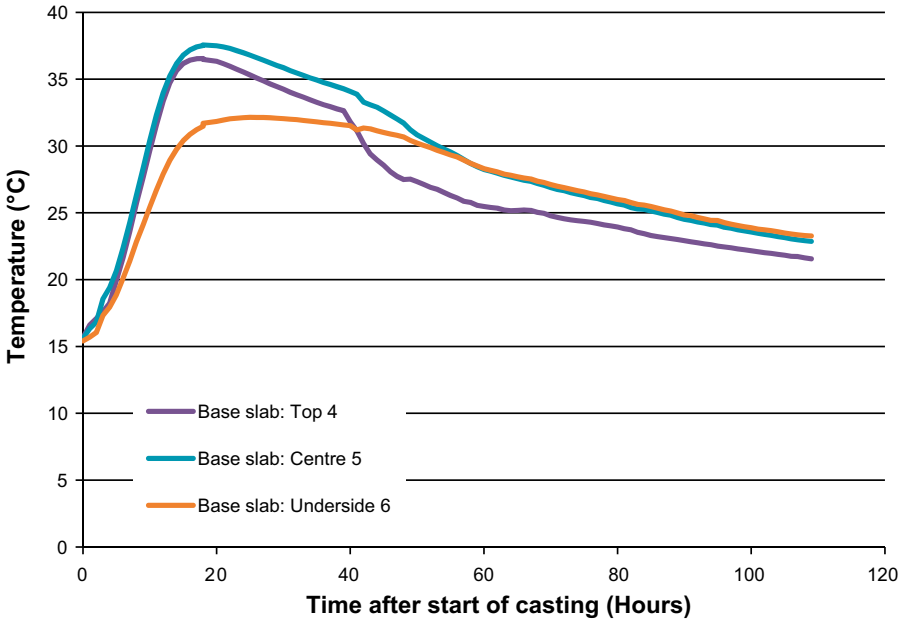

Figure A-7. Temperature in the base slab until 108 hours after start of casting.

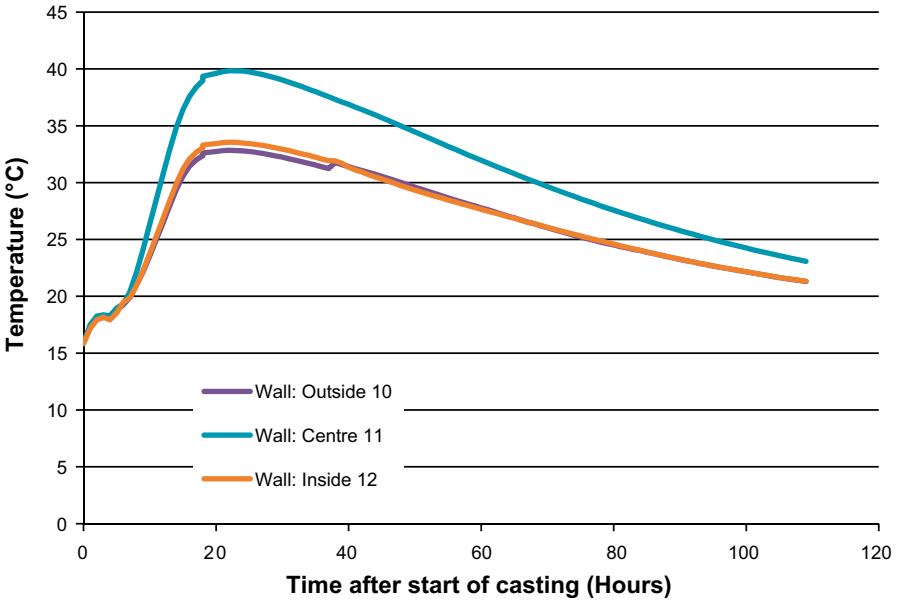

Figure A-8. *Temperature in the walls until 108 hours after start of casting.*

Strain

The results from the strain measurements are inconsistent; see Figure A-9 to Figure A-11. Neighbouring sensors which should display comparable readings differ greatly. Some sensors register a slight tension before turning towards compression at the beginning of the measurement, whereas others do not. There is no explanation for this behaviour except possible disturbance by casting and vibration of the concrete. All sensors show an extremely rapid increase of compressive strain with increasing temperature in the initial stages of hydration. This is typical for strain measurements on hardening concrete. However, the recorded values in strain do not fit the registered temperature increase of about 20 °C. At full restraint, this temperature increase would equal a maximum possible strain of about −200 µm/m (the thermal expansion coefficient of concrete is approximately 10^{-6} and the temperature increase is around 20 °C). In the present study, strain values of up to −350 µm/m were registered. The reason for this phenomenon cannot be investigated further within the limitations of this study.

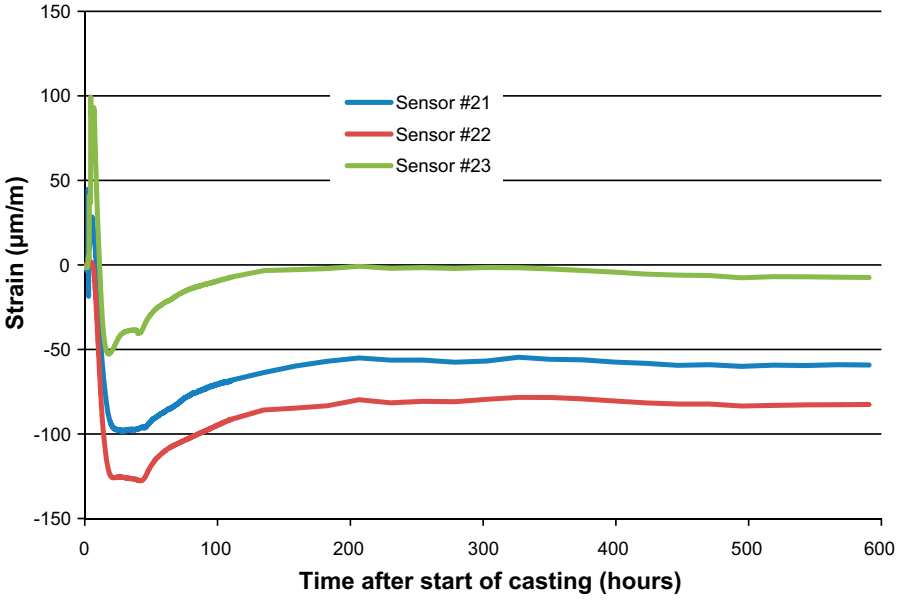

Figure A-9. *Strain results for the base slab of section 1.*

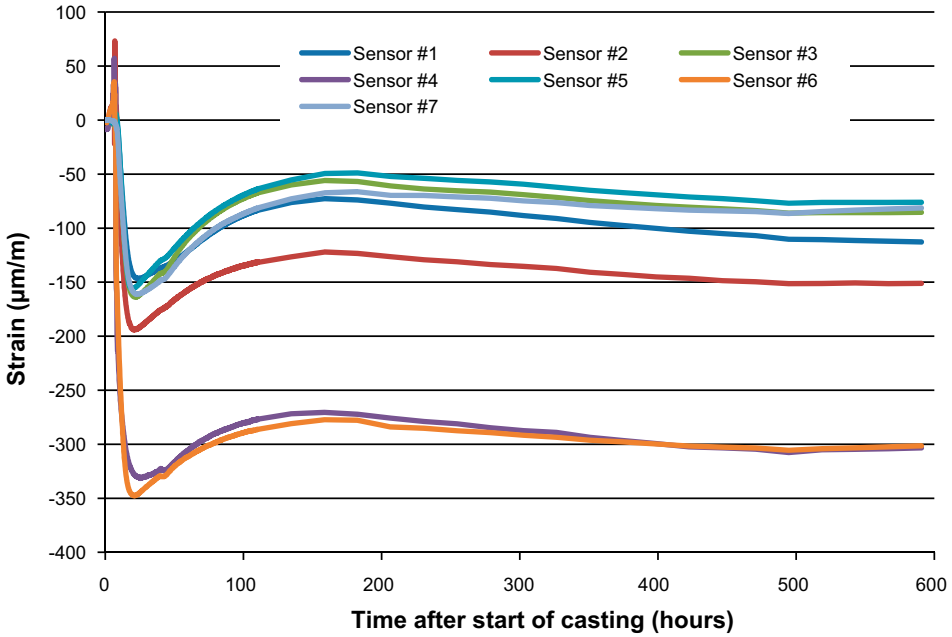

Figure A-10. *Strain results for the lower part of the wall of section 1.*

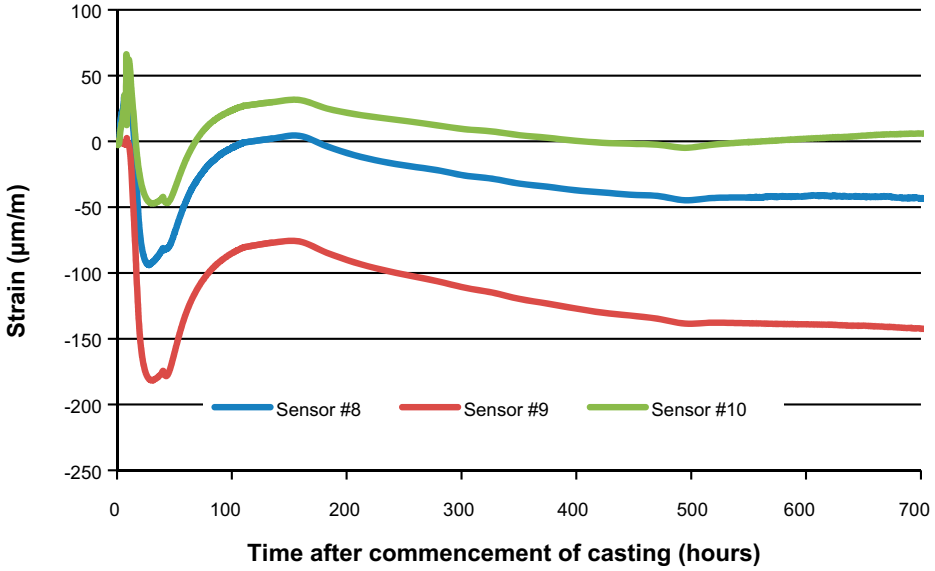

Figure A-11. *Strain results for the wall of section 1 about 500 mm below the top of the wall.*

Due to the problems with the evaluation of the strain measurements, three combinations of temperature and strain that seem "most logic" have been chosen for base slab, lower wall and upper wall (see Figure A-12 to Figure A-14). These are the measurements with the least disturbance in the beginning. Observe that, as explained earlier, the measured strain increase in compression for the actual restraint situation does not really fit the temperature increase. The registered strain in compression is in between 120 µm/m for the base slab and 170 µm/m for the upper wall. This would equal a restraint of 0.60 and 0.85 respectively.

However, according to theory, the restraint for the slab in the actual situation is not higher than 0.1 to 0.2 due to friction from the underground. The restraint for lower and upper wall should therefore be even lower since these parts are cast together with the slab but have a larger distance from the ground (origin of restraint). Typically, the restraint is lower in the top part of a wall.

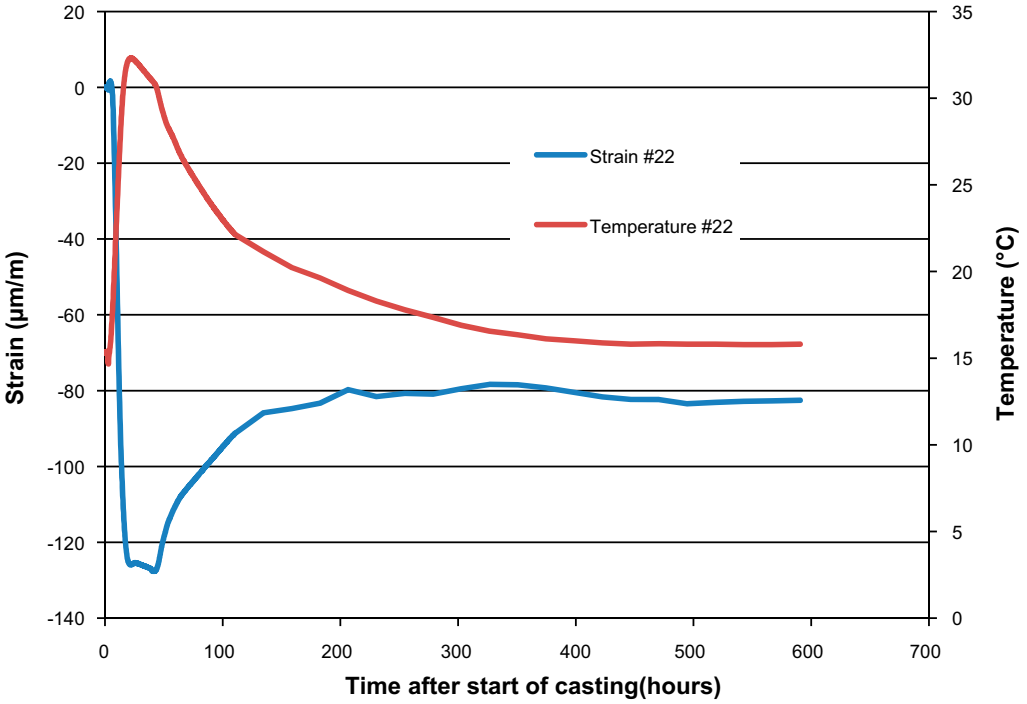

Figure A-12. *Chosen strain measurement for the base slab.*

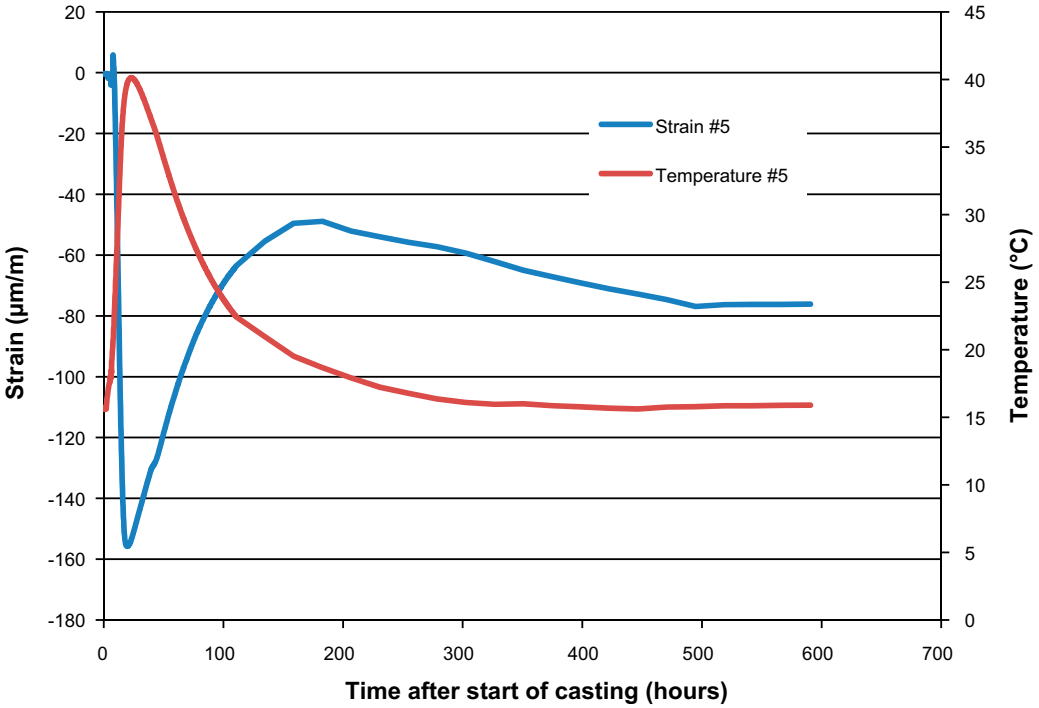

Figure A-13. *Chosen strain measurement for the lower part of the wall.*

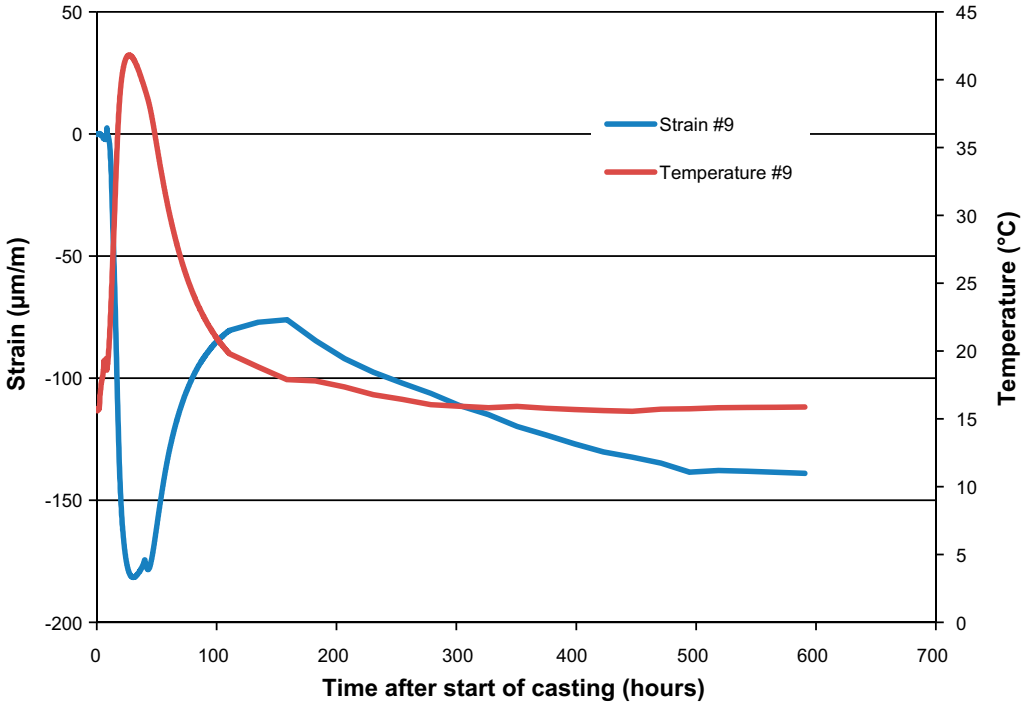

Figure A-14. Chosen strain measurement for the upper part of the wall.

A4.3 Casting of section 2

Temperature

The temperature measurement results from the thermocouple setup was used for evaluation, see Table A-3, Figure A-15 and Figure A-16. Sensors #13, #14 and #15 were chosen for the wall and sensor #20, for the joint. An increase in temperature was noticed in the wall of section 1 after casting section 2. This is considered by increasing the temperature in the boundaries from 24 hours after casting until 72 hours after casting. The 24 hours delay is due to the retardation of the concrete used for casting section 2.

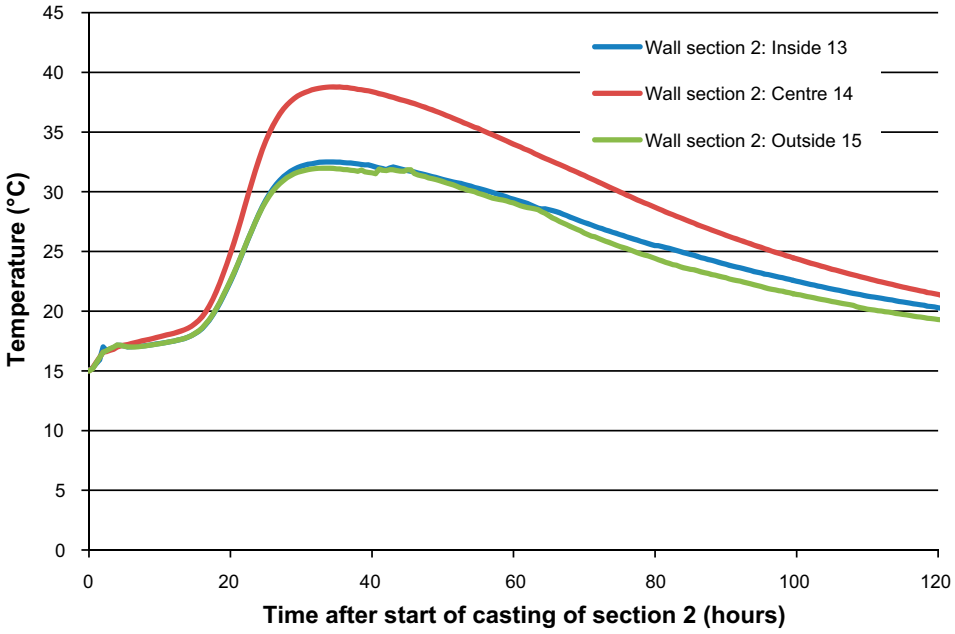

Figure A-15. Temperature results for the lower wall until 120 hours after casting started.

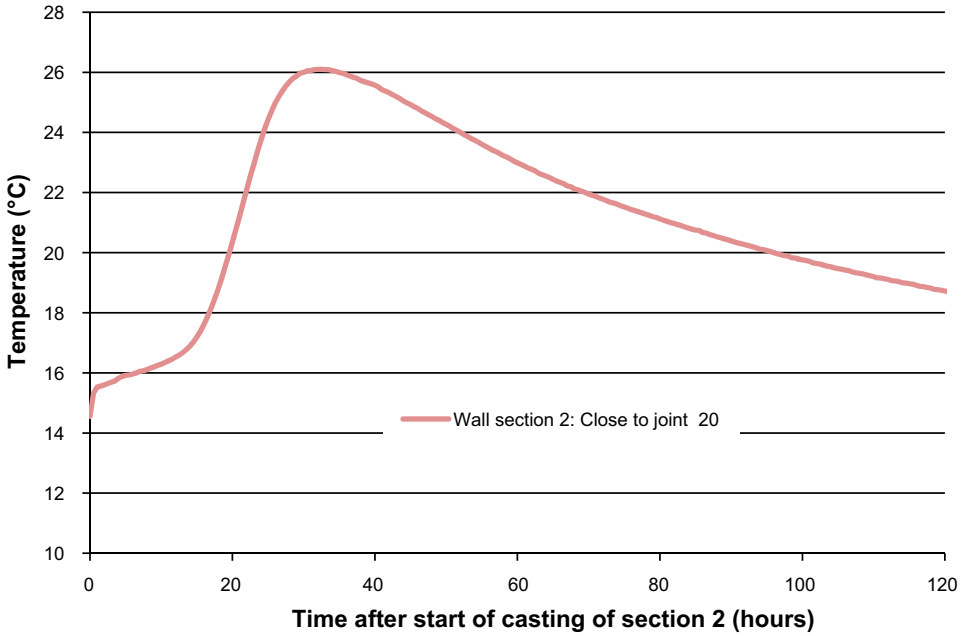

Figure A-16. *Temperature results for the lower wall about 750 mm above the joint until 120 hours after casting started.*

Table A-3. Temperatures used in the analysis. Linear interpolation is done automatically in the used software. Calculation time 1 000 h.

Boundary	Time (h)	Temperature (°C)
Air, formwork	0	18
	24	18
	48	20
	72	20
	96–1 000	16
Rock, gravel, mature slab	0–1 000	16
Fresh concrete	0	16

Strain

The problems with the strain measurements observed for section 1 occur also in section 2. The results from the strain measurement are inconsistent; see Figure A-17 and Figure A-18. Neighbouring sensors which should display comparable readings differ greatly. Some sensors register a slight tension before turning towards compression at the beginning of the measurement, some do not. There is no explanation for this behaviour except possible disturbance by casting and vibration of the concrete. All sensors show an extremely rapid increase of compressive strain with increasing temperature in the initial stages of hydration. This is typical for strain measurements on hardening concrete. The recorded values in strain fit the registered temperature increase of about 20 °C somewhat better, compared to section 1. At full restraint, this temperature increase would equal a maximum possible strain of about −200 μm/m. However, the wall is not subjected to 100 % restraint. According to theory, the present situation (length/height, slab width, length of the wall) would equal a restraint of 0.5 to 0.6 at the bottom of the wall and 0 to 0.25 at the top of the wall. These values can either be calculated using elastic 3D FEA or be found in the literature.

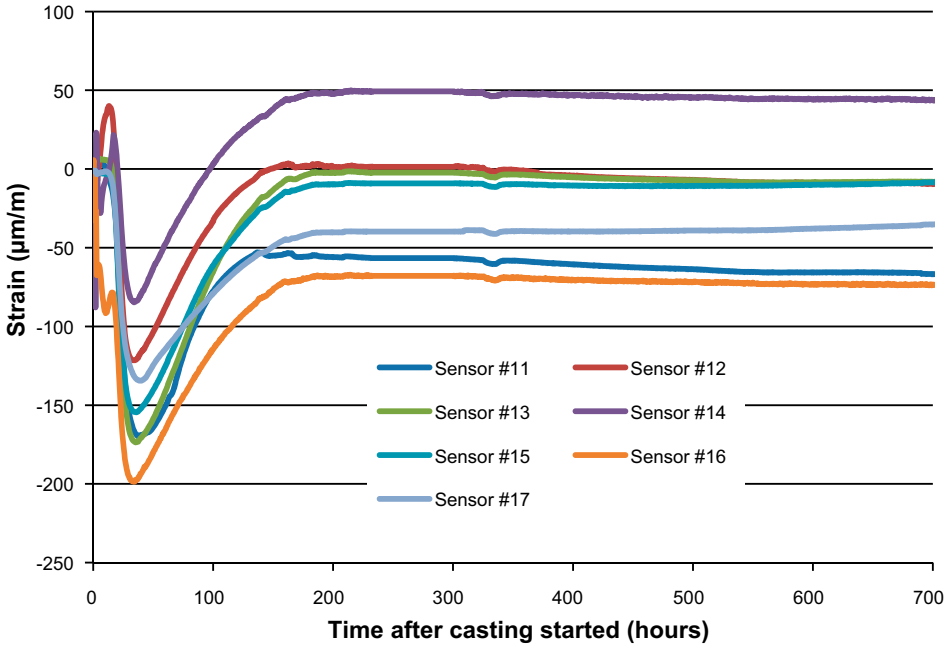

Figure A-17. *Strain results for the lower part of the wall, section 2 about 750 mm above the joint.*

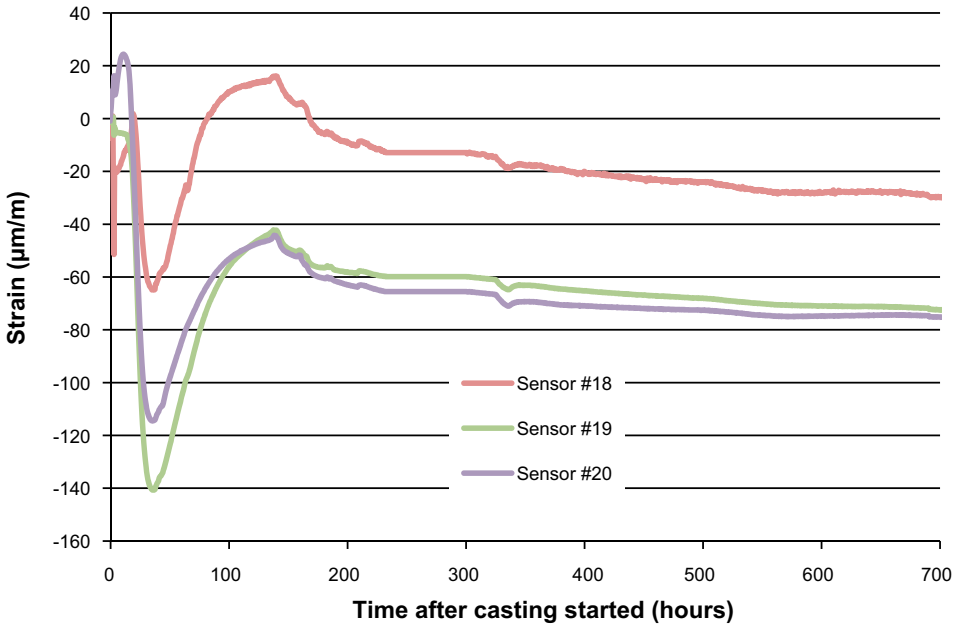

Figure A-18. *Strain results for the upper wall, section 2, about 500 mm below the top of the wall.*

The measurements with the least disturbance in the beginning were chosen for evaluation. Observe that, as explained earlier, the measured strain increase in compression for the actual restraint situation does not really fit the temperature increase. The registered strain in compression is in between 160 µm/m for the lower wall and 140 µm/m for the upper wall. This would equal a restraint of 0.80 and 0.70 respectively. According to theory, the present situation would equal a restraint of 0.5 to 0.6 at the bottom of the wall and 0 to 0.25 at the top of the wall. If the restraint were in fact as high as 0.80, the wall would most likely have cracked. However, no cracks were indicated by cracking events in the logged strain measurements or by visual inspection.

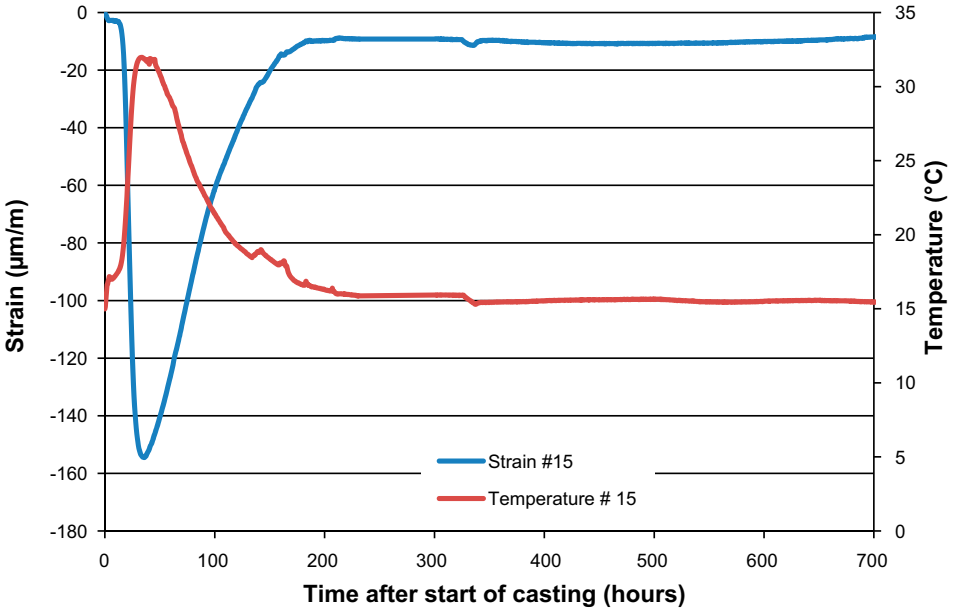

Figure A-19. *Chosen strain measurement for the lower part of the wall, sensor #15.*

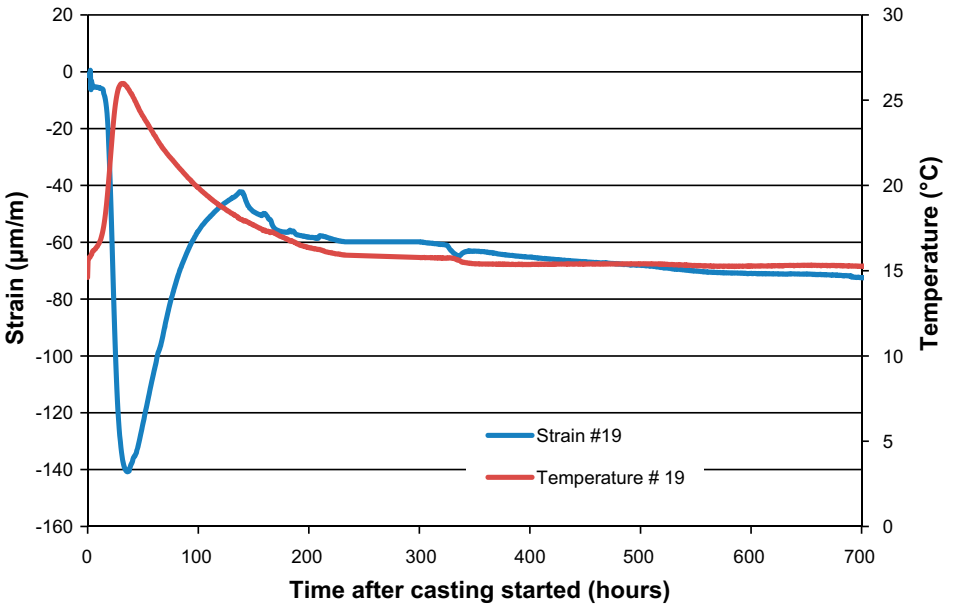

Figure A-20. *Chosen strain measurement for the upper part of the wall, sensor #19.*

A5 Adaption of heat parameters, calculated values and comparison with measurements

A5.1 Section 1

By adjusting the values for Wc and BetaD, the calculated heat development and the measured temperature were fit in an iterative process. This was necessary since no data regarding heat of hydration or other parameters required for parametrization were available. BetaD is called the acceleration factor and is commonly used to adjust the calculated heat development for accelerating admixtures or additions. Wc describes the total heat developed by the cement. Using a BetaD of 2.0 and reducing Wc to 250 000 J/g resulted in comparable temperature development in simulation and measurement.

Calculated and measured temperatures are compared in Figure A-21 and Figure A-22. The fit for the maximum temperature developed is good for both slab and wall. The bottom sensor in the slab can be calculated satisfactory too. A somewhat larger difference is noted for the sensors close to the top of the slab and close to the formwork. This is not uncommon when comparing measured and calculated values. It may be due to effects like heat agglomeration between formwork stiffeners or increased heat flow through metal formwork parts. These effects are difficult to incorporate in a simulation.

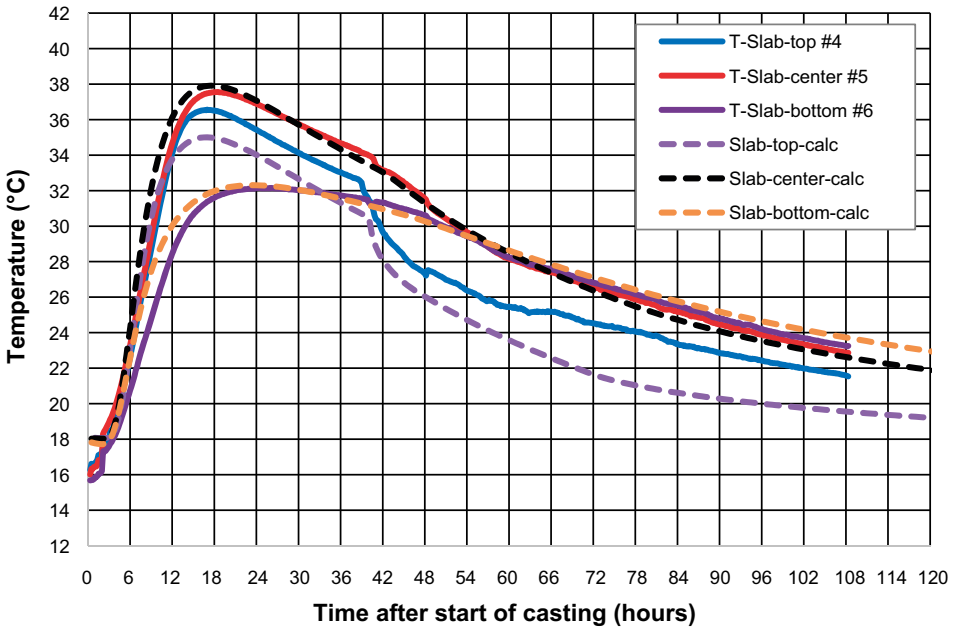

Figure A-21. *Comparison of measured and calculated temperature for the slab, section 1.*

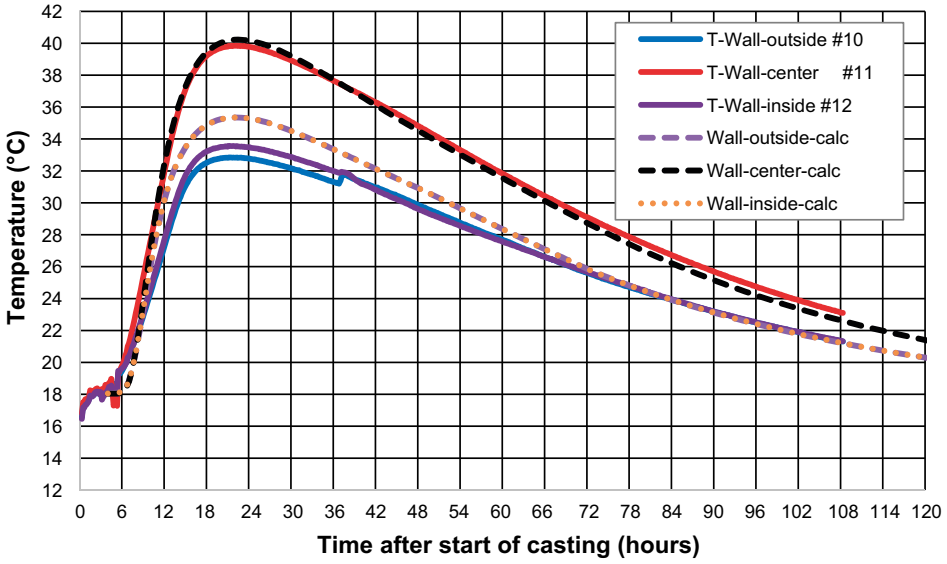

Figure A-22. *Comparison of measured and calculated temperature for the wall, section 1. Please note that "wall-outside-calc" and "wall-inside-calc" partly cover each other.*

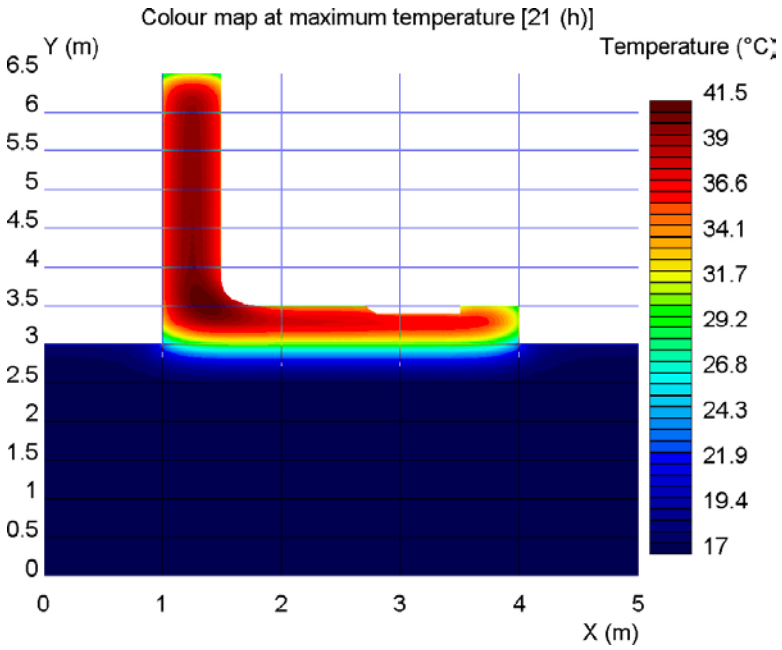

Figure A-23. *Simulated maximum temperature in section 1.*

A5.2 Section 2

The heat parameters for Wc and BetaD were not changed when simulating section 2. The starting temperatures had to be adjusted to fit the surrounding conditions, see Table A-3. One material parameter, te0, was adjusted to include the effect of the increased retarder dosage. Te0 just moves the start of the hydration process parallel in time, thus representing a retarder when used with negative sign.

The simulation of section 2 can thus be seen as validation for the adjusted heat parameters. Again, the maximum temperature is very close in simulation and measurement. The deviation close to the formwork is comparable to section 1. The temperature development close to the joint could be simulated with acceptable result.

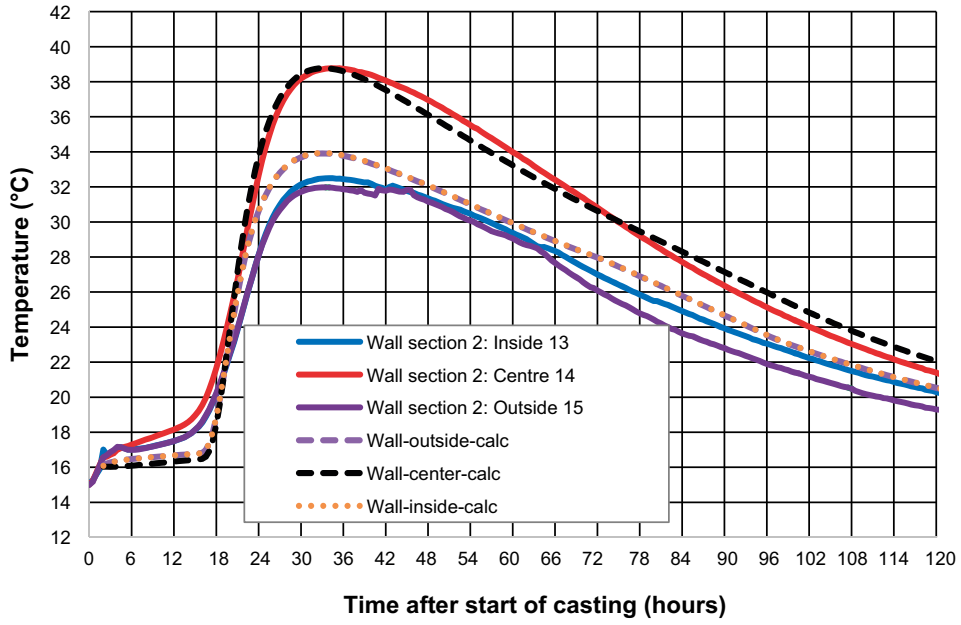

Figure A-24. *Comparison of measured and calculated temperature for the wall, section 2.Please note that "wall-outside-calc" and "wall-inside-calc" partly cover each other.*

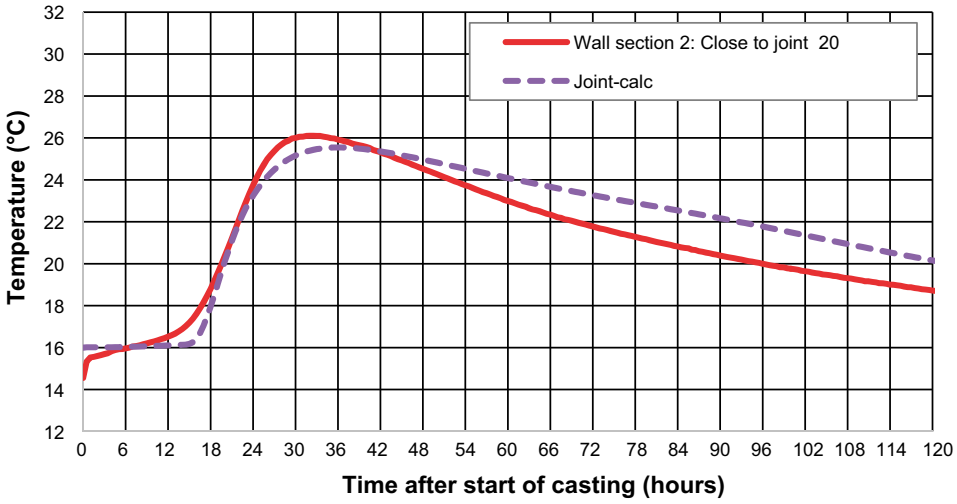

Figure A-25. *Comparison of measured and calculated temperature for the joint, section 2.*

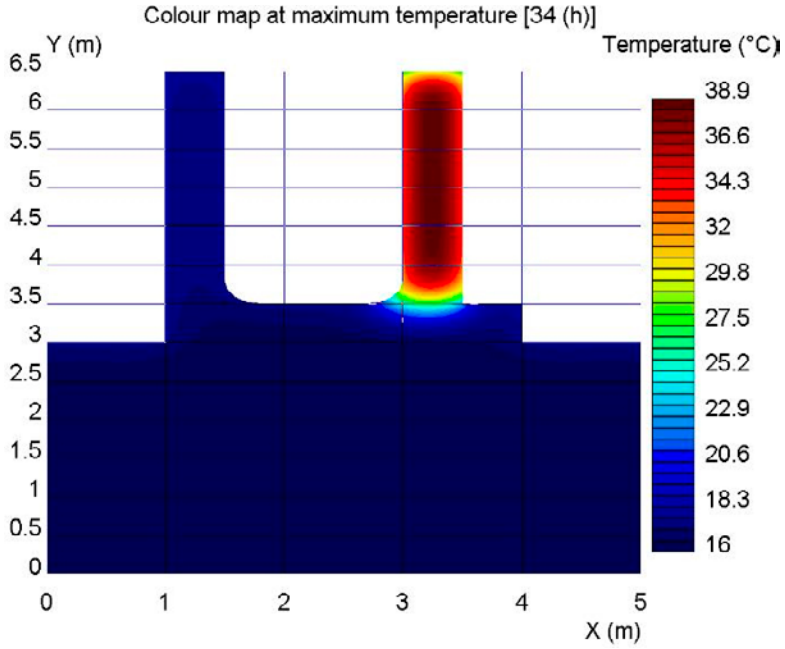

Figure A-26. *Simulated maximum temperature in section 2.*

A5.3 Final heat parameters

The heat development of the concrete used in the test castings can be satisfyingly simulated in ConTest Pro, using the parameters in Figure A-27. Using the tested parameters of a self-compacting concrete as starting points simplified the process. When attempting to simulate structures with a different geometry under different environmental conditions, one can expect to achieve a good prediction of the actual heat development when using these parameters.

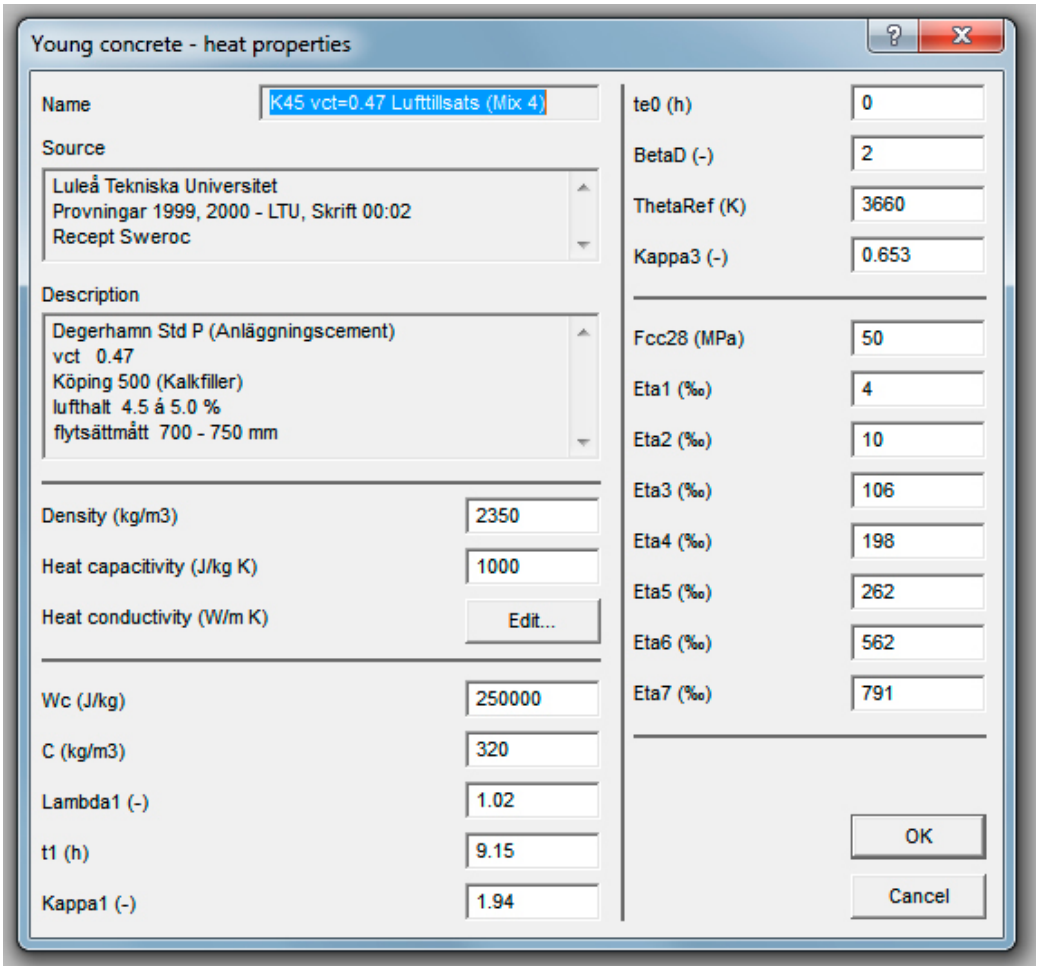

Figure A-27. *Deduced heat parameters.*

A6 Strain calculation and comparison with measurements

Inspections showed that no cracks had formed in the concrete structures during the period until the start of the stress test. This was verified both by visual inspections and from the strain measurements where cracking would be indicated by sudden changes in the measured strain.

A6.1 Section 1

Due to the inconsistent nature of the results from strain measurements, only an indicative comparison of measurement and simulation is possible.

The restraint situation for section 1 was modelled without any restraint from the underlying slab. This is justified by that the smooth surface of the underlying slab and double friction reducing layers in between the old and newly cast structure.

In the simulation, the strain is expressed as strain ratio, i.e. the ratio between actual strain and strain capacity of the concrete in a timeline. Figure A-28 to Figure A-30 show the results. The general shape alignment of the measured and simulated curves is good for the lower wall but differs quite a lot for slab and upper wall. Observe that the actual values are not even close in measurement and simulation, i.e. there is no tension measured but tension is simulated for example in the lower wall. This is due to that in the measurements; there is an unexplainable high compression during the temperature rise in the concrete.

The calculated low strain ratio is consistent with the absence of cracks. It is, however, questionable, if there really is no tension at all in the structure as the measurements indicate.

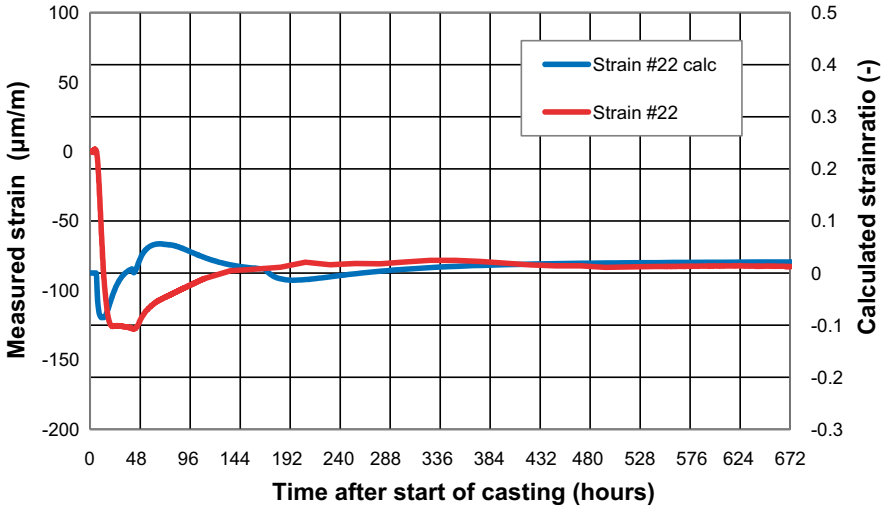

Figure A-28. *Comparison between measured and calculated strain for the slab, section 1.*

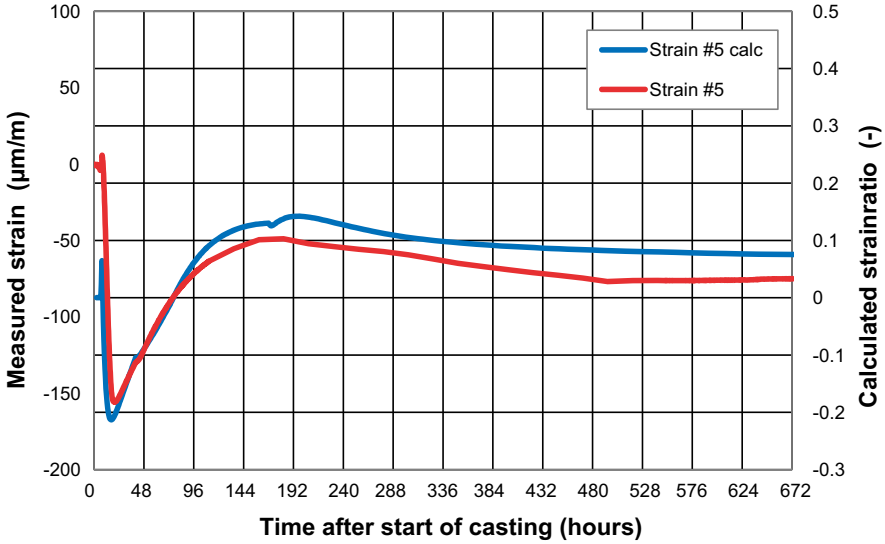

Figure A-29. *Comparison between measured and calculated strain for the lower part of the wall, section 1.*

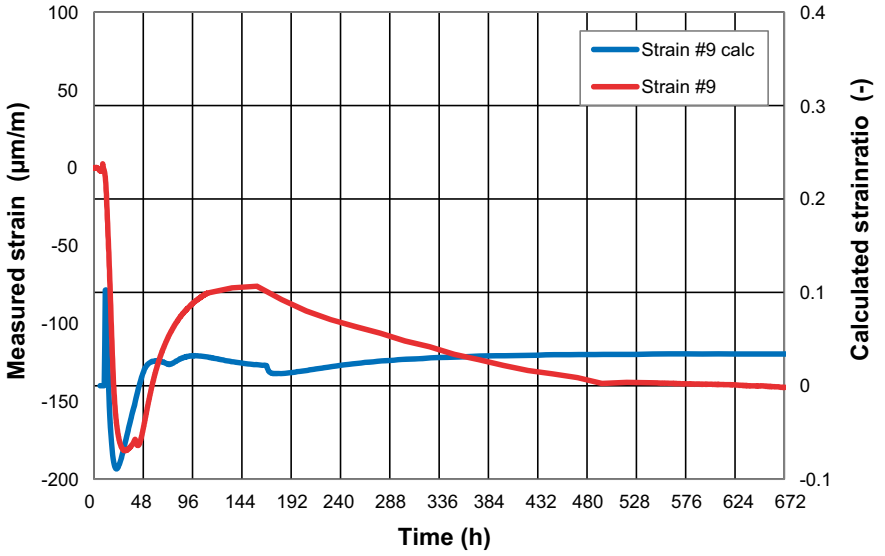

Figure A-30. *Comparison between measured and calculated strain for the upper part of the wall, section 1.*

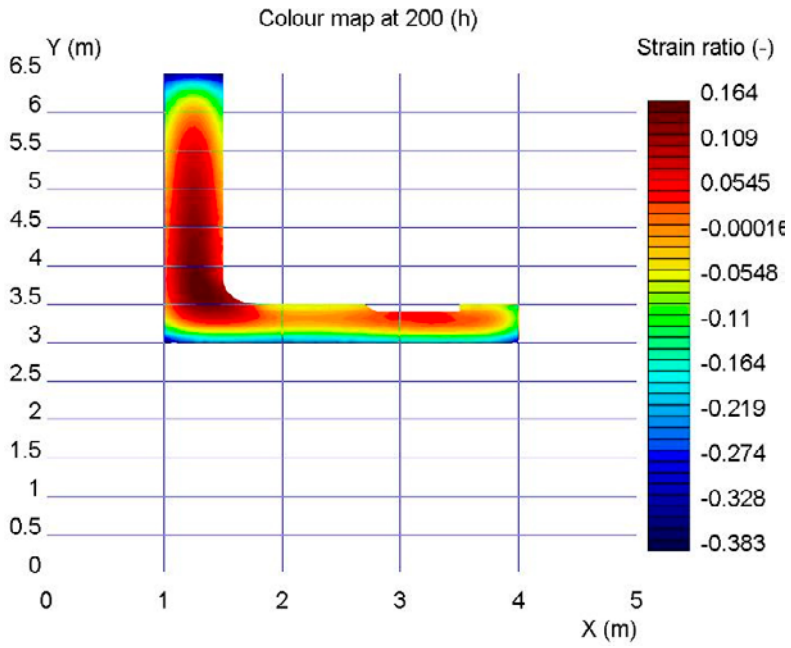

Figure A-31. *Simulated maximum strain ratio in the cross section, section 1.*

A6.2 Section 2

The restraint for section 1 was modelled according to experience since the strain measurements could not be used to calculate a degree of restraint. This is due to the inconsistent results of the strain measurements. The entire base slab was used as restraining part for the simulation of the stresses in section 2. This is on the safe side.

The comparison of simulation and measurement is displayed in Figure A-32 and Figure A-33. The general shape of the measured and simulated curve is very similar for the lower wall but differs quite a lot for the upper wall. Observe that the actual values are not even close in measurement and simulation, i.e. there is no tension measured but tension is simulated for example in the lower wall. This is due to that in the measurements, there is an unexplainable high compression during the temperature rise (expansion phase) in the concrete.

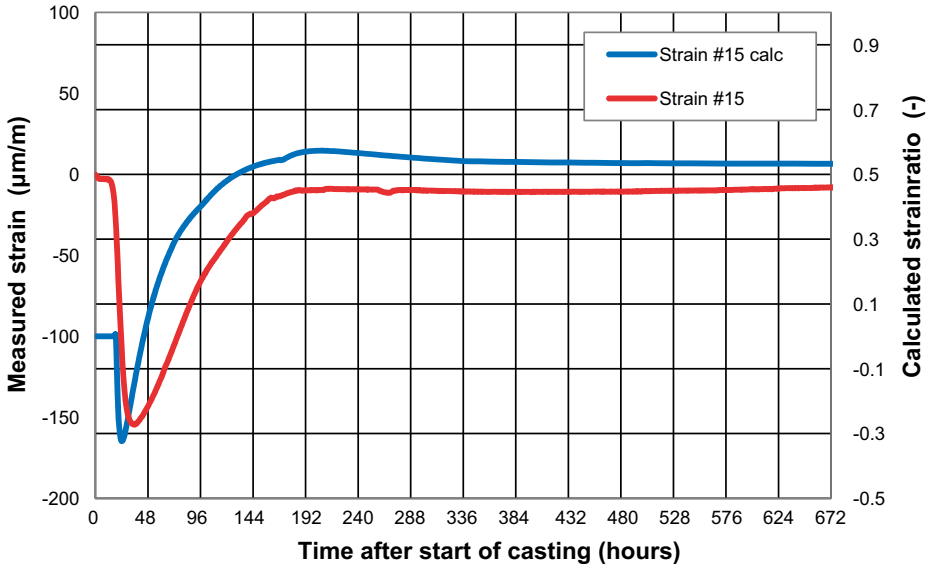

Figure A-32. *Comparison between measured and calculated strain for the lower wall, section 2.*

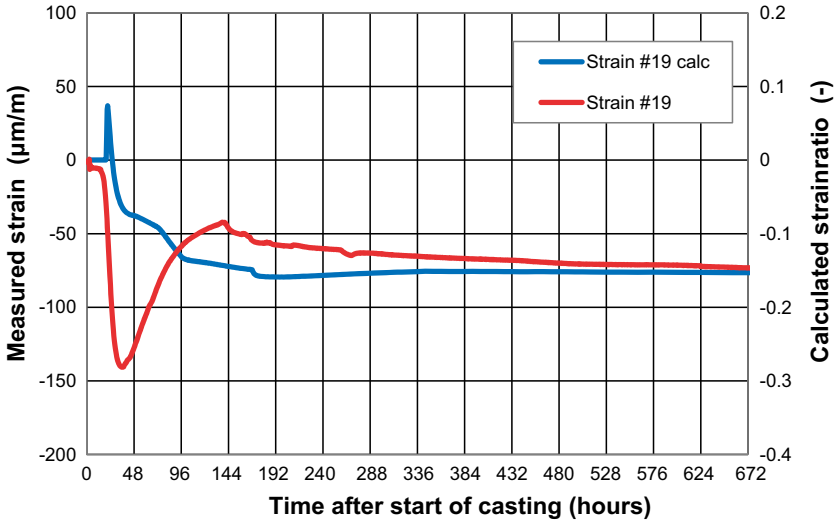

Figure A-33. *Comparison between measured and calculated strain for the upper wall, section 2.*

The difference in the shape of the blue curves (calculation) in Figure A-32 and Figure A-33 is due to that in the used software, the upper parts of the wall are according to theory in compression. In the upper part of the wall (Figure A-33), the calculation gives tension for a short period of time. This can be explained by the rising concrete height which was included into the model. This gives an age difference of the concrete over height, resulting in a higher temperature in the lower parts of the wall in the initial stages of the hydration. This temperature difference expresses itself as tension for a short period of time.

The calculated strain ratio in the lower part of the wall is around 0.60. It is known from experience that structures tend to crack if the strain ratio exceeds 0.80. Thus, the simulation is consistent with the absence of cracks. It is questionable if there really is no tension at all in the structure as most of the measurements indicate.

There is one single strain gauge in the lower part of the wall (#14) that actually registered tension, see Figure A-35. The maximum value is 48 µm/m after 200 hours. The point of time is consistent with the simulation. The actual value of 48 µm/m can be recalculated to a strain ratio, using the strain capacity value of 108 µm/m for concrete with granite aggregates from Bamforth (2007).

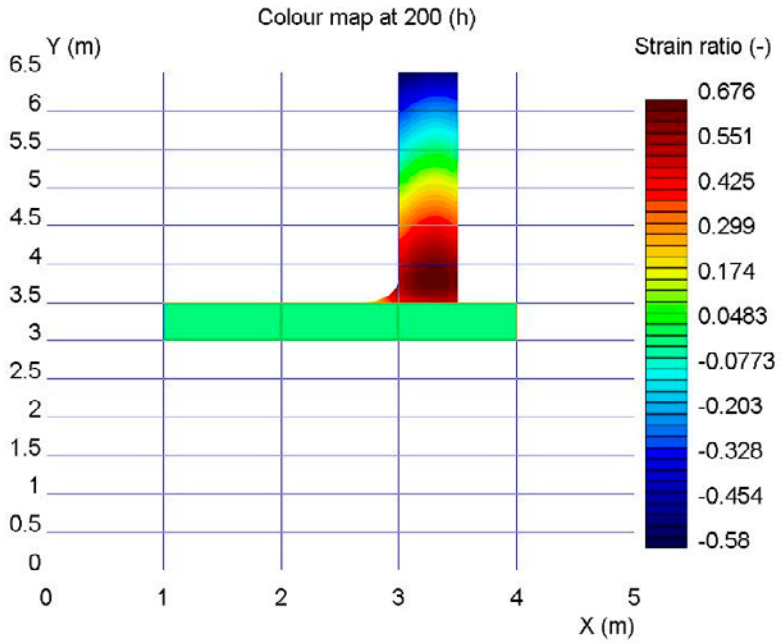

Figure A-34. *Simulated maximum strain ratio in the cross section, section 2.*

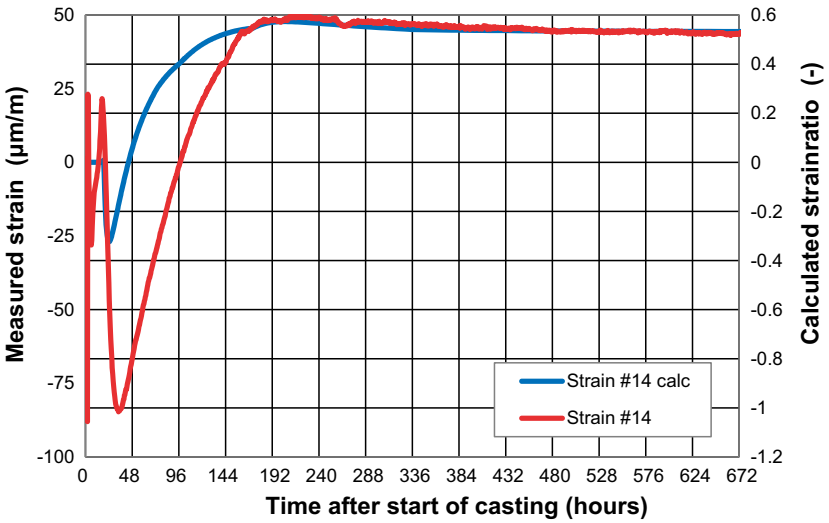

Figure A-35. *Measured and calculated strain for sensor #14.*

This would give a "measured" strain ratio of 0.44 which is not too far from the calculated value of 0.57 for the position of the strain gauge. A slight adjustment of the stress parameters would result in a better fit. However, to do so is not reliable with only one measurement.

A6.3 Final stress parameters

Only the compressive strength was changed compared to the original setup of stress parameters, see Figure A-36. Further adjustments were not possible since the strain measurements were inconsistent and did not allow for calculations of restraint or reliable analysis of the strain development. At present time, the chosen material parameters cannot be adjusted further since reliable strain measurements do not exist.

Considering the pre-warming of the planned test casting in TAS08, one can expect that modelling the restraint according to experience and existing models and using the material parameters deduced here for heat and stress, the resulting measures will be on the safe side.

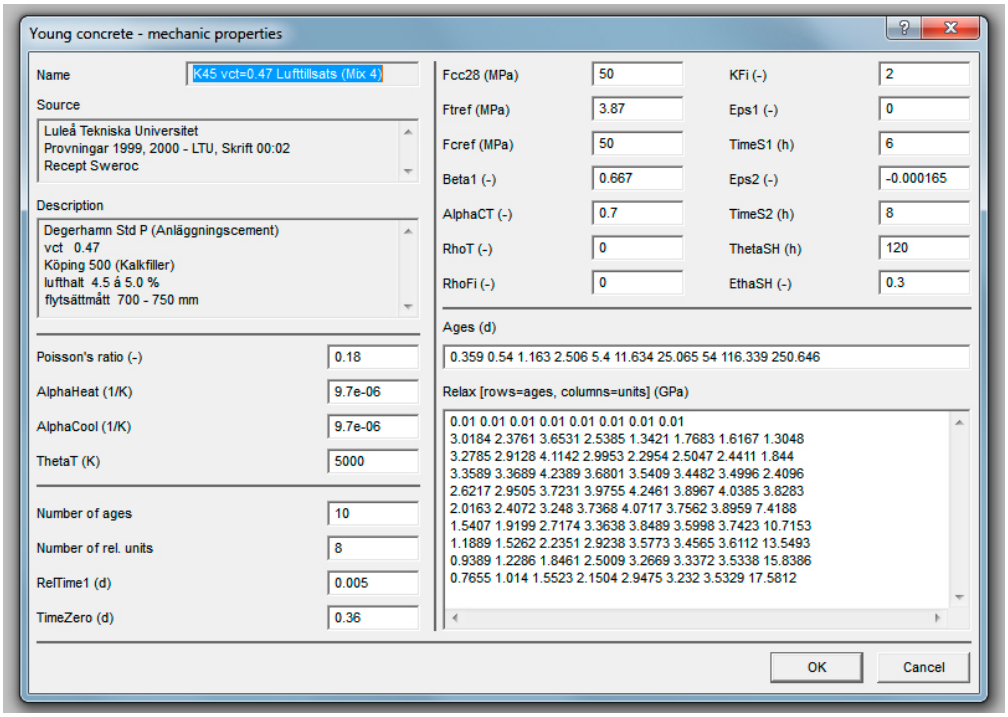

Figure A-36. *Deduced stress parameters.*

Appendix B

D:\Work\SKB\TAS05\TAS05_et1_S.CPR: Report

B1 Software and project information

B1.1 Software

System name: ConTeSt System version: 1.0
Developed by: JEJMS Concrete AB

B1.2 Project

Original filename: D:\Work\SKB\TAS05\TAS05_et1_T.CPR Created: 2018.06.01 12.34.11
Created by: swecvo on CNU21810QY
Current filename: D:\Work\SKB\TAS05\TAS05_et1_S.CPR Last change: 2018.06.06 22.15.54
Last change by: swecvo on CNU21810QY

B2 Geometry and time

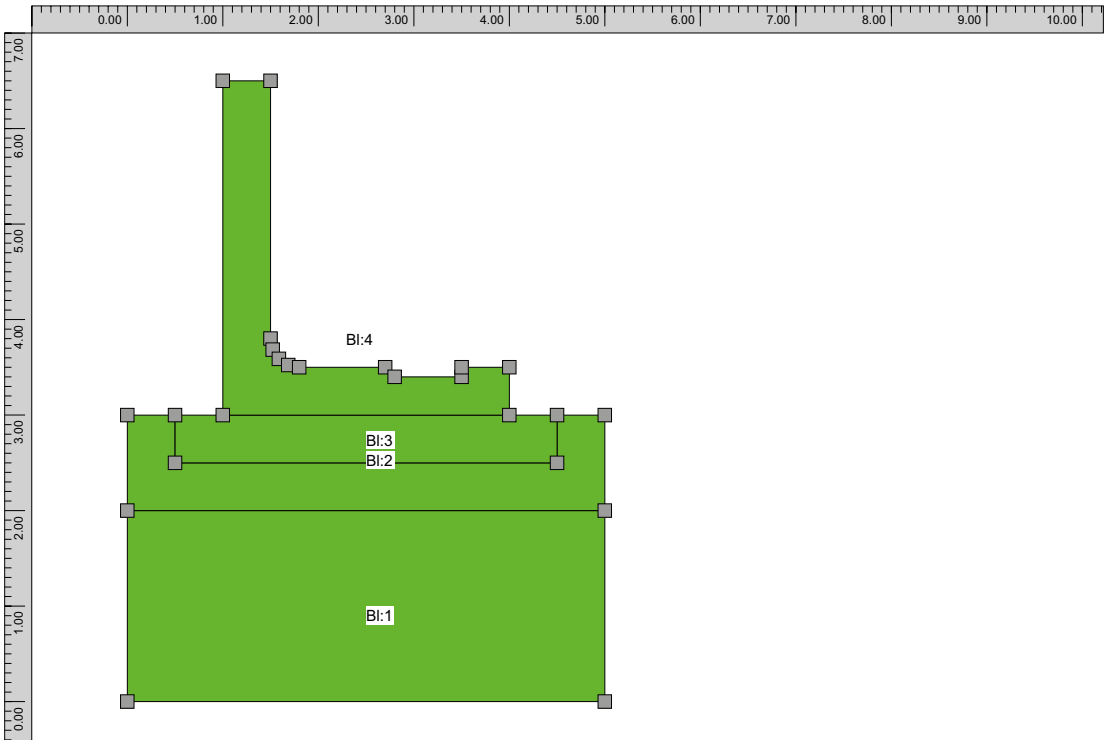

Figure B-1. *Geometry of section 1.*

B2.1 Description

B2.1.1 Blocks

Block 1: (5.000;0.000) - (5.000;2.000) - (0.000;2.000) - (0.000;0.000)

Block 2: (0.000;3.000) - (0.000;2.000) - (5.000;2.000) - (5.000;3.000) - (4.500;3.000) - (4.500;2.500) - (0.500;2.500) - (0.500;3.000)

Block 3: (0.500;2.500) - (4.500;2.500) - (4.500;3.000) - (4.000;3.000) - (1.000;3.000) - (0.500;3.000)

Block 4: (4.000;3.000) - (4.000;3.500) - (3.500;3.500) - (3.500;3.400) - (2.800;3.400) - (2.700;3.500) - (1.800;3.500) - (1.685;3.523) - (1.588;3.588) - (1.523;3.685) - (1.500;3.800) - (1.500;6.500) - (1.000;6.500) - (1.000;3.000)

B2.1.2 Computation time

Total time length: 1 000 (h)

B3 Element size

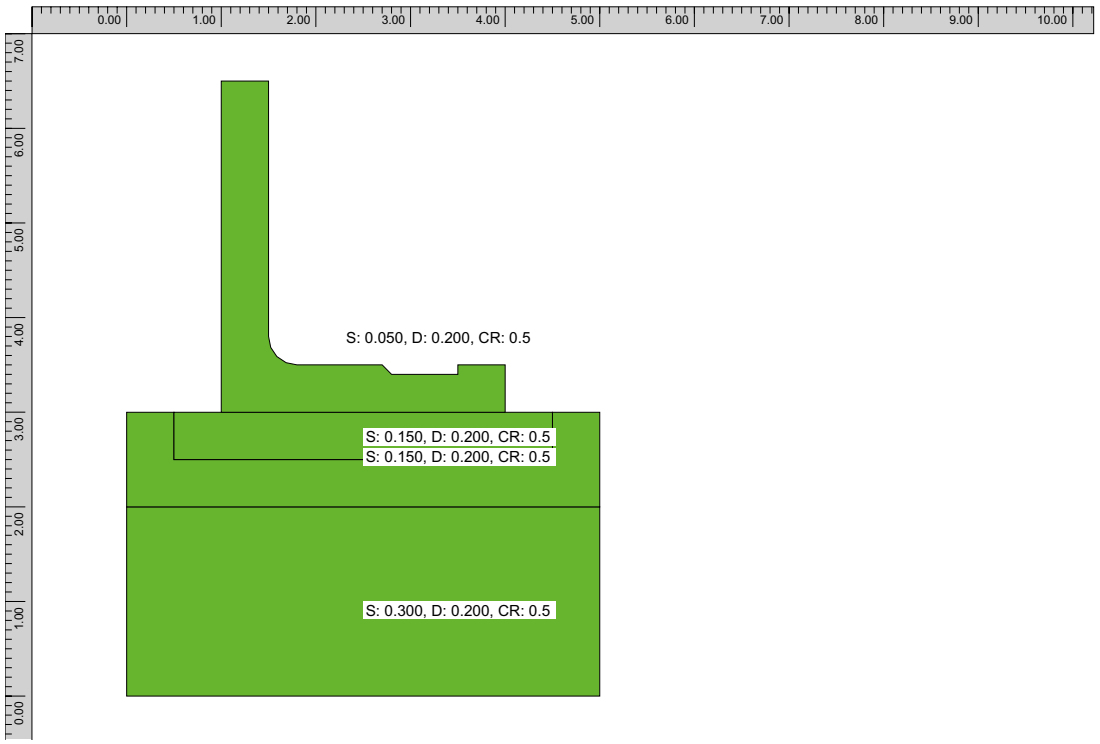

Figure B-2. *Element size for meshing, section 1.*

B4 Computation mesh

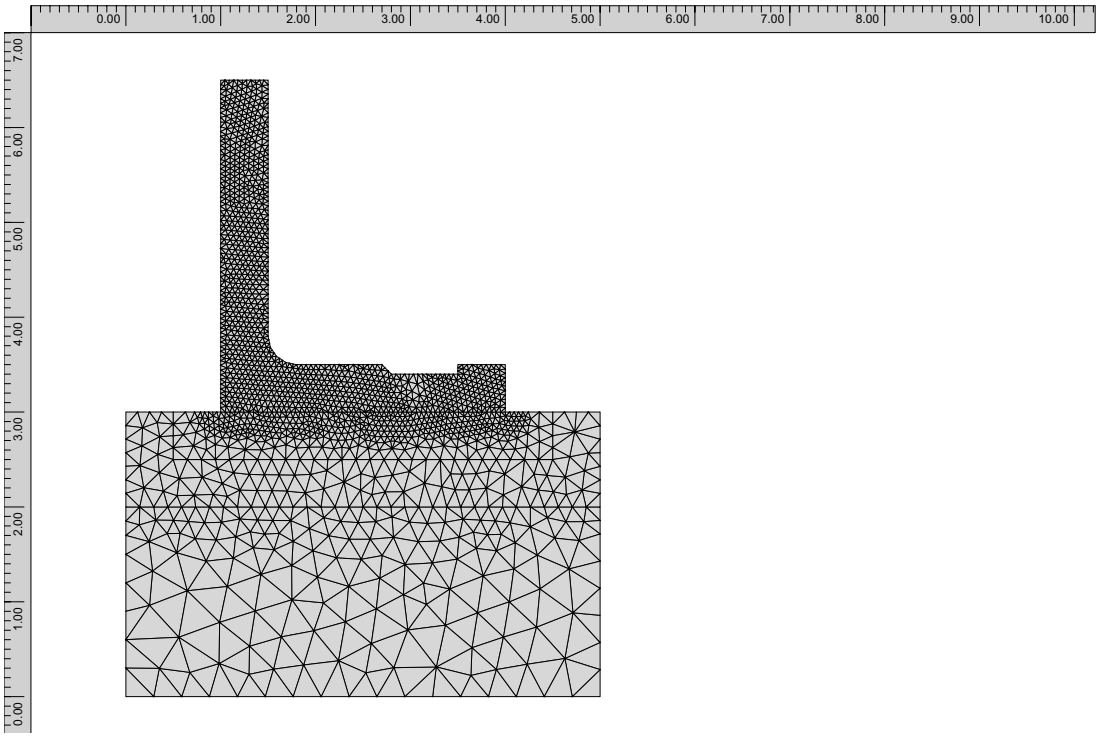

Figure B-3. *Finite element mesh for section 1.*

B5 Heat properties

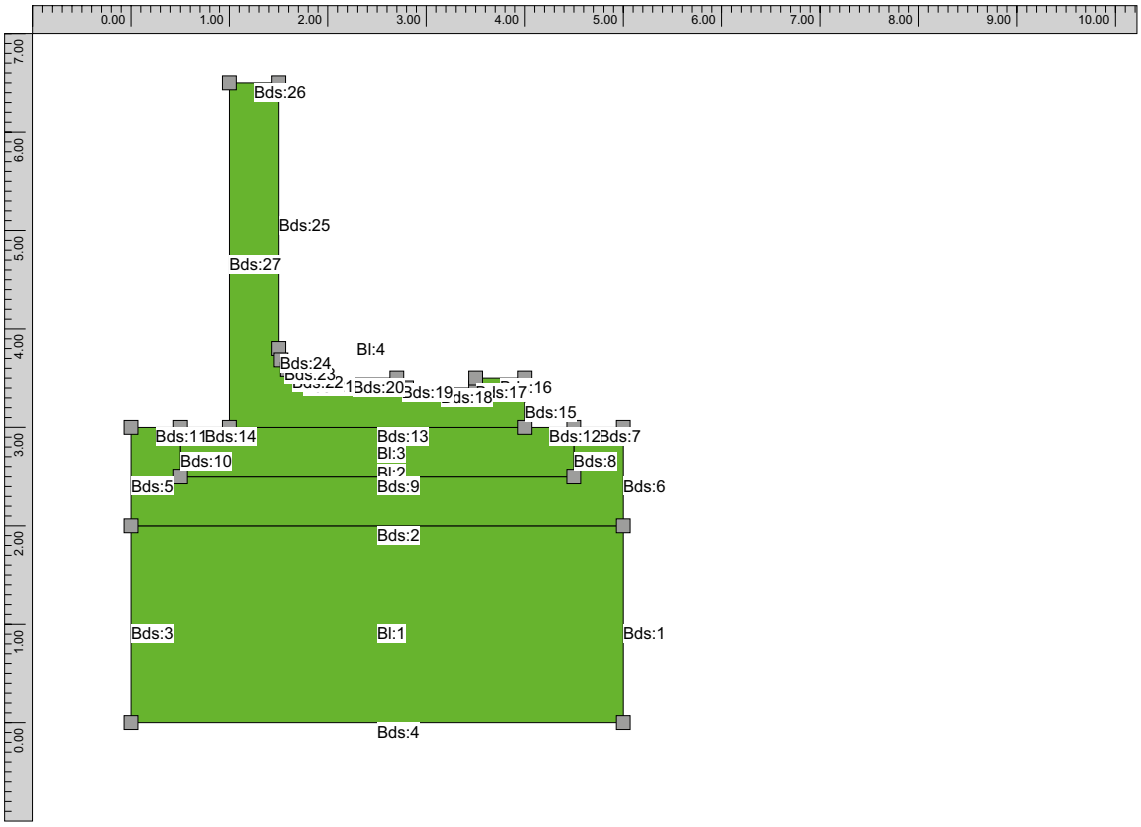

Figure B-4. *List of boundaries, section 1.*

B5.1 Description

B5.1.1 Block type list

SCC-mod-TAS05: Young concrete Start temperature:

Constant: 18.0

Material definition: K45 vct = 0.47 Lufttillsats (Mix 4) (str) Source

Luleå Tekniska Universitet

Provningar 1999, 2000 – LTU, Skrift 00:02 Recept Sweroc

Description

Degerhamn Std P (Anläggningscement) vct 0.47

Köping 500 (Kalkfiller)

lufthalt 4.5 á 5.0 %

flytsättmått 700–750 mm Original material parameters

Density: 2 350 (kg/m³), Heat cap. 1 000 (J/(kg·K))

Heat cond. (W/m²K) as piece-wise linear function of equivalent time of maturity (h), (equ. time; heat cond.): (0;2.1), (12;2.1), (24;1.7), (10000;1.7),

C 363 (kg/m³), Wc 325000 (J/kg), Lambda1 1.02 (-), t1 9.15 (h), Kappa1 1.94 (-)

te0 0 (h), BetaD 1 (-), ThetaRef 3660 (K), Kappa3 0.653 (-)

Eta6 4 (‰), Eta8 10 (‰), Eta12 106 (‰), Eta18 198 (‰), Eta24 262 (‰), Eta72 562 (‰), Eta168 791 (‰)

Fcc28 68 (MPa)

Following material parameters are changed by the user

C 320 kg/m3

Wc 250 000 (J/kg)
BetaD 2 (-)
Fcc28 50 (MPa)

mature concrete: Other material Start temperature:
Constant: 17.0
Material definition: Mature C32/40 w0/C = 0.45 AEA (str) Source
Luleå University of Technology, Sweden Tests during 1995 to 2004
Adjustment to a “general” data base 2006 Description
Moderate heat cement (Degerhamn OPC) from Cementa AB in Sweden. Primarily aimed for use in civil engineering structures.
Original material parameters
Density: 2 350 (kg/m³), Heat cap. 1 000 (J/(kg·K))
Heat cond. (W/m²K) as piece-wise linear function of equivalent time of maturity (h), (equ. time; heat cond.): (0;1.7), (12;2.1), (24;1.7), (10000;1.7),

Gravel: Other material Start temperature:
Constant: 17.0
Material definition: Coarse grained soil Source
Luleå University of Technology 1997 Description
e.g. till, moraine and gravel Original material parameters
Density: 2 200 (kg/m³), Heat cap. 1 400 (J/(kg·K)) Heat cond. 2.1 (W/m²K)

Rock: Other material Start temperature: Constant: 17.0
Material definition: Rock (str) Source
Luleå University of Technology 1997 Description
Original material parameters
Density: 2 650 (kg/m³), Heat cap. 850 (J/(kg·K)) Heat cond. 3.7 (W/m²K)

B5.1.2 Block connection list

Block 1: Rock
Block 2: Gravel
Block 3: mature concrete
Block 4: SCC-mod-TAS05, simulate filling

B5.1.3 Boundary type list

free surface Temperature
Piece-wise linear (time (h);temp. (°C)) (0;18) (24;20) (48;20) (72;17)
Wind velocity Constant 2 (m/s)
Heat transfer coefficient Constant 30 (W/m²K)
Supplied heat Constant 0 (W/m²)
Rock
Temperature Constant 17 (°C)
Heat transfer coefficient
Constant 80 (W/m²K)
Supplied heat Constant 0 (W/m²)
Form wall 21mm Temperature
Piece-wise linear (time (h);temp. (°C)) (0;18) (24;20) (48;20) (72;17)
Wind velocity Constant 2 (m/s)
Heat transfer coefficient

Piece-wise constant (time (h);htc (W/m²K)) (0:6.66667)
Wood 0.021 (m)
(168:500)
Free Surface Supplied heat
Constant 0 (W/m²) Form corner 40mm
Temperature
Piece-wise linear (time (h);temp. (°C)) (0;18) (24;20) (48;20) (72;17)
Wind velocity Constant 2 (m/s)
Heat transfer coefficient
Piece-wise constant (time (h);htc (W/m²K)) (0:3.5)
Wood 0.04 (m)
(168:500)
Free Surface Supplied heat
Constant 0 (W/m²) Form slab top 18mm
Temperature
Piece-wise linear (time (h);temp. (°C)) (0;18) (24;20) (48;20) (72;17)
Wind velocity Constant 2 (m/s)
Heat transfer coefficient
Piece-wise constant (time (h);htc (W/m²K)) (0:7.77778)
Wood 0.018 (m)
(40:500)
Free Surface Supplied heat
Constant 0 (W/m²) Form slab boxout 40mm
Temperature
Piece-wise linear (time (h);temp. (°C)) (0;18) (24;20) (48;20) (72;17)
Wind velocity Constant 2 (m/s)
Heat transfer coefficient
Piece-wise constant (time (h);htc (W/m²K)) (0:3.5)
Wood 0.04 (m)
(168:500)
Free Surface Supplied heat
Constant 0 (W/m²)
Moving Boundary: Moving boundary Temperature
Constant 20 (°C) Wind velocity
Constant 1 (m/s) Heat transfer coefficient
Constant 500 (W/m²K) Free Surface
Supplied heat Constant 0 (W/m²)

B5.1.4 Boundary connection list

Boundary segment 1: adiabatic (no heat flow)
Boundary segment 2: inner segment (full thermal contact)
Boundary segment 3: adiabatic (no heat flow)
Boundary segment 4: Rock
Boundary segment 5: adiabatic (no heat flow)
Boundary segment 6: adiabatic (no heat flow)
Boundary segment 7: free surface
Boundary segment 8: inner segment (full thermal contact)
Boundary segment 9: inner segment (full thermal contact)

Boundary segment 10: inner segment (full thermal contact)
Boundary segment 11: free surface
Boundary segment 12: free surface
Boundary segment 13: inner segment (full thermal contact)
Boundary segment 14: free surface
Boundary segment 15: Form slab top 18mm
Boundary segment 16: Form slab top 18mm
Boundary segment 17: Form slab boxout 40mm
Boundary segment 18: Form slab boxout 40mm
Boundary segment 19: Form slab boxout 40mm
Boundary segment 20: Form slab top 18mm
Boundary segment 21: Form corner 40mm
Boundary segment 22: Form corner 40mm
Boundary segment 23: Form corner 40mm
Boundary segment 24: Form corner 40mm
Boundary segment 25: Form wall 21mm
Boundary segment 26: free surface
Boundary segment 27: Form wall 21mm

B5.1.5 Inner point type list

B.5.1.6 Simulation of filling process for young concrete

Surface position as a piece-wise linear func. of time (time (h); y-coord. (m)) (0;3), (6.5;6.5.,

B6 Plane-surface analysis

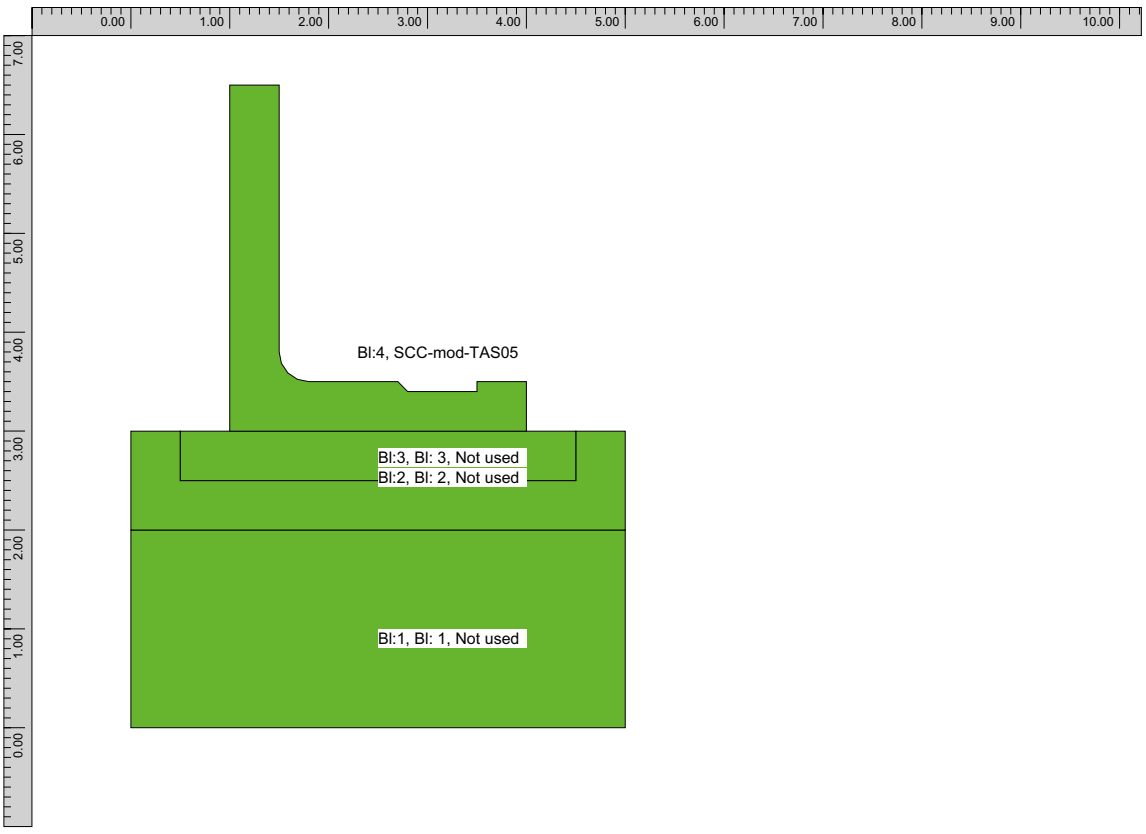

Figure B-5. *Blocks used in stress calculation, section 1.*

B6.1 Description

B6.1.1 Stress case

Default time stepping Translation

Free (0.000)

Rotation around X-axis Free (0.000)

Rotation around Y-axis Full restraint (1.000)

B6.1.2 Block data list

Block 4: SCC-mod-TAS05

B6.1.3 Block type list

SCC-mod-TAS05: Young concrete

Material definition: K45 vct = 0.47 Lufttillsats (Mix 4) (str) Source

Luleå Tekniska Universitet

Provningar 1999, 2000 – LTU, Skrift 00:02 Recept Sweroc

Description

Degerhamn Std P (Anläggningscement) vct 0.47

Köping 500 (Kalkfiller)

lufthalt 4.5 á 5.0 %

flytsättmått 700–750 mm

Original material parameters

Po-ratio 0.18 (-), AlfaHeat 9.7e-06 (1/K), AlfaCool 9.7e-06 (1/K) ThetaT 5000 (K), RelaxTime1 0.005 (d), TimeZero 0.36 (d)

Fcc28 68 (MPa), Fcref 62 (MPa), Ftref 3.87 (MPa)

Beta1 0.667 (-), Alfact 0.7 (-), RaaT 0 (-), RaaFi 0 (-)

KFi 2 (-), Eps1 0 (-), TimeS1 6 (h)

Eps2 -0.000165 (-), TimeS2 8 (h), ThetaSH 120 (h), EthaSH 0.3 (-)

Relax: Age 0.359 (d), Units (GPa) 0.01 0.01 0.01 0.01 0.01 0.01 0.01 0.01

Relax: Age 0.54 (d), Units (GPa) 3.0184 2.3761 3.6531 2.5385 1.3421 1.7683 1.6167 1.3048

Relax: Age 1.163 (d), Units (GPa) 3.2785 2.9128 4.1142 2.9953 2.2954 2.5047 2.4411 1.844

Relax: Age 2.506 (d), Units (GPa) 3.3589 3.3689 4.2389 3.6801 3.5409 3.4482 3.4996 2.4096

Relax: Age 5.4 (d), Units (GPa) 2.6217 2.9505 3.7231 3.9755 4.2461 3.8967 4.0385 3.8283

Relax: Age 11.634 (d), Units (GPa) 2.0163 2.4072 3.248 3.7368 4.0717 3.7562 3.8959 7.4188

Relax: Age 25.065 (d), Units (GPa) 1.5407 1.9199 2.7174 3.3638 3.8489 3.5998 3.7423 10.7153

Relax: Age 54 (d), Units (GPa) 1.1889 1.5262 2.2351 2.9238 3.5773 3.4565 3.6112 13.5493

Relax: Age 116.339 (d), Units (GPa) 0.9389 1.2286 1.8461 2.5009 3.2669 3.3372 3.5338 15.8386

Relax: Age 250.646 (d), Units (GPa) 0.7655 1.014 1.5523 2.1504 2.9475 3.232 3.5329 17.5812

Following material parameters are changed by the user Fcc28 50 (MPa)

Fcref 50 (MPa)

mature concrete: Other material

Material definition: Mature C32/40 w0/C = 0.45 AEA (str) Source

Luleå University of Technology, Sweden Tests during 1995 to 2004

Adjustment to a “general” data base 2006 Description

Moderate heat cement (Degerhamn OPC) from Cementa AB in Sweden. Primarily aimed for use in civil engineering structures.

Original material parameters

Po-ratio 0.18 (-), E-modulus 33.5 (GPa), AlfaHeat 1e-05 (1/K) Fcc 48 (MPa), Ftref 3.45 (MPa)

Rock: Other material
Material definition: Rock (str) Source
Luleå University of Technology 1997 Description
Original material parameters
Po-ratio 0.2 (-), E-modulus 30 (GPa), AlfaHeat 1e-05 (1/K) Fcc 30 (MPa), Ftref 3 (MPa)

B7 Heat computation results

B7.1 Temperature curves

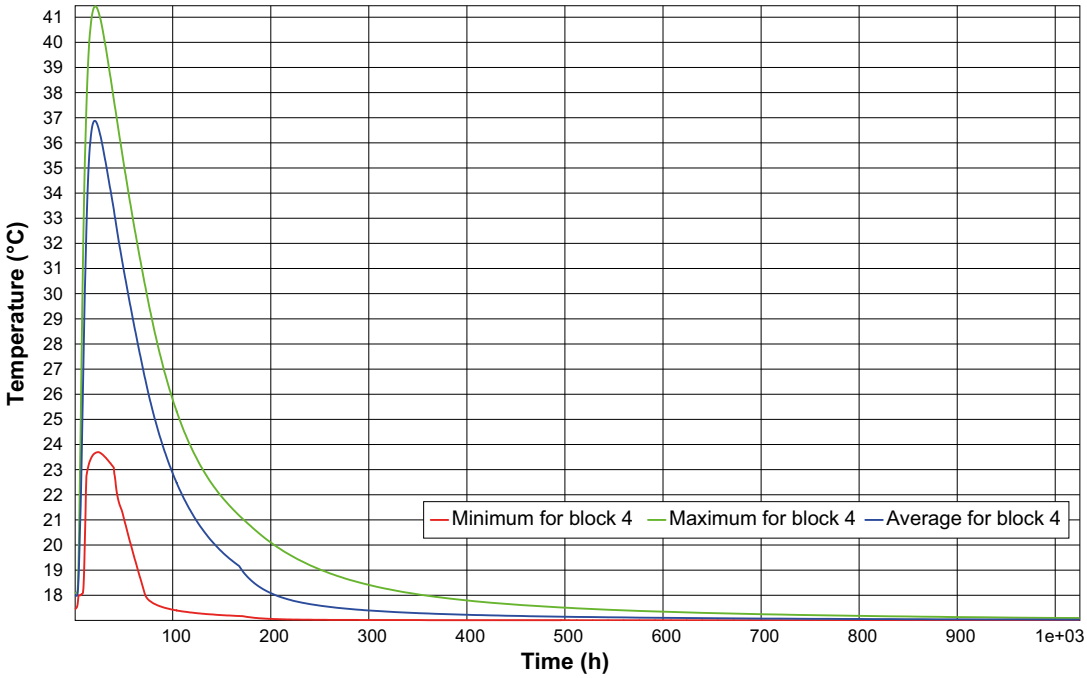

Figure B-6. *Temperature development, section 1 (minimum, maximum and average).*

B7.2 Temperature slab

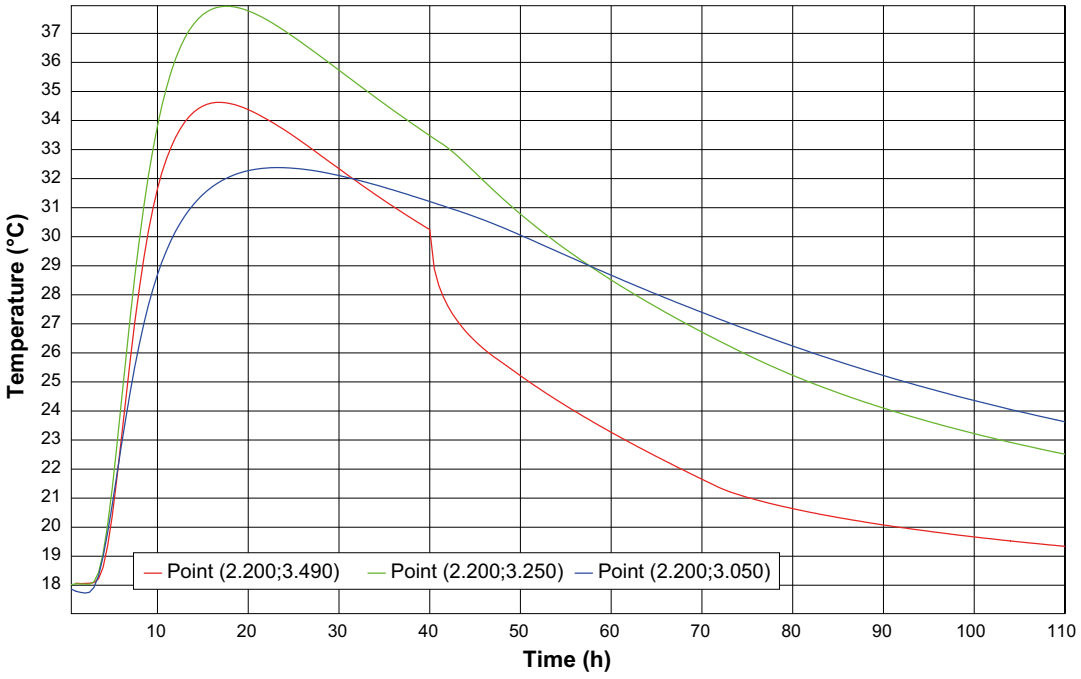

Figure B-7. *Calculated temperature development in the slab, section 1, position of the temperature gauges.*

B7.3 Temperature wall

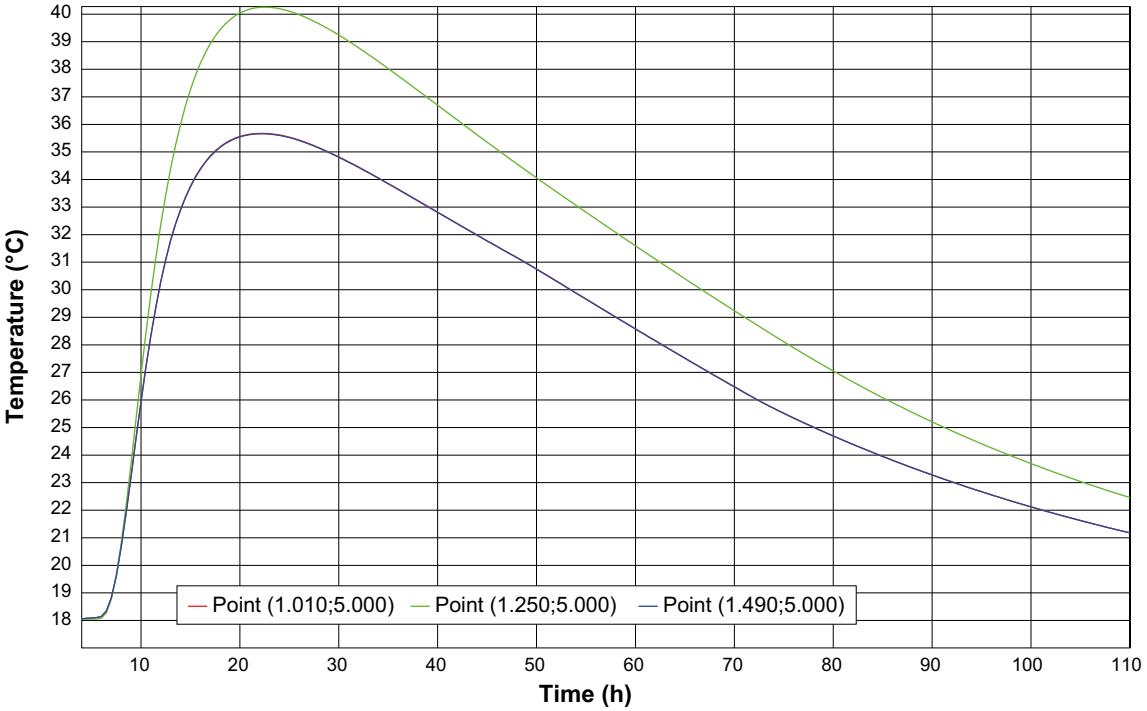

Figure B-8. *Calculated temperature development in the wall, section 1, position of the temperature gauges.*

B7.4 Temperature max

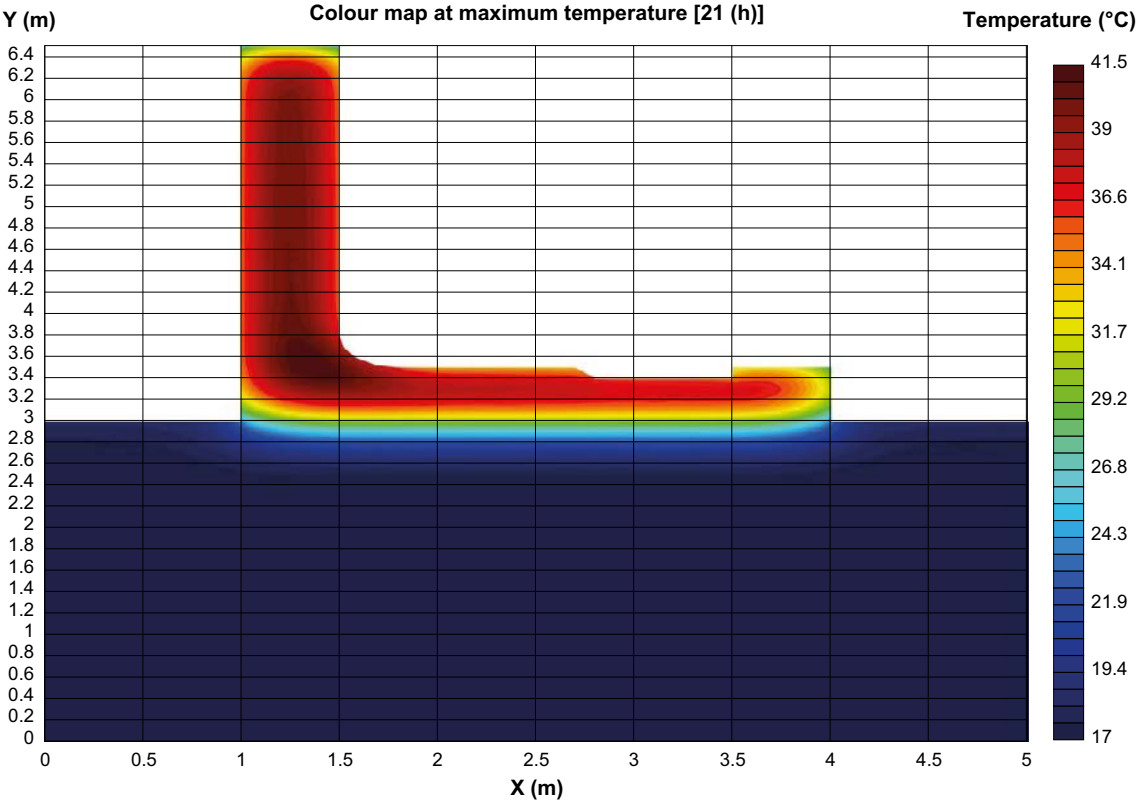

Figure B-9. *Highest temperature in section 1, 21 hours after casting, temperature distribution in the cross section.*

B8 Plane-surface computation results

B8.1 Strain ratio curves

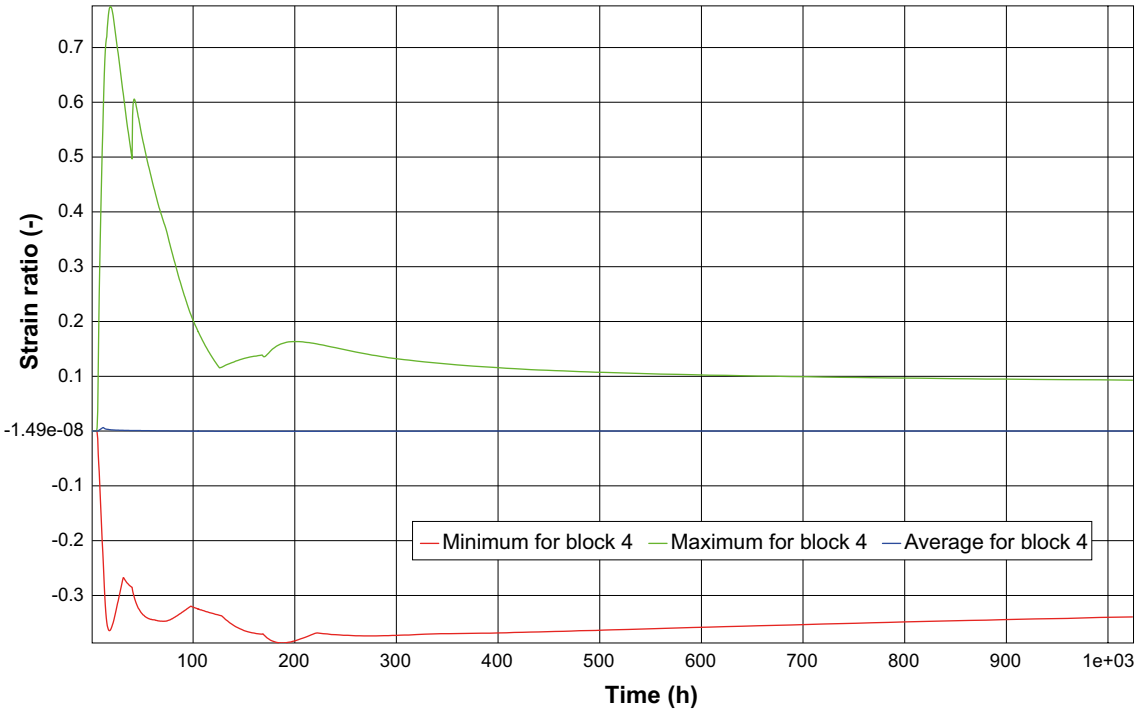

Figure B-10. *Calculated strain ratio, section 1 (minimum, maximum and average).*

B8.2 Strain ratio points

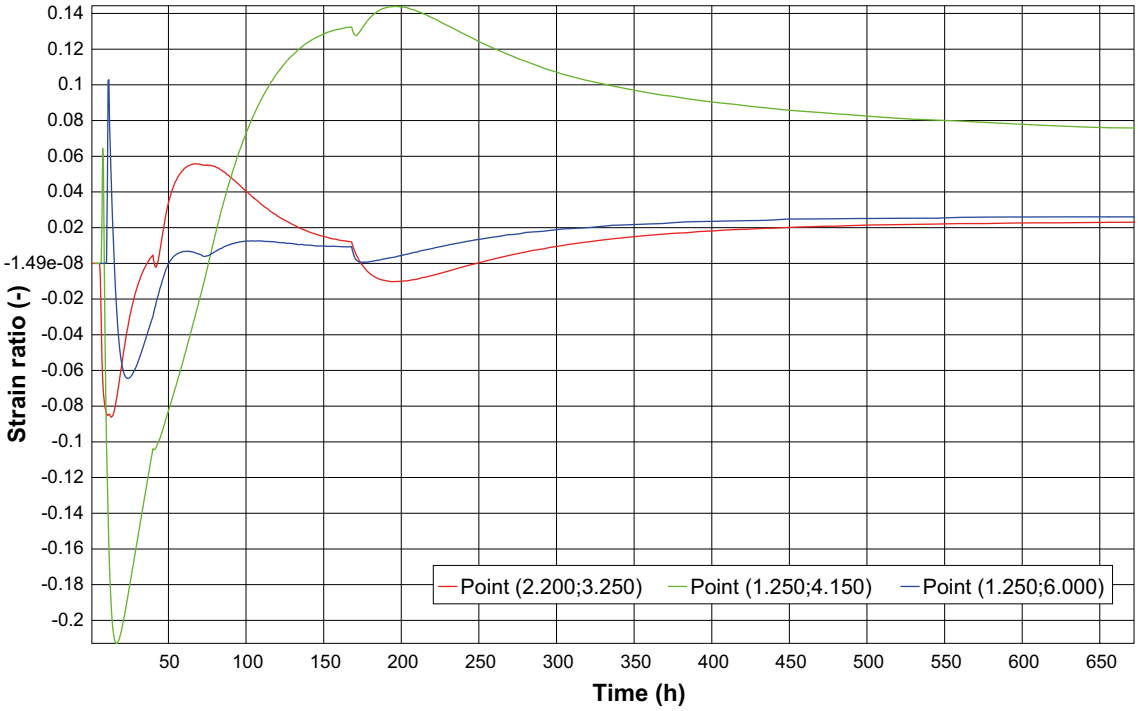

Figure B-11. *Calculated strain ratio, section 1, position of the strain gauges.*

B8.3 Early strain ratio

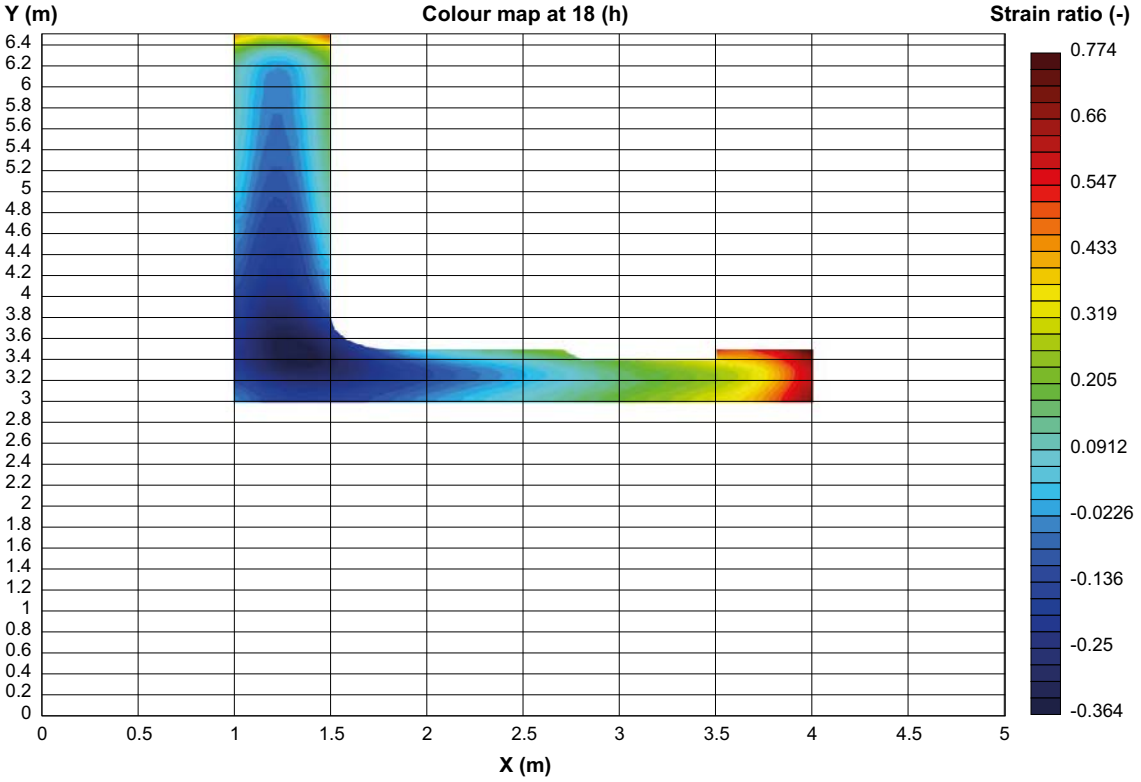

Figure B-12. *Maximum strain ratio in section 1, 18 hours after casting, distribution in the cross section.*

B8.4 Late strain ratio

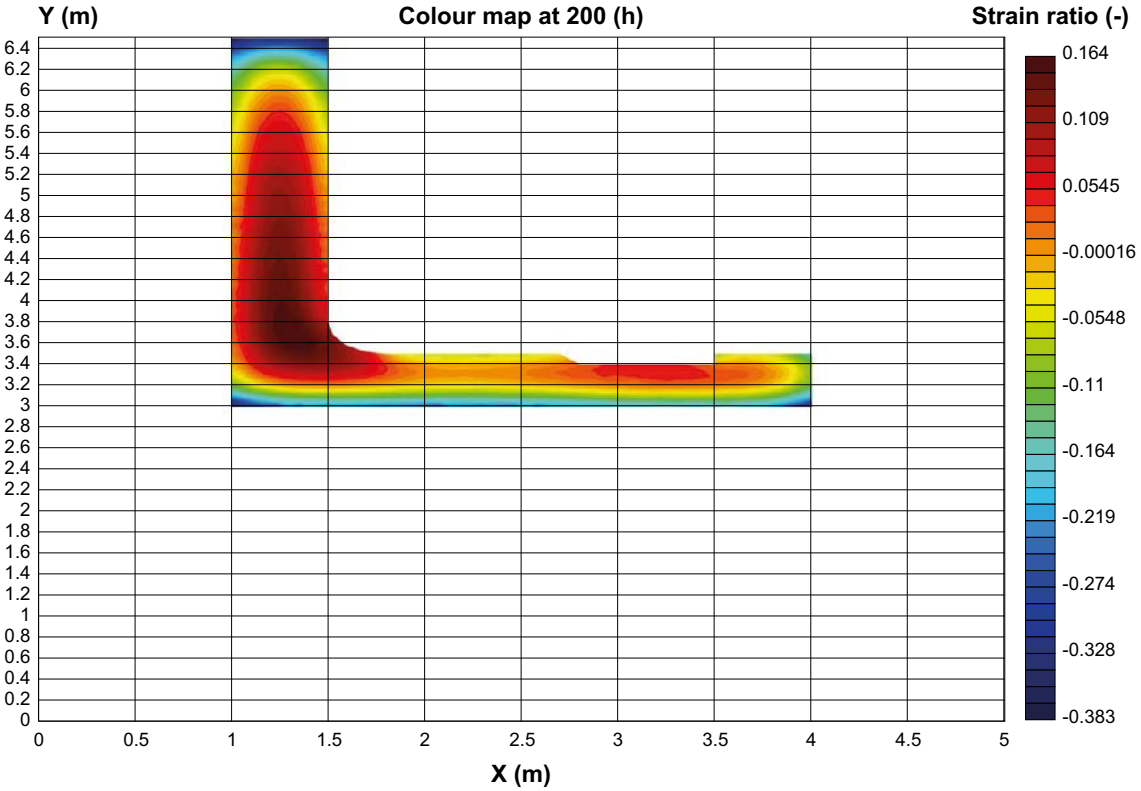

Figure B-13. ***S****train ratio in section 1, 2nd peak, 200 hours after casting, distribution in the cross section.*

Appendix C

D:\Work\SKB\TAS05\TAS05_et2_S.CPR: Report

C1 Software and project information

C1.1 Software

System name: ConTeSt System version: 1.0
Developed by: JEJMS Concrete AB

C1.2 Project

Original filename: D:\Work\SKB\TAS05\TAS05_et1_T.CPR Created: 2018.06.01 12.34.11
Created by: swecvo on CNU21810QY
Current filename: D:\Work\SKB\TAS05\TAS05_et2_S.CPR Last change: 2018.06.06 22.18.09
Last change by: swecvo on CNU21810QY

C2 Geometry and time

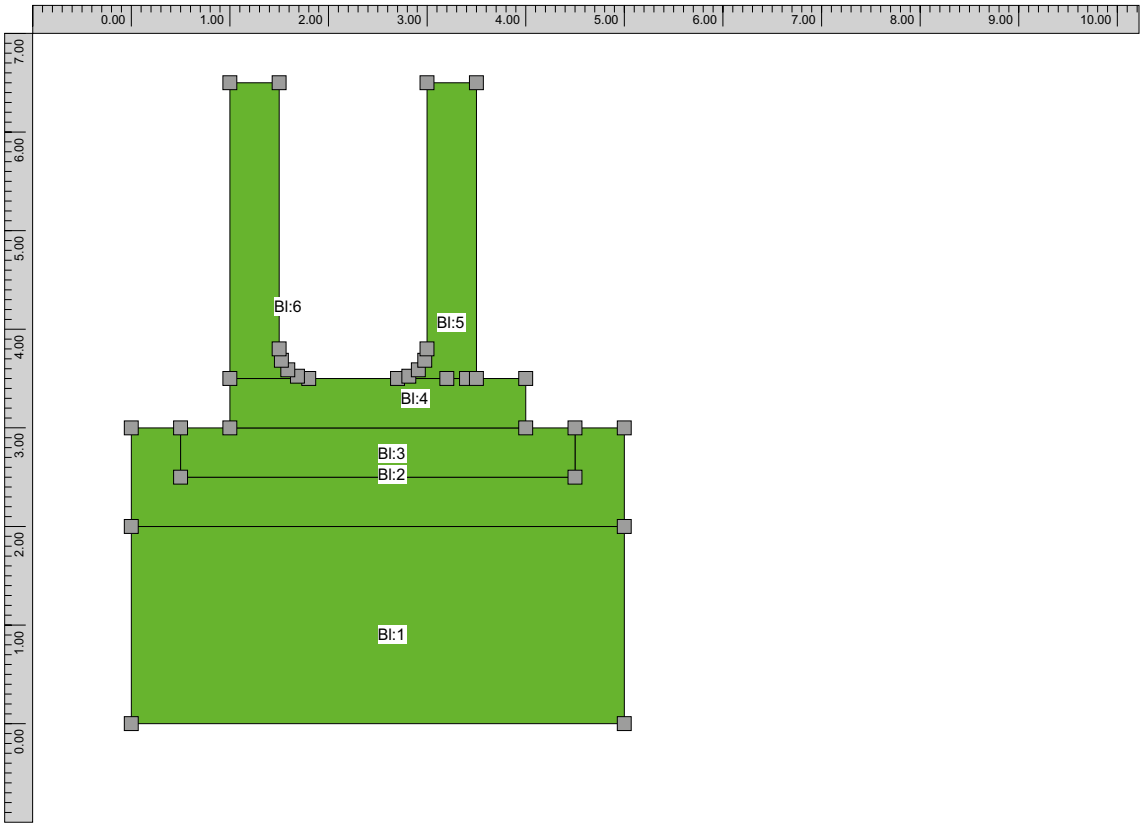

Figure C-1. *Geometry of section 2.*

C2.1 Description

C2.1.1 Blocks

Block 1: (5.000;0.000) - (5.000;2.000) - (0.000;2.000) - (0.000;0.000)

Block 2: (0.000;3.000) - (0.000;2.000) - (5.000;2.000) - (5.000;3.000) - (4.500;3.000) - (4.500;2.500) - (0.500;2.500) - (0.500;3.000)

Block 3: (0.500;2.500) - (4.500;2.500) - (4.500;3.000) - (4.000;3.000) - (1.000;3.000) - (0.500;3.000)

Block 4: (4.000;3.000) - (4.000;3.500) - (3.500;3.500) - (3.400;3.500) - (3.200;3.500) - (2.700;3.500) - (1.800;3.500) - (1.000;3.500) - (1.000;3.000)

Block 5: (3.000;3.800) - (2.977;3.685) - (2.912;3.588) - (2.815;3.523) - (2.700;3.500) - (3.200;3.500) - (3.400;3.500) - (3.500;3.500) - (3.500;6.500) - (3.000;6.500)

Block 6: (1.800;3.500) - (1.685;3.523) - (1.588;3.588) - (1.523;3.685) - (1.500;3.800) - (1.500;6.500) - (1.000;6.500) - (1.000;3.500)

C2.1.2 Computation time

Total time length: 1 000 (h)

C3 Element size

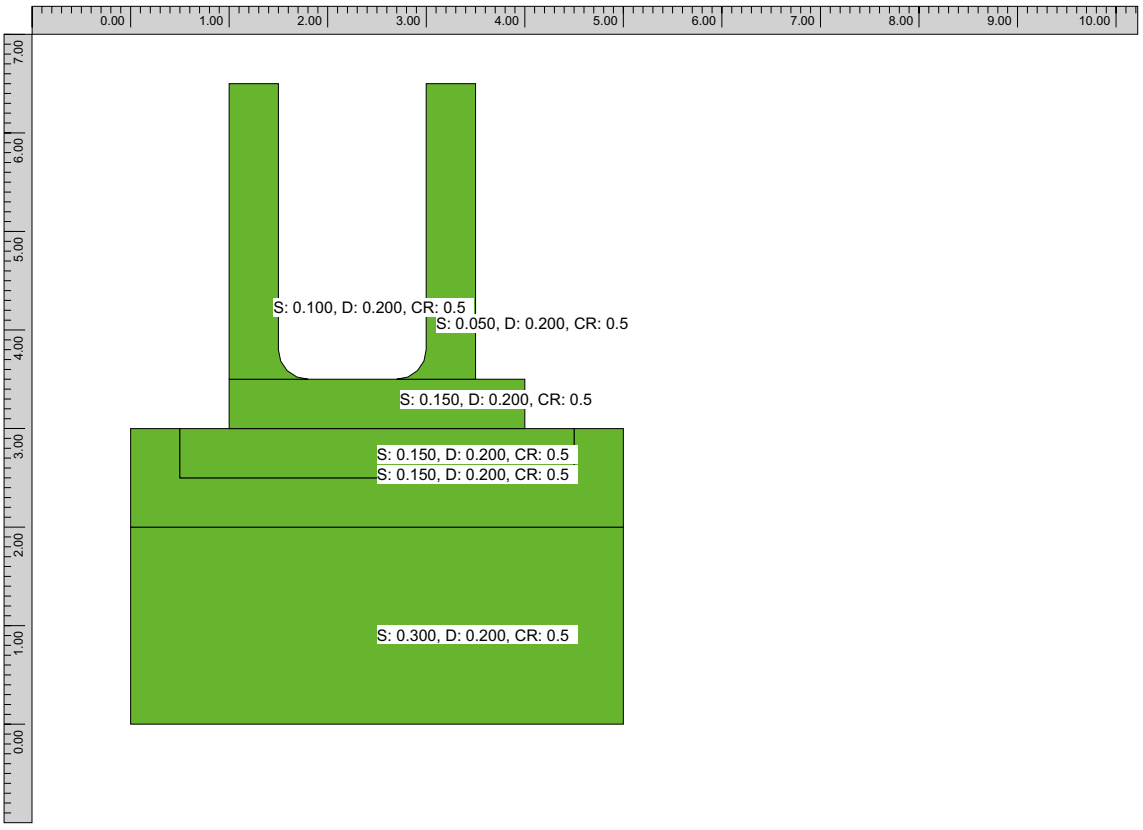

Figure C-2. *Element size for meshing, section 2.*

C4 Computation mesh

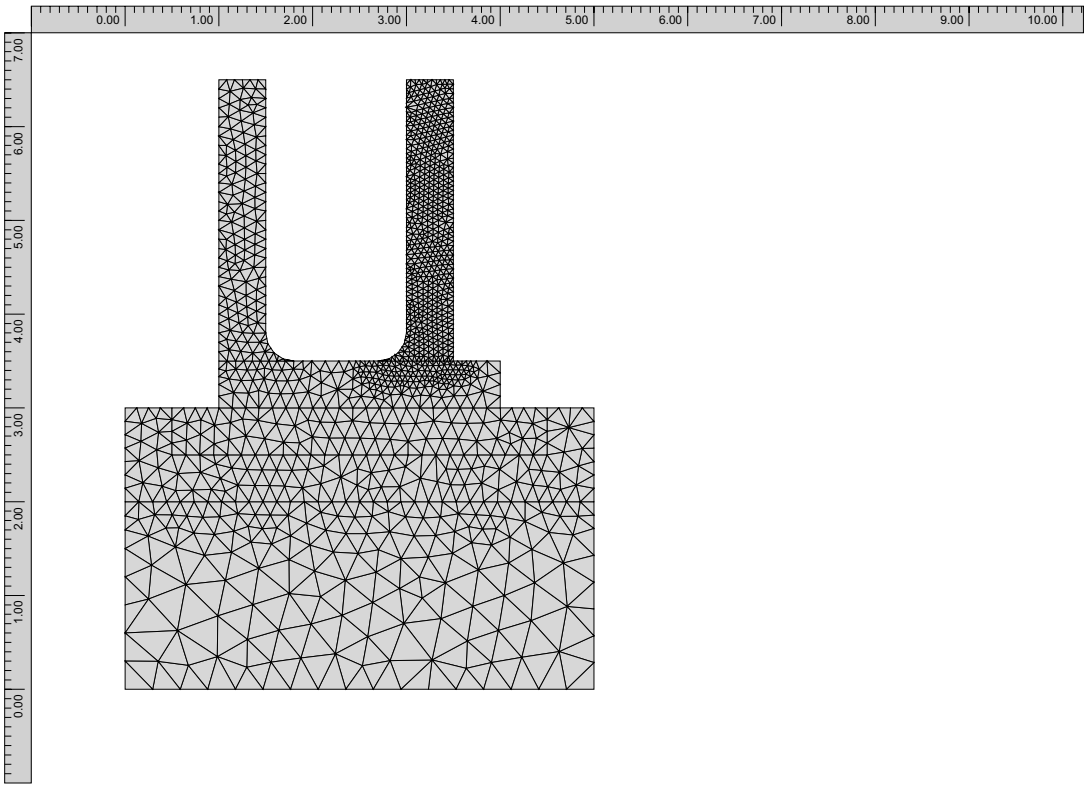

Figure C-3. *Finite element mesh for section 2.*

C5 Heat properties

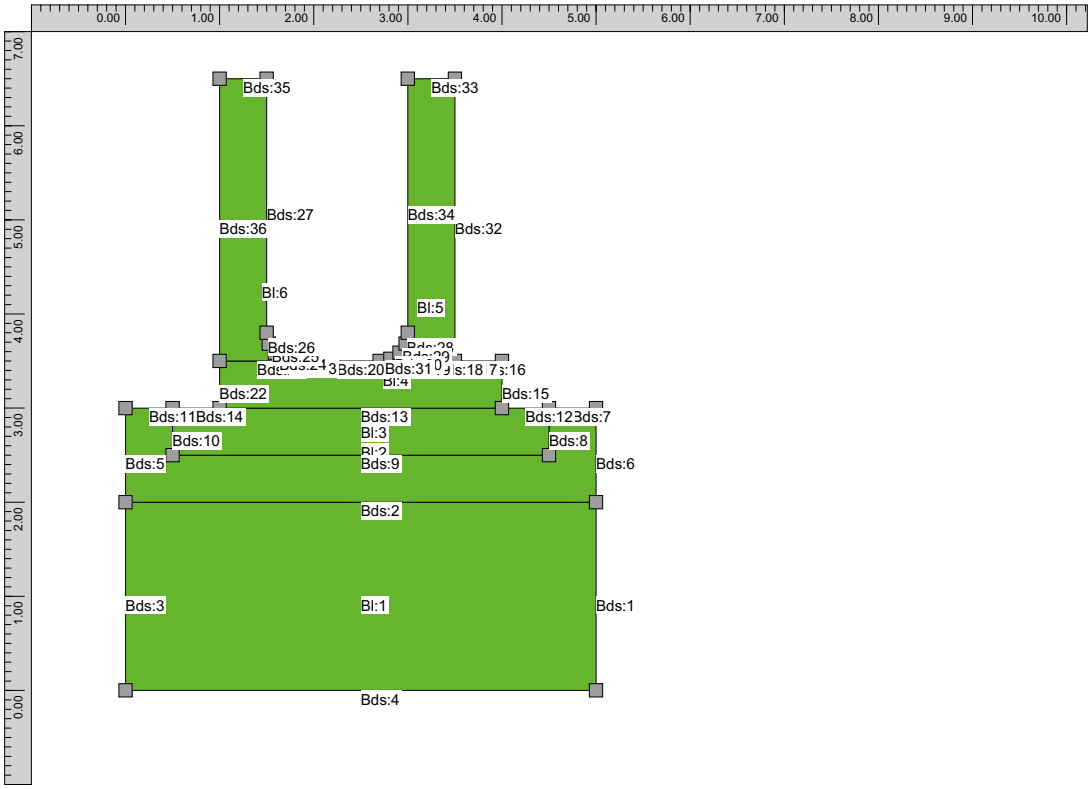

Figure C-4. *List of boundaries, section 2.*

C5.1 Description

C5.1.1 Block type list

SCC-mod-TAS05: Young concrete Start temperature:

Constant: 16.0

Material definition: K45 vct = 0.47 Lufttillsats (Mix 4) (str) Source

Luleå Tekniska Universitet

Provningar 1999, 2000 – LTU, Skrift 00:02 Recept Sweroc

Description

Degerhamn Std P (Anläggningscement) vct 0.47

Köping 500 (Kalkfiller)

lufthalt 4.5 á 5.0 %

flytsättmått 700–750 mm Original material parameters

Density: 2 350 (kg/m³), Heat cap. 1 000 (J/(kg·K))

Heat cond. (W/m²K) as piece-wise linear function of equivalent time of maturity (h), (equ. time; heat cond.): (0;2.1), (12;2.1), (24;1.7), (10000;1.7),

C 363 (kg/m³), Wc 325000 (J/kg), Lambda1 1.02 (-), t1 9.15 (h), Kappa1 1.94 (-)

te0 0 (h), BetaD 1 (-), ThetaRef 3660 (K), Kappa3 0.653 (-)

Eta6 4 (‰), Eta8 10 (‰), Eta12 106 (‰), Eta18 198 (‰), Eta24 262 (‰), Eta72 562 (‰), Eta168 791 (‰)

Fcc28 68 (MPa)

Following material parameters are changed by the user

C 320 (kg/m³)

Wc 250 000 (J/kg)

te0 -20 (h)

BetaD 2 (-)

Fcc28 50 (MPa)

mature concrete: Other material Start temperature:

Constant: 16.0

Material definition: Mature C32/40 w0/C = 0.45 AEA (str) Source

Luleå University of Technology, Sweden Tests during 1995 to 2004

Adjustment to a “general” data base 2006 Description

Moderate heat cement (Degerhamn OPC) from Cementa AB in Sweden. Primarily aimed for use in civil engineering structures.

Original material parameters

Density: 2 350 (kg/m³), Heat cap. 1 000 (J/(kg·K))

Heat cond. (W/m²K) as piece-wise linear function of equivalent time of maturity (h), (equ. time; heat cond.): (0;1.7), (12;2.1), (24;1.7), (10000;1.7),

Gravel: Other material Start temperature:

Constant: 16.0

Material definition: Coarse grained soil Source

Luleå University of Technology 1997 Description

e.g. till, moraine and gravel Original material parameters

Density: 2 200 (kg/m³), Heat cap. 1 400 (J/(kg·K)) Heat cond. 2.1 (W/m²K)

Rock: Other material Start temperature: Constant: 16.0

Material definition: Rock (str) Source

Luleå University of Technology 1997 Description

Original material parameters

Density: 2 650 (kg/m³), Heat cap. 850 (J/(kg·K)) Heat cond. 3.7 (W/m²K)

C5.1.2 Block connection list

Block 1: Rock
Block 2: Gravel
Block 3: mature concrete
Block 4: mature concrete
Block 5: SCC-mod-TAS05, simulate filling
Block 6: mature concrete

C5.1.3 Boundary type list

free surface Temperature
Piece-wise linear (time (h);temp. (°C)) (0;18) (24;18) (48;20) (72;20) (96;16)
Wind velocity Constant 1 (m/s)
Heat transfer coefficient Constant 30 (W/m²K)
Supplied heat Constant 0 (W/m²)
Rock
Temperature Constant 16 (°C)
Heat transfer coefficient Constant 80 (W/m²K)
Supplied heat Constant 0 (W/m²)
Form wall 21mm Temperature
Piece-wise linear (time (h);temp. (°C)) (0;18) (24;18) (48;20) (72;20) (96;16)
Wind velocity Constant 2 (m/s)
Heat transfer coefficient
Piece-wise constant (time (h);htc (W/m²K)) (0:6.66667)
Wood 0.021 (m)
(168:500)
Free Surface Supplied heat
Constant 0 (W/m²) Form corner 40mm
Temperature
Piece-wise linear (time (h);temp. (°C)) (0;18) (24;18) (48;20) (72;20) (96;16)
Wind velocity Constant 2 (m/s)
Heat transfer coefficient
Piece-wise constant (time (h);htc (W/m²K)) (0:3.5)
Wood 0.04 (m)
(168:500)
Free Surface Supplied heat
Constant 0 (W/m²) Form slab top 12mm
Temperature
Piece-wise linear (time (h);temp. (°C)) (0;18) (24;20) (48;20) (72;17)
Wind velocity Constant 2 (m/s)
Heat transfer coefficient
Piece-wise constant (time (h);htc (W/m²K)) (0:11.6667)
Wood 0.012 (m)
(30:500)
Free Surface Supplied heat
Constant 0 (W/m²) Form slab boxout 40mm
Temperature
Piece-wise linear (time (h);temp. (°C)) (0;18) (24;20) (48;20) (72;17)

Wind velocity Constant 2 (m/s)
Heat transfer coefficient
Piece-wise constant (time (h);htc (W/m²K)) (0:3.5)
Wood 0.04 (m)
(168:500)
Free Surface Supplied heat
Constant 0 (W/m²)
Moving Boundary: Moving boundary Temperature
Constant 18 (°C) Wind velocity
Constant 1 (m/s) Heat transfer coefficient
Constant 500 (W/m²K) Free Surface
Supplied Heat
Constant 0 (W/m²)

C5.1.4 Boundary connection list

Boundary segment 1: adiabatic (no heat flow)
Boundary segment 2: inner segment (full thermal contact)
Boundary segment 3: adiabatic (no heat flow)
Boundary segment 4: Rock
Boundary segment 5: adiabatic (no heat flow)
Boundary segment 6: adiabatic (no heat flow)
Boundary segment 7: free surface
Boundary segment 8: inner segment (full thermal contact)
Boundary segment 9: inner segment (full thermal contact)
Boundary segment 10: inner segment (full thermal contact)
Boundary segment 11: free surface
Boundary segment 12: free surface
Boundary segment 13: inner segment (full thermal contact)
Boundary segment 14: free surface
Boundary segment 15: free surface
Boundary segment 16: Form wall 21mm
Boundary segment 17: inner segment (full thermal contact)
Boundary segment 18: inner segment (full thermal contact)
Boundary segment 19: inner segment (full thermal contact)
Boundary segment 20: free surface
Boundary segment 21: inner segment (full thermal contact)
Boundary segment 22: free surface
Boundary segment 23: free surface
Boundary segment 24: free surface
Boundary segment 25: free surface
Boundary segment 26: free surface
Boundary segment 27: free surface
Boundary segment 28: Form corner 40mm
Boundary segment 29: Form corner 40mm
Boundary segment 30: Form corner 40mm
Boundary segment 31: Form corner 40mm
Boundary segment 32: Form wall 21mm

Boundary segment 33: free surface
Boundary segment 34: Form wall 21mm
Boundary segment 35: free surface
Boundary segment 36: free surface

C5.1.5 Inner point type list

C5.1.6 Simulation of filling process for young concrete

Surface position as a piece-wise linear func. of time (time (h); y-coord. (m)) (0;3.5), (3.5;6.5),

C6 Plane-surface analysis

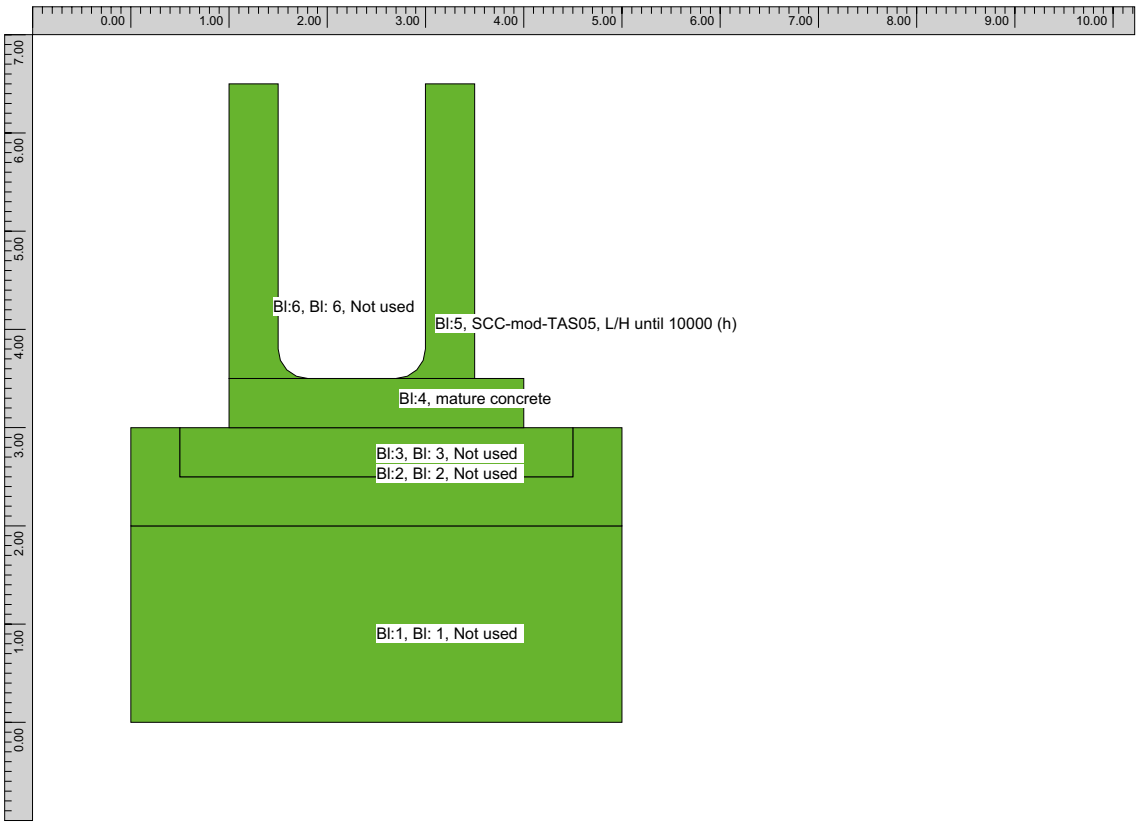

Figure C-5. *Blocks used in stress calculation, section 2.*

C6.1 Description

C6.1.1 Stress case

Default time stepping Translation
Free (0.000)
Rotation around X-axis Free (0.000)
Rotation around Y-axis Full restraint (1.000)
Resilience: LH-based
Structure length: 12.500 (m) Data source: Standard
Resilience reduction length and width dependent
Data source: External file C:\Program Files (x86)\ConTeSt\redH3.0m.rrt Length = 0.000 (m) : [width(m),red]
(0.400;0.500) (0.800;0.500) (1.200;0.500)
Length = 2.500 (m) : [width(m),red] (0.400;0.500) (0.800;0.500) (1.200;0.500)

Length = 7.000 (m) : [width(m),red] (0.400;0.720) (0.800;0.750) (1.200;0.780)
Length = 15.000 (m) : [width(m),red] (0.400;1.000) (0.800;1.000) (1.200;1.000)

C6.1.2 Block data list

Block 4: mature concrete

C6.1.3 Block type list

SCC-mod-TAS05: Young concrete
Material definition: K45 vct = 0.47 Lufttillsats (Mix 4) (str) Source
Luleå Tekniska Universitet
Provningar 1999, 2000 – LTU, Skrift 00:02 Recept Sweroc
Description
Degerhamn Std P (Anläggningscement) vct 0.47
Köping 500 (Kalkfiller)
lufthalt 4.5 á 5.0 %
flytsättmått 700–750 mm Original material parameters
Po-ratio 0.18 (-), AlfaHeat 9.7e-06 (1/K), AlfaCool 9.7e-06 (1/K) ThetaT 5000 (K), RelaxTime1 0.005 (d), TimeZero 0.36 (d)
Fcc28 68 (MPa), Fcref 62 (MPa), Ftref 3.87 (MPa)
Beta1 0.667 (-), Alfact 0.7 (-), RaaT 0 (-), RaaFi 0 (-)
KFi 2 (-), Eps1 0 (-), TimeS1 6 (h)
Eps2 -0.000165 (-), TimeS2 8 (h), ThetaSH 120 (h), EthaSH 0.3 (-)
Relax: Age 0.359 (d), Units (GPa) 0.01 0.01 0.01 0.01 0.01 0.01 0.01 0.01
Relax: Age 0.54 (d), Units (GPa) 3.0184 2.3761 3.6531 2.5385 1.3421 1.7683 1.6167 1.3048
Relax: Age 1.163 (d), Units (GPa) 3.2785 2.9128 4.1142 2.9953 2.2954 2.5047 2.4411 1.844
Relax: Age 2.506 (d), Units (GPa) 3.3589 3.3689 4.2389 3.6801 3.5409 3.4482 3.4996 2.4096
Relax: Age 5.4 (d), Units (GPa) 2.6217 2.9505 3.7231 3.9755 4.2461 3.8967 4.0385 3.8283
Relax: Age 11.634 (d), Units (GPa) 2.0163 2.4072 3.248 3.7368 4.0717 3.7562 3.8959 7.4188
Relax: Age 25.065 (d), Units (GPa) 1.5407 1.9199 2.7174 3.3638 3.8489 3.5998 3.7423 10.7153
Relax: Age 54 (d), Units (GPa) 1.1889 1.5262 2.2351 2.9238 3.5773 3.4565 3.6112 13.5493
Relax: Age 116.339 (d), Units (GPa) 0.9389 1.2286 1.8461 2.5009 3.2669 3.3372 3.5338 15.8386
Relax: Age 250.646 (d), Units (GPa) 0.7655 1.014 1.5523 2.1504 2.9475 3.232 3.5329 17.5812
Following material parameters are changed by the user Fcc28 50 (MPa)
Fcref 50 (MPa)

mature concrete: Other material
Material definition: Mature C32/40 w0/C = 0.45 AEA (str) Source
Luleå University of Technology, Sweden Tests during 1995 to 2004
Adjustment to a “general” data base 2006 Description
Moderate heat cement (Degerhamn OPC) from Cementa AB in Sweden. Primarily aimed for use in civil engineering structures.
Original material parameters
Po-ratio 0.18 (-), E-modulus 33.5 (GPa), AlfaHeat 1e–05 (1/K) Fcc 48 (MPa), Ftref 3.45 (MPa)

Rock: Other material
Material definition: Rock (str) Source
Luleå University of Technology 1997 Description
Original material parameters
Po-ratio 0.2 (-), E-modulus 30 (GPa), AlfaHeat 1e–05 (1/K) Fcc 30 (MPa), Ftref 3 (MPa)

C7 Heat computation results

C7.1 Temperature curves

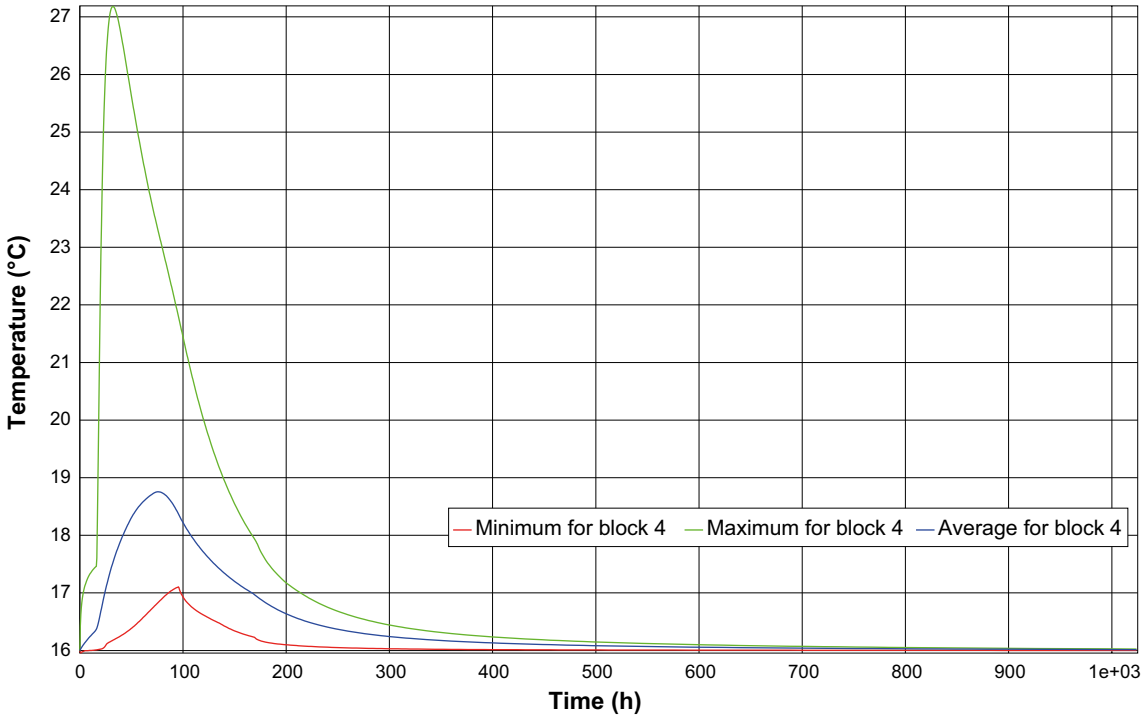

Figure C-6. *Calculated temperature development, section 2 (minimum, maximum and average).*

C7.2 Temperature wall

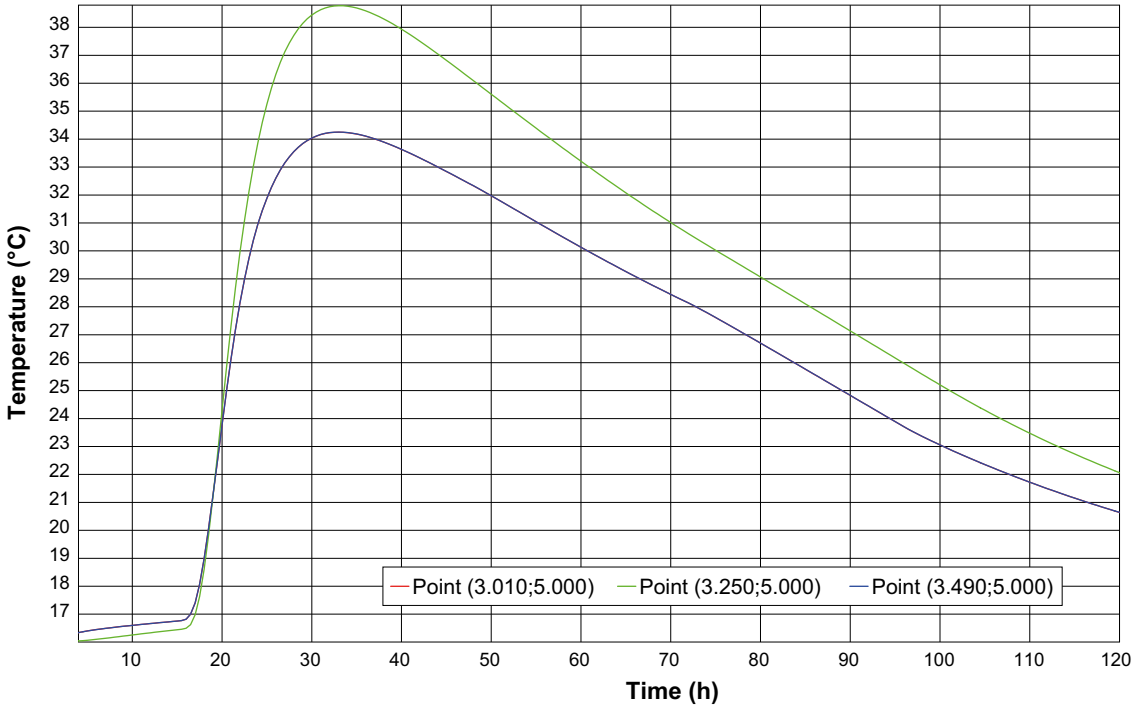

Figure C-7. *Calculated temperature development in the wall, section 2, position of the temperature gauges.*

C7.3 Maximum temperature

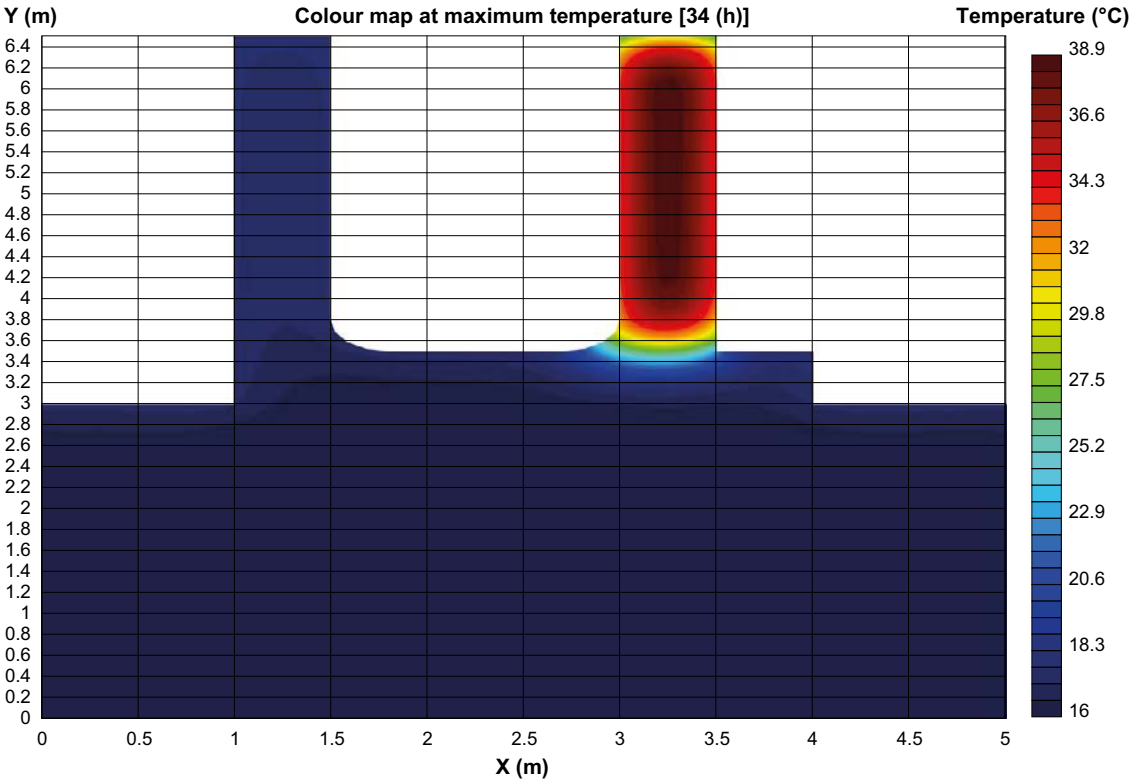

Figure C-8. *Highest temperature in section 2, 34 hours after casting, temperature distribution in the cross section.*

C8 Plane-surface computation results

C8.1 Strain ratio curves

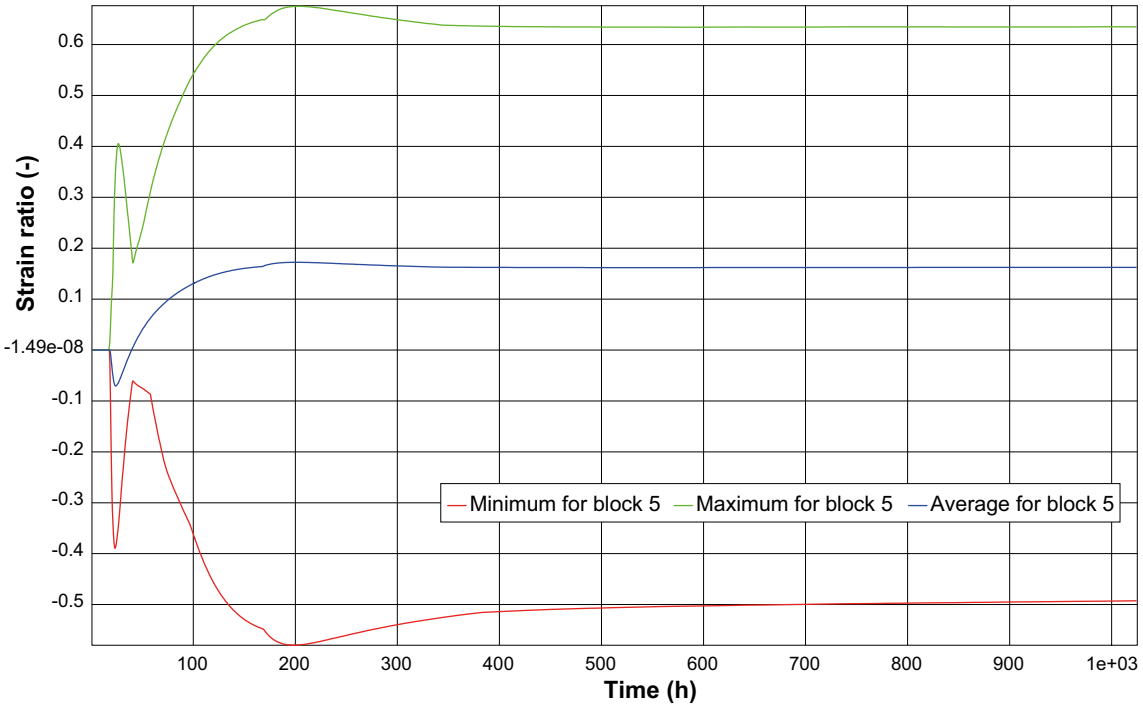

Figure C-9. *Calculated strain ratio, section 2 (minimum, maximum and average).*

C8.2 Strain ratio points

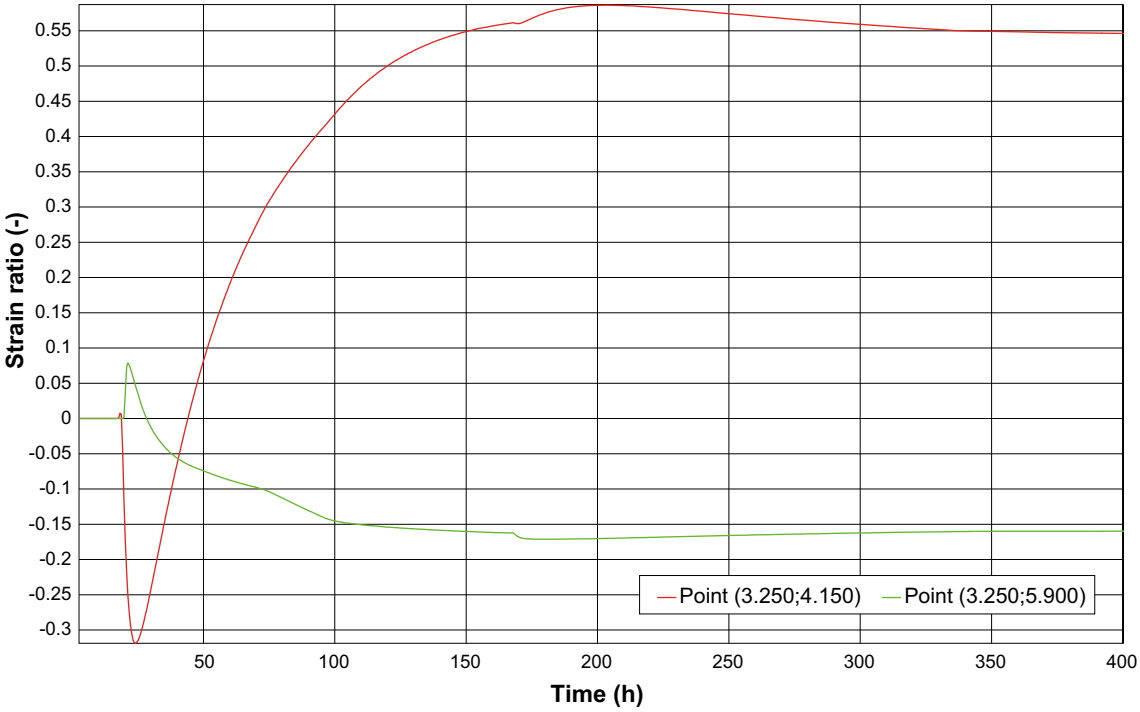

Figure C-10. *Calculated strain ratio, section 2, position of the strain gauges.*

C8.3 Maximum strain ratio

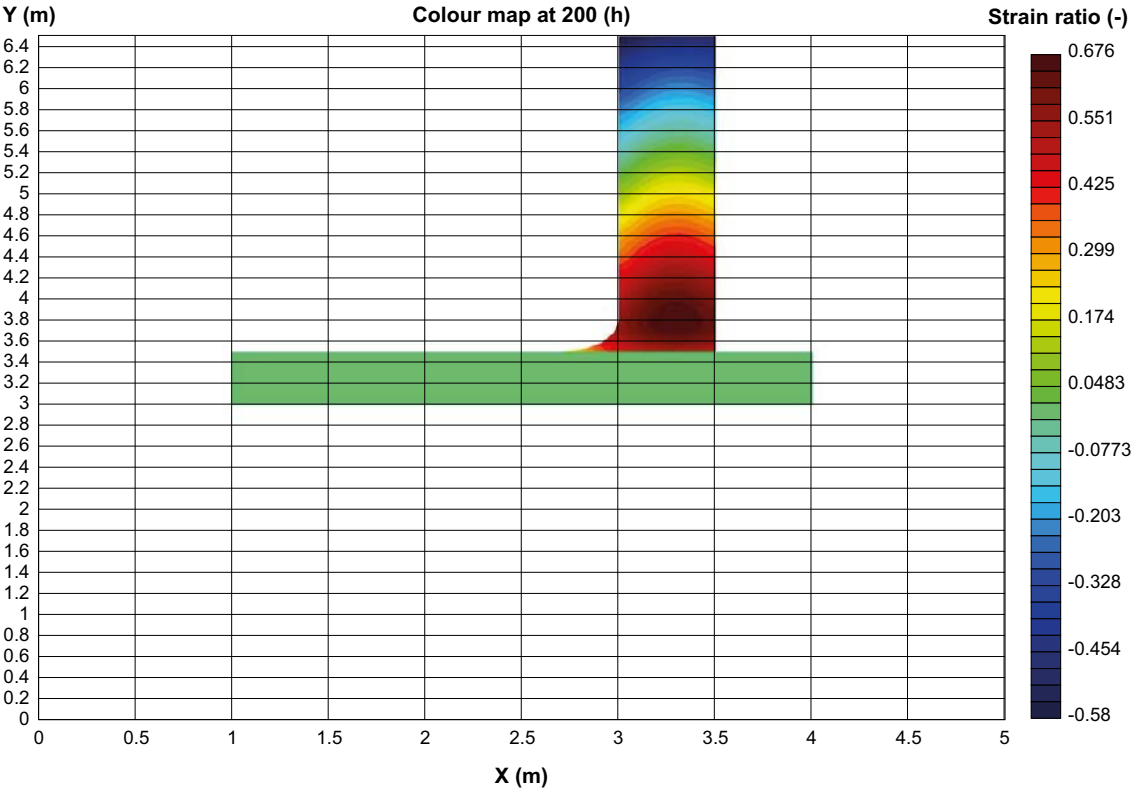

Figure C-11. *Maximum strain ratio in section 2, 200 hours after casting, distribution in the cross section.*

Arkitektkopia AB, Bromma, 2019

SKB is responsible for managing spent nuclear fuel and radioactive waste produced by the Swedish nuclear power plants such that man and the environment are protected in the near and distant future.

skb.se